Fiber Tension Loss During the
Winding and Cure of a Filament Wound Composite Case

by

Paul M. Northrop

Thesis submitted to the Faculty of the
Virginia Polytechnic Institute and State University
in partial fulfillment of the requirements for the degree of

MASTER OF SCIENCE

in

Engineering Mechanics

APPROVED:

A. C. Loos, Chairman

C. E. Knight, Jr.

J. W. Grant

C. H. Stern

February 1992
Blacksburg, Virginia

Fiber Tension Loss During The

Winding and Cure of a Filament Wound Composite Case

by

Paul M. Northrop

Committee Chairman: Alfred C. Loos

Department of Engineering Science and Mechanics

(ABSTRACT)

During the fabrication of a filament-wound composite case, which includes the winding and cure stages, the tension in the fiber can change significantly. If the level of fiber tension decreases excessively during fabrication, fiber slippage and clumping can occur. The resulting resin rich areas can significantly decrease the strength of the composite case.

The objectives of the present investigation were 1) to measure the change in fiber tension during the winding and cure of a composite case wound with prepreg material, and 2) to calculate the change in tension during cure using a simulation computer program. Of particular interest was the loss of fiber tension due to resin flow (RFTL).

A total of twenty-four tension loss experiments were performed using Amoco's Thornel T40 fiber and T40/1908 prepreg materials. The parameters which were varied in the experiments were spool tension, oven heating rate, and the number of composite layers.

Some of the experiments were designed to isolate and measure RFTL by comparing the changes in tension of winds of dry fiber and prepreg material. This method was not successful due to a similarity in prepreg and dry fiber tension loss characteristics.

Low spool tensions were found to result in more tension loss due to resin flow (RFTL). RFTL was also greater for an increased number of layers, but was not affected by oven heating rate.

During winding, significant tension loss occurred, probably due to deformation of the prepreg tow at room temperature.

The change in fiber tension during cure was calculated using an existing cure simulation code (FWCURE) which was modified in this work to include the contribution to fiber tension made by the thermal expansion of the mandrel during cure. The revised code is called FWEXPAND. By adjusting the permeability model in FWEXPAND, the fiber tension during the cure of a single layer wind was accurately calculated. The predicted total RFTL of two multi-layer winds agreed reasonably well with the measured RFTL, but the rate of tension loss was overpredicted. Complete RFTL and full compaction occurred during the first ramp of the cure cycle in all of the experiments.

Acknowledgements

My thanks go out to several people who have contributed in different ways. Foremost, I would like to thank my sweet wife, Tammie, whose encouragment during difficult moments and sensitivity to life in graduate school made it a feasible pursuit.

I also thank Dr. Loos for his helpful advise through the entire project. His assistance was immeasurable. In addition, Dr. Stern was very helpful during our "brainstorming" sessions at critical points in the research. Thank you.

Assembling and maintaining the experimental equipment was greatly facilitated by Danny Reed, Bob Simonds and George Lough. Thank you all.

Finally, I am grateful to Thiokol Corporation who sponsored this research.

Table of Contents

1.0 Introduction 1

1.1 Overview of the Most Common Fabrication Processes 1

1.2 Filament Winding Process 3

1.2.1 General Description of the Filament Winding Process 4

1.2.2 Problems Associated with Fiber Tension Loss 5

1.2.3 Mechanisms of Fiber Tension Loss During Winding and Cure 6

1.3 Objective of This Study 9

2.0 Literature Survey of Modeling Techniques and Experimental Measurements 11

3.0 Numerical Simulation 16

3.1 Simulation of Cure Without Mandrel Expansion Effects (FWCURE) 16

3.2 Addition of Mandrel Expansion Effects to FWCURE (FWEXPAND) 18

4.0 Experimental Methodology, Equipment and General Procedure 30

4.1 Methodology 30

4.2 Equipment 35

4.3 General Procedure 42

5.0 Results 50

5.1 Dry Fiber Winds - Experimental Verification of the Mandrel Expansion Model 50

5.2 Dry Fiber versus Prepreg Winds - Experimental Method of Determining Resin Flow Tension Loss (RFTL) 54

5.3 Repeatability and Parametric Studies of the Experimental Data 65

5.3.1 Repeatability of Tension Loss During Winding 67

5.3.2 Repeatability of Tension Loss During Cure 73

5.3.3 Parametric study of the effect of Spool Tension on RFTL . . . 77

5.3.4 Parametric Study of the Effect of Oven Ramp Rate on RFTL 79

5.3.5 Parametric Study of the Effect of the Number of Layers on RFTL 81

5.4 Comparison of Measured and Calculated Mandrel Strain and Pressure 84

5.4.1 Single Layer Winds 84

5.4.2 Multi-layer Winds 95

6.0 Summary, Conclusions, and Future Research 109

6.1 Summary and Conclusions 109

6.2 Future Research 112

Bibliography 114

Appendix A: Calculation of Fiber Tension from Mandrel Hoop Strain 116

Appendix B: Permeability Models 119

Appendix C: Experimental Data 123

VITA 125

List of Figures

Figure 1. Mechanisms of Fiber Tension Loss During Winding and Cure 7
Figure 2. Computation flowchart of the cure submodel in FWCURE 17
Figure 3. Computation flowchart of the Tension Loss Submodel in FWCURE 19
Figure 4. Concentric cylinders used to model the thermal stresses and strains in the mandrel and composite layers 21
Figure 5. Free body diagram of the mandrel and one layer of composite 25
Figure 6. Viscosity profile for a typicl hot-melt resin system. 32
Figure 7. Tension measurement / delivery eye used to place prepreg rovings on the mandrel (by Kent Call) [10]. 37
Figure 8. Aluminum mandrel instrumented with strain gages and thermocouples 38
Figure 9. Equipment used to acquire strain and temperature data 40
Figure 10. Measured strain, apparent strain and actual strain for a typical experiment (Wind 28 - dry T40 fiber) 47
Figure 11. Manufacturer-specified apparent strain and measured apparent strain for M&M CEA-13-250UW-120 strain gages mounted on aluminum 48
Figure 12. Mandrel strain for a single, continuous layer of dry T40 fiber (Wind 28) - verification of the mandrel expansion model 51
Figure 13. Typical cure cycle used in this study (Wind 14a) 57
Figure 14. Mandrel strains for single layer dry fiber versus prepreg winds (2.5 lb spool tension, Wind 16/17) 58
Figure 15. Mandrel strain for single layer dry fiber versus prepreg winds (5.0 lb spool tension, Wind 15/14a) 59

Figure 16. Mandrel strain for single layer dry fiber versus prepreg winds (8.0 lb spool tension, Wind 18/19) 60
Figure 17. Mandrel strain for 2 layers of dry fiber versus prepreg winds (5.0 lb spool tension, Wind 20/21) 61
Figure 18. Mandrel strain for 3 layers of dry fiber versus prepreg winds (5.0 lb spool tension, Wind 22/23) 62
Figure 19. Mandrel strain for 3 layers of dry fiber versus prepreg winds (5.0 lb spool tension, Wind 12/13) 63
Figure 20. Variation of mandrel strain during the winding of dry T40 fiber . . . 71
Figure 21. Variation of mandrel strain during the winding of T40/1908 prepreg 72
Figure 22. Repeatability of mandrel strain for single layer winds of T40/1908 prepreg (5.0 lb spool tension, 1.0 °C/min. ramp rate) 74
Figure 23. Repeatability of mandrel strain for single layer winds of T40/1908 prepreg (8.0 lb spool tension, 0.5 °C/min. ramp rate) 75
Figure 24. Effect of spool tension on mandrel strain for single layer winds of T40/1908 prepreg (2.5, 5.0 and 8.0 lb spool tensions) 78
Figure 25. Effect of oven ramp rate on mandrel strain for single layer winds of T40/1908 prepreg (0.2, 0.5, 1.0, and 2.0 °C/min. ramp rates) . . . 80
Figure 26. Effect of the number of layers on mandrel strain for 1, 2, 3, and 5-layer winds of T40/1908 prepreg (5.0 lb spool tension, 1.0 °C/min. ramp rate) 83
Figure 27. Porosity-permeability characteristics of four permeability models by Tzeng, Cai and Gutowski, and two models by Lundström 86
Figure 28. Measured and calculated mandrel strains for a single layer of T40/1908 prepreg (5.0 lb spool tension, Wind 14a) 87
Figure 29. Measured and calculated mandrel pressure and resin viscosity for a single layer wind of T40/1908 prepreg (5.0 lb spool tension,

Wind 14a) 88
Figure 30. Micrographs of a single tow of uncured and cured T40/1908 prepreg 90
Figure 31. Measured and calculated mandrel strains for a single layer of T40/1908 prepreg (2.5 lb spool tension, Wind 17) 92
Figure 32. Measured and calculated mandrel strains for a single layer of T40/1908 prepreg (8.1 lb spool tension, Wind 19) 93
Figure 33. Effect of increased initial resin volume fraction on simulated mandrel strain (2.5 lb spool tension, Wind 17) 94
Figure 34. Measured and calculated mandrel pressures for a 2-layer wind of T40/1908 prepreg during the first ramp of the heatup (Wind 21) . . . 96
Figure 35. Effect of using full winding tension on mandrel pressure for a 2-layer simulation (Wind 21) 98
Figure 36. Measured and calculated mandrel pressures for a 2-layer wind of T40/1908 prepreg during the full heatup period (Wind 21) 99
Figure 37. Measured and calculated mandrel pressures for a 3-layer wind of T40/1908 prepreg during the first ramp of the heatup (Wind 23) . . 100
Figure 38. Measured and calculated mandrel pressures for a 3-layer wind of T40/1908 prepreg during the full heatup period (Wind 23) 101
Figure 39. Calculated fiber tension in a 3-layer wind of T40/1908 prepreg (Wind 23) 103
Figure 40. Effect of changing the distribution of initial tension in each layer on mandrel pressure for a 3-layer wind of T40/1908 prepreg (Wind 23) 104
Figure 41. Effect of permeability on calculated mandrel pressure for a 3-layer wind of T40/1908 prepreg (Wind 23) 106
Figure 42. Effect of the maximum fiber volume fraction, V_{fmax}, on calculated mandrel pressure for a 3-layer wind of T40/1908 prepreg (Wind

23) 107
Figure 43. Free body diagram of the mandrel and one layer of composite . . . 117

List of Tables

Table 1. Typical cure cycle used for full-scale filament wound cases at Thiokol Corporation, and a typical cycle used for the cases wound in this study 44

Table 2. Material properties used to simulate the thermally-induced mandrel strain resulting from a single, continuous layer of dry T40 fiber . . . 52

Table 3. Winding parameters used in the six pairs of dry fiber-prepreg experiments 55

Table 4. Experiments performed using T40/1908 prepreg material 66

Table 5. T40/1908 prepreg winds used in the Stress Retention Factor (SRF) repeatability study 68

Table 6. Dry T40 fiber winds used in the Stress Retention Factor (SRF) repeatability study 69

Table 7. T40/1908 prepreg winds used to study the repeatability of tension loss during cure 76

Table 8. T40/1908 prepreg winds used to study the effect of spool tension on experimentally measured RFTL 77

Table 9. T40/1908 prepreg winds used to study the effect of oven ramp rate on experimentally measured RFTL 81

Table 10. T40/1908 winds used to study the effect of the number of layers on experimentally measured RFTL 82

Table 11. Winds simulated using FWEXPAND 84

1.0 Introduction

1.1 Overview of the Most Common Fabrication Processes

The use of composite materials has grown steadily over the past thirty years. There are several methods used to fabricate parts using thermoset composite materials. The two general classes of fabrication processes are closed-mold and open-mold processes.

Examples of closed-mold processes are compression (matched-die) molding, injection molding, and resin transfer molding (RTM). Closed-molds are two-piece male and female molds, usually made from metal. The primary characteristics of a molded object are a controlled surface finish on both sides and dimensional repeatability from part to part.

Compression molding is used in large scale production of parts requiring high dimensional accuracy. In this process, a wet or prepreg (fiber is pre-impregnated with resin and partially cured in a separate manufacturing step) lay-up is placed on one of the matched dies, which are heated, and the other die is pressed against it, applying heat and mechanical pressure to the lay-up. This causes consolidation (the removal of excess resin to achieve optimal fiber/resin content) and cure of the part.

Injection molding also utilizes a male and female mold, but continuous fiber reinforcement material is not present. Instead, only the resin, and perhaps a filler, is used. The heated resin is forced by a ram or screw into a cooled mold. The part is then ejected from the mold. This process is used extensively in the toy, automotive, and appliance industries where a very high number of parts are produced.

Resin transfer molding involves the low pressure injection of resin into a low cost mold which tightly encloses a fiber preform. A preform is a three-dimensional, finished-shape textile object constructed from knit, braided, or woven fiber. The injected resin infiltrates the fiber preform, displacing the air ahead of it. After the resin has saturated the entire preform, the part is cured and removed from the mold. The primary advantages of this technique are 1) enhanced through-the-thickness strength due to the 3-D weave or stitching in the preform, 2) the use of high-speed, automated textile technology to reduce cost, and 3) the finished-shape preforms reduce the bonding and fastening requirements of sub-parts.

The open-mold processes include vacuum-bag and autoclave molding, pultrusion and pulforming, and filament winding. In the vacuum-bag and autoclave molding processes, the fiber/resin system is first laid up by hand or by an automated method such as a tape lay-up machine. In both processes, the part is sealed in a vacuum atmosphere to draw out any trapped air or volatile gasses released by the resin during cure, which would create voids and reduce the part's strength. The bagging assembly includes four layers of material adjacent to the composite part: 1) a porous, non-sticking teflon layer to allow excess resin to leave the part, 2) a layer of bleeder material to absorb the excess resin released during consolidation, 3) a non-porous teflon layer to contain the resin in the bleeder, and 4) the vacuum bag as the outermost layer to contain the vacuum. After the part is laid up and bagged, it must be cured and consolidated. This is where the two methods differ. In vacuum-bag processing, the part is exposed only to elevated temperature in an oven, but in autoclave molding, the part is exposed to elevated temperature and pressure to assist in the consolidation process. Though these methods are labor-intensive and expensive, they do produce parts which have low void content and good consolidation, resulting in good mechanical properties.

Pultrusion and pulforming are continuous, high volume processing techniques in which continuous lengths of resin-impregnated fiber are pulled through one or more forming dies to impart the desired cross-section and resin content to the material. The material is next cured by heat from a tunnel oven, heated dies, or by an energy source of microwave or radio frequency. The difference between pultrusion and pulforming is that pultrusion can only generate straight, constant-shape, constant-volume parts; whereas by using a series of dies, pulforming can be used to make curved parts which have changing shape and volume. This is necessary for parts such as automotive leaf springs and stiffening ribs for cylindrical pressure vessels. The advantages of both processes are rapid production rates and reduced material scrappage, resulting in reduced cost. However, the main disadvantage is that only unidirectional fiber orientation is possible.

1.2 Filament Winding Process

Filament winding has been used by the aerospace industry and in other commercial markets for many years. Winding done in the aerospace industry is highly specialized, geared to superior performance (primarily due to high specific strength properties), but at a premium price. The commercial sector, however, stresses lower production costs while taking advantage of other composite material properties such as high corrosion resistance and electrical resistivity. In general, filament winding is economical because it is a fully automated, high-speed, continuous process, and is suitable for fabricating large parts. However oven curing, as opposed to autoclave curing, is typically used, consolidation is poor, void content is high, and mechanical properties are diminished.

1.2.1 General Description of the Filament Winding Process

The filament winding process consists of wrapping rovings of continuous fiber (2000-12000 fiber filaments per roving) over a mandrel in an orientation tailored to carry the applied service loads. One way to categorize the types of filament winding is according to the state of the resin when the part is wound. In wet winding the fiber is saturated with low viscosity, uncured resin just before being wound onto the mandrel. In dry winding, the fiber roving is a prepreg material which is composed of the fiber and partially cured resin. In either case, the fiber roving spacing and orientation are subject to close control by the winding machine, and many layers of composite are wound onto the mandrel until sufficient thickness is built up. The process is completed by curing the part and removing it from the mandrel.

Another categorization of the filament winding process applies to the winding pattern and the machines necessary to accomplish each pattern. The two main categories are hoop (circumferential) winding and helical (longitudinal) winding. In hoop winding, the rovings of fiber are wound nearly perpendicular to the mandrel axis, i.e., in the mandrel circumferential direction. Each path around the mandrel is called a circuit. To lay down a continuous layer of material, the fiber delivery system must advance one bandwidth (the width of one roving) along the mandrel axis for every rotation of the mandrel. This results in a series of adjacent circuits. This simple pattern can be wound using a lathe-type machine, but the resulting parts are limited to cylinders or shells which have no integral end enclosures and have low axial strength.

In helical winding, the fiber rovings are placed in a more-nearly axial direction on the mandrel. The winding angle, defined as the angle between the fiber direction and the mandrel axis, is fixed such that in a typical 10-circuit pattern, the fiber path advances one tenth of the part circumference plus one tenth of the bandwidth per circuit. A helical winding machine can produce parts which have integral end enclosures and significant axial strength, making this the necessary winding machine for producing pressure vessels.

In all winding processes, the fiber is wound under tension to make the rovings lie in straight, collimated paths within the composite case. However, during the winding and cure stages of fabrication, the fiber tension can change significantly, resulting in several potential problems.

1.2.2 Problems Associated with Fiber Tension Loss

The distribution of fiber tension in a filament wound part is very important. In addition to maintaining control of fiber position, fiber tension provides the pressure needed for compaction of the part. If the tension is too low, the compaction pressure imposed by one layer on the layers under it will be too low, resulting in resin rich areas between the layers of fiber. These areas are inherently weaker than areas of the material which have an optimal proportion of fiber and resin. This resin rich area is susceptible to delamination and matrix cracking when service loads are imposed. This adverse effect may not reveal itself until the part fails during testing or service.

In addition to the potential for delamination, if the fiber tension drops to zero, the normal (radial) force between the layers of composite vanishes, and the friction force holding the rovings in their as-wound positions disappears. The rovings would then be free to slide, buckle, and bunch up, resulting in unevenly distributed fibers which do not lie in parallel paths. When the resin cures and locks the fiber in this position, the composite case will experience strength degradation.

Just as low fiber tension can cause problems, so can excessively high tension. Differences in thermal expansion between the mandrel and composite during the cure stage can produce high levels of tension in the fiber. If the resin gels while the fiber is in this state, the fiber tension is "locked in" as a residual stress. This also reduces the part's load-carrying capability, which is the burst strength for pressure vessels.

1.2.3 Mechanisms of Fiber Tension Loss During Winding and Cure

The level of fiber tension during the fabrication of a filament-wound part varies with position within the part and with the stage of fabrication. Figure 1 illustrates the

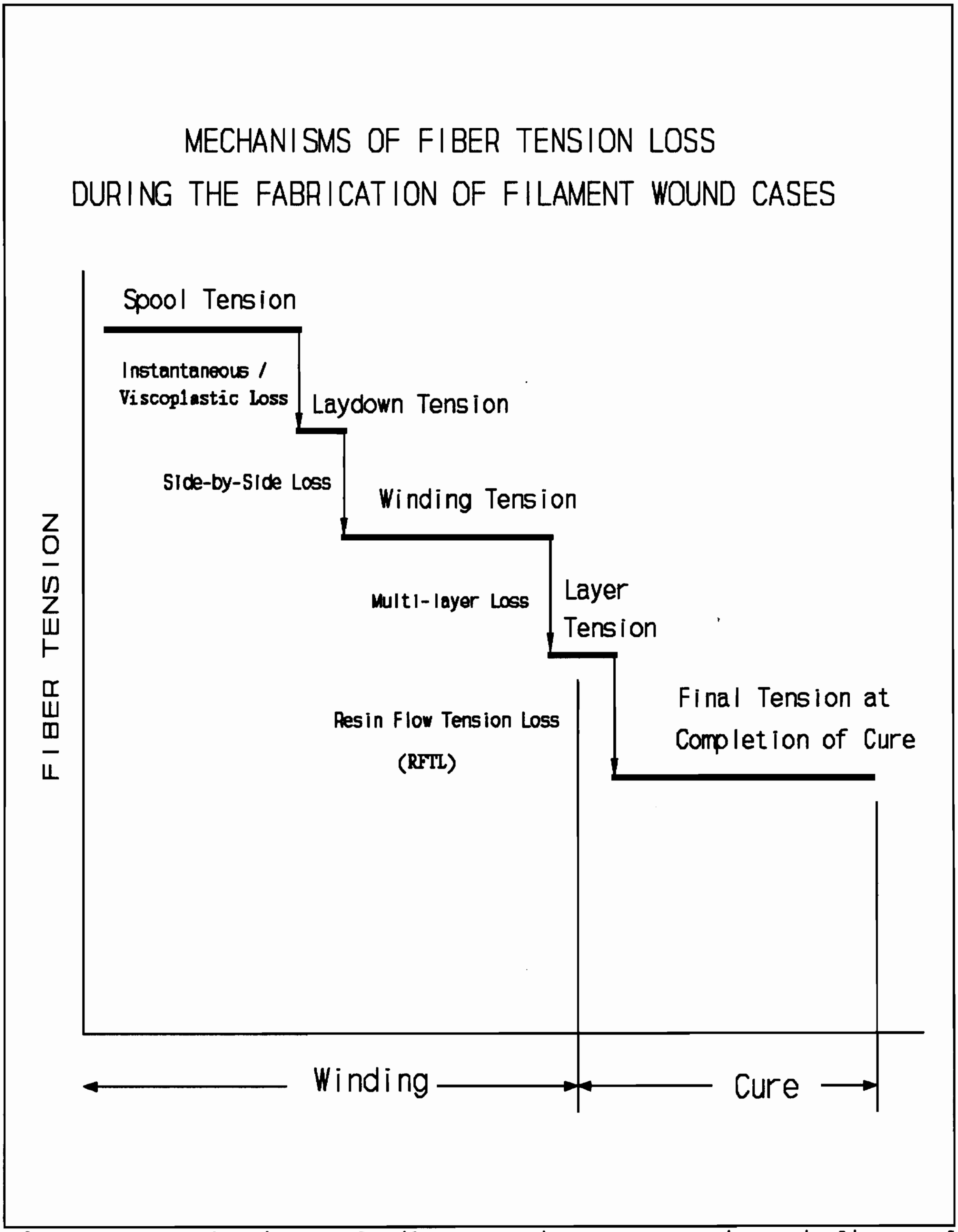

Figure 1. Mechanisms of Fiber Tension Loss During Winding and Cure

mechanisms which can cause a change in tension during the fabrication process, which is composed of the winding and cure stages.

During the winding stage, the fiber has spool tension just prior to being wrapped around the mandrel/composite assembly. For wet winding, the round fiber tow flattens as it lays down on the mandrel, causing an instantaneous tension loss, which results in the laydown tension. This loss is somewhat reduced, and occurs more slowly with prepreg winding because the prepreg roving is contained in a viscoplastic resin. As each circuit within a layer is laid down, it compresses the assembly over an area which extends beyond its bandwidth, causing previous circuits to reside on a smaller radius. This is called side-by-side tension loss, which results in the winding tension. Most composite cases consist of many layers, built up with layer upon layer. Multi-layer tension loss occurs when the layer currently being wound further compresses the mandrel and the previously-wound composite layers, causing all layers to reside on a smaller radius. These three modes of tension loss all occur during the winding stage of fabrication. After the case has been completely wound, and three of the four mechanisms of tension loss have occurred (instantaneous, side-by-side, and multi-layer), the fiber is in a state of tension called layer tension.

In the cure stage, the assembly is placed in an oven to accomplish consolidation (removal of excess resin) and full cure of the resin. During cure, the assembly is heated to a temperature sufficient to cause the resin viscosity to decrease enough to allow fiber compaction and void expulsion, but not so high as to cause the resin to cure before consolidation occurs. When the resin viscosity is low enough, the fibers tend to move inward to a smaller radius due to the inward radial component of the fiber tension. This fiber movement displaces the resin, which must simultaneously flow outward through the fiber network. This fiber movement results in the fourth mechanism of tension loss, called resin flow tension loss (**RFTL**), which continues until either 1) the radial component of the fiber tension decreases enough to equal the viscous drag forces imposed by the resin, or 2) the resin gels, locking the fiber at its final position and tension.

Not shown in Figure 1, yet a significant contributor to an increase in fiber tension, is the thermal expansion of the mandrel/composite assembly during cure. The coefficient of thermal expansion of the metallic mandrel is generally higher than that of the fiber. This introduces thermal stresses in both materials, with the mandrel going into compression and the fiber experiencing tension. The timing of resin cure relative to the assembly's state of thermal dilatation dictates the degree to which this thermally-induced fiber tension becomes residual stress in the composite.

1.3 Objective of This Study

The overall objective of this research is to investigate the fiber tension loss during the fabrication of a filament-wound composite case constructed with Thornel T-40/ERL-1908 prepreg material, manufactured by Amoco Performance Products. The following items are specific goals within this general objective:

1) To experimentally quantify the viscoplastic/side-by-side and resin flow

mechanisms of tension loss

2) To develop a mandrel expansion model for inclusion in the cure simulation code (FWCURE) in order to compare experimental and simulation data

3) To modify the permeability model in FWCURE so the rate and degree of simulated tension loss during cure concurs with the experimental data

Prior to discussing the work toward these objectives, Section 2.0 provides a literature review of some of the simulation techniques and experimental work already done in the area of filament winding. Section 3.0 describes the general logic of the cure simulation code (FWCURE), and the theory behind the mandrel expansion model added to it (FWEXPAND). Section 4.0 describes the experimental methodology, equipment and procedures used, followed by Section 5.0 which provides the experimental and simulation results.

2.0 Literature Survey of Modeling Techniques and Experimental Measurements

Within the last decade, there have been several significant efforts to model the filament winding process in order to reduce manufacturing costs and improve performance. Without a simulation capability, a manufacturer will either 1) spend a significant amount of money to produce a limited number of trial parts, or 2) not attempt to optimize the process. Therefore, several investigators have modeled the physics of the filament winding process, and have also performed experimental work to validate and/or improve the performance of the models.

Spencer [1] developed an analytical model for predicting the residual stress state, resin cure state, and layer locations in multi-layer cylinders using spool tension, mandrel type, resin viscosity, and cure cycle as the process parameters. The model utilizes submodels for stress analysis, cure kinetics, resin flow, and heat transfer. To verify the model, four cylinders were wound and cured. The final layer locations were determined by sectioning the cylinders and examining the cross-sections using photomicrographs. The average residual hoop stress in the cylinders was measured by cutting sample rings from the cylinders. Strain gages mounted on the rings in the hoop direction provided strain data necessary for determination of the average residual hoop stress in the cylinder.

Cai and Gutowski [2] developed a process model for the winding of cylindrical shells, with a focus on the consolidation process. This model addresses two different cases. The first case applies to wet winding, where the resin viscosity is low and the fluid flow is nearly completed during the winding operation. Here, the material deformation after winding is determined almost solely by the transverse fiber deformation behavior. The second case addresses prepreg winding, where the resin is semi-solid, and the main flow process occurs during cure. The stresses and deformations due to winding are determined by treating the prepreg material as a linear elastic solid material. This stress information is then used as an input to the consolidation model.

The experimental program conducted by Cai and Gutowski addressed these two cases. In both sets of experiments, constant viscosity silicone fluids were used in place of polymeric resin. Wet winding was represented using low viscosity fluid and fiber rovings having a small cross-section, and dry winding was represented using a high viscosity fluid and rovings having large cross-sections. The primary experimental parameters were the total pressure and fluid pressure at the mandrel/layer interface. These pressures were measured using force sensor resistors and pressure transducers, respectively. Pressure build-up was monitored because it provided insight into the time-dependent resin flow and consolidation which occurred during the winding and cure processes.

Springer, Calius, and co-workers [3,4,5,6,7] developed a one-dimensional model which relates spool tension, winding speed, and cure cycle to the thermal, chemical, and mechanical behavior of an open-ended cylinder during fabrication. This model, which was later made two-dimensional, consists of five submodels which generate 1) temperature, cure kinetics, and viscosity changes; 2) resin flow and fiber motion; 3) stress and strain; 4) void determination; and 5) strength estimates. Experimental studies [4] were performed to validate this model. Temperature and strain were measured at various locations in the mandrel and composite material, and good agreement was found between the data and the model predictions.

Based in part on the work of Springer et al, Tzeng [8] developed a computer code called FWCURE which simulates fiber motion during the cure stage of fabrication. It is an improvement of the original one-dimensional model of Calius and Springer [6,7] in that it performs a two-dimensional analysis, and can therefore be used to study composite cases which have end enclosures. In addition, anisotropic resin flow and the variation of permeability due to fiber motion and consolidation are considered. Validation experiments were performed wherein the temperatures throughout a vessel having end enclosures were measured. Excellent agreement was found between this data and the model's predictions.

Nguyen [9] developed WACSAFE, a stress analysis code to be used in conjunction with FWCURE. The code simulates the stresses and strains developed in the mandrel and case during winding and cure. In this model, an initial fiber stress (the winding tension) interacts structurally with the mandrel, and also with the composite sub-layers as the winding process proceeds. The stress distribution throughout the mandrel/case assembly is determined using a procedure which involves turning "on" element stiffnesses and nodal loads in an incremental fashion to reflect the winding process. When WACSAFE is coupled with FWCURE, the entire fabrication process is simulated.

In an effort to verify the performance of FWCURE and WACSAFE, Call [10] performed two sets of experiments using the wet winding process. One set was performed to determine the value of an empirical constant in the permeability model of FWCURE, and the other set was performed to determine the degree of instantaneous tension loss which occurs during winding, as discussed in Section 1.0. This type of tension loss in not modeled by WACSAFE, and must therefore be determined empirically.

The permeability-related experiments provided a basis for "backing out" the value of a constant in the permeability-porosity equation. This constant directly affects the rate of fiber tension loss, which occurs when the resin viscosity is sufficiently low. A low viscosity resin system and three different types of fiber rovings were used in the study, and a comparison of the experimental and analytical tension loss showed good agreement for two out of three types of fiber. Only the low filament-count rovings showed poor agreement.

The instantaneous tension loss study was performed using a combination of experimental data and analytical modeling. It was found that the instantaneous tension loss is a function of the type of fiber/resin system, the spool tension, and even of the type of mandrel (stiffness) used. Therefore, since excessive experiments would be needed to cover all the possible winding situations, an instantaneous tension loss model is needed.

Knight [11] performed a separate experimental study for the purpose of 1) verifying the accuracy of WACSAFE-generated residual stresses following winding, and 2) correlating residual stress with the case burst strength. In the experiments, the hoop strain in the cylindrical mandrels was measured for comparison with the analytical results. The model was found to accurately predict the mandrel strain produced during winding, meaning the average residual stress was also well predicted. The case burst strength was found to decrease significantly if the average layer tension, or average residual stress, dropped below zero. However, the strength was relatively constant for all positive values of average residual stress.

The work presented in this investigation is similar in focus to the work done by Call [10] in that fiber tension loss is studied. However, rather than studying tension loss during the wet winding process, the tension loss during the fabrication of a prepreg-wound case is examined. Prepreg material is composed of fiber rovings which have been pre-impregnated with resin and then partially cured.

3.0 Numerical Simulation

3.1 Simulation of Cure Without Mandrel Expansion Effects (FWCURE)

The numerical simulation performed in this study is based on the FWCURE model developed by Tzeng [8]. A complete explanation of the analytical basis for this code, as well as its numerical implementation, is given in Tzeng [8]. However, a general explanation of the function of FWCURE is provided here to help the reader understand the modifications to the code in the present investigation.

FWCURE is composed of two separate submodels. The first is the cure model which calculates the temperature distribution in the filament wound assembly, and the resin degree of cure and viscosity in the composite case during cure. The second submodel is the layer tension loss model which calculates resin flow, fiber displacement, fiber tension variation, and fiber/resin distribution for each layer of the composite case during cure.

A computation flow chart for the cure model is shown in Figure 2. This model is composed of three submodels: a heat transfer model, a kinetics model, and a viscosity model. After receiving the geometry, material properties, initial conditions, and boundary conditions for the problem, the heat transfer model calculates the temperature throughout the assembly using the heat generation calculated in the kinetics model as an internal heat source. Integration of the cure rate calculated in the kinetics model gives the degree of cure, which is used in the viscosity model, together with the calculated temperatures, to determine the resin viscosity. The temperature and resin viscosity are then used in the

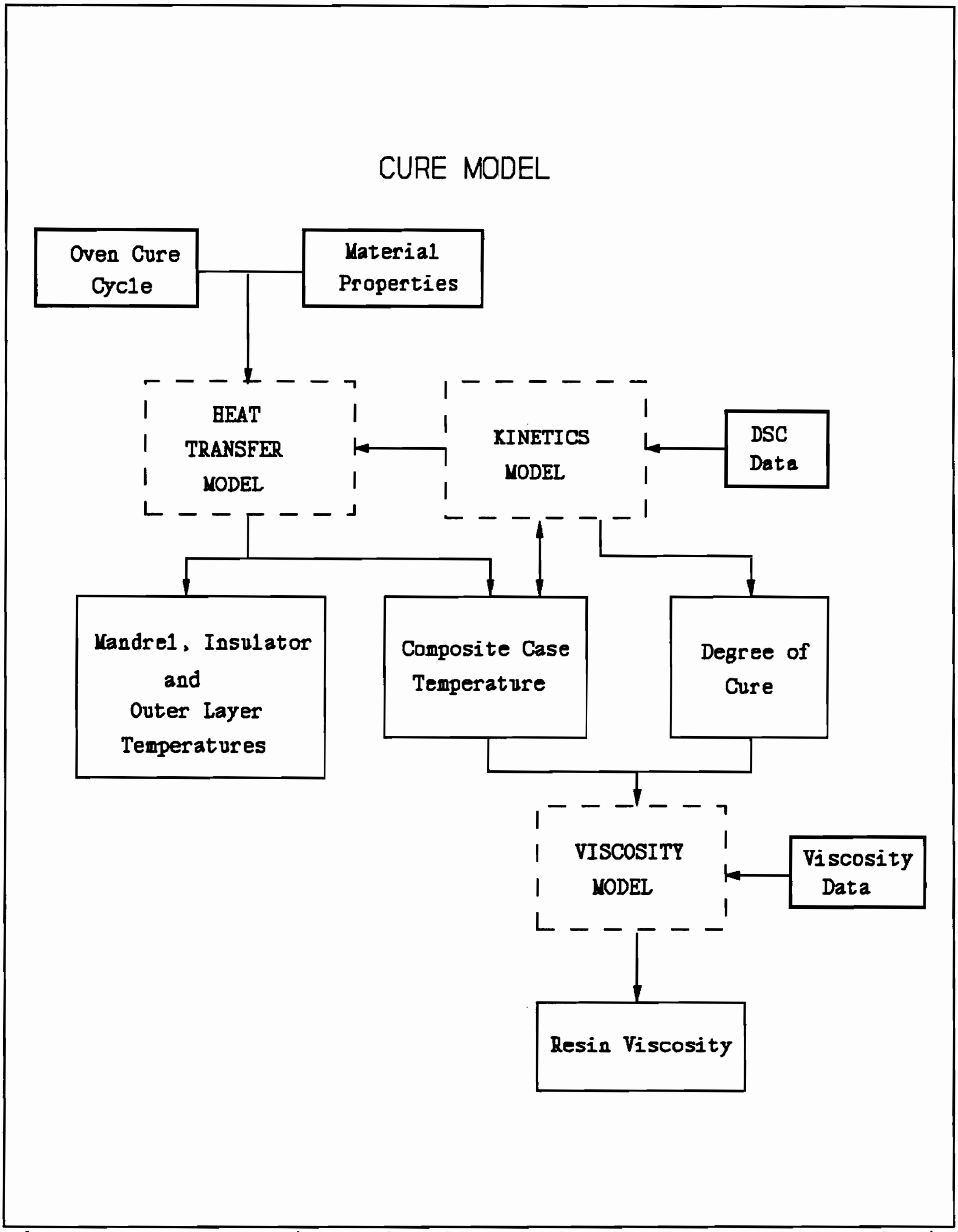

Figure 2. Computation flowchart of the cure submodel in FWCURE

calculation of resin flow and fiber motion in the layer tension loss model.

The calculations performed in the layer tension loss model are represented in Figure 3. The resin pressure field is calculated from the fiber tension and element curvature. The permeability of the fiber tow is calculated in the permeability model using the resin volume fraction. Once the pressure field, permeability, and resin viscosity are known, the resin flow rate and displacement are calculated in the flow model. The fiber movement in the inward radial direction is taken to be equal to the outward resin displacement. New element curvatures are calculated based on the fiber movement from which an updated fiber tension is obtained.

In FWCURE, the fiber tension is affected by thermal effects in the assembly only in that the thermal strain of the fiber is considered. The dimensions of the mandrel are assumed to be unaffected by changes in temperature. This aspect of the problem has been addressed by adding a simple mandrel deformation model to FWCURE.

3.2 Addition of Mandrel Expansion Effects to FWCURE (FWEXPAND)

The addition of the effects of mandrel expansion to FWCURE requires the calculation of the thermally-induced fiber stress. This stress is the result of a difference in the coefficients of thermal expansion of the mandrel and composite material. Once this component of fiber stress is known, it can be added to the reduction of stress (tension loss) due to resin flow, which is already calculated by FWCURE. The revised code, called FWEXPAND, performs this combining of stress effects.

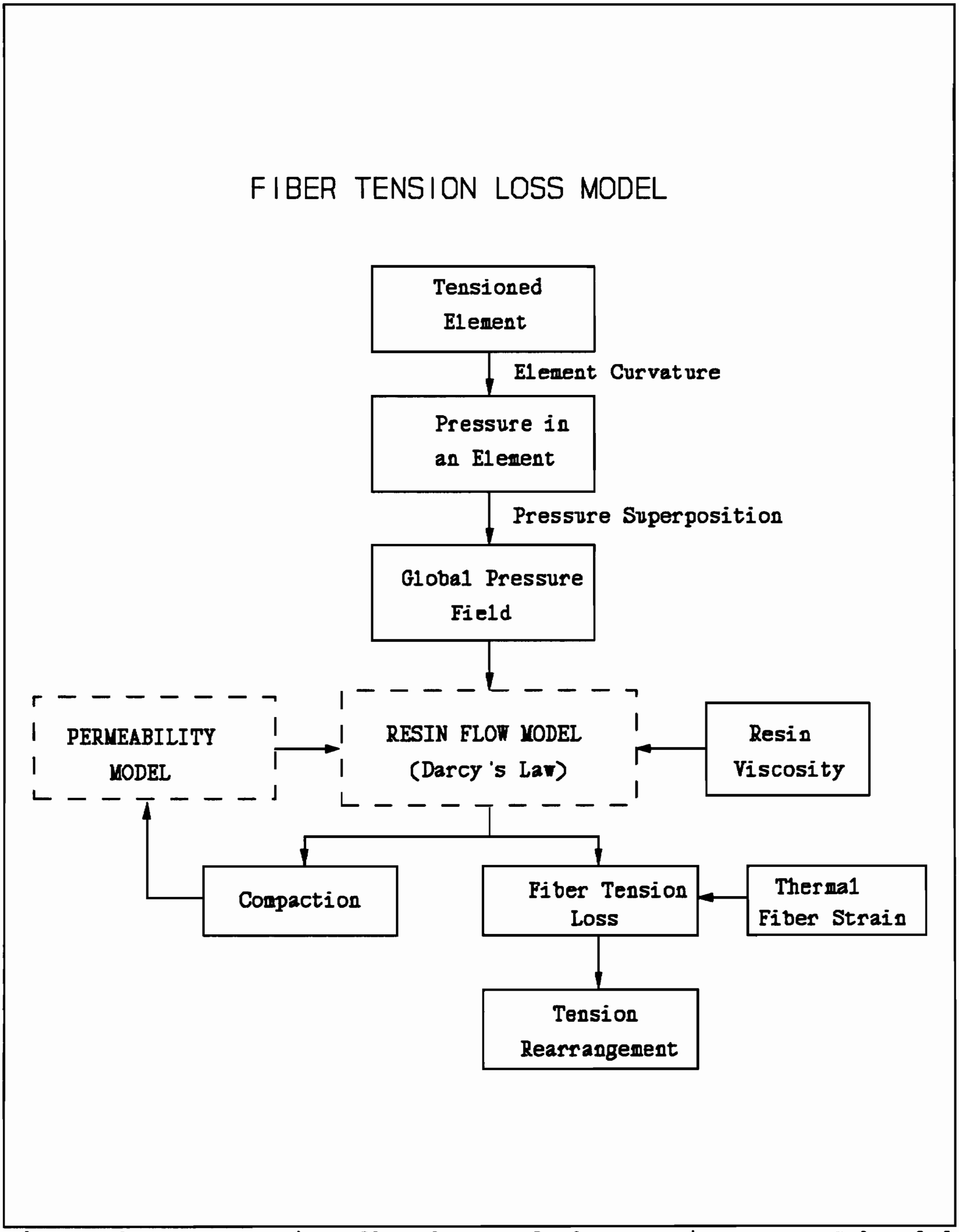

Figure 3. Computation flowchart of the Tension Loss Submodel in FWCURE

The analysis used to calculate the thermally-induced fiber stress was derived by Faupel [12]. In this analysis, the cylindrical, wound assembly is viewed in cross-section as a set of concentric rings, with the innermost ring being the mandrel and the outer rings being 'K' layers of composite material. Figure 4 illustrates this configuration, which also represents the geometry of the experimental work. Each layer in the assembly has a stiffness, a temperature change, a coefficient of thermal expansion, and a thickness.

The total strain of the wound assembly can be derived by considering the thermal response of the mandrel to an increase in temperature of the wound assembly. The response is the sum of two additive effects. The first effect is the free expansion of the mandrel. In this case, the thermal strain of the mandrel would be

$$\epsilon_{free} = \alpha_m \, \Delta T_m \tag{3.1}$$

where α_m is the mandrel coefficient of thermal expansion, and ΔT_m is the change in temperature at the center of the mandrel.

The second effect is where the mandrel experiences an increase in temperature, but is surrounded by a rigid body (the composite case) which totally constrains it from expanding. In this case, the mandrel would experience a thermally-induced stress which results in a mechanical strain of:

$$\epsilon_{constrained} = \frac{\sigma_h}{E_m} - \nu_m \frac{\sigma_z}{E_m} \tag{3.2}$$

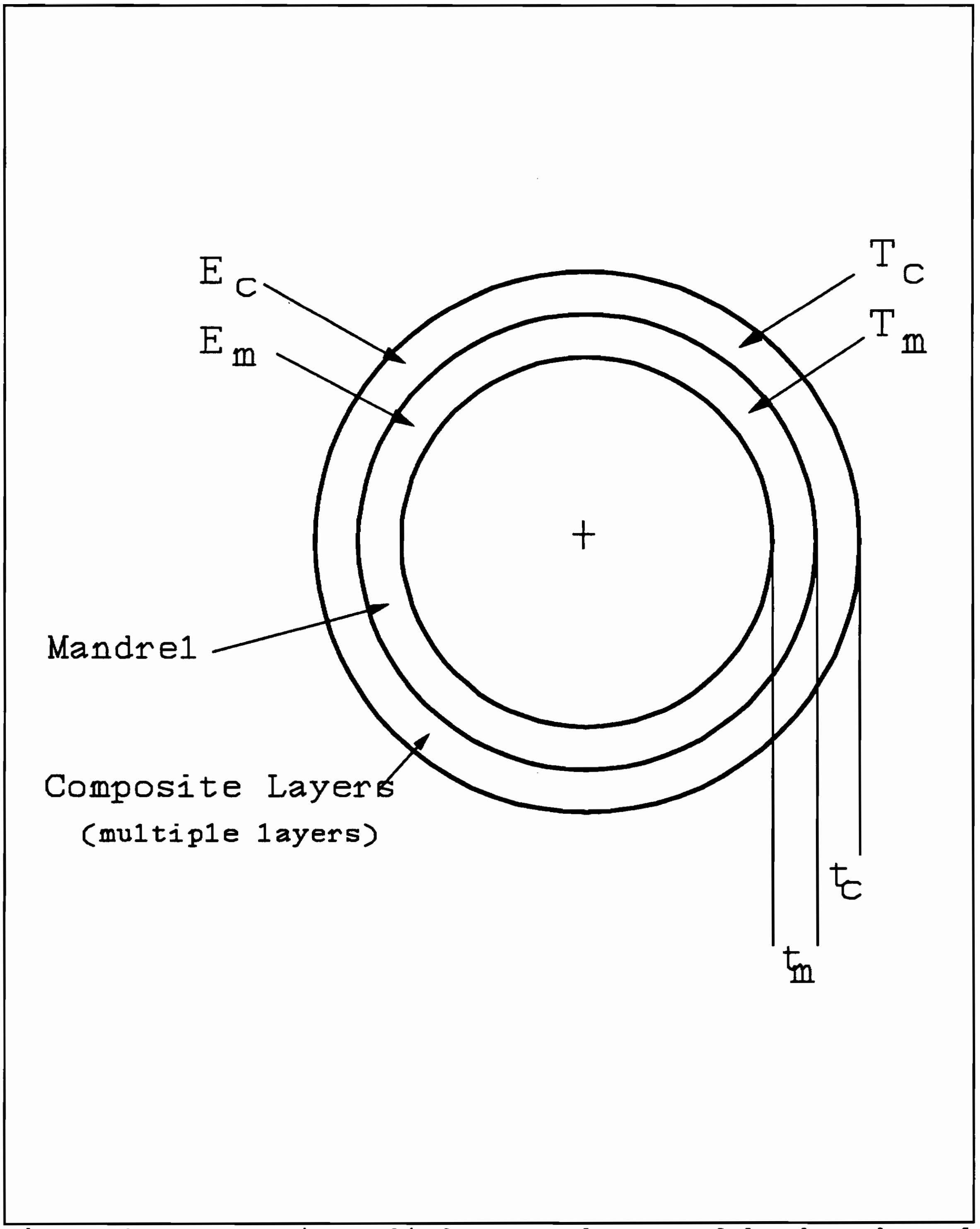

Figure 4. Concentric cylinders used to model the thermal stresses and strains in the mandrel and composite layers

where σ_h is the thermally-induced hoop stress in the mandrel, σ_z is the thermally-induced axial stress in the mandrel, E_m is the mandrel modulus of elasticity, and ν_m is Poisson ratio for the mandrel. Since the cylindrical, wound assembly is not constrained in the axial direction, the stress in the axial direction, σ_z, is zero, and Equation 3.2 reduces to

$$\epsilon_{constrained} = \frac{\sigma_h}{E_m} \tag{3.3}$$

Therefore, the total strain of the mandrel is the sum of the free thermal strain and the mechanical strain.

$$\begin{aligned} \epsilon_m &= \epsilon_{free} + \epsilon_{constrained} \\ &= \alpha_m \Delta T_m + \frac{\sigma_{h_m}}{E_m} \end{aligned} \tag{3.4}$$

The assembly expands as a unit because of the interface pressure which exists between the layers. Therefore, the total strain of the mandrel and every composite layer are equal. This assumes that the thickness-to-diameter ratio of the wound assembly is small enough that the strain can be taken to be constant through the thickness of the assembly. In this case, the total strain of the assembly, including the mandrel and all composite layers, is given by the general expression:

$$\begin{aligned} \epsilon_{assembly} &= \epsilon_{free} + \epsilon_{constrained} \\ &= \alpha \Delta T + \frac{\sigma_h}{E} \end{aligned} \qquad (3.5)$$

Therefore, from Equation 3.5, the average hoop stress in the mandrel and composite layers are

$$\begin{aligned} (\sigma_h)_m &= E_m(\epsilon_{assembly} - \alpha_m \Delta T_m) \\ (\sigma_h)_{c_n} &= E_{c_n}(\epsilon_{assembly} - \alpha_{c_n} \Delta T_{c_n}) \quad , n=1,K \end{aligned} \qquad (3.6)$$

where $\varepsilon_{assembly}$ is the strain of the entire assembly, E_m is the modulus of elasticity of the mandrel, E_{cn} is the modulus of elasticity of the n^{th} composite layer in the hoop direction, α_m and α_{cn} are the coefficients of thermal expansion of the mandrel and n^{th} composite layer in the hoop direction, ΔT_m and ΔT_{cn} are the change in temperature at the middle of the mandrel and n^{th} composite layer, and K is the number of composite layers.

From the equilibrium of forces in the hoop direction, an expression for the strain of the assembly, $\varepsilon_{assembly}$, can be developed. Consider the case where there is only one composite layer, as shown in Figure 5. The total force in the mandrel must equal the total force in the composite layer.

$$\begin{aligned} \Sigma F_h &= 0 \\ F_m + F_c &= 0 \end{aligned} \tag{3.7}$$

The forces in the mandrel and composite layer are equal to the product of the hoop stress and the cross-sectional areas of each layer as follows:

$$\begin{aligned} F_m &= (\sigma_h)_m \, A_m \\ F_c &= (\sigma_h)_c \, A_c \end{aligned} \tag{3.8}$$

The areas A_m and A_c are equal to the product of the cylinder thicknesses (t_m and t_c) and an arbitrary axial length, chosen to be unity. Therefore, $A_m=t_m$ and $A_c=t_c$. The thickness of each composite layer, t_c, is reduced by a factor equal to the fiber volume fraction of the composite material. The reduced layer thickness is called the equivalent fiber layer thickness, t_f. Combining Equations 3.6, 3.7 and 3.8 results in an expression for the thermal strain of the assembly:

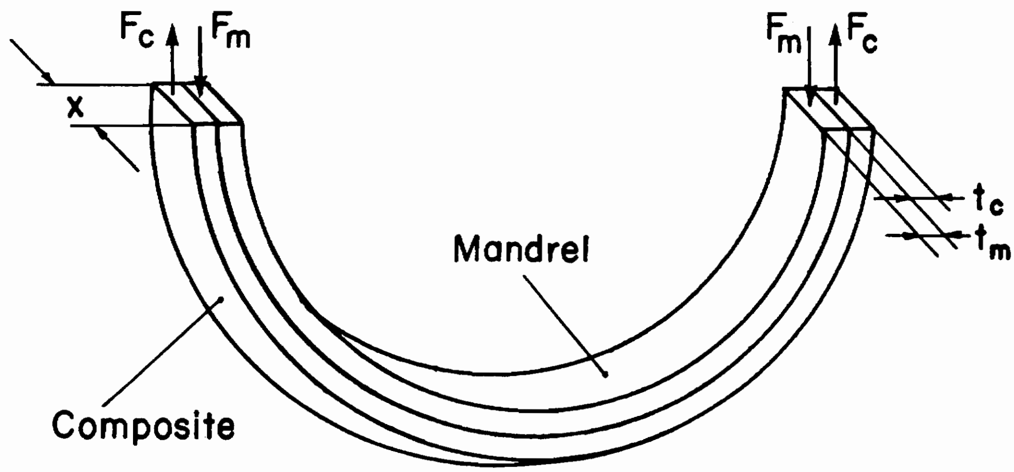

Figure 5. Free body diagram of the mandrel and one layer of composite

$$\epsilon_{assembly} = \frac{t_m E_m \alpha_m \Delta T_m + t_f E_f \alpha_f \Delta T_c}{t_m E_m + t_f E_f} \qquad (3.9)$$

Since the composite layer thickness has been reduced to the equivalent fiber layer thickness, the elastic modulus and coefficient of thermal expansion of the fiber (E_f and α_f) have been used for the composite properties in Equation 3.9. For 'n' composite layers, Equation 3.9 would be

$$\epsilon_{assembly} = \frac{t_m E_m \alpha_m \Delta T_m + t_{f_1} E_{f_1} \alpha_{f_1} \Delta T_{c_1} + \ldots + t_{f_n} E_{f_n} \alpha_{f_n} \Delta T_{c_n}}{t_m E_m + t_{f_1} E_{f_1} + \ldots + t_{f_n} E_{f_n}} \qquad (3.10)$$

where n=1,K and K is the number of composite layers. Since the thickness, t_f, and the coefficient of thermal expansion, α_f, are the same for each composite layer, Equation 3.10 can be written as

$$\epsilon_{assembly} = \frac{t_m E_m \alpha_m \Delta T_m + (t_f \alpha_f E_f)(\Delta T_{c_1} + \ldots + \Delta T_{c_n})}{t_m E_m + t_f E_f K} \qquad (3.11)$$

Substituting Equation 3.11 into Equations 3.6 yields the hoop stresses in the mandrel and each composite layer due to temperature changes of ΔT_m and ΔT_{cn}, respectively.

In FWEXPAND, the stress in the mandrel is then used to calculate the mandrel hoop strain for comparison with experimental mandrel strain. The thermally-induced fiber stresses are incorporated with the fiber stress changes due to resin flow to generate the net fiber stress during cure.

In order to understand the integration of the thermally-induced fiber stress into FWCURE, a review of the calculation procedures in FWCURE is in order. At the beginning of cure, the initial fiber stress in each composite layer is calculated from the initial layer tensions. The fiber stress is used to construct a global pressure field through the thickness of the composite case. The pressure field is determined by first calculating the pressure in each layer due to the fiber stress as follows:

$$p = \frac{\sigma_{total} t_f}{r} \tag{3.12}$$

where p is the pressure at the center of the layer, σ_{total} is the total stress in the fiber, t_f is the equivalent thickness of the fiber in the layer, and r is the radius from the axis of the mandrel to the center of the layer.

The layer pressures are then superimposed through the thickness of the composite case to generate a global pressure field in the case. The pressure gradient across each layer, the resin viscosity, and the fiber tow permeability are substituted into Darcy's Law to determine the rate of resin flow through the layer. The assumption is then made that the inward displacement of the fiber during a given time step is equal to the distance which the resin flows during that same time step. From the fiber displacement, a new radius of curvature for the layer is calculated, from which an updated fiber strain and stress are calculated. This fiber stress is then used during the next time step to calculate a new pressure gradient, as described above. This sequence is repeated each time step, and the fiber tension continues to decrease until either 1) the fiber tension reaches zero, or 2) full compaction of the fiber has occurred, reducing the resin flow to zero.

In FWEXPAND, the sequence of calculations performed for tension loss due to resin flow is identical to that performed in FWCURE. But at the end of each time step the incremental thermally-induced fiber stress, which occurred during that time step, is calculated using Equations 3.11 and 3.6, and then summed with the reduction in stress due to resin flow. This summation process occurs as shown below:

$$\sigma_{total,new} = \sigma_{total,old} + (\sigma_{rf,new} - \sigma_{rf,old}) + \sigma_{th,incr} \qquad (3.13)$$

where, $\sigma_{total,new}$ = total fiber stress at the end of the current time step

$\sigma_{total,old}$ = total fiber stress from the previous time step

$\sigma_{rf,new}$ = current fiber stress associated only with resin flow and not affected by thermal stress

$\sigma_{rf,old}$ = previous fiber stress associated only with resin flow and not affected by thermal stress

$\sigma_{th,incr}$ = *incremental* fiber stress which was thermally-induced by the change in temperature *since the previous time step*

The cumulative net fiber stress, σ_{total}, is the stress which is used in Equation 3.12 to calculate the global pressure field at each time step.

For single layer winds, the fiber stress, σ_{total}, is converted to fiber tension, from which the mandrel strain is calculated using Equation 4.1. For multi-layer winds, the total fiber stress, σ_{total}, is used to calculate mandrel pressure using Equation 3.12.

FWEXPAND was developed to study the effects of RFTL in the experiments done in this study. Therefore, due to the assumptions made in developing the mandrel expansion model, the use of FWEXPAND is valid only for hoop direction winds using cylindrical mandrels without end enclosures. The thickness-to-diameter ratio of the wound assembly should be low enough that the strain can be assumed to be constant through the thickness. In addition, it should only be used for the RFTL portion of the cure cycle when the resin viscosity and degree of cure are low, and the composite properties are fiber-dominated.

4.0 Experimental Methodology, Equipment and General Procedure

4.1 Methodology

The parameter of interest in this study is fiber tension. As discussed in Section 1.0, if the fiber tension in a filament wound structure drops to zero during winding or cure, the structure's final strength can decrease significantly. This investigation examines the tension variation during the cure of prepreg-wound cylindrical shells. Tension can decrease due to inward fiber movement in the radial direction. The only resistance to this movement is the viscous drag force imposed as the fiber network moves through the resin. As defined in Section 1.0, this tension decrease due to fiber motion is called Resin Flow Tension Loss (RFTL). The initial resin viscosity in prepreg material is high enough that significant RFTL does not occur at room temperature. Only during cure, when elevated temperatures reduce the resin viscosity, does this mechanism of tension loss become appreciable.

Offsetting the RFTL during cure is the thermal interaction of the mandrel and composite materials. Metal mandrels tend to have higher coefficients of thermal expansion than composite materials. As the cure cycle progresses and the assembly temperature increases, the mandrel attempts to expand more than the composite material surrounding it. This introduces compressive hoop stresses in the mandrel and tensile stresses in the fiber. The net change in fiber strain is the sum of decreased strain due to RFTL and increased strain due to thermally-induced stress.

Integral to the change in fiber stress (or tension) with time is the resin "flow window", which is the period of time during which RFTL can occur. The duration of this window is a function of both resin viscosity and fiber tension. For any given viscosity, higher fiber tension will result in more fiber motion. The resin viscosity changes as a result of two opposing mechanisms: a melting mechanism which causes decreased viscosity, and the molecular cross-linking associated with the cure of a thermoset resin which causes increased viscosity. Therefore, as the assembly heats up, the viscosity initially decreases because the melting mechanism dominates the cross-linking effect. But with sufficient time and temperature, the molecular cross-linking mechanism replaces the melting mechanism and the viscosity of the resin increases. Ultimately, the resin becomes a rubbery solid. Figure 6 shows this bowl-shaped viscosity profile for a typical hot-melt resin system. It is during this period of low viscosity that RFTL occurs.

In order to measure and study RFTL, two different approaches have been taken. Each one is designed to remove, or account for, the effect of mandrel expansion on fiber tension during cure in order to isolate the effects of RFTL on fiber tension. The first method, which is purely experimental, attempts to empirically remove thermal effects from the measured data. The second method involves a comparison of experimental and analytical data, where the effects of mandrel expansion have been included in the analytical solution. An explanation of the experimental fiber tension measurements is given at this point.

Fiber tension cannot be measured directly after the roving has been wound onto the mandrel. Therefore, an indirect method is to measure the hoop strain in the mandrel

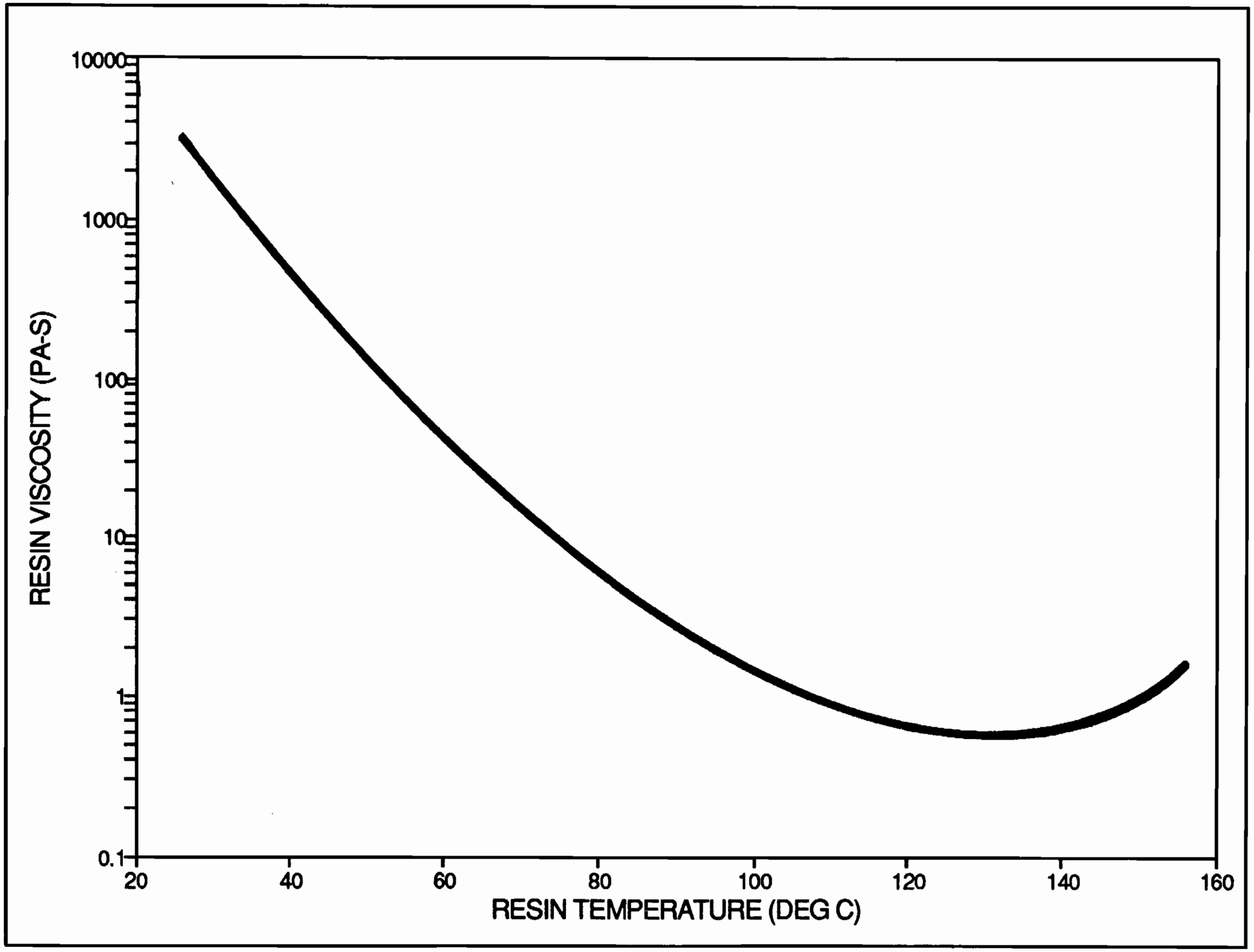

Figure 6. Viscosity profile for a typicl hot-melt resin system.

caused by the tensioned fiber, from which the tension can be calculated [10,11]. The equation relating mandrel hoop strain to fiber tension for a single layer of fiber is developed in Appendix B. The equation is:

$$T = -E_m \epsilon B t \tag{4.1}$$

where T is the fiber tension (force), E_m is the mandrel modulus of elasticity, B is the bandwidth of one roving of fiber, ε is the mandrel hoop strain, and t is the mandrel thickness.

In the case of multi-layer winds, Equation 4.1 cannot be used. Therefore, rather than calculating the fiber tension, the mandrel pressure can be used as a measure of the total effect of the tension in all of the wound layers. This pressure can be calculated from the measured strain using thin shell theory which, for orthotropic shells, is only valid where the thickness-to-diameter ratio is much less than 1/10. In this study, for the mandrel and one layer of composite, the ratio is 1/110. From this well known analysis, the mandrel stress in the hoop direction is:

$$\sigma_h = -\frac{p r_m}{t_m} \tag{4.2}$$

where t_m is the mandrel thickness, and r_m is the average mandrel radius. Therefore, the pressure imposed on the mandrel by the outer layers is:

$$p = -\frac{\sigma_h t_m}{r_m} = -\frac{E_m \epsilon_h t_m}{r_m} \tag{4.3}$$

where E_m is the mandrel modulus of elasticity, and ε_h is the mandrel hoop strain. Conversely, the mandrel strain can be calculated as:

$$\epsilon_h = -\frac{p r_m}{E_m t_m} \tag{4.4}$$

If an article is wound and then subject to an increase in temperature, the change in measured strain is a result of both RFTL and thermally-induced stresses. Therefore, in order to measure RFTL, the thermally-induced strain must be subtracted from the measured strain. (Strain gages measure only stress-induced strain, not thermal strain [13].)

The purely empirical method of subtracting out the thermally-induced strain involves performing pairs of experiments. Each pair is composed of one wind using prepreg material and the other wind using dry fiber only (the same type of fiber as is in the prepreg material). Both winds are performed using the same mandrel, spool tension, bandwidth and cure cycle. As discussed above, the mandrel strain measured during the cure of the prepreg wind includes both RFTL and thermally-induced strain, whereas the strain measured from the dry fiber wind is the result of thermal effects only. By subtracting the strain from the dry fiber wind from that of the prepreg wind, one should gain insight into the strain due to RFTL. This data can then be compared with the tension variation simulated by FWCURE, which accounts for changes due to fiber motion, but makes no provision for thermally-induced stress. However, as will be discussed in Section 5.2, this method did not provide a useful measure of RFTL.

The second method used in this study to account for the thermal effects on fiber tension involves the use of a modified version of FWCURE, called FWEXPAND. FWEXPAND includes a calculation of the thermal strain of the assembly during cure, and the resulting stresses induced in the fiber and mandrel. The thermal stress in the fiber is summed with the stress changes due to fiber motion to determine the net affect on fiber tension. This simulated data from FWEXPAND is then compared with the experimental prepreg wind data, which includes stress changes from both sources.

4.2 Equipment

The equipment used to perform the experiments are a converted machining lathe, an instrumented mandrel, a roving tension measurement and delivery system, a data acquisition system and a programmable oven. The lathe, the tension measurement device, and the mandrel were assembled and used by Call [10] and by Knight [11] for the studies discussed in Section 2.0. A thorough description if this equipment can be found in reference [10], but a brief description will be given here.

The lathe is a South Bend Model 'A' machining lathe. Attached to the tool carriage of the lathe is a tension measurement device, which also serves as a delivery eye. The axial feed rate of the tool carriage can be adjusted so that the delivery eye moves along the mandrel one roving bandwidth for each revolution of the mandrel. In this manner, a continuous layer of material can be wound onto the mandrel with a winding angle which is nearly circumferential (within 1°). The winding angle is the acute angle formed by the fiber roving and the mandrel axis.

The tension measurement/delivery eye device is shown in Figure 7. It is composed of two stationary pulleys on the outside with a pivoting pulley between them. The pivoting pulley is attached to a supporting arm which contacts a load cell. The fiber lies across the pulley in such a manner that increased tension in the fiber causes increased voltage output from the load cell. This output is read using a Vishay P3500 load cell indicator and was calibrated with the tension in the roving using dead weights.

Tension was maintained in the roving using a mechanical tensioner, called an Unwind Tension Compensator, built by Compensating Tension Controls, Incorporated. It is a mechanical device which has a tension sensing unit which provides feedback to a friction brake device. The friction brake device maintains a constant tension in the roving of fiber.

The aluminum mandrel used in these experiments, shown in Figure 8, has an outside diameter of 6.0 inches and a thickness of 0.05 inches. It was instrumented for use

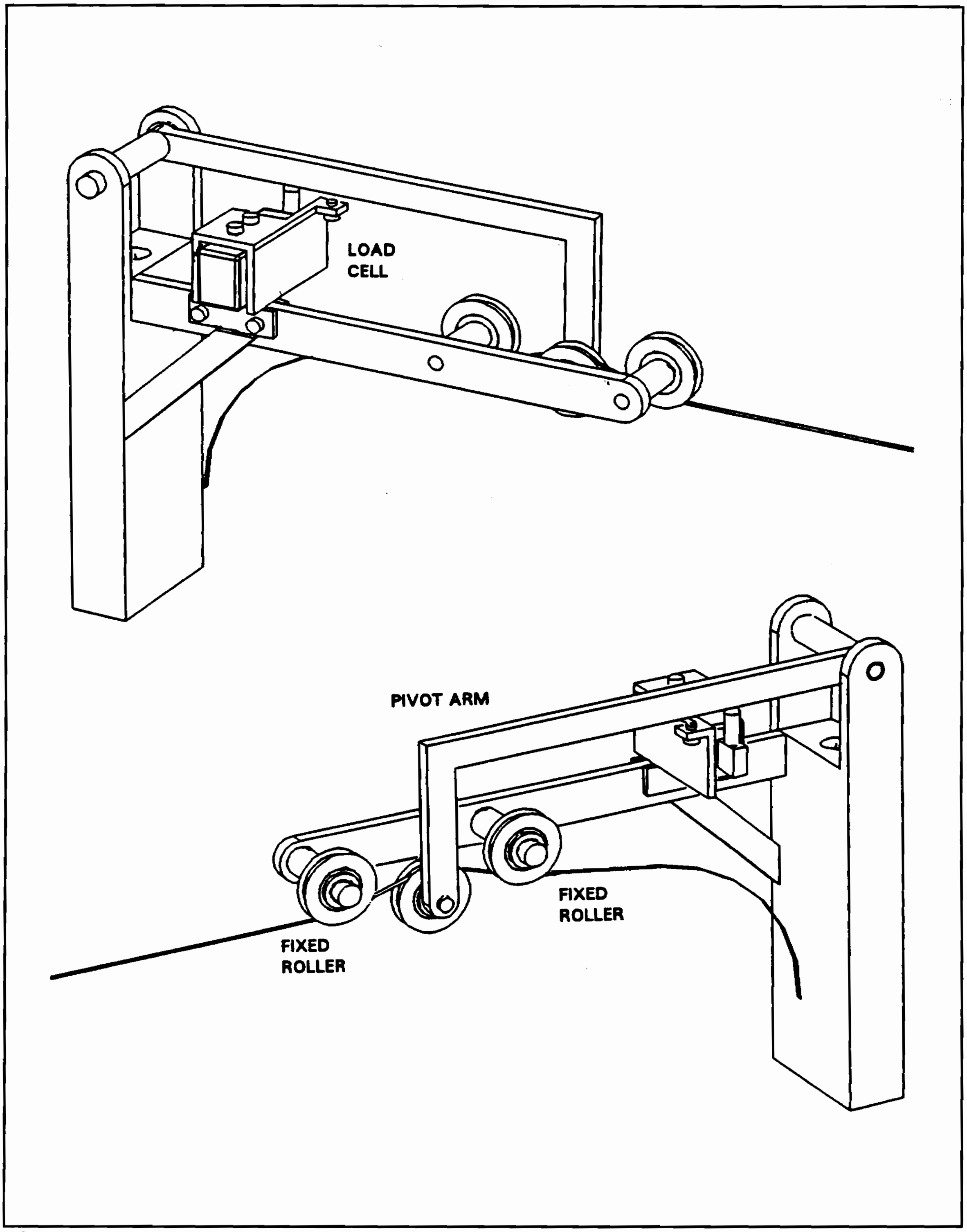

Figure 7. Tension measurement / delivery eye used to place prepreg rovings on the mandrel (by Kent Call) [10].

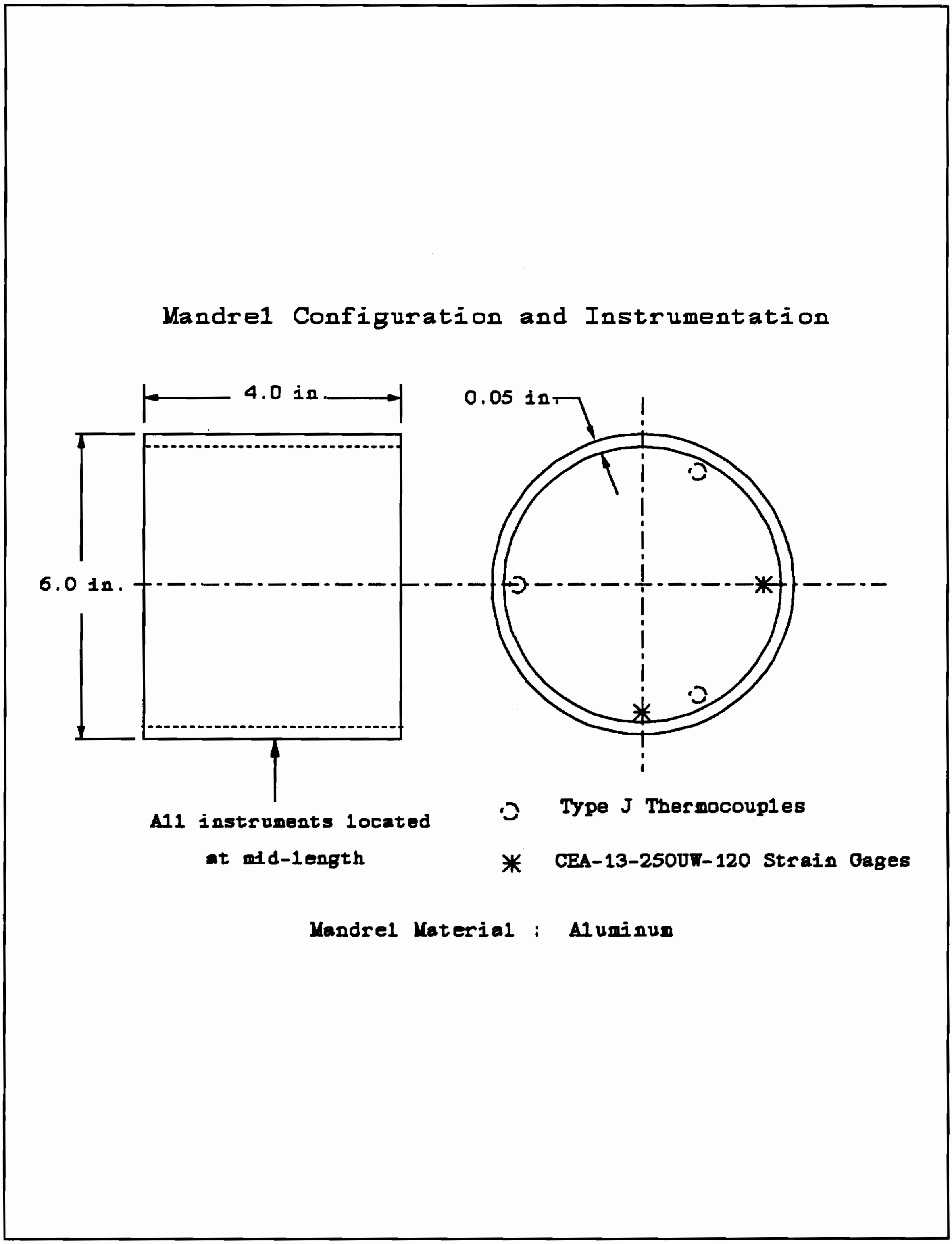

Figure 8. Aluminum mandrel instrumented with strain gages and thermocouples

at elevated temperatures using two CEA-13-250UW-120 strain gages, made by Measurements Group, and three Type J thermocouples. All five instruments were mounted at mid-length on the inner surface of the mandrel. The strain gages were oriented in the circumferential (hoop) direction to measure hoop strain, and were separated by 90° to average any variation of strain in the circumferential direction. To minimize the "apparent" strain caused by a difference in gage/specimen thermal expansion coefficients, the gages are "matched" to aluminum. The two strain gages were mounted to the mandrel using M-Bond 600 high temperature adhesive, and high temperature, shielded lead wires were attached. The three thermocouples were mounted 120° apart to detect any circumferential variation in temperature.

In order to provide a means for winding the rovings onto the open-ended mandrel, a steel shaft held two aluminum endcaps against the ends of the mandrel. To avoid thermal stresses during cure, the shaft and endcaps were used only in the winding stage, and were removed before cure.

The instruments used to measure and record the strain and temperature data are illustrated in Figure 9. The main components of the system are 1) the mandrel, where strain and temperature are measured, 2) Wheatstone Bridge circuits for use with the strain gages, 3) a strain gage voltage source and signal amplifier, and 4) a data acquisition system (DAS). The two strain gages were used in quarter bridge Wheatstone Bridge circuits. A Measurements Group model 2120 strain amplifier supplied the excitation voltage (V_s) to the Wheatstone Bridge and amplified the output voltage (V_o), which was

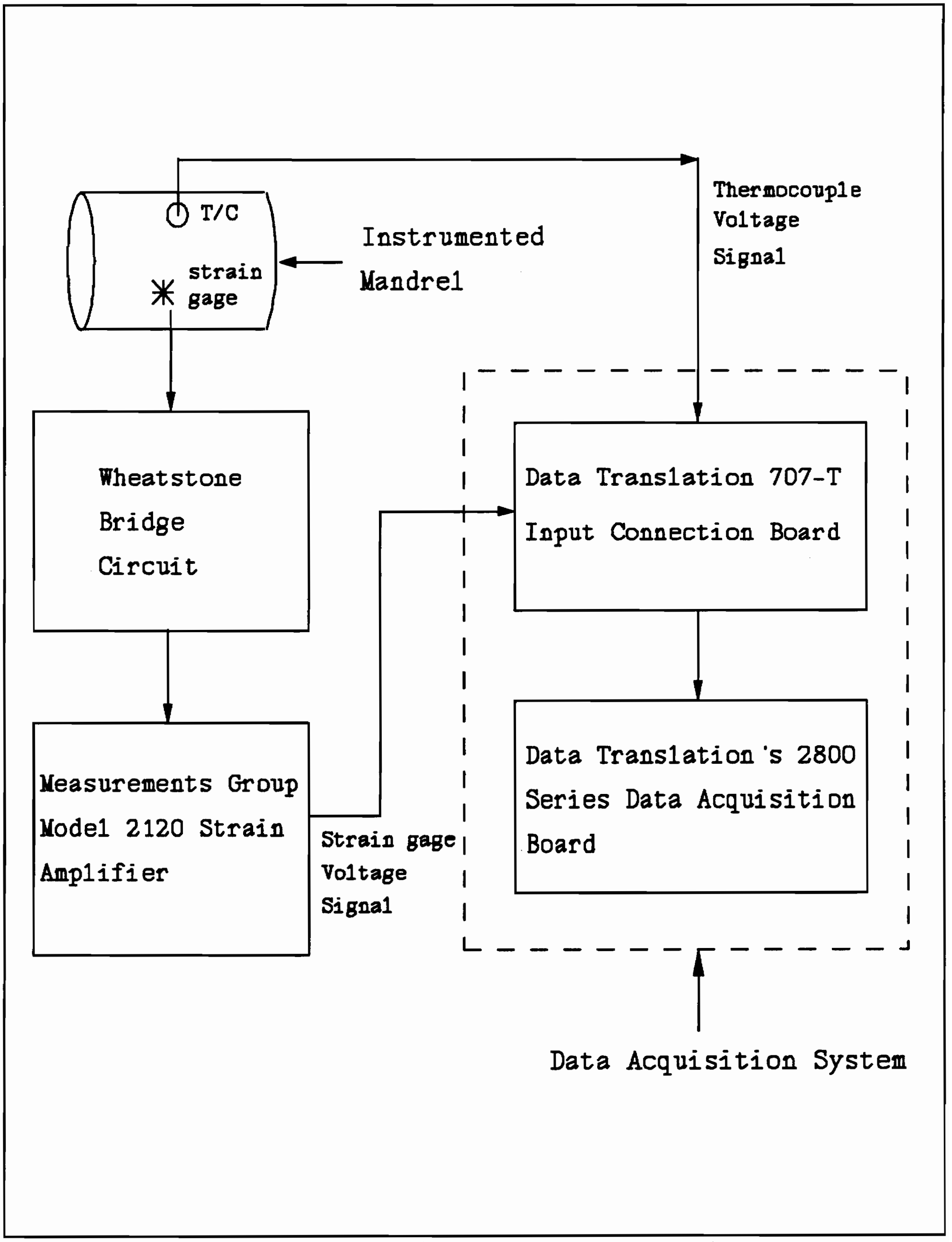

Figure 9. Equipment used to acquire strain and temperature data

then input to the data acquisition system. The thermocouple voltages went directly to the DAS.

The DAS, made by Data Translation, is composed of a 707-T input connection board and a 2800-series data acquisition board, which was located in an IBM PC. The 707-T board receives unamplified voltages from the thermocouples and partially amplified strain gage voltages from the 2120 strain amplifier. The 707-T board has positions for 16 single-ended (SI) input channels or 8 differential input (DI) channels. Because DI channels can filter out noise which is common to the high and low ends of each channel, this type of input was chosen over the SI input channels. In addition to the five channels needed for the three thermocouples and two strain gages on the mandrel, one channel received input from a thermocouple which measures oven temperature, and one acts as a cold (reference) junction for converting thermocouple voltages into temperature values.

The 2800-series data acquisition board, located in the PC, receives the input signals from the 707-T board. The primary function of the 2800 board is to sample the voltages from each channel, amplify the signals and perform analog/digital conversion. The digital value of the sampled voltages are then recorded on disk in the PC. The functioning of the DAS is controlled by a BASIC program. This program performs the following tasks:

- Converts the sampled voltages to units of microstrain and degrees Celsius.
- Averages the data over a specified time interval to smooth noise in the signals.

- Switches the level of amplification of the strain voltages during cure to provide 1) higher gain with low level signals for greater accuracy, and 2) lower gain with high level signals to avoid saturation of the A/D converter.
- Amplifies the low thermocouple voltages (microvolts) with a maximum gain to maintain accurate temperature measurements.

The last piece of equipment, used in the cure stage of the experiments, was a Fisher Scientific programmable oven. It was capable of providing up to six ramp-hold steps in a cure cycle. It also had a port in the top of the oven to allow passage of leadwires from the mandrel to the DAS.

4.3 General Procedure

The prepreg material investigated in this study was Thornel T-40/ERL-1908 made by Amoco Performance Products. It is referred to in this work as T40/1908. It is composed of a proprietary, toughened, hot-melt, epoxy resin (ERL-1908), and a continuous, 12k carbon fiber tow made from polyacrylonitrile precursor. The prepreg system was designed for the manufacture of rocket motor cases and other pressure vessels in which optimal tensile strength is required.

The general experimental procedure includes both winding and cure stages. The winding stage has three steps including 1) attaching the endcaps to the mandrel, 2) winding the dry fiber or prepreg roving onto the mandrel/endcap assembly, and 3) removing the endcaps from the mandrel. Each step causes a change in the mandrel hoop strain, so the effect of each step on strain was measured. The strain was first zeroed (by balancing the two quarter bridge circuits using the strain amplifier) before the endcaps were mounted. This balance setting was not changed throughout the winding and cure stages. The mandrel strain was recorded again after each of the three steps listed above, with the final strain reading providing the strain needed for calculating the winding tension, as described in Section 4.1.

The 3-pulley tension measurement device was calibrated using the technique outlined by Call [10]. The strain amplifier and DAS were calibrated using the calibration shunt resistance in the 2120 strain amplifier. The precision shunt resistor has a resistance equal to the resistance of a strain gage which is strained to 1000$\mu\varepsilon$.

Securing the ends of the wound roving to the mandrel was very important since any slippage would keep the mandrel from experiencing full thermal stress and strain, which could be mistaken as RFTL. Therefore, the ends of the fiber or prepreg were held to the mandrel by overwrapping them with three or four successive circuits. Later, during cure, as the wound assembly heated up, the increased fiber tension would produce a greater clamping pressure on the free ends. At the end of a wind, the technique used to perform the overwrap was to wind the final 3-4 circuits over a separate loop of roving. The free end was threaded through the loop and pulled under the final circuits using the loop. The loop was then discarded.

After winding the dry fiber or prepreg onto the mandrel and then removing the endcaps, the assembly was placed in the programmable oven for the cure stage of the experiment. During this time, the data acquisition system was used to collect mandrel strain, mandrel temperature and oven temperature. The oven cycles used were not intended to fully cure the prepreg, but rather only to allow enough time for RFTL to occur. Therefore, in comparison with the cure cycles used at Thiokol on full scale filament wound articles, which are much larger in diameter and thicker in cross-section, the hold times were much shorter. However, the same ramp rates and hold temperatures were used. This is shown in Table 1. The relatively small and thin assembly used in this

Table 1. Typical cure cycle used for full-scale filament wound cases at Thiokol Corporation, and a typical cycle used for the cases wound in this study

	1st Ramp (°C/min)	Hold Temp (°C)	Hold Time (hrs)	2nd Ramp (°C/min)	Hold Temp (°C)	Hold Time (hrs)
Typical Thiokol Cycle	0.8	100	8	0.8	155	16
Experimental Cycle	1.0	100	0.5	1.0	155	0.5

study had a rapid thermal response and most of the RFTL was found to occur during the first ramp, rendering irrelevant the duration of the first hold time.

In order to wind a continuous, even layer of material onto the mandrel, the feed rate on the lathe was adjusted to 0.12 inch/revolution so that adjacent circuits of T40/1908 prepreg were just touching each other. This lathe setting resulted in a distance of 0.12

inch between the leading edges of successive circuits, which is very close the prepreg bandwidth of 0.125 inch. However, the dry T40 fiber roving had a narrower bandwidth (0.088 inch) when wound onto the mandrel. For the pairs of winds in which dry T40 fiber and T40/1908 prepreg were compared, it was important to have equal amounts of fiber per axial length of the mandrel for both winds. Therefore, since both the dry fiber and prepreg rovings contain 12k filaments, the dry fiber winds were wound using the same lathe feed rate as was used for the prepreg winds (0.12 inch/rev). As a result, the dry fiber winds had "actual" bandwidths of 0.088 inch, but "apparent" bandwidths of 0.12 inch.

The dry fiber wind used to validate the mandrel expansion model had an even, continuous layer of fiber, obtained using an appropriate lathe feed rate (Section 5.1).

The type of strain gages used to measure mandrel hoop strain were chosen to be "matched" to the test part, which in this case was the aluminum mandrel. To be "matched" means that the alloy used in the grid of the gage has approximately the same coefficient of thermal expansion as aluminum. However, this match is not exact, and for each lot of gages the manufacturer provides apparent strain specifications, which is a plot of indicated strain versus temperature. The manufacturer generated this data by mounting gages to flat, unconstrained aluminum plates and measuring the indicated strain over a wide temperature range. This is called apparent strain because the strain indication is not induced by an externally applied or thermally induced load.

There are two sources of apparent strain. First, the electrical resistivity of the grid conductor is somewhat temperature dependent. Second, due to a difference in coefficients of thermal expansion, there is a differential thermal expansion between the grid conductor and the test part to which the gage is bonded. To the extent that this differential expansion occurs, the grid is mechanically strained, and therefore experiences a change in resistance.

The manufacturer-provided apparent strain specifications, are accurate only for the specific test article to which the gages were bonded. Therefore, a separate test was done for the specific gages mounted on the mandrel. This was necessary because the magnitude of strain imposed by the tensioned fiber was relatively low (1000 microstrain or 0.1% max.), and the apparent strain could be a significant part of the measured strain. The apparent strain must be subtracted from the measured strain to obtain the actual strain. Figure 10 shows the effect of apparent strain on the measured strain for a typical experiment. Figure 11 shows a plot of the supplier's apparent strain and the apparent strain measured and used in this study.

There was one problem encountered in performing the experiments which should be mentioned. This problem involved the narrowing of the prepreg bandwidth during winding. There are a series of six rollers or pulleys between the supply spool and the mandrel which impart tension, measure tension, and guide the prepreg onto the mandrel. At room temperature, the T40/1908 prepreg has a lot of tack and drape. The tackiness would cause the roving to climb up the sidewall of a pulley, and the low drape would cause the prepreg to roll inward onto itself, narrowing its bandwidth. This narrowing

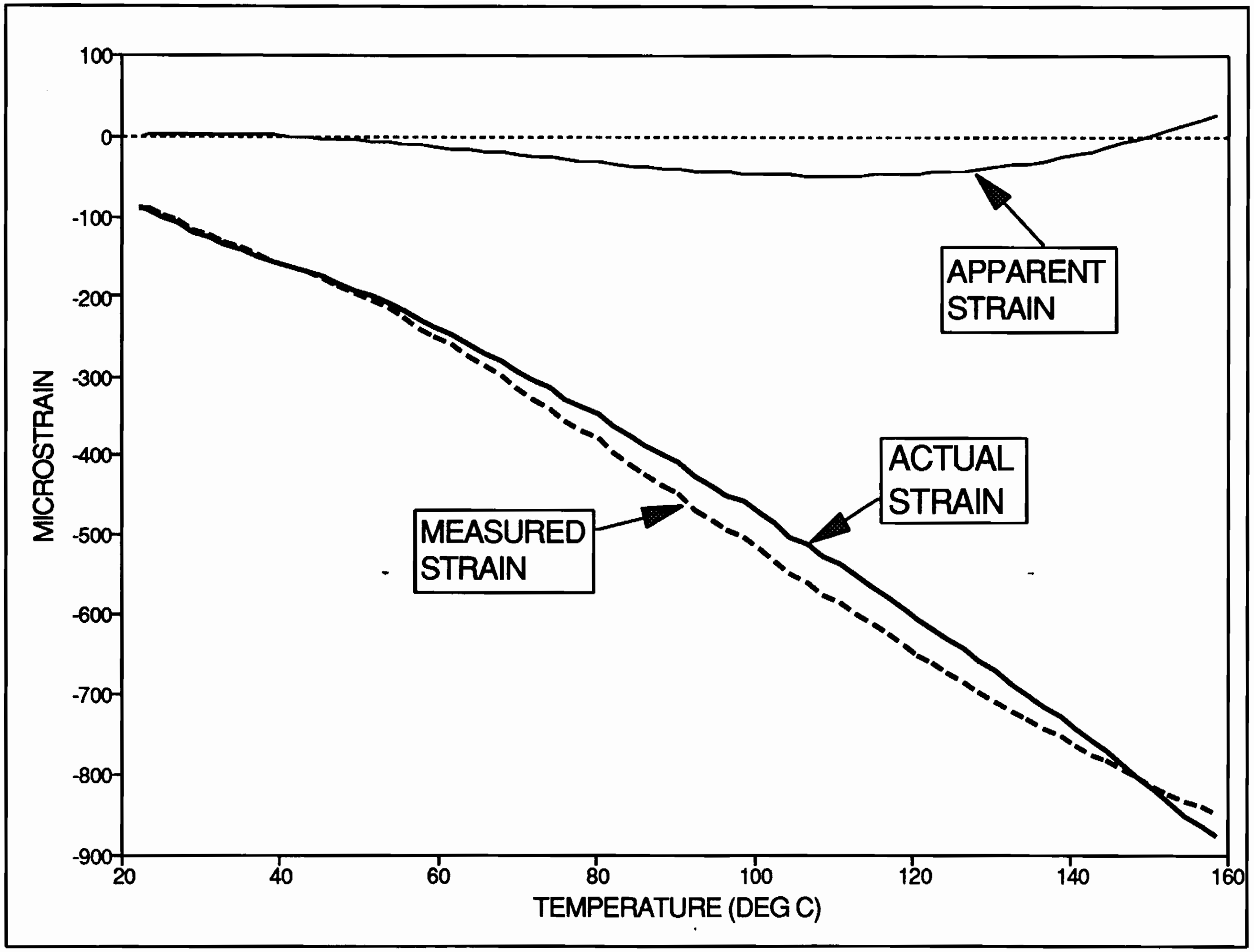

Figure 10. Measured strain, apparent strain and actual strain for a typical experiment (Wind 28 - dry T40 fiber)

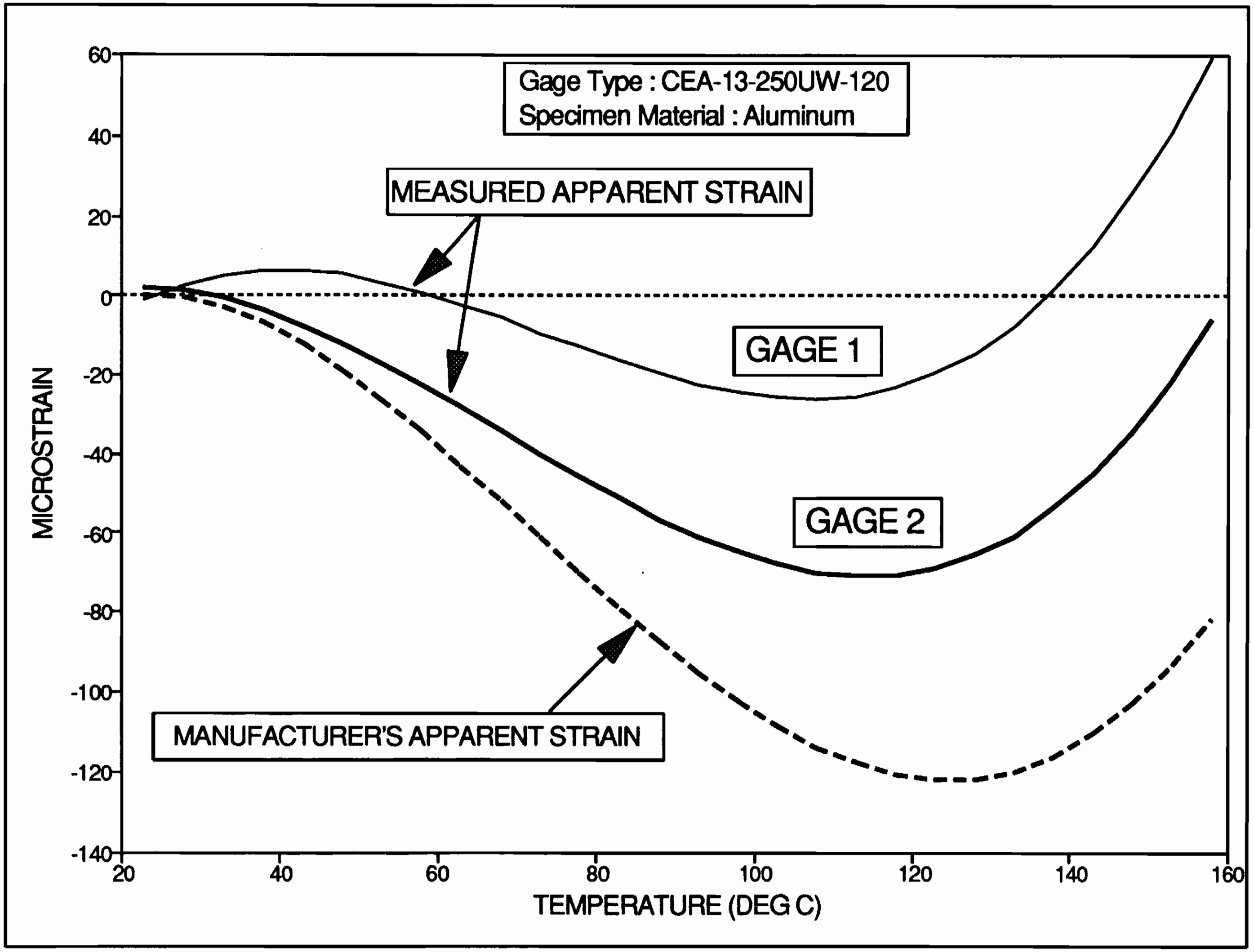

Figure 11. Manufacturer-specified apparent strain and measured apparent strain for M&M CEA-13-250UW-120 strain gages mounted on aluminum

effect was amplified by the lateral force exerted on the roving by the smaller tension measurement pulleys, which control the placement of the roving on the mandrel. In an attempt to remedy this, the tack and drape of the prepreg was reduced by using the prepreg in a frozen state. Even then, the bandwidth and layer thickness of the prepreg windings was not optimal.

5.0 Results

5.1 Dry Fiber Winds - Experimental Verification of the Mandrel Expansion Model

To account for the effect of mandrel expansion on fiber tension during cure, FWCURE was modified by the addition of a mandrel expansion model. A description of this model was provided in Section 3.2. Experiments were run to verify the accuracy of the model. The parameter used to compare the simulation results with the experimental data was mandrel hoop strain. In the experiments, a single layer of dry T40 fiber was wound onto the 0.05 inch thick aluminum mandrel. Dry fiber was used rather than prepreg because the effects of resin flow would not be present. The configuration of the wound assembly consists of two concentric rings of material which have different material properties and thicknesses. These properties, which include the moduli of elasticity in the hoop direction and the coefficients of thermal expansion, are listed with the layer thicknesses in Table 2. The thickness of the fiber layer was determined by measuring the as-wound widths of several circuits of fiber. This was done using a micrometer under magnification. The fiber tow was assumed to be rectangular in cross section. Therefore, dividing the tow cross-sectional area by the measured bandwidth gave the fiber layer thickness.

Mandrel strain was measured as the wound assembly was heated to 160°C at a rate of 1 °C/minute. Figure 12 shows the measured and calculated mandrel strain and temperatures.

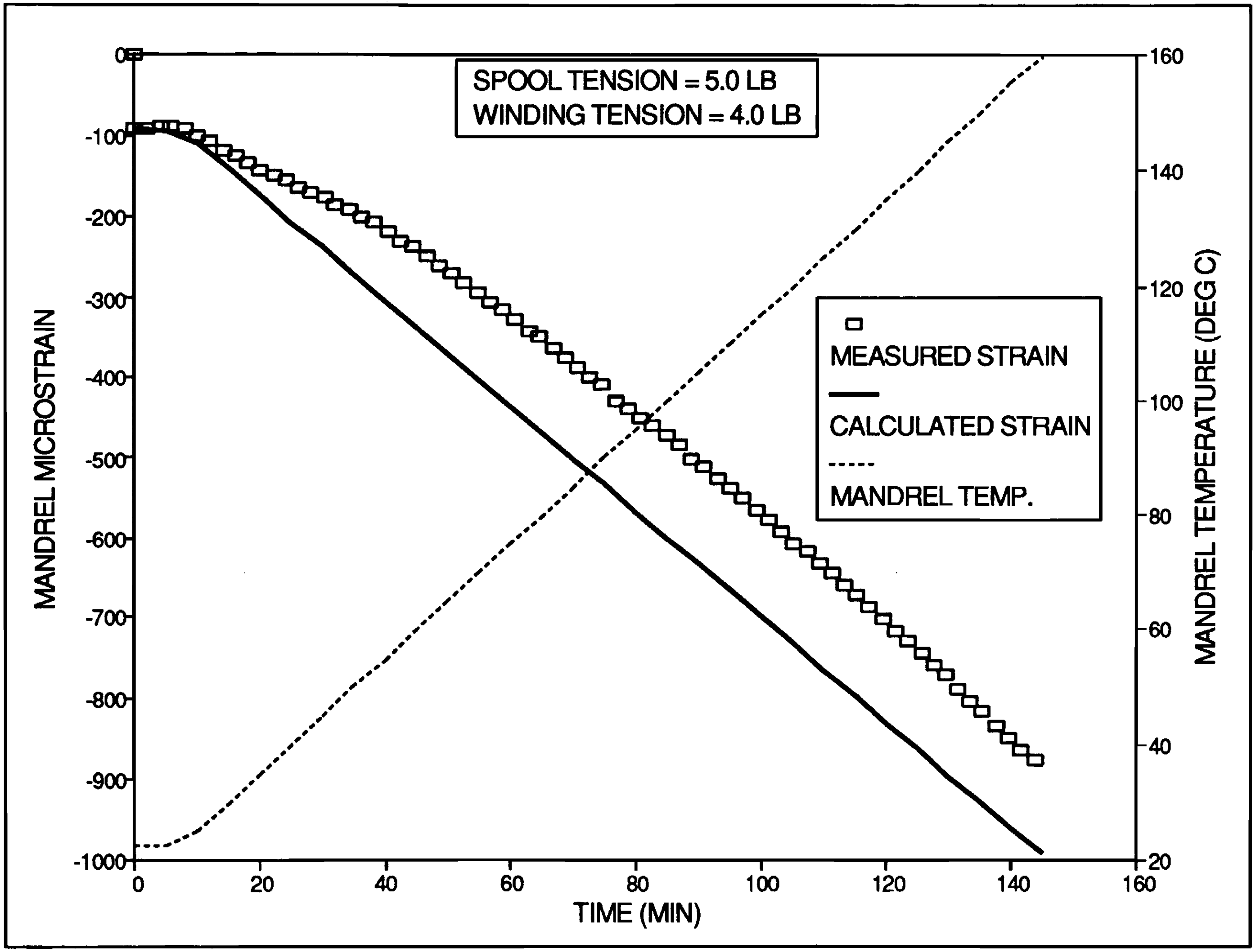

Figure 12. Mandrel strain for a single, continuous layer of dry T40 fiber (Wind 28) - verification of the mandrel expansion model

Table 2. Material properties used to simulate the thermally-induced mandrel strain resulting from a single, continuous layer of dry T40 fiber

	Aluminum Mandrel	T40 Fiber
Modulus of Elasticity, Msi (GPa)	10 (69)	42 (290)
Coeff. of Thermal Expansion, ppm/°F (ppm/°C)	13.3 (23.9)	-0.42 (-0.75)
Thickness, inch (mm)	0.050 (1.27)	0.0043 (0.11)

The thermally-induced strains in the mandrel are compressive (negative) because free expansion of the mandrel is restricted by the presence of the fiber layer. In fact, with a negative coefficient of thermal expansion, the fiber would normally contract during heatup. This, combined with the high fiber stiffness, causes mandrel compression in the hoop direction. The calculated strain is linear with time because the mandrel heating rate is linear with time, and the thermal expansion is proportional to the increase in temperature. However, as shown in Figure 12, the experimental strain is somewhat nonlinear in the early portion of the heatup.

There are two possible causes for the non-linearity in the experimental strain. The first is the possibility of fiber slippage due to inadequate anchoring of the fiber to the mandrel. In all of the experiments, the ends of the fiber tows were pinned to the mandrel by overwrapping three to four successive circuits over the free ends. These free ends could possibly slip as fiber tension increases. The second possible cause is the compaction of the filaments within each tow as the tension increases. As the mandrel expands and the tension in each tow increases, the radial component of this tension would cause a packing of the individual filaments up to the point of full compaction. At that point, the multi-filament tow would behave more like a solid, continuous material.

To investigate the possibility of slippage of the ends of the fiber tows, a separate experiment was run in which a section of dry T40 fiber tow was wrapped around the mandrel using a relatively low tension level (2.5 lb). One free end of the tow was clamped to the mandrel by overwrapping it with the next circuit. The overwrap length was limited to one-half of the mandrel circumference. Tension was then applied to the other tow end. The tension was measured using the 3-pulley tension measurement device. As the applied tension was increased to 14 pounds, no fiber slippage was observed. Since the tow ends are normally overwrapped by much more then one-half of the mandrel circumference, and since higher tension would only increase the locking pressure on the free end, it was concluded that the free ends of the fiber tow were well anchored to the mandrel using the overwrap technique.

Two other possible causes of the non-linear increase in strain are fiber breakage and inelastic behavior of the fiber. Concerning the former, no visible fiber breakage was observed following heatup. Also, in the absence of a cured resin matrix to redistribute the load from broken fibers to unbroken fibers, the onset of fiber breakage would have propagated through the entire tow. As for the latter possibility, the manufacturer of T40 fiber (Amoco) specifies the elastic recovery of the fiber to be 100%.

Therefore, after considering the four possible sources of non-linearity, it was concluded that the most probable cause was fiber compaction.

In Figure 12, after full compaction has occurred (time≈60 min), the measured strain is essentially linear. During this period, the calculated strain is parallel to the measured strain, which validates the mandrel expansion model.

5.2 Dry Fiber versus Prepreg Winds - Experimental Method of Determining Resin Flow Tension Loss (RFTL)

As discussed in Section 4.1, the rationale for performing pairs of prepreg/dry fiber experiments was to experimentally separate the effect of mandrel expansion from the effect of RFTL on fiber tension during cure. To do this, dry T40-12k fiber rovings were used which are the same fiber rovings used to fabricate the T40/1908 prepreg. Therefore, the thermal stress imposed by the fiber on the mandrel should be the same for both types of winds. The resin would not contribute to the prepreg stiffness due to low resin viscosity during cure. Using this approach, the mandrel strain induced by the dry fiber would be subtracted from the prepreg-induced mandrel strain, and the difference would provide a measure of RFTL.

Six such pairs of winds were performed in this effort. Table 3 shows the winding parameters used in the twelve experiments. With the exception of Wind 12 and 13, two

Table 3. Winding parameters used in the six pairs of dry fiber-prepreg experiments

Wind Number	No. of Layers	Material	Spool Tension lb, (N)	Winding Tension lb, (N)	Stress Ret. Factor (Wind./Spool Ten.)
16	1	T40	2.4 (10.7)	1.3 (5.8)	0.54
17	1	T40/1908	2.5 (11.1)	0.8 (3.5)	0.32
15	1	T40	5.0 (22.2)	4.1 (18.2)	0.82
14a	1	T40/1908	5.0 (22.2)	1.5 (6.6)	0.30
18	1	T40	7.5 (33.4)	5.4 (24.0)	0.72
19	1	T40/1908	8.1 (36.0)	3.8 (16.9)	0.47
20	2	T40	5.0 (22.2)	4.8 (21.4)	0.96
21	2	T40/1908	5.3 (23.6)	3.3 (14.7)	0.62
22	3	T40	5.2 (23.1)	4.6 (20.5)	0.88
23	3	T40/1908	5.1 (22.7)	1.9 (8.5)	0.37
12	3	T40	5.0 (22.2)	4.1 (18.2)	0.82
13	3	T40/1908	5.0 (22.2)	2.5 (11.1)	0.50

(1) Spool Tension was measured during winding using the 3-pulley tension measurement device
(2) Winding Tension is calculated from the mandrel strain after room temperature fiber tension loss has occurred. For multi-layer winds, the indicated winding tension reflects the strain imposed after winding only the first layer
(3) Stress Retention Factor = Winding Tension / Spool Tension

parameters were held constant for all of the winds in Table 3. The apparent bandwidth (distance between the leading edge of successive circuits) was 0.12 inch (3.048×10^{-3} m), and the oven cycle was:

1st Ramp/Hold → 1°C/min ramp from room temperature to 100°C, 30 minute hold

2nd Ramp/Hold → 1°C/min ramp from 100°C to 155°C, 30 minute hold

Cooldown → approximately 2°C/min ramp from 155°C to room temperature

The ramp rates for Wind 12 and 13 were 2°C/minute.

Figures 13-19 show the results of the experiments. Figure 13 shows the full oven cycle used in these experiments, and highlights the heatup portion of the cycle which is the focus of this investigation. In Figures 14-19, the mandrel strain and temperature for each pair of dry fiber/prepreg experiments are presented. In each figure, the dry fiber and prepreg mandrel temperature histories were the same. Figures 14-16 show the single layer winds (Wind 16/17, 15/14a, 18/19), with 2.5, 5.0 and 8.0 lbs of spool tension, respectively. Figures 17-19 show one 2-layer set and two 3-layer sets of winds, respectively. The spool tension was 5.0 lb in all of the multi-layer winds. In this discussion, mandrel hoop strain is the parameter presented, but it should be remembered that mandrel strain is caused by fiber tension, which is the actual parameter of interest.

First, note in all six figures the difference in initial mandrel strain between the prepreg and dry fiber winds. The difference is due to a difference in the Stress Retention Factors (SRF), which is defined as the ratio of winding tension to spool tension. Since the dry fiber winds all have much higher SRF than the prepreg winds, the dry fiber winds start with higher winding tension. The prepreg tension loss during winding will be

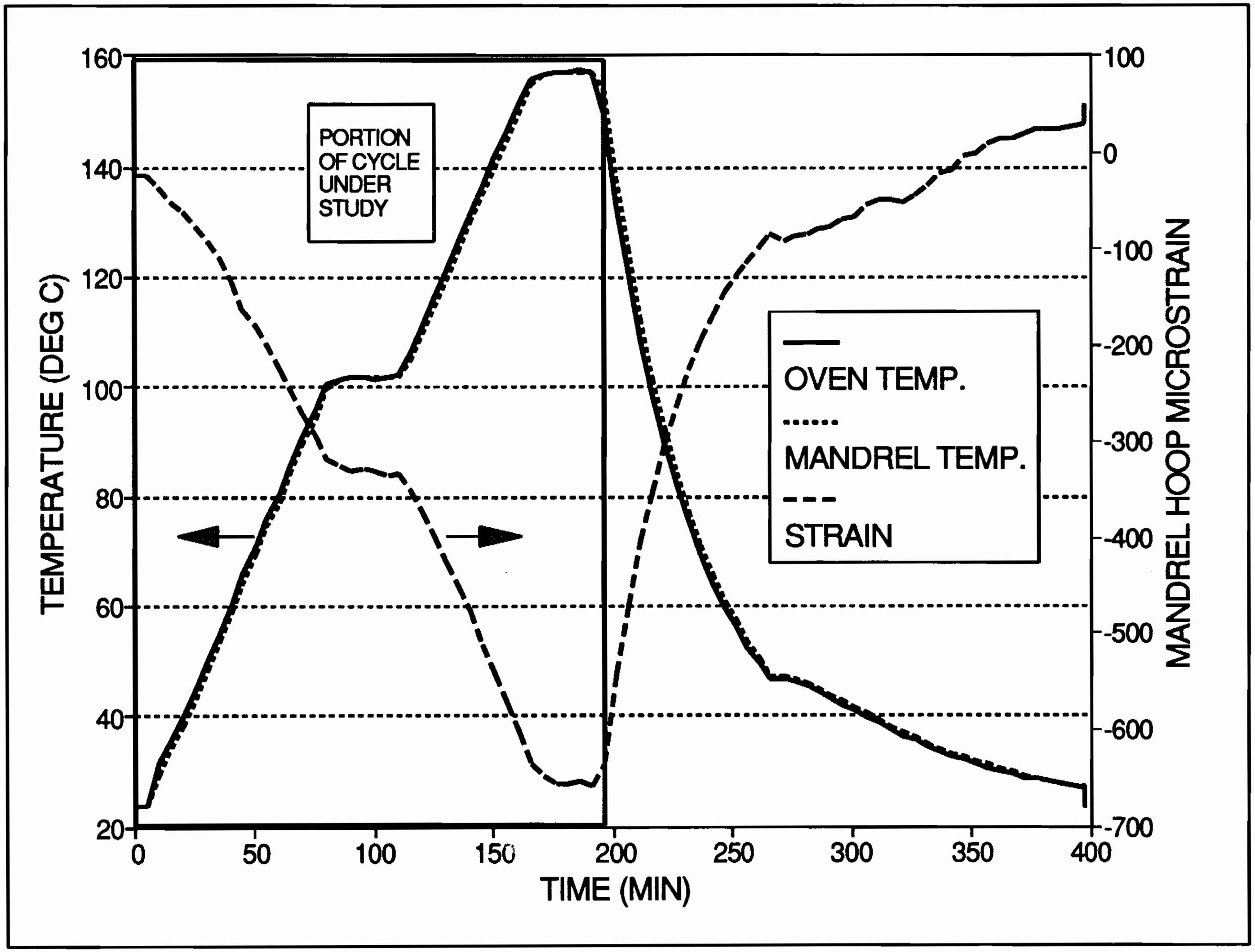

Figure 13. Typical cure cycle used in this study (Wind 14a)

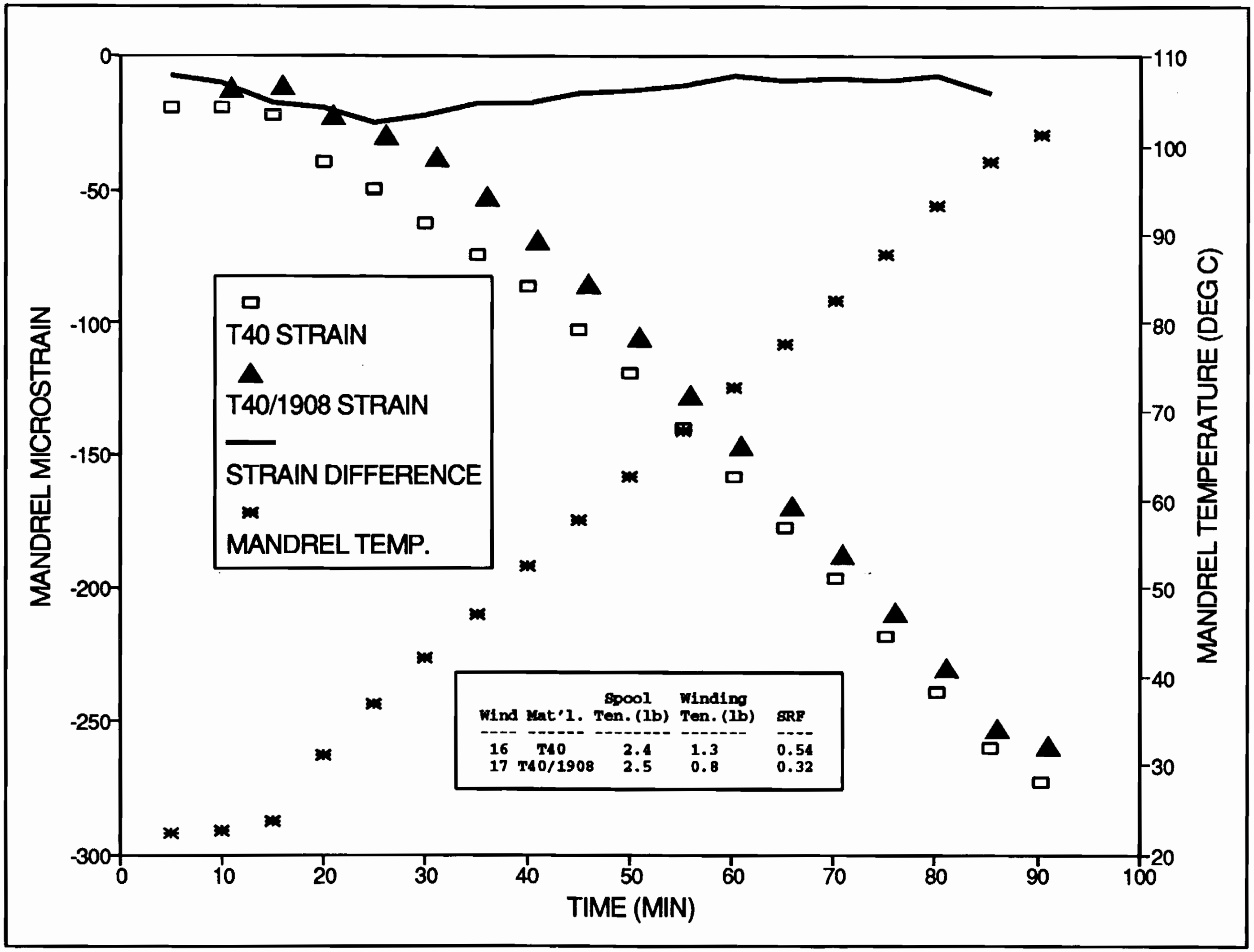

Figure 14. Mandrel strains for single layer dry fiber versus prepreg winds (2.5 lb spool tension, Wind 16/17)

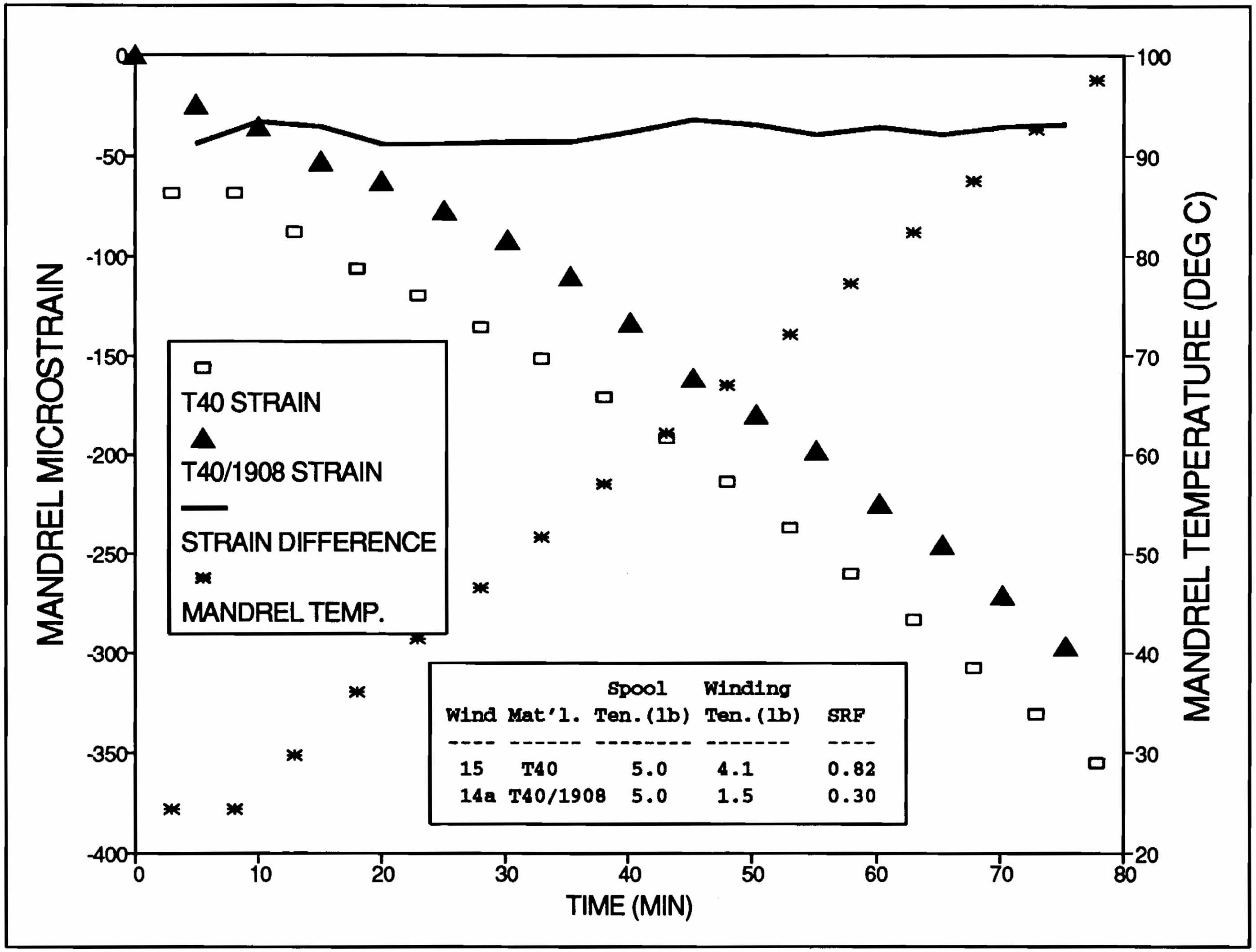

Wind	Mat'l.	Spool Ten.(lb)	Winding Ten.(lb)	SRF
15	T40	5.0	4.1	0.82
14a	T40/1908	5.0	1.5	0.30

Figure 15. Mandrel strain for single layer dry fiber versus prepreg winds (5.0 lb spool tension, Wind 15/14a)

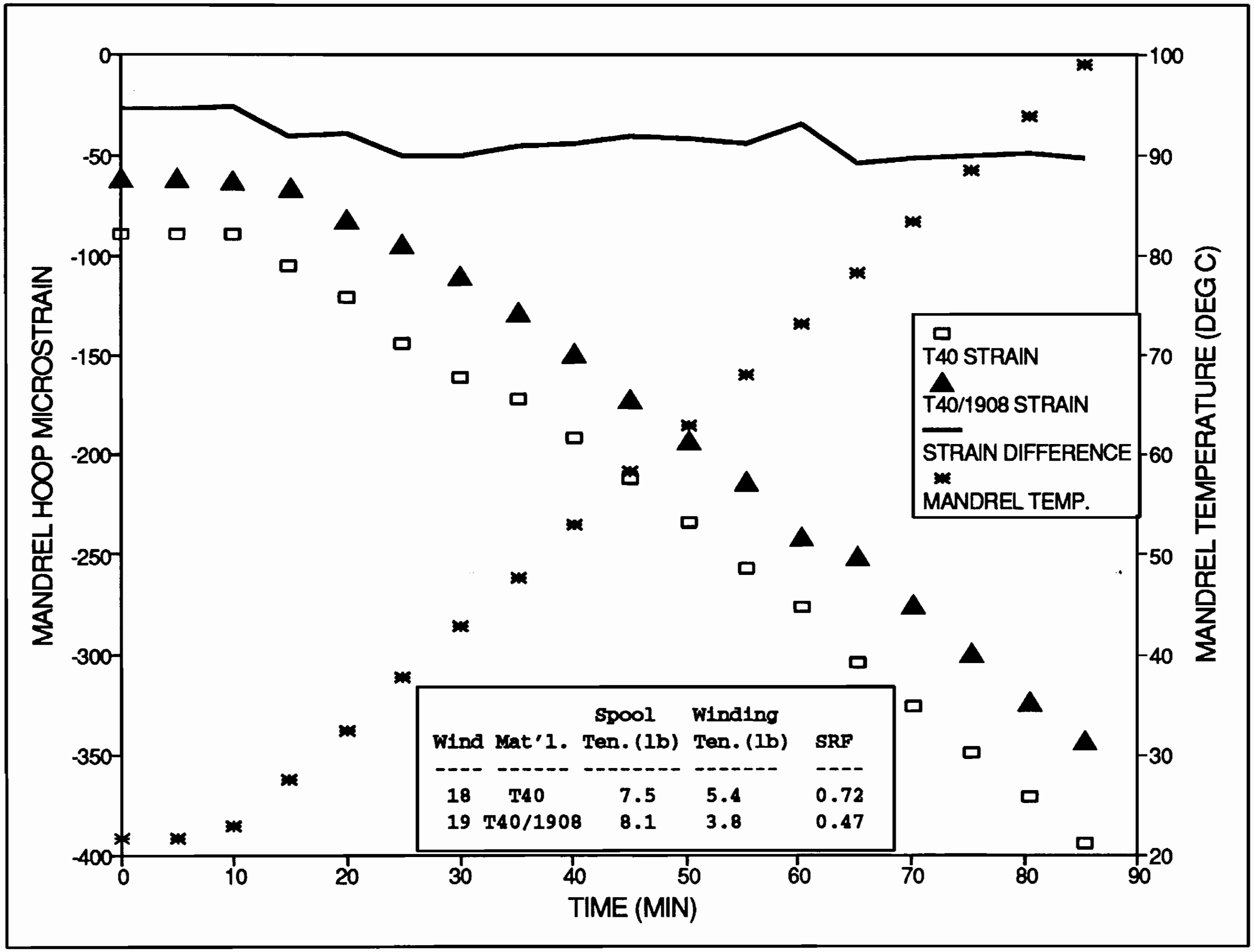

Figure 16. Mandrel strain for single layer dry fiber versus prepreg winds (8.0 lb spool tension, Wind 18/19)

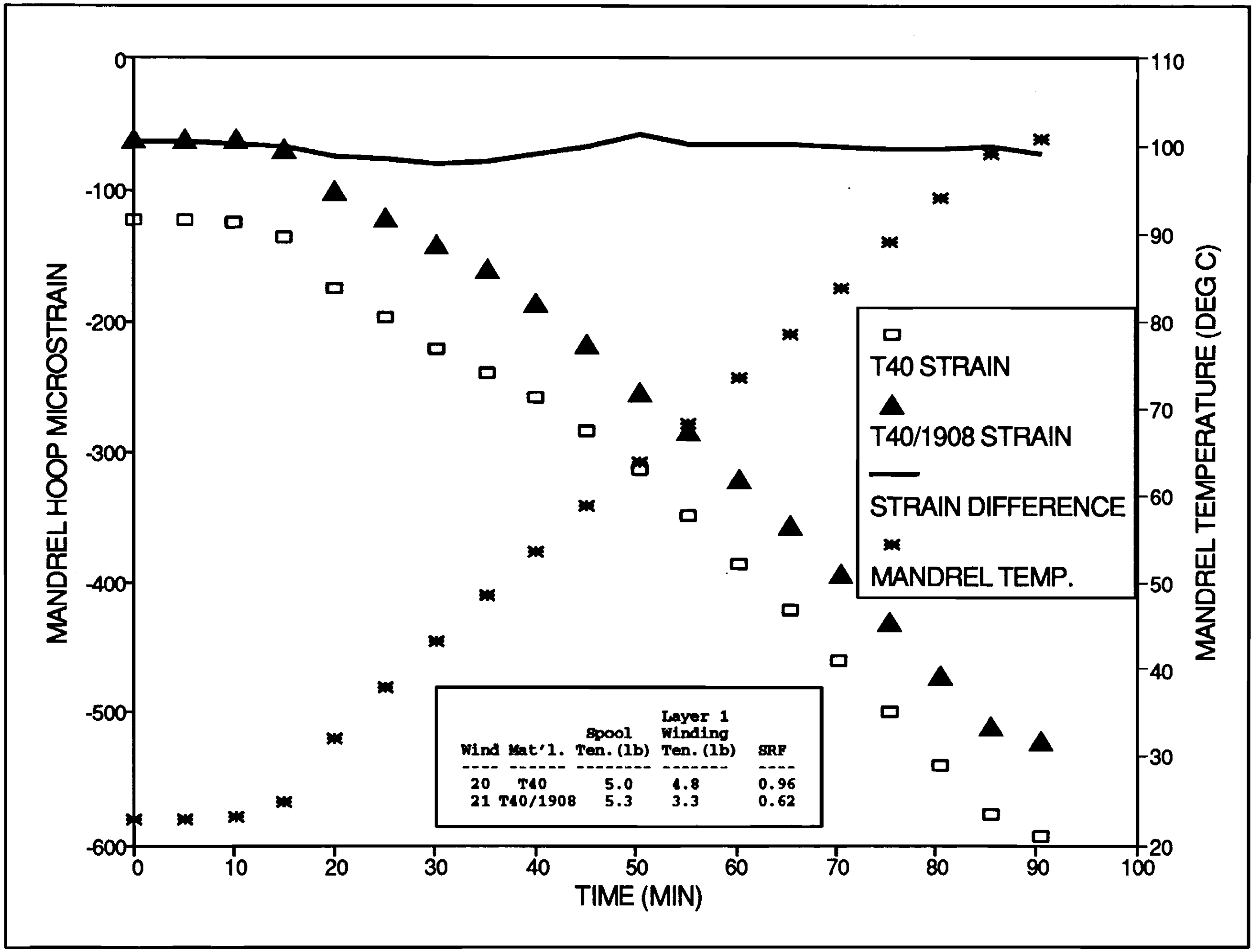

Figure 17. Mandrel strain for 2 layers of dry fiber versus prepreg winds (5.0 lb spool tension, Wind 20/21)

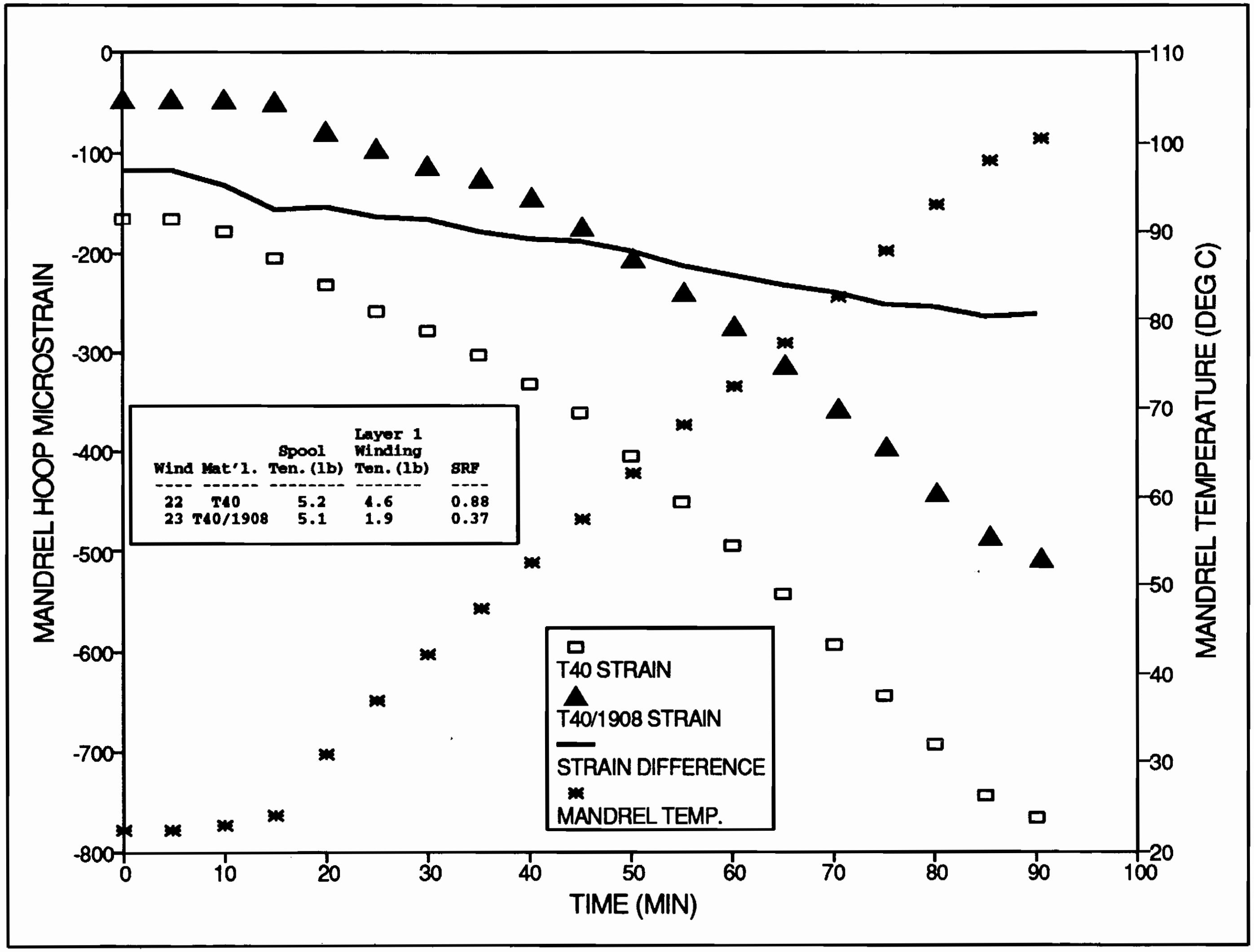

Figure 18. Mandrel strain for 3 layers of dry fiber versus prepreg winds (5.0 lb spool tension, Wind 22/23)

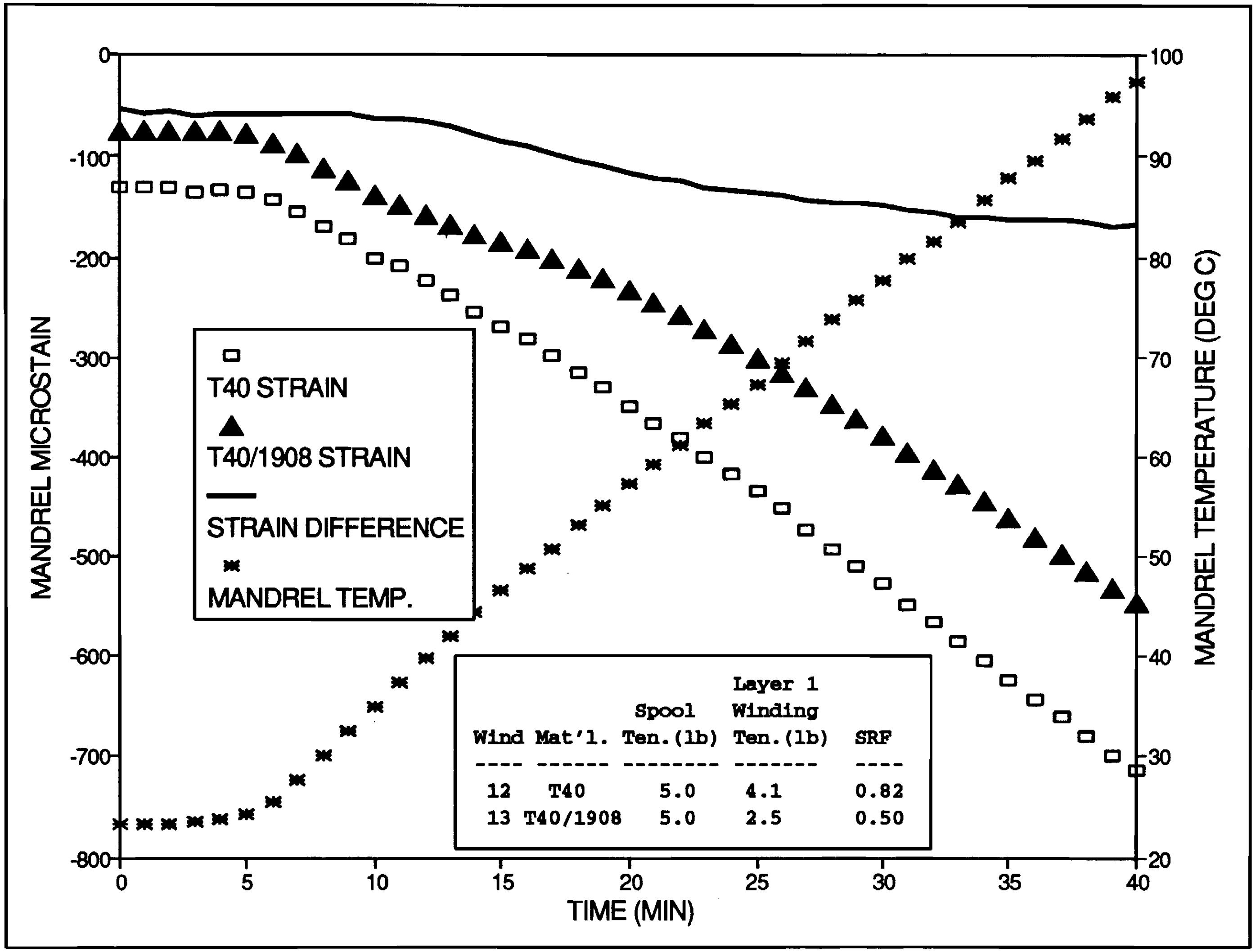

Figure 19. Mandrel strain for 3 layers of dry fiber versus prepreg winds (5.0 lb spool tension, Wind 12/13)

discussed in more detail in Section 5.3.1.

Second, upon initiation of heatup, the two mandrel strain curves start out with a shallow slope and become steeper with time, eventually becoming linear. At the point where the curves become linear, it is felt that fiber compaction has reached completion and the increase in mandrel strain is due only to the thermal stress imposed by the fully compacted layer of fiber around the mandrel.

The important observation here is that not only is compaction occurring in the prepreg, which would be expected due to the flow of resin, but it also occurs in the dry fiber. In both cases, as the mandrel expands, the fiber tension increases. The increased tension causes a packing force which is transverse to the fiber direction. The difference is that in the dry fiber tow, the resistance to this force is the sliding friction between individual fibers, whereas in the prepreg the resistance is due to the viscous flow of resin. With increased time/temperature and tension, the fibers are fully compacted into an arrangement where movement is no longer possible. From then on, the mandrel strain increases linearly.

The third observation to make from Figures 14-16 for the single layer winds, is that both before and after full compaction has occurred, the dry fiber and prepreg strain curves are parallel, and the difference between the two strain curves remains constant with time. Since both contain the same quantity and type of fiber, one would expect the thermally-induced strain to be parallel. But since the difference in the curves is also fairly constant through the compaction process, little information about the effect of RFTL can be deduced from the single layer winds.

The fourth observation is that the paralleling of mandrel strain between dry fiber and prepreg winds is independent of spool tension. The same trend can be seen in each of Figures 14-16.

In the set of 2-layer winds (Wind 20/21), shown in Figure 17, the same trend is seen as in the single layer winds. However, in the two sets of three layer winds (Wind 22/23 and 12/13), shown in Figures 18-19, an appreciable difference in strain can be seen. In both sets of winds, the strain for the prepreg wind increases more slowly than for the dry fiber wind reflecting greater tension loss due to resin flow than due to dry fiber compaction. The average increase in the <u>difference</u> between the dry fiber and prepreg strain curves for the two sets of 3-layer winds is about 125$\mu\varepsilon$. For a single layer wind, this would represent about 7.5 lb of tension loss; but since the differential change in mandrel strain was the result of three layers, one can make the rough approximation that the average tension loss in each layer due to RFTL was 2.5 lb.

Unfortunately, due to the unanticipated amount of compaction which occurs in the dry fiber winds, this method of comparing the difference in strain between the dry fiber and prepreg winds could not be used to measure RFTL.

5.3 Repeatability and Parametric Studies of the Experimental Data

This section presents the experimental results of the single layer winds of T40/1908 prepreg. These experiments were performed to determine the repeatability of the data and the effects of changing two of the processing parameters: the spool tension during winding and the oven ramp rate during cure. Table 4 shows the test matrix for all of the prepreg winds, which includes ten single layer winds and two multi-layer winds.

Table 4. Experiments performed using T40/1908 prepreg material

Wind No.	No. of Layers	Spool Tension(1) lb (N)	Winding Tension(2) lb (N)	Stress Retention Factor(3) (SRF)	Oven Ramp Rate (°C/min)
17	1	2.5 (11.1)	0.8 (3.5)	0.32	1.0
10	1	5.0 (22.2)	2.4 (10.7)	0.48	1.0
10a2	1	5.5 (24.5)	3.7 (16.5)	0.67	1.0
14a	1	5.0 (22.2)	1.5 (6.6)	0.30	1.0
19	1	8.1 (36.0)	3.8 (16.9)	0.47	1.0
25	1	7.9 (35.1)	4.0 (17.8)	0.51	0.2
24	1	8.0 (35.6)	3.0 (13.3)	0.38	0.5
26	1	8.1 (36.0)	3.0 (13.3)	0.37	0.5
27	1	8.2 (36.5)	3.9 (17.3)	0.48	0.5
29	1	7.7 (34.2)	2.5 (11.1)	0.33	2.0
21	2	5.3 (23.6)	3.3 (14.7)	0.62	1.0
23	3	5.1 (22.7)	1.9 (8.5)	0.37	1.0

(1) Spool Tension was measured during winding using the 3-pulley tension measurement device
(2) Winding Tension is calculated from the mandrel strain after room temperature fiber tension loss has occurred. For multi-layer winds, the indicated data reflect the strain imposed after winding only the first layer
(3) Stress Retention Factor = Winding Tension / Spool Tension

All winds had a circuit-to-circuit spacing of 0.12 inches (3.05×10^{-3} m). This spacing was used in an attempt to wind an even, continuous layer of prepreg onto the mandrel.

Two sets of experiments are analyzed here. First, in order to confirm the repeatability of the experimental data, all winds which have the same nominal spool tension and oven ramp rate are compared. Second, a parametric study was performed to measure the effect of spool tension and oven ramp rate on RFTL. The first set of winds in the parametric study (17,10,10a2,14a,19) had a constant oven ramp rate of 1 °C/min and the nominal spool tension was varied from 2.5 lb (11.1 N) to 8.0 lb (35.6 N). In the second set of winds (19,24,25,26,27,29), the nominal spool tension was held constant at 8.0 lb and the oven ramp rate was varied from 0.2 to 2.0 °C/min.

No comparable parametric study was performed for the multi-layer winds. The purpose of the multi-layer experiments was to determine the ability of FWEXPAND to simulate the effect of RFTL in these winds. This is discussed in Section 5.4.2.

5.3.1 Repeatability of Tension Loss During Winding

The groups of winds which compose the repeatability studies are subsets of the winds in Table 4. The repeatability of the Stress Retention Factor (SRF) during winding was studied using the winds shown in Table 5. The SRF for the 5.0 lb winds averages 0.48 ± 0.18 (38% of average), and for the 8.0 lb winds it averages 0.42 ± 0.09 (21% of average). Overall for the nine winds the average SRF was 0.44 ± 0.14 (32% of average). Two observations concerning this data can be made. First, the low average SRF reflects a relatively large amount of tension loss in that 56% of the spool tension is lost in the

Table 5. T40/1908 prepreg winds used in the Stress Retention Factor (SRF) repeatability study

Wind No.	No. of Layers	Spool Tension lb (N)	Winding Tension lb (N)	Stress Retention Factor (SRF)	Oven Ramp Rate (°C/min)
10	1	5.0 (22.2)	2.4 (10.7)	0.48	1.0
10a2	1	5.5 (24.5)	3.7 (16.5)	0.67	1.0
14a	1	5.0 (22.2)	1.5 (6.6)	0.30	1.0
19	1	8.1 (36.0)	3.8 (16.9)	0.47	1.0
25	1	7.9 (35.1)	4.0 (17.8)	0.51	0.2
24	1	8.0 (35.6)	3.0 (13.3)	0.38	0.5
26	1	8.1 (36.0)	3.0 (13.3)	0.37	0.5
27	1	8.2 (36.5)	3.9 (17.3)	0.48	0.5
29	1	7.7 (34.2)	2.5 (11.1)	0.33	2.0

winding stage, before cure begins. A comparable calculation for all of the dry T40 fiber winds in Table 6 gave an average SRF of 0.77 ± 0.23 (30% of average), which is higher than the average prepreg SRF by 0.33. Second, the repeatability of the SRF is not very good, with a total deviation from average of 32% for the prepreg winds. The following sources are possible contributors to this error:

- Variation of spool tension during winding - the readout from the load cell in the tension measurement device typically changed ±5% during winding
- Actual difference in SRF between winds - possibly caused by different amounts of bandwidth narrowing (described in Section 4.3) and the resulting

Table 6. Dry T40 fiber winds used in the Stress Retention Factor (SRF) repeatability study

Wind No.	No. of Layers	Spool Tension lb (N)	Winding Tension lb (N)	Stress Retention Factor (SRF)	Oven Ramp Rate (°C/min)
16	1	2.4 (10.7)	1.3 (5.8)	0.54	1.0
15	1	5.0 (22.2)	4.6 (20.5)	0.92	1.0
11a	1	5.0 (22.2)	4.3 (19.1)	0.86	1.0
11	1	5.1 (22.7)	4.1 (18.2)	0.80	1.0
28	1	5.0 (22.2)	4.0 (17.8)	0.80	1.0
18	1	7.5 (33.4)	5.4 (24.0)	0.72	1.0

difference in the shape of the tow cross-section

However, of significance is the large amount of tension loss (low SRF) in the prepreg compared to that in the dry fiber. The tension loss in the prepreg occurred at room temperature prior to the cure stage and the associated low resin viscosity. During the time period between winding and the start of cure (30-60 minute interval), significant tension loss occurs. There are two possible explanations for this. First, it may be due to the plastic deformation and flattening of the resin impregnated tow bundle. The flattening of the prepreg tow causes a time-dependent decrease in mandrel strain. Second, the fiber and resin may behave like a parallel spring/dashpot mechanical system in which the elastic fiber serves as the spring and the soft, plastic resin serves as the dashpot.

Because the fiber and matrix are partially bonded together, the tensioned fiber exerts shear stress on the resin, which deforms plastically over a period of time. Equilibrium occurs when the shear stress exerted by the fiber is balanced by the opposing stress in the resin. In either case, the time-dependency of the mandrel strain relaxation is in contrast to the tension loss in the dry fiber tow which occurs virtually instantaneously.

The loss of tension during winding was investigated by performing a set of experiments using dry fiber and prepreg material. The objective of these experiments was to measure mandrel strain during the winding operation to observe fiber tension immediately following contact with the mandrel. To minimize the twisting of the strain gage leadwires during the measurement, the axial length of the mandrel on which winds were placed was limited to one inch. This length was determined by previous measurements which showed that the gages only detect strain caused by circuits which are located within 0.5 inch of the gages. The DAS was set to record data every 3 seconds, which was the maximum frequency available.

Figures 20 and 21 show mandrel strain versus time for the dry fiber and prepreg relaxation experiments during four phases of the winding operation, including: 1) when the mandrel is free of any loading by the endcaps or windings, 2) when the endcaps are installed, 3) during the actual winding process, and 4) when the endcaps are removed. Of greatest interest is the third phase. In Figure 20, for the dry fiber experiment, the mandrel strain increases in magnitude from about -12$\mu\varepsilon$ to -90$\mu\varepsilon$, and then holds constant at -90$\mu\varepsilon$ over the next 20 minutes. No strain relaxation was observed, which indicates

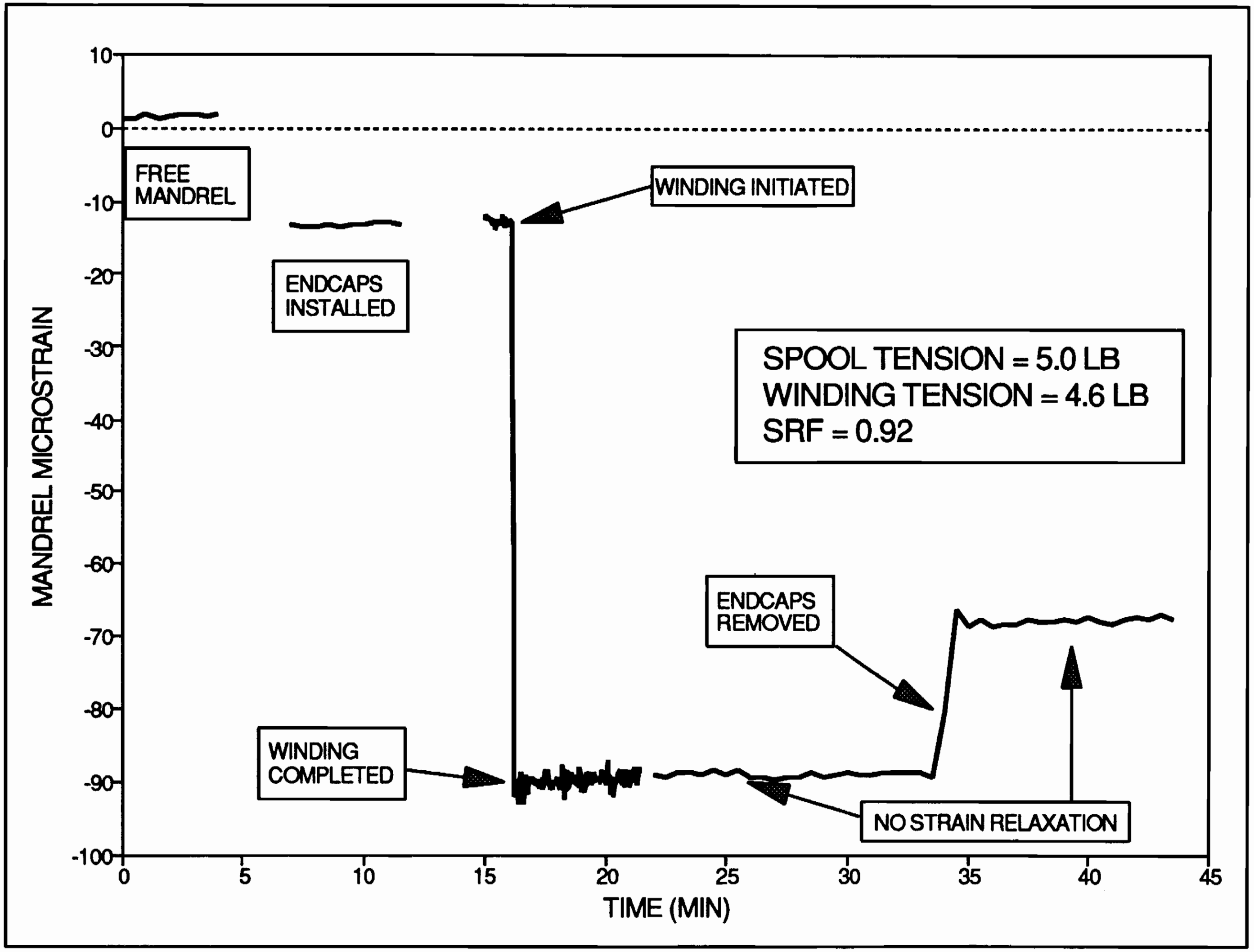

Figure 20. Variation of mandrel strain during the winding of dry T40 fiber

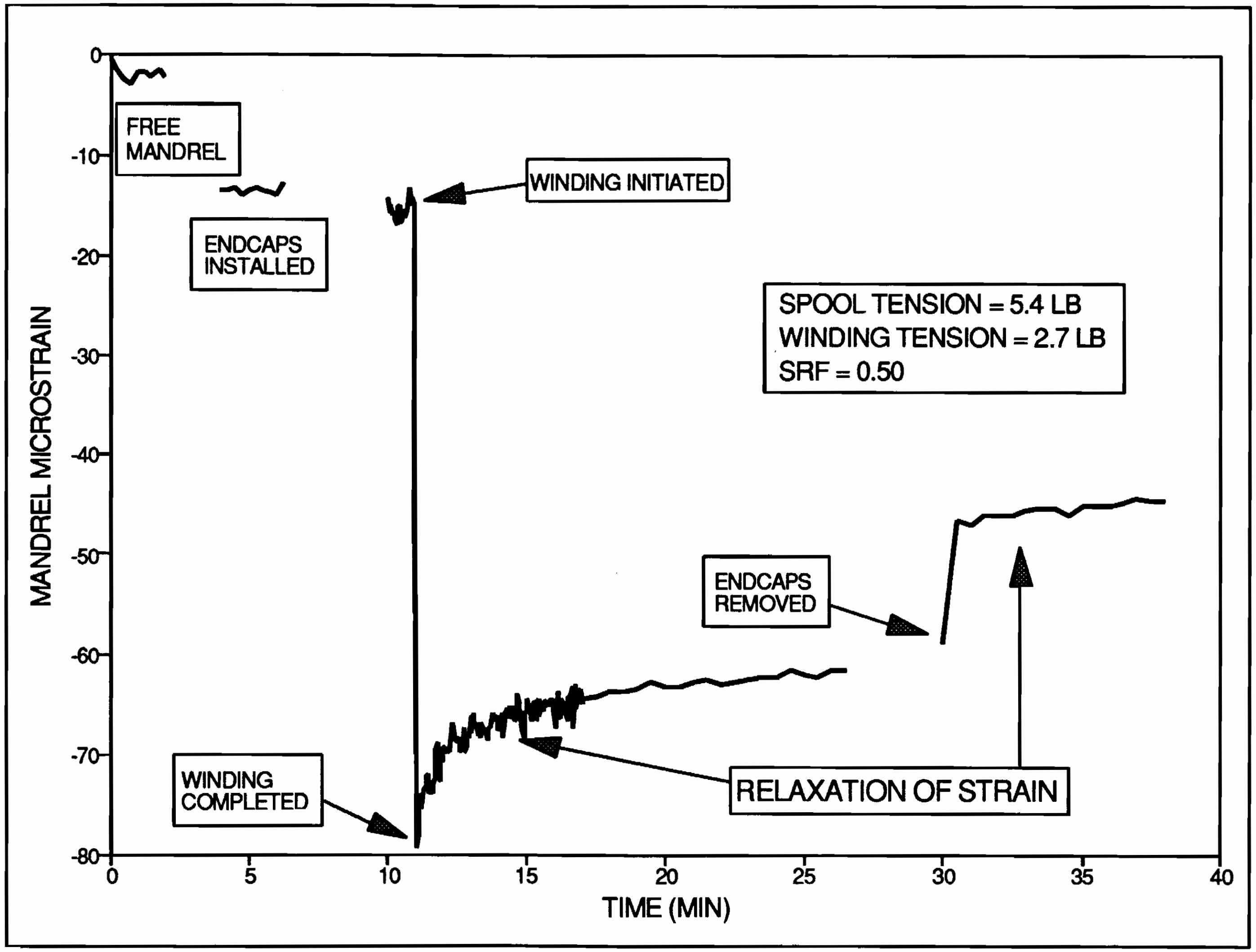

Figure 21. Variation of mandrel strain during the winding of T40/1908 prepreg

that all of the tension loss was instantaneous upon contact with the mandrel. This loss was approximately 8% of the spool tension.

In Figure 21, for the prepreg wind, the mandrel strain increases from about -15με to -80με and then decreases asymptotically to about -60με. This relaxation of strain represents a loss of about 30% of the spool tension, due entirely to what has been called viscoplastic tension loss (VTL). However, the total tension loss was about 50%. The remaining 20% loss occurred during the 3 second interval between data acquisitions and is assumed to consist of both VTL and side-by-side tension loss. Call [10] found that for the same mandrel, the side-by-side loss for wet winding ranged from 17-23%, depending on the material wound, and was independent of spool tension. This is roughly equal to the 20% loss which was unaccounted for above. If an analog strain recorder was used it would not be limited by minimum logging intervals, and would provide a better measure of the viscoplastic and side-by-side tension loss.

5.3.2 Repeatability of Tension Loss During Cure

The repeatability of tension loss during cure (RFTL) can be seen in Figures 22 and 23 which show mandrel strain and temperature for the six winds shown in Table 7. The objective of this study was to determine the repeatability of the experimental data when the processing parameters were held constant. Figure 22 presents the data for three winds which all have nominal spool tensions of 5.0 lb and ramp rates of 1 °C/min, and Figure 23 presents three winds which have spool tensions of 8.0 lb and ramp rates of 0.5 °C/min.

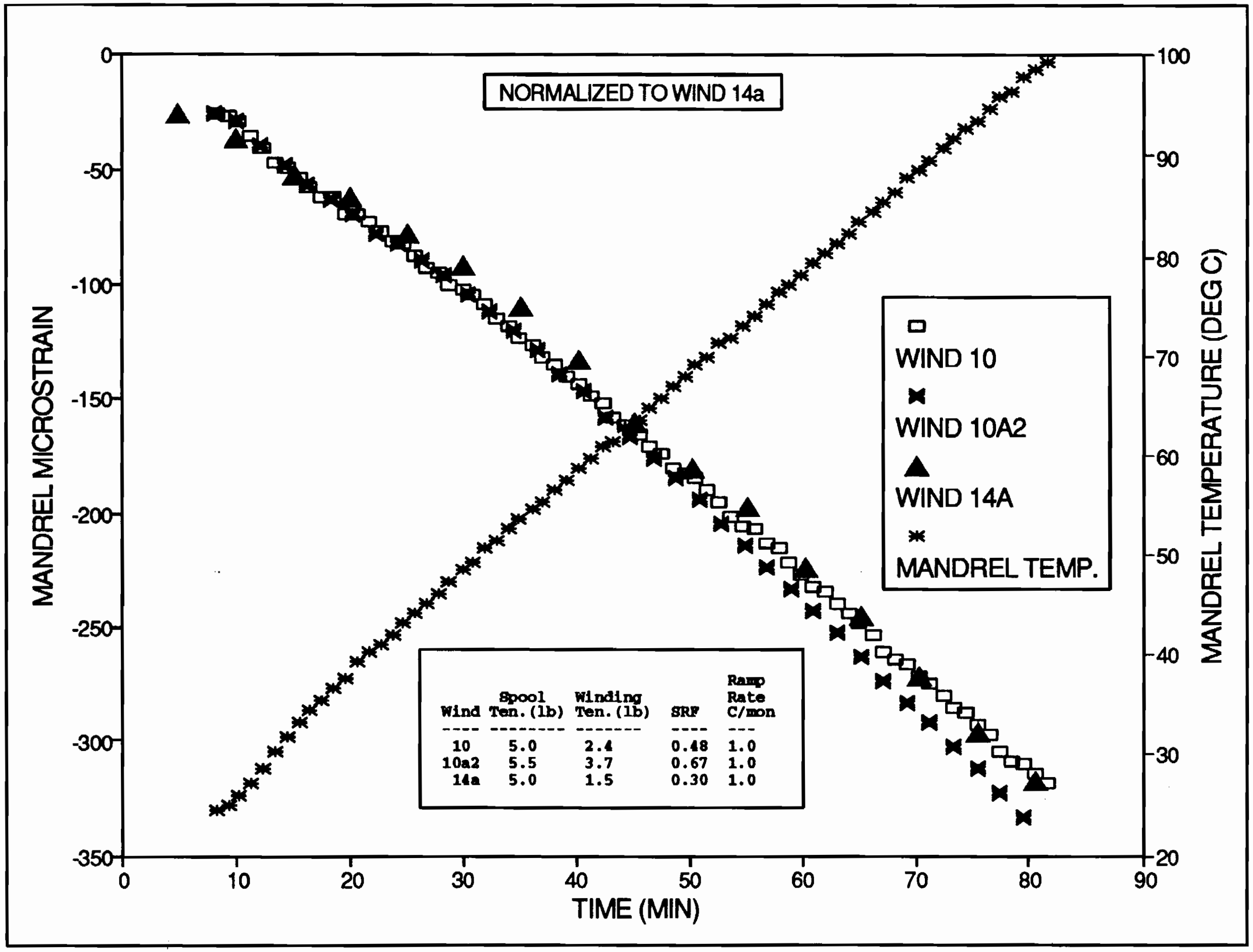

Figure 22. Repeatability of mandrel strain for single layer winds of T40/1908 prepreg (5.0 lb spool tension, 1.0 °C/min. ramp rate)

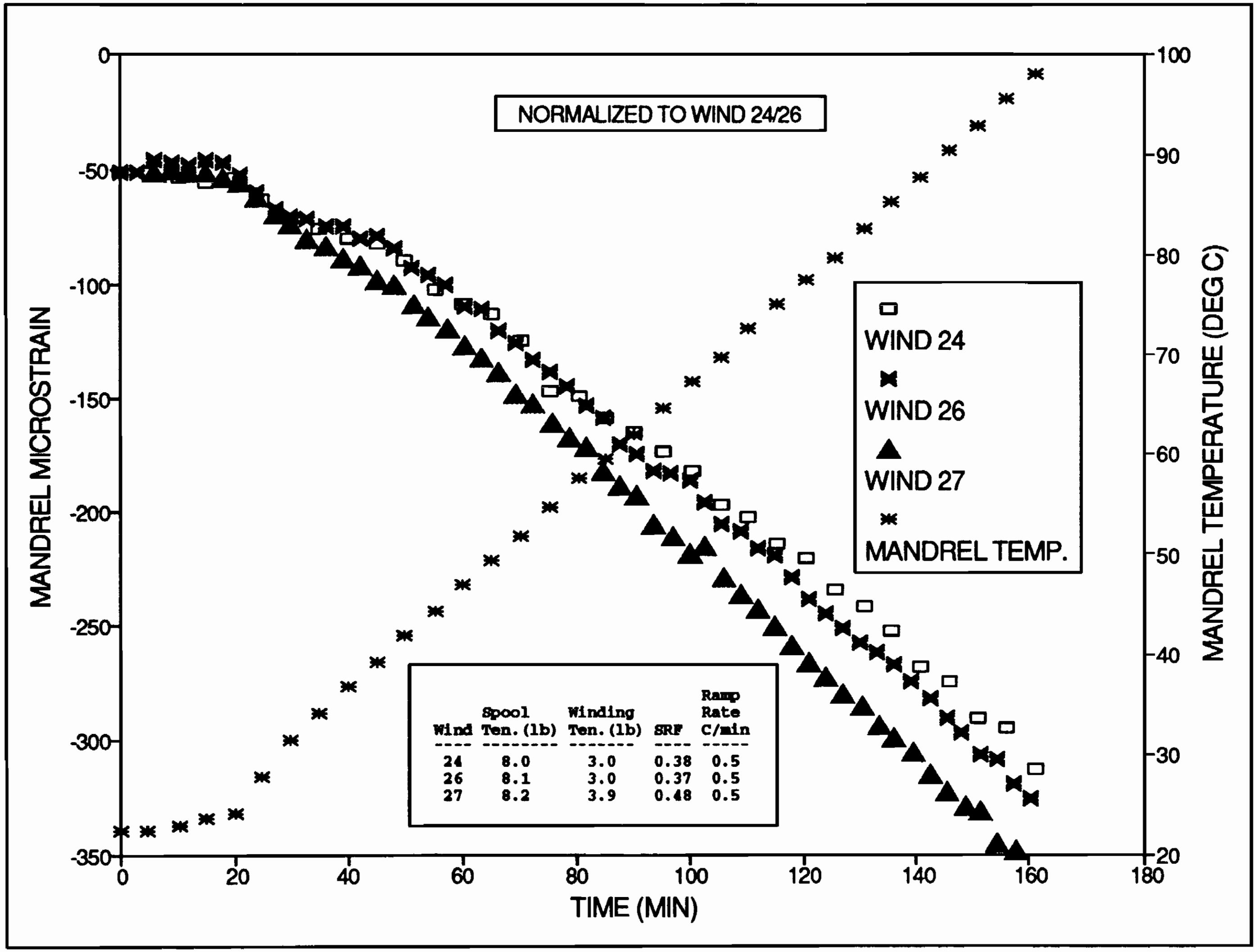

Figure 23. Repeatability of mandrel strain for single layer winds of T40/1908 prepreg (8.0 lb spool tension, 0.5 °C/min. ramp rate)

Table 7. T40/1908 prepreg winds used to study the repeatability of tension loss during cure

Wind No.	No. of Layers	Spool Tension lb (N)	Winding Tension lb (N)	Stress Retention Factor (SRF)	Oven Ramp Rate (°C/min)
10	1	5.0 (22.2)	2.4 (10.7)	0.48	1.0
10a2	1	5.5 (24.5)	3.7 (16.5)	0.67	1.0
14a	1	5.0 (22.2)	1.5 (6.6)	0.30	1.0
24	1	8.0 (35.6)	3.0 (13.3)	0.38	0.5
26	1	8.1 (36.0)	3.0 (13.3)	0.37	0.5
27	1	8.2 (36.5)	3.9 (17.3)	0.48	0.5

In order to remove the initial difference in strain, caused by differences in tension loss during winding, the strain curves in both figures have been normalized. This normalization involved shifting the curves in the positive or negative strain direction so that the initial mandrel strain was the same for each case. The mandrel temperature, which was the same for all winds, is shown as well for reference.

The curves in Figure 22 show very good repeatability, especially in the early portion of the curve (10-40 min) where most of the RFTL occurs. Even at the end of the ramp, the strain values vary by only 25με. In Figure 23, Wind 27 experiences less tension loss during the 30-50 minute interval than do Winds 24 and 26. There were no anomalies in the experimental procedure for this wind, except that there was less bandwidth narrowing. The bandwidth for Wind 27 was estimated at 0.09-0.11 inches, and was 0.06-0.11 inches for Winds 24 and 26. A narrower bandwidth results in a greater layer thickness and more potential for tow deformation and flattening. This flattening would tend to reduce the mandrel strain in those winds where bandwidth narrowing was more prominent.

5.3.3 Parametric study of the effect of Spool Tension on RFTL

Table 8 shows the winds used to empirically study the effect of spool tension on tension loss during cure. These winds were all cured using a ramp rate of 1 °C/minute.

Table 8. T40/1908 prepreg winds used to study the effect of spool tension on experimentally measured RFTL

Wind No.	No. of Layers	Spool Tension lb (N)	Winding Tension lb (N)	Stress Retention Factor (SRF)	Oven Ramp Rate (°C/min)
17	1	2.5 (11.1)	0.8 (3.5)	0.32	1.0
10	1	5.0 (22.2)	2.4 (10.7)	0.48	1.0
10a2	1	5.5 (24.5)	3.7 (16.5)	0.67	1.0
14a	1	5.0 (22.2)	1.5 (6.6)	0.30	1.0
19	1	8.1 (36.0)	3.8 (16.9)	0.47	1.0

Figure 24 shows mandrel strain and temperature for the five winds in Table 8. Three of these winds had spool tensions of 5.0 lb, and the other two had 2.5 and 8.0 lb spool tensions. The same mandrel temperatures was used for all five winds. With all winds

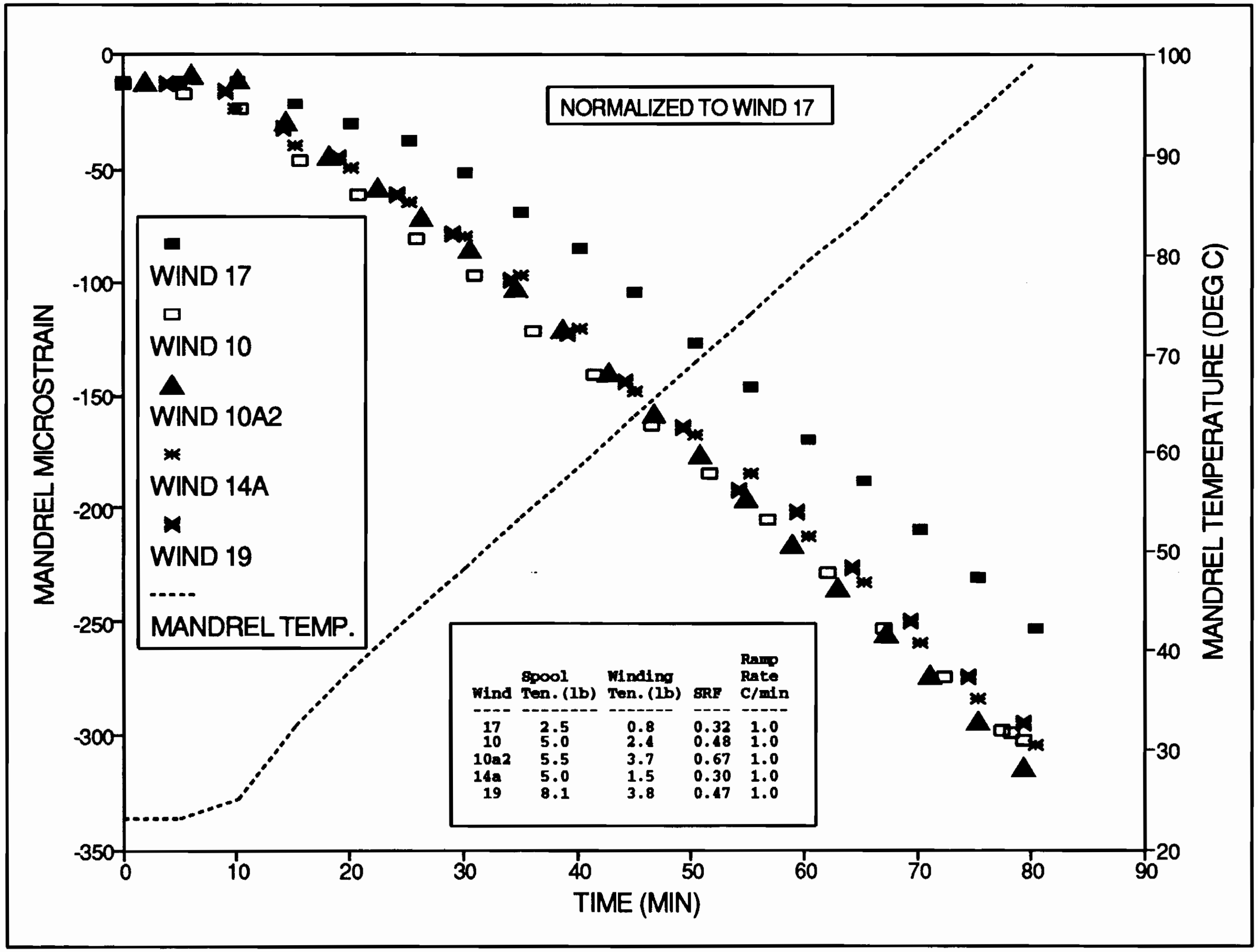

Figure 24. Effect of spool tension on mandrel strain for single layer winds of T40/1908 prepreg (2.5, 5.0 and 8.0 lb spool tensions)

normalized to account for differences in tension loss during winding, as described previously, the mandrel strain for the winds having spool tensions of 5.0 and 8.0 lb are nearly identical. But the wind having 2.5 lb of spool tension (Wind 17) experiences significantly less strain buildup and more tension loss during heatup. One explanation for this deviation from the higher tension winds is as follows. At higher levels of spool tension (5.0 lb and above), the fibers in the prepreg experience a substantial, though limited, amount of compaction during winding. But the lower spool tension of 2.5 lb causes less compaction, leaving more matrix through which the fibers can migrate during cure. In all of the winds, maximum compaction is achieved by approximately 60 minutes into cure, as shown by the linearity of the data.

5.3.4 Parametric Study of the Effect of Oven Ramp Rate on RFTL

Table 9 shows the winds used to empirically study the effect of oven ramp rate on tension loss during cure. Since the ramp rate is different for several of these winds, the mandrel strain data shown in Figure 25 is plotted against mandrel temperature rather than time. Three of these winds had a ramp rate of 0.5 °C/min and the other three were heated at 0.2, 1.0, and 2.0 °C/min. Again, all of the winds were normalized to account for differences in tension loss during winding. With the exception of the anomalous behavior of Wind 27, discussed previously, all of the winds experience the same approximate mandrel strain. This can be explained from Figure 6 in that the viscosity profile of the resin is the same for all heating rates (1.0 - 10.0 °C/min) up to a resin

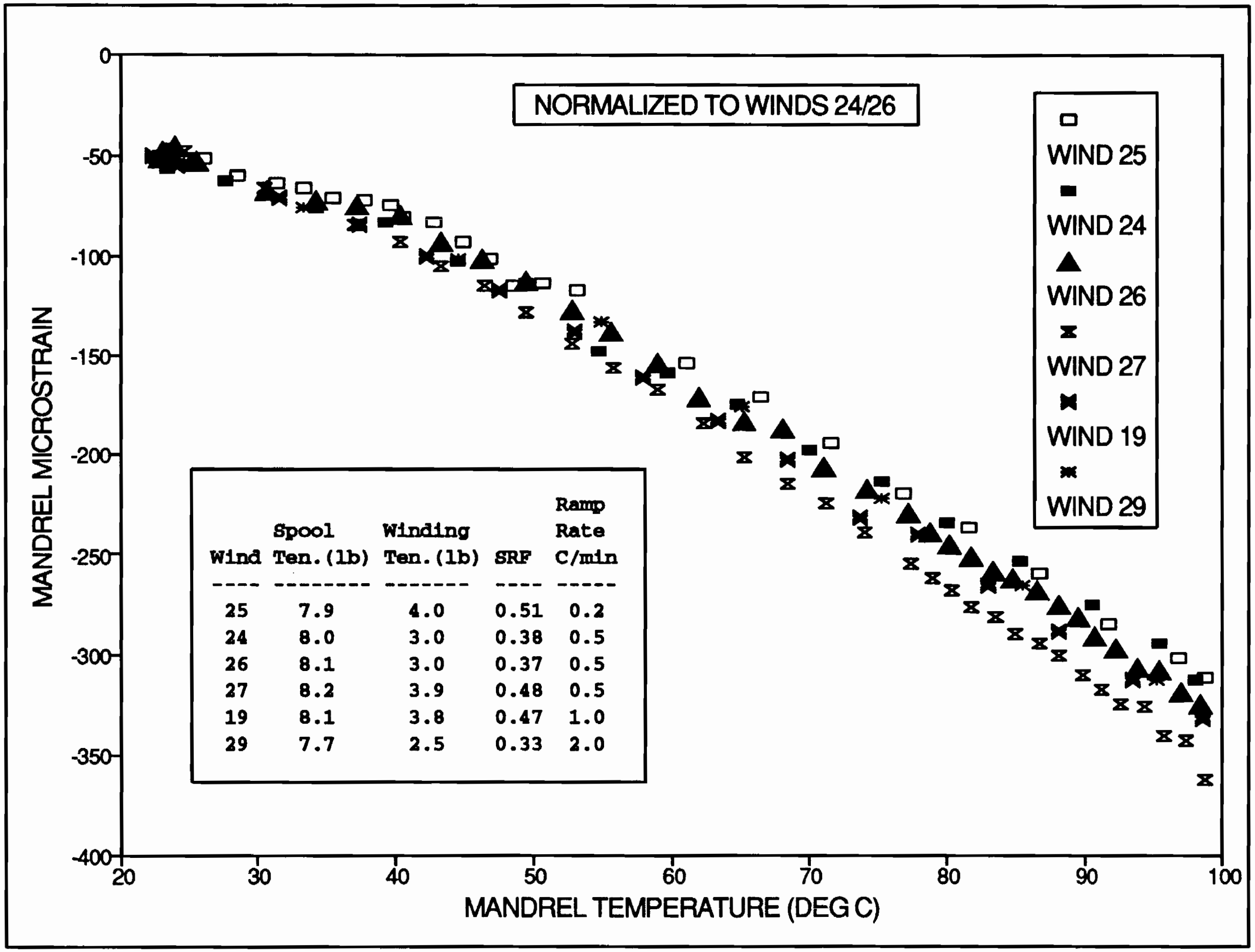

Wind	Spool Ten. (lb)	Winding Ten. (lb)	SRF	Ramp Rate C/min
25	7.9	4.0	0.51	0.2
24	8.0	3.0	0.38	0.5
26	8.1	3.0	0.37	0.5
27	8.2	3.9	0.48	0.5
19	8.1	3.8	0.47	1.0
29	7.7	2.5	0.33	2.0

Figure 25. Effect of oven ramp rate on mandrel strain for single layer winds of T40/1908 prepreg (0.2, 0.5, 1.0, and 2.0 °C/min. ramp rates)

Table 9. T40/1908 prepreg winds used to study the effect of oven ramp rate on experimentally measured RFTL

Wind No.	No. of Layers	Spool Tension lb (N)	Winding Tension lb (N)	Stress Retention Factor (SRF)	Oven Ramp Rate (°C/min)
25	1	7.9 (35.1)	4.0 (17.8)	0.51	0.2
24	1	8.0 (35.6)	3.0 (13.3)	0.38	0.5
26	1	8.1 (36.0)	3.0 (13.3)	0.37	0.5
27	1	8.2 (36.5)	3.9 (17.3)	0.48	0.5
19	1	8.1 (36.0)	3.8 (16.9)	0.47	1.0
29	1	7.7 (34.2)	2.5 (11.1)	0.33	2.0

temperature of 85°C. Therefore, the ability of the resin and fiber to flow or migrate is the same for all of these winds, and virtually full compaction and RFTL has occurred by the time a difference in heating rate has caused a difference in resin viscosity.

5.3.5 Parametric Study of the Effect of the Number of Layers on RFTL

Table 10 shows the winds used to empirically study the effect of the number of layers on tension loss during cure. All of these winds had a ramp rate of 1°C/min and a nominal spool tension of 5.0 lb. Figure 26 shows the mandrel strain during heatup for Winds 10, 21, 23 and 31 representing 1, 2, 3 and 5-layer winds. Only one single layer wind (Wind 10) is shown to provide clarity in the figure. Wind 10 is representative of the three single layer winds in Table 10, as can be seen in Figure 22.

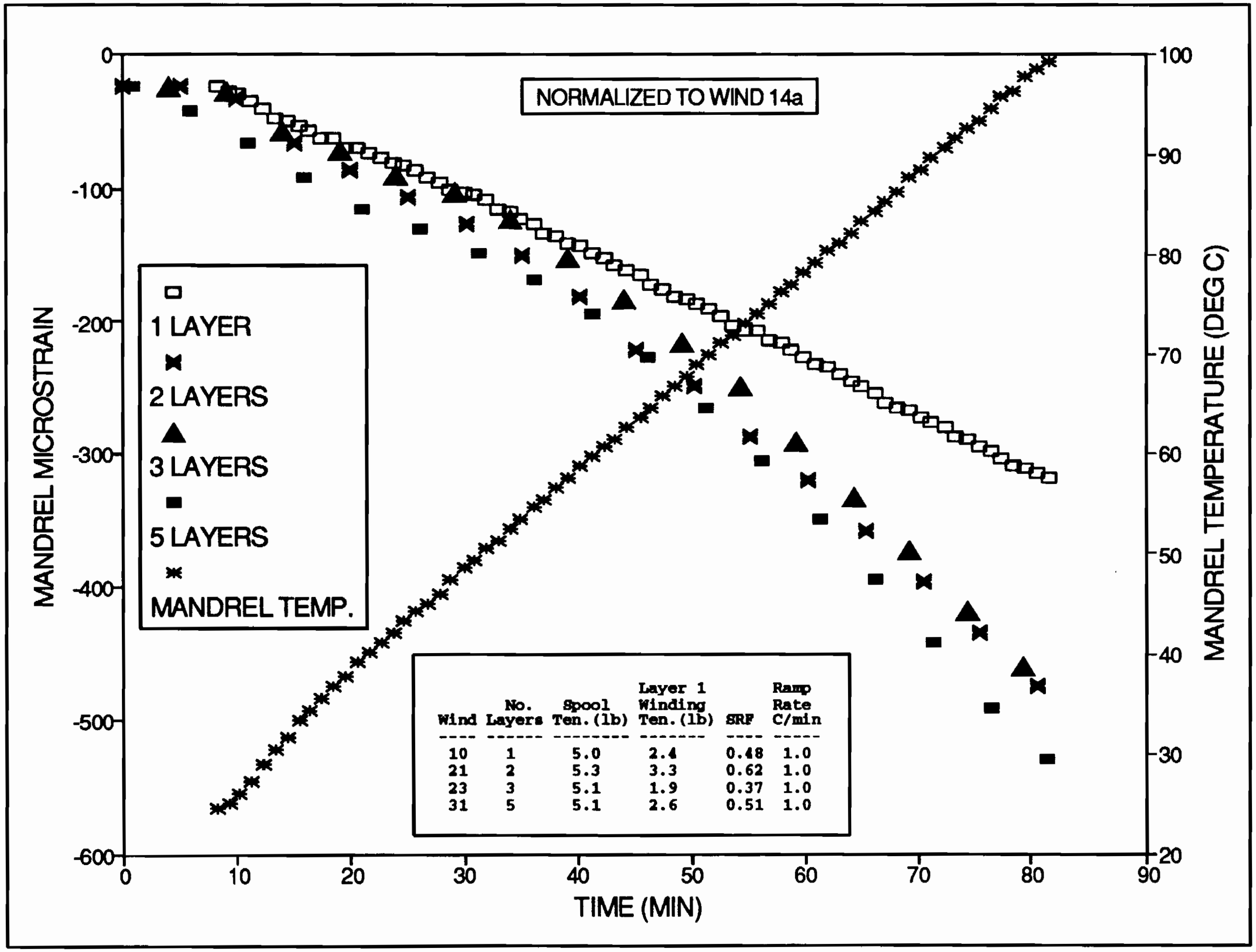

Figure 26. Effect of the number of layers on mandrel strain for 1, 2, 3, and 5-layer winds of T40/1908 prepreg (5.0 lb spool tension, 1.0 °C/min. ramp rate)

Table 10. T40/1908 winds used to study the effect of the number of layers on experimentally measured RFTL

Wind No.	No. of Layers	Spool Tension lb (N)	Winding Tension lb (N)	Stress Retention Factor (SRF)	Oven Ramp Rate (°C/min)
10	1	5.0 (22.2)	2.4 (10.7)	0.48	1.0
10a2	1	5.5 (24.5)	3.7 (16.5)	0.67	1.0
14a	1	5.0 (22.2)	1.5 (6.6)	0.30	1.0
21	2	5.3 (23.6)	3.3 (14.7)	0.62	1.0
23	3	5.1 (22.7)	1.9 (8.5)	0.37	1.0
30	1	7.8 (34.7)	2.4 (10.7)	0.31	1.0
31	5	5.1 (22.7)	2.6 (11.6)	0.51	1.0

In Figure 26, it can be seen that increasing the number of layers has little effect on the rate of tension loss since the slopes of all four curves are approximately equal during the 10-35 minute time interval. However, the slopes of the curves for the multi-layer winds continue to increase up to the 60-80 minute interval, when compaction is nearly complete and the curves are nearly linear. This shows that, though the rates of tension loss are nearly equal, resin flow occurs for a longer period of time with an increasing numbers of layers. The effect of RFTL on mandrel strain can be seen by extrapolation of the linear portions of the curves to the onset of heatup (time=10 minutes). The difference in strain between the four extrapolated lines at 10 minutes represents the overall effect of RFTL on mandrel strain. As expected, the difference in strain increases with an increasing number of layers since there is more excess resin which flows to the outer surface of the composite.

5.4 Comparison of Measured and Calculated Mandrel Strain and Pressure

The computer code FWEXPAND, which predicts the change in fiber tension during cure due to RFTL and mandrel expansion, was used to simulate five of the prepreg winds discussed in Section 5.3. These winds, shown in Table 11, include three single layer winds each having different spool tensions, and two multi-layer winds (2 and 3-layer).

Table 11. Winds simulated using FWEXPAND

Wind No.	No. of Layers	Experimen. Spool Tension lb (N)	Experimental Winding Tension lb (N)	Simulated Layer Tensions, lb		
				Layer 1	Layer 2	Layer 3
17	1	2.5 (11.1)	0.8 (3.5)	0.8	---	---
14a	1	5.0 (22.2)	1.5 (6.6)	1.5	---	---
19	1	8.1 (36.0)	3.8 (16.9)	3.8	---	---
21	2	5.3 (23.6)	3.3 (14.7)	1.0	3.3	---
23	3	5.1 (22.7)	1.9 (8.5)	0.5	1.0	1.9

5.4.1 Single Layer Winds

The first step in performing the simulations was to construct a permeability model which best represents the flow of resin through the as-wound fiber network. The best way to do this was to adjust the empirical constants in the permeability model so that the calculated data matched the measured data. Since mandrel strain is used as the experimental measurement of fiber tension, it will be used as the parameter for comparison with the single layer simulations.

Four different permeability models were considered for use in these simulations. All of them relate permeability to porosity, which is equal to the resin volume fraction of the composite. Two were cited by Lundström [14], including one which assumes a hexagonal fiber arrangement and the other a quadratic arrangement. Also investigated were models developed by Cai and Gutowski [2] and by Tzeng [8]. The form of each of these models is provided in Appendix B. The models have empirical constants which were varied to achieve a fit between the measured and calculated mandrel strains in Wind 14a. This wind was selected because it is a single layer wind with an average level of spool tension (5.0 lb), and the unknown multi-layer effects would not be a complicating factor. Figure 27 shows porosity versus permeability for the four permeability models and the values of the empirical constants. Cai and Gutowski's model was found to provide the best fit and was therefore used in the simulations.

The fit for Wind 14a is shown in Figures 28 and 29, which show the measured and calculated mandrel strains and pressures for Wind 14a. The experimental pressures in Figure 29 were calculated from the experimental strains using Equation 4.3 in Section 4.1. All of the simulations in this study used a layer thickness equal to the thickness of

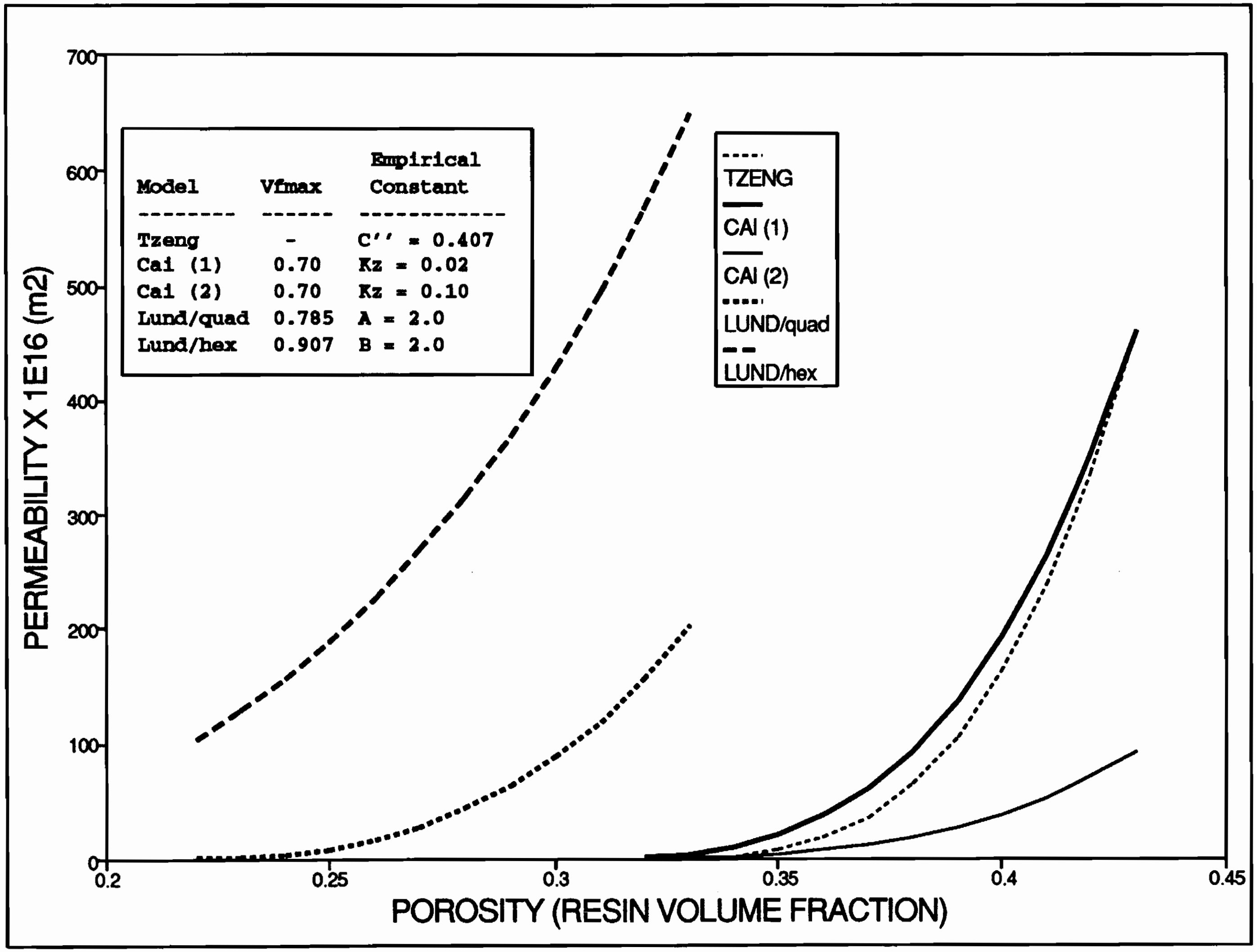

Figure 27. Porosity-permeability characteristics of four permeability models by Tzeng, Cai and Gutowski, and two models by Lundström

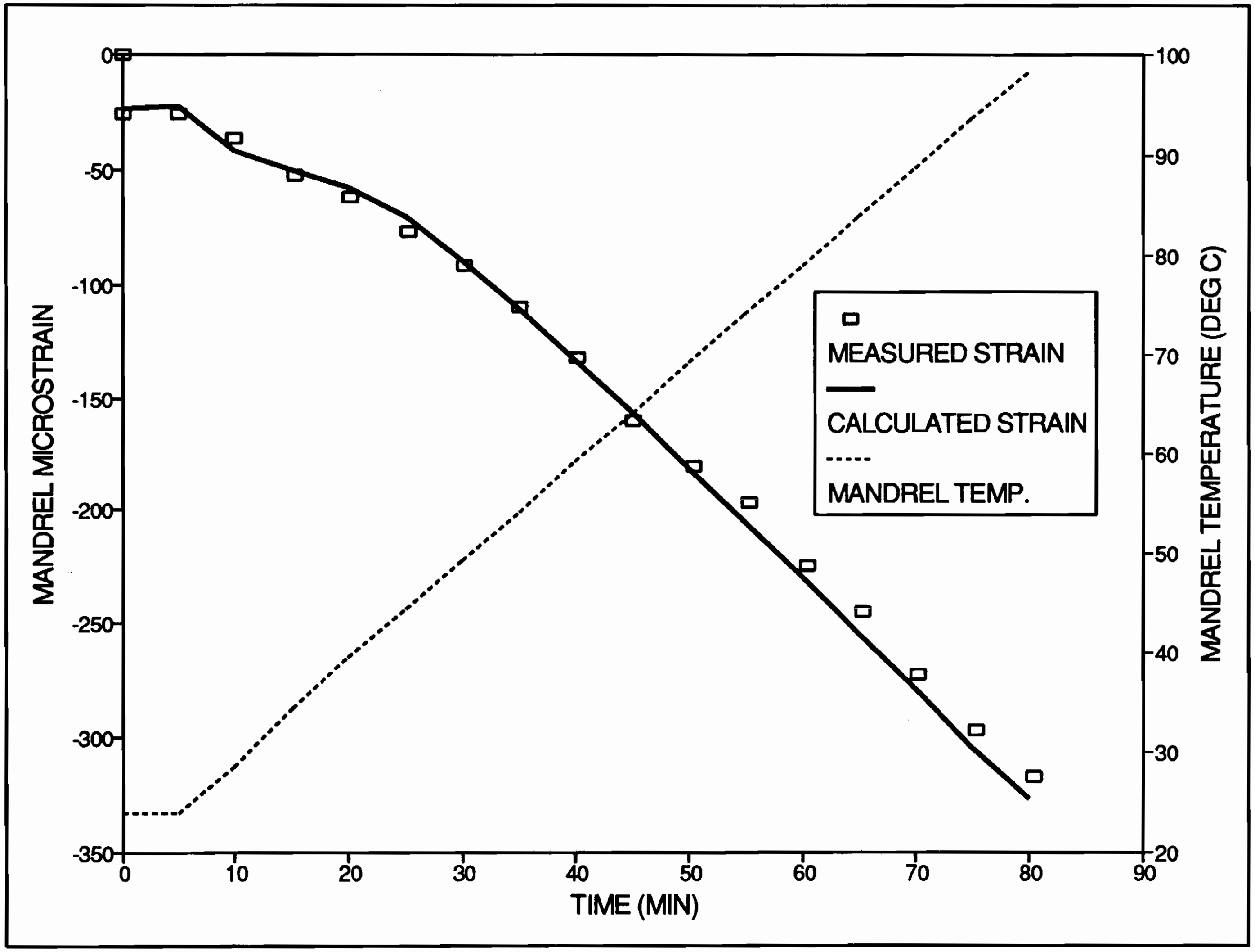

Figure 28. Measured and calculated mandrel strains for a single layer of T40/1908 prepreg (5.0 lb spool tension, Wind 14a)

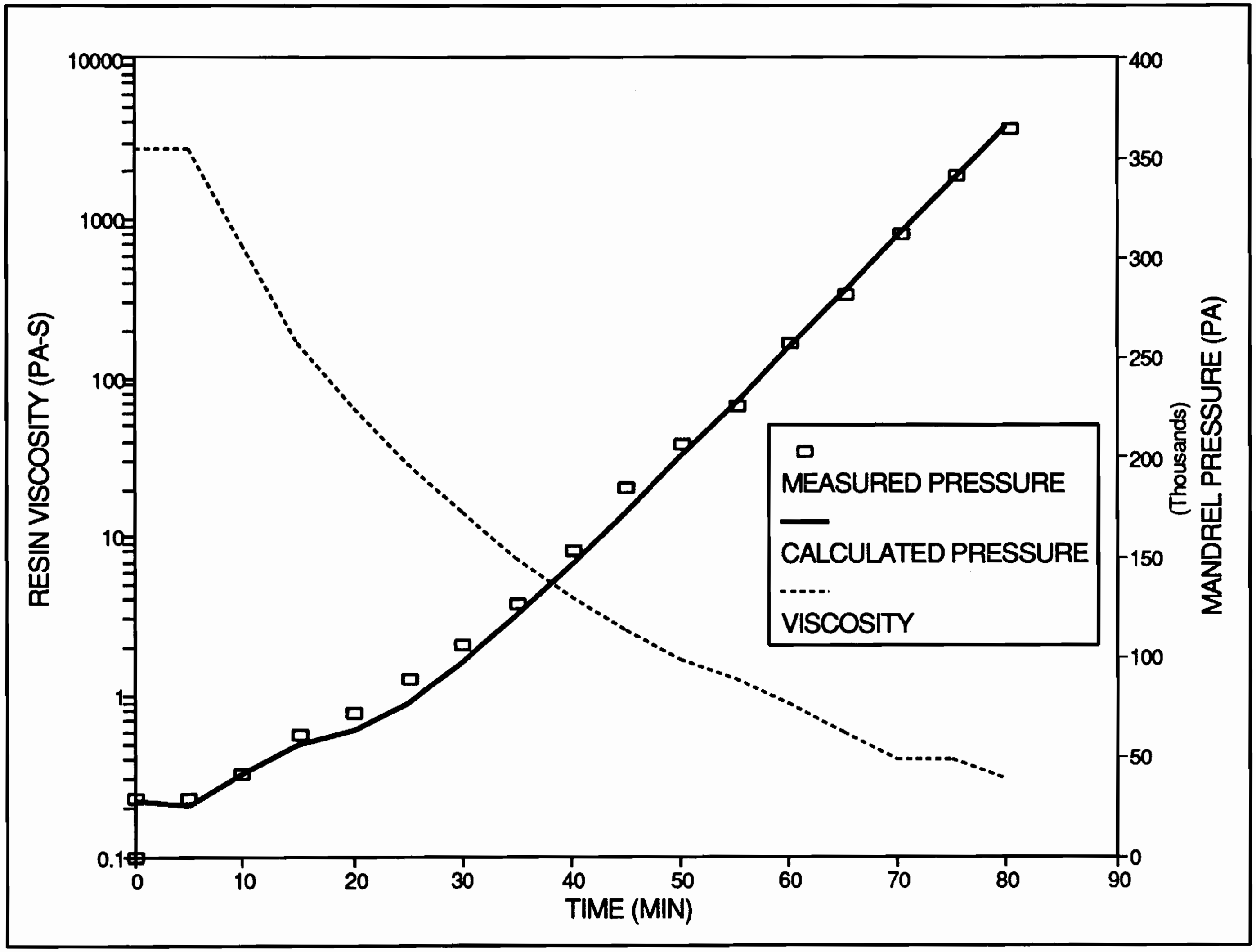

Figure 29. Measured and calculated mandrel pressure and resin viscosity for a single layer wind of T40/1908 prepreg (5.0 lb spool tension, Wind 14a)

the fiber component of the prepreg. The reasons for this were discussed in Section 3.2. This thickness was calculated by multiplying the thickness of the prepreg tow by the fiber volume fraction of the prepreg.

To provide a check on the initial and final resin volume fractions used to perform the fit, micrographs were taken of the cross-sections of uncured and cured prepreg tows. The cured sample was taken from Wind 14a. The micrographs were digitized and analyzed using a PC-based graphics program which quantifies the proportion of resin and fiber in the micrographs.

The micrographs, shown in Figure 30, were taken at 400x and 1000x power. The 400x pictures of the uncured and cured specimens show the reduction in overall thickness of the prepreg due to consolidation. Having higher resolution, the 1000x pictures were used to evaluate resin volume fraction. The resin volume fraction was 0.43 for the uncured specimen and 0.31 for the cured specimen. The supplier's specification for resin content was 0.41, which is relatively close to the measured uncured specimen value of 0.43. Since the supplier's specification of resin content is more representative of the material as a whole, the simulations were run using a resin volume fraction of 0.41 as the initial value. The final resin volume fraction in the simulation is the value at which flow decreases to zero and fiber motion and compaction stop. This minimum resin volume fraction is specified in the permeability model as a maximum fiber volume fraction, $V_{f,max}$. In performing the fit of simulation results to Wind 14a data, the optimal value of $V_{f,max}$ was found to be 0.70. This is very close to the fiber volume fraction of 0.69 determined

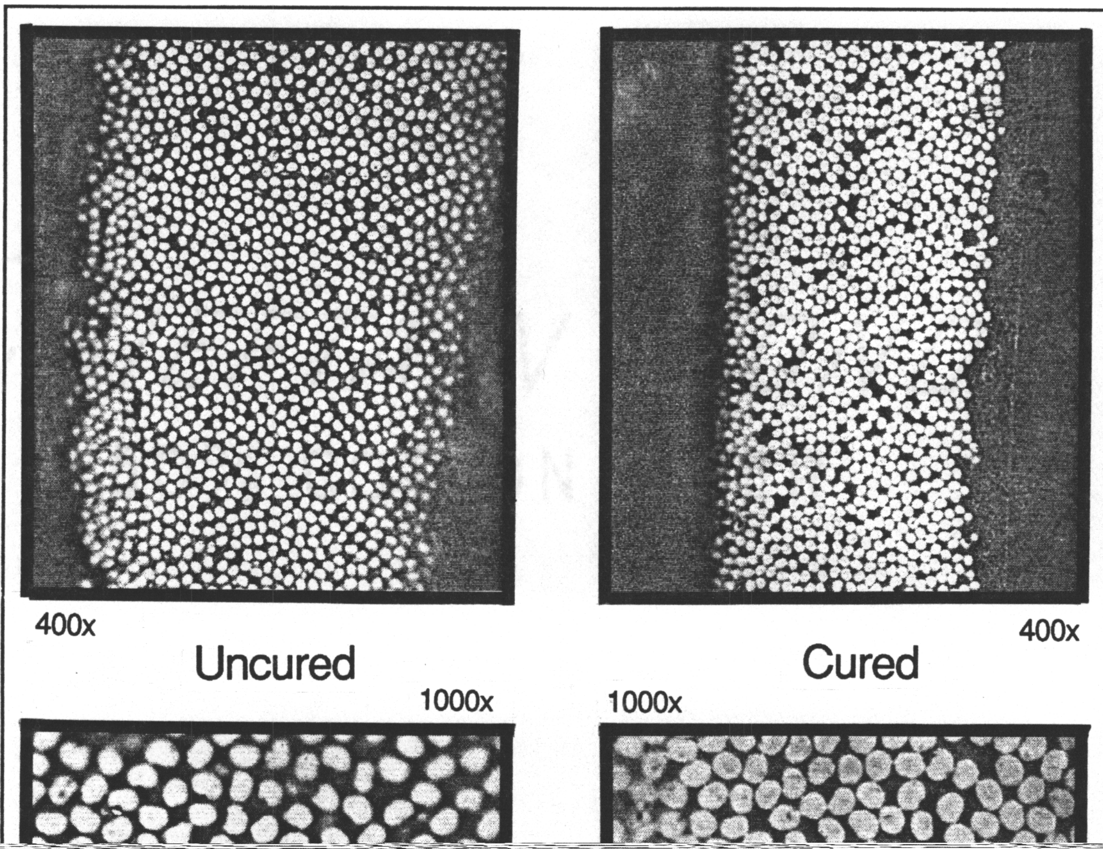

400x
Uncured
1000x
400x
Cured
1000x

from the cured specimen micrograph.

Using the new permeability model, two other single layer winds having different spool tensions were simulated. Figures 31 and 32 show these results for Winds 17 and 19, which have spool tensions of 2.5 and 8.0 lb, respectively. In Figure 32, where the spool tension was 8.0 lb, the simulated strain again fits the data quite well. However, in Figure 31 where the spool tension was 2.5 lb, the measured tension loss is greater than the calculated tension loss, as seen by the slower build-up of strain. The reason for the difference was discussed in Section 5.3.3. At higher spool tensions (5.0 lb and above) there is a larger amount of fiber consolidation which occurs during winding. The consolidation creates a lower effective resin volume fraction at the beginning of cure. However, the lower spool tension (2.5 lb) does not cause as much consolidation during winding so the effective resin volume fraction at the beginning of cure is higher. Since the same manufacturer-specified value of resin volume fraction is used in the simulation of all three winds, the amount of resin flow and fiber tension loss which occurs in the low spool tension wind is underpredicted. Figure 33 shows the effect of increasing the initial resin volume fraction in the simulation from 0.41 to 0.44. The simulation is moderately improved.

A better way to approach the problem may be to fit the permeability model to the data from a very low spool tension wind (1.0 lb or less) in which very little winding consolidation has occurred and the resulting effective resin volume fraction is approximately equal to the manufacturer-specified resin volume fraction. Then when

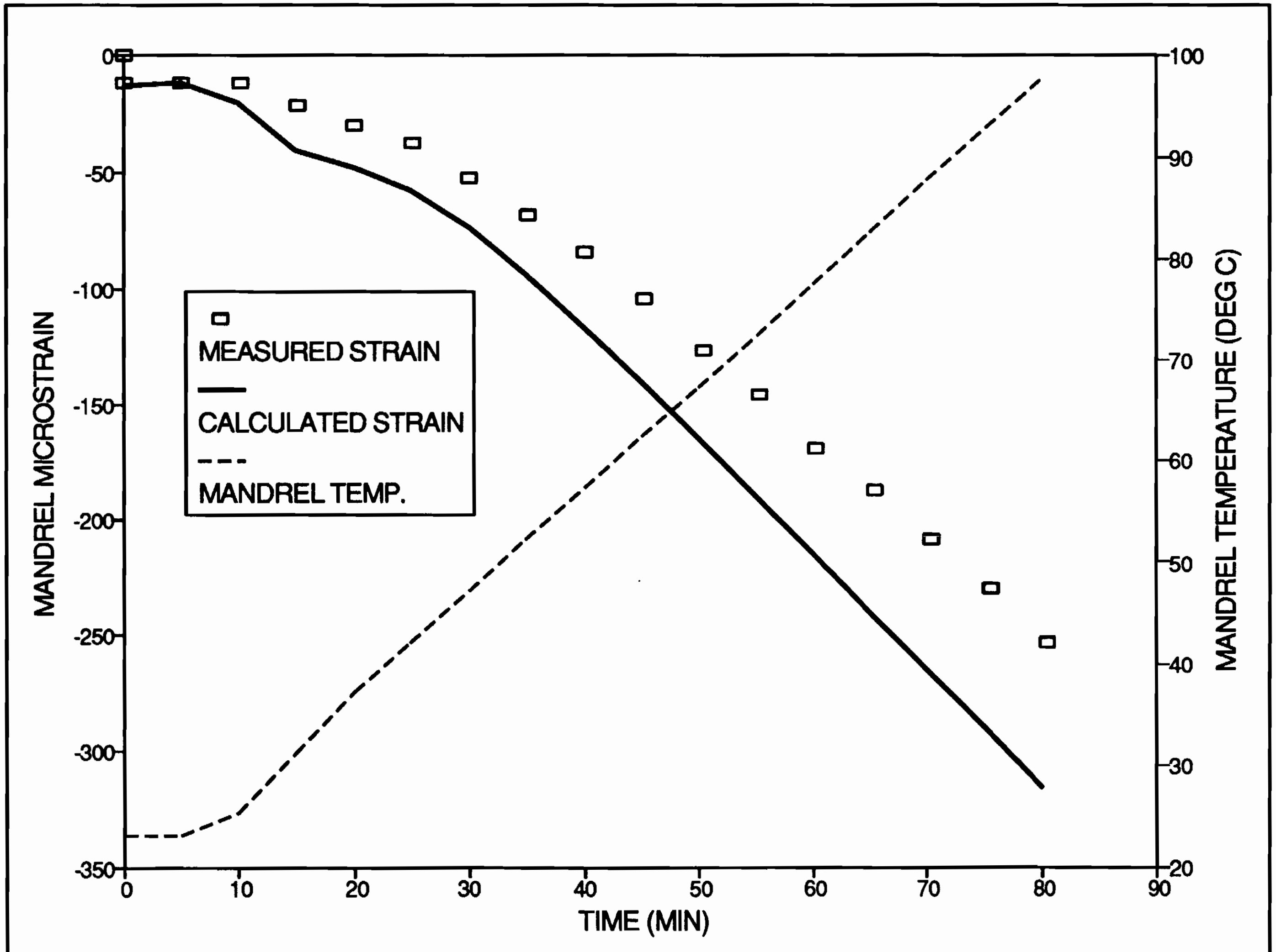

Figure 31. Measured and calculated mandrel strains for a single layer of T40/1908 prepreg (2.5 lb spool tension, Wind 17)

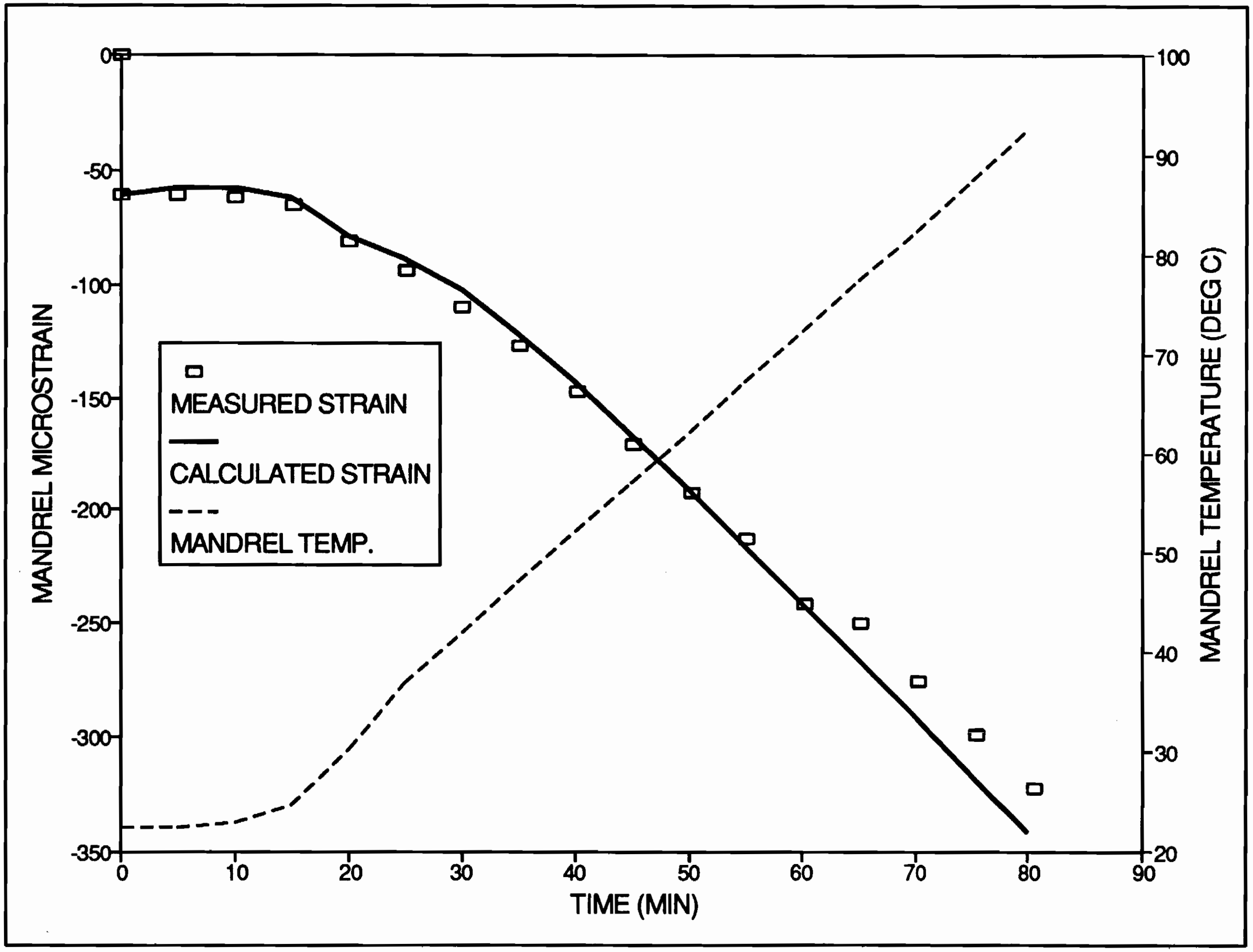

Figure 32. Measured and calculated mandrel strains for a single layer of T40/1908 prepreg (8.1 lb spool tension, Wind 19)

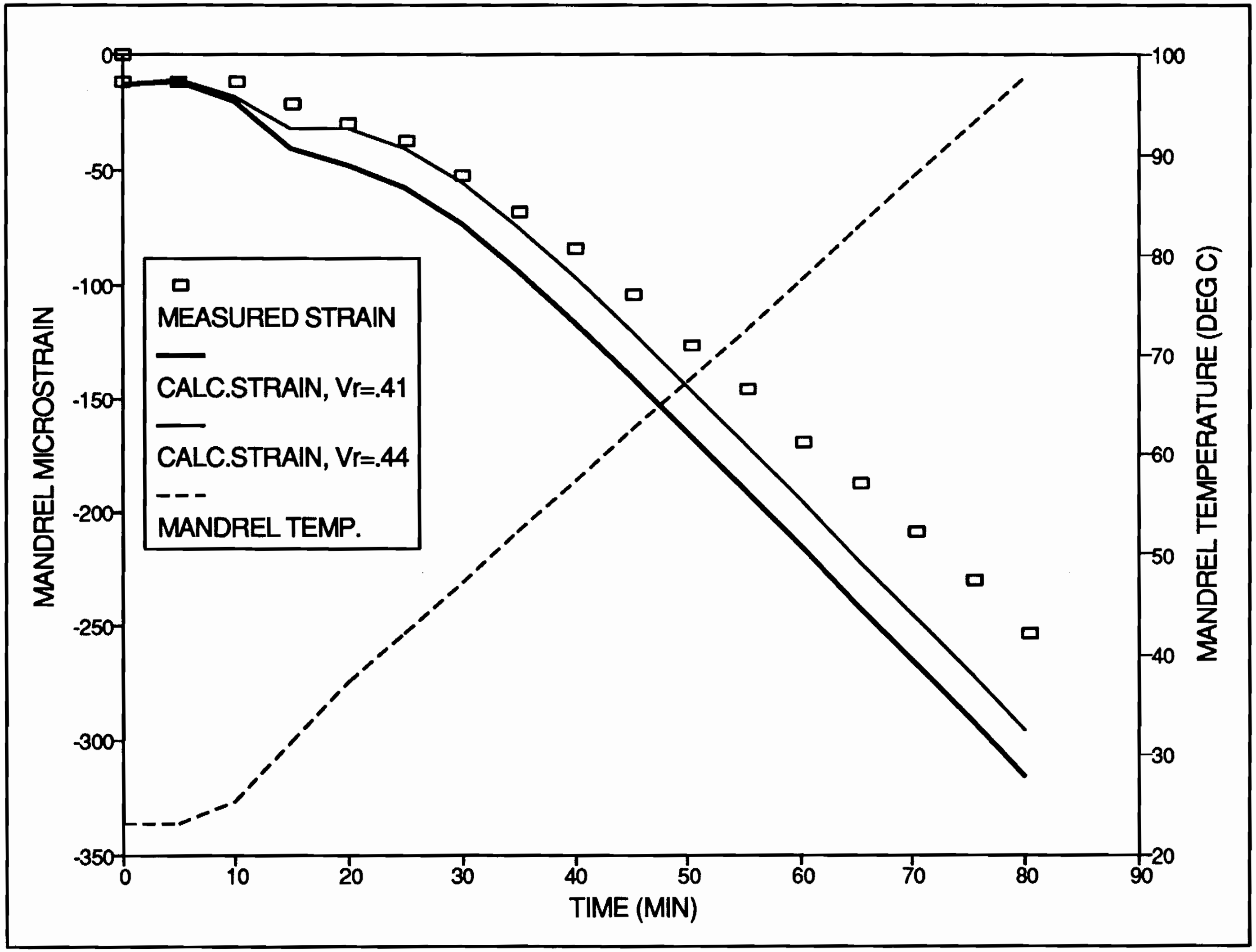

Figure 33. Effect of increased initial resin volume fraction on simulated mandrel strain (2.5 lb spool tension, Wind 17)

simulating the winds having higher spool tensions, the resin volume fraction used in the simulation would need to be lowered to approximate the effective resin volume fraction.

5.4.2 Multi-layer Winds

In multi-layer winds, Multi-Layer tension loss also occurs, as shown in Figure 1. This occurs when the outer layers cause an inward deformation of the inner layers and mandrel reducing the tension of the inner layers. The tension in each layer at the end of the entire wind is referred to as the Layer Tension, which generally decreases from the outer to the inner layers. Because of the variation in layer tensions, the mandrel strain measured during winding can only be used to determine the winding tension of the first layer, but not its final layer tension. To simulate a multi-layer wind, however, the initial tension in each layer must be specified. In this study, it has been assumed that the layer tension in the outermost layer is equal to the measured winding tension of the innermost layer. Then the tensions in the inner layers are reduced from the outer layer tension level to account for multi-layer loss. The tension of the inner layers is reduced to a level which will achieve agreement between the measured and calculated initial mandrel pressures.

Using the permeability model developed for the single layer winds, the two multi-layer winds shown in Table 10 were simulated. The first of these, Wind 21, had two layers and was wound with a spool tension of 5.3 lb (23.6 N). Figure 34 shows the measured and calculated mandrel pressures for Wind 21. In the simulation, the layer

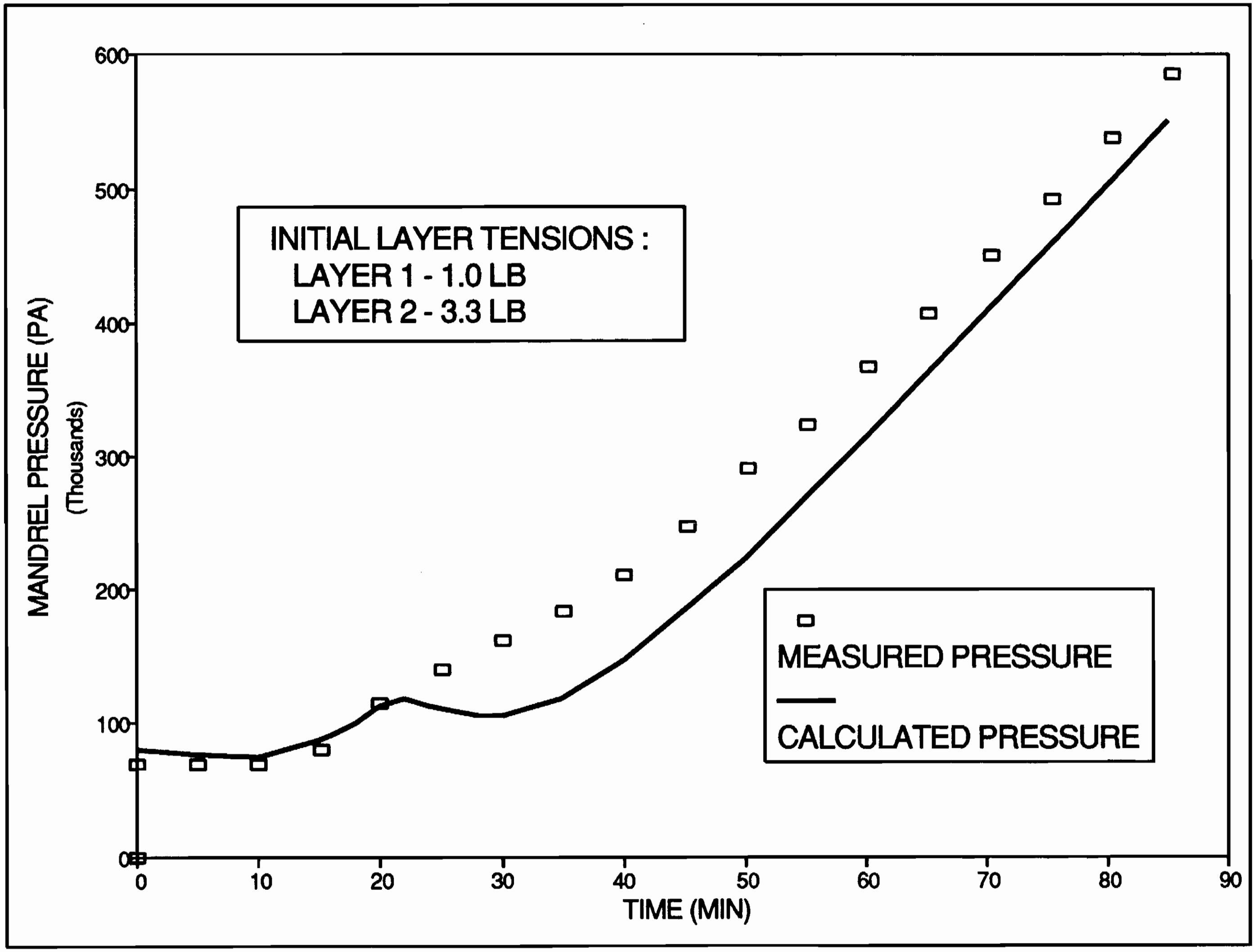

Figure 34. Measured and calculated mandrel pressures for a 2-layer wind of T40/1908 prepreg during the first ramp of the heatup (Wind 21)

tension in the second (outer) layer was assumed to be 3.3 lb (14.7 N) since that was the measured winding tension of the first layer. The layer tension of the first layer was then chosen to be 1.0 lb so that the initial pressure matched the experimental data. As shown in Figure 35, if the inner layer tension is not reduced and the full winding tension of 3.3 lb is used in both layers the initial mandrel pressure is overpredicted. The simulations show an accelerated tension loss effect during the 20-40 minute timeframe. However, the measured and calculated data begin to converge at about 80 minutes. In fact, as shown in Figure 36, during the intermediate hold temperature and during the second heatup ramp the calculated mandrel pressure agrees well with the measured mandrel pressure.

A three layer wind (Wind 23) was then simulated. The initial layer tensions in the simulation were again chosen to achieve a match in the calculated and measured initial mandrel pressure. The results of this simulation are shown in Figures 37 and 38. Again, the simulation over-predicts the effect of tension loss during the first ramp of the heatup. But when the full heatup time period is considered, shown in Figure 38, the measured and calculated pressure curves agree after the intermediate hold temperature. This indicates that the simulation predicts the tension loss to occur quite rapidly, i.e., during the first 20-50 minutes of the heatup; but the measured tension loss occurs more slowly, taking at least 80-90 minutes to occur.

In an attempt to explain the difference between the measured and calculated mandrel pressures, sensitivity studies of three parameters were performed using the three-layer wind. These parameters are 1) the initial fiber tension, 2) the empirical constant

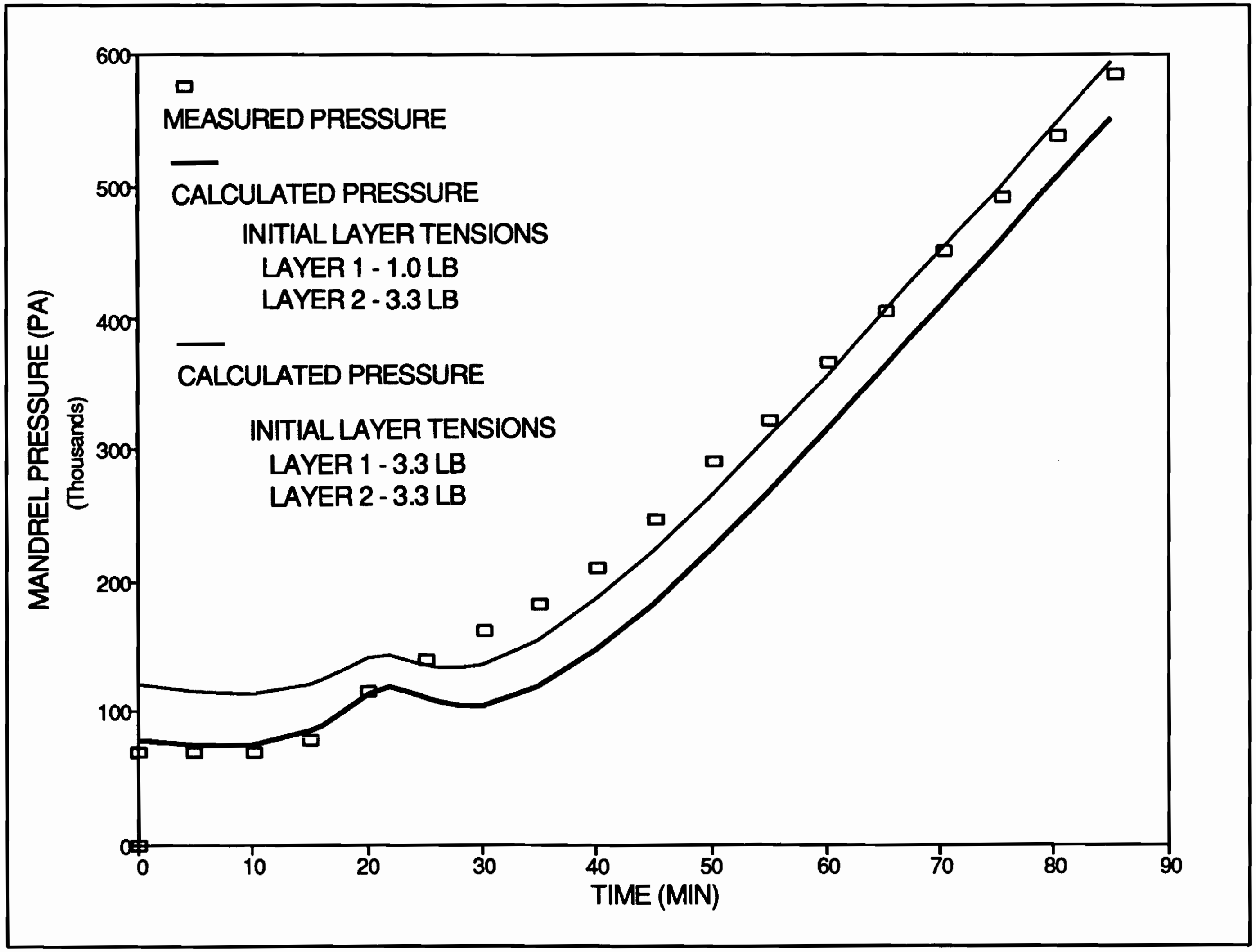

Figure 35. Effect of using full winding tension on mandrel pressure for a 2-layer simulation (Wind 21)

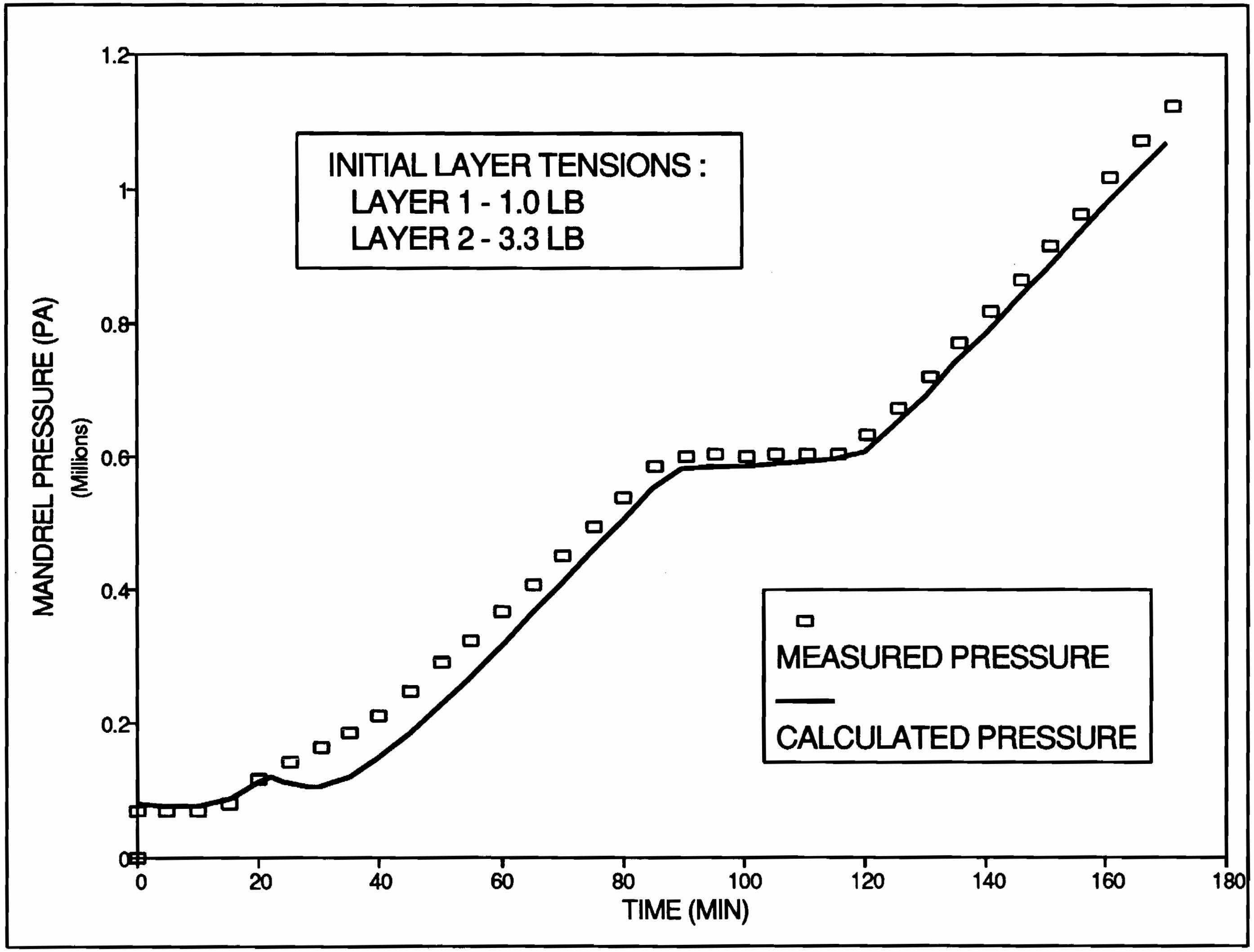

Figure 36. Measured and calculated mandrel pressures for a 2-layer wind of T40/1908 prepreg during the full heatup period (Wind 21)

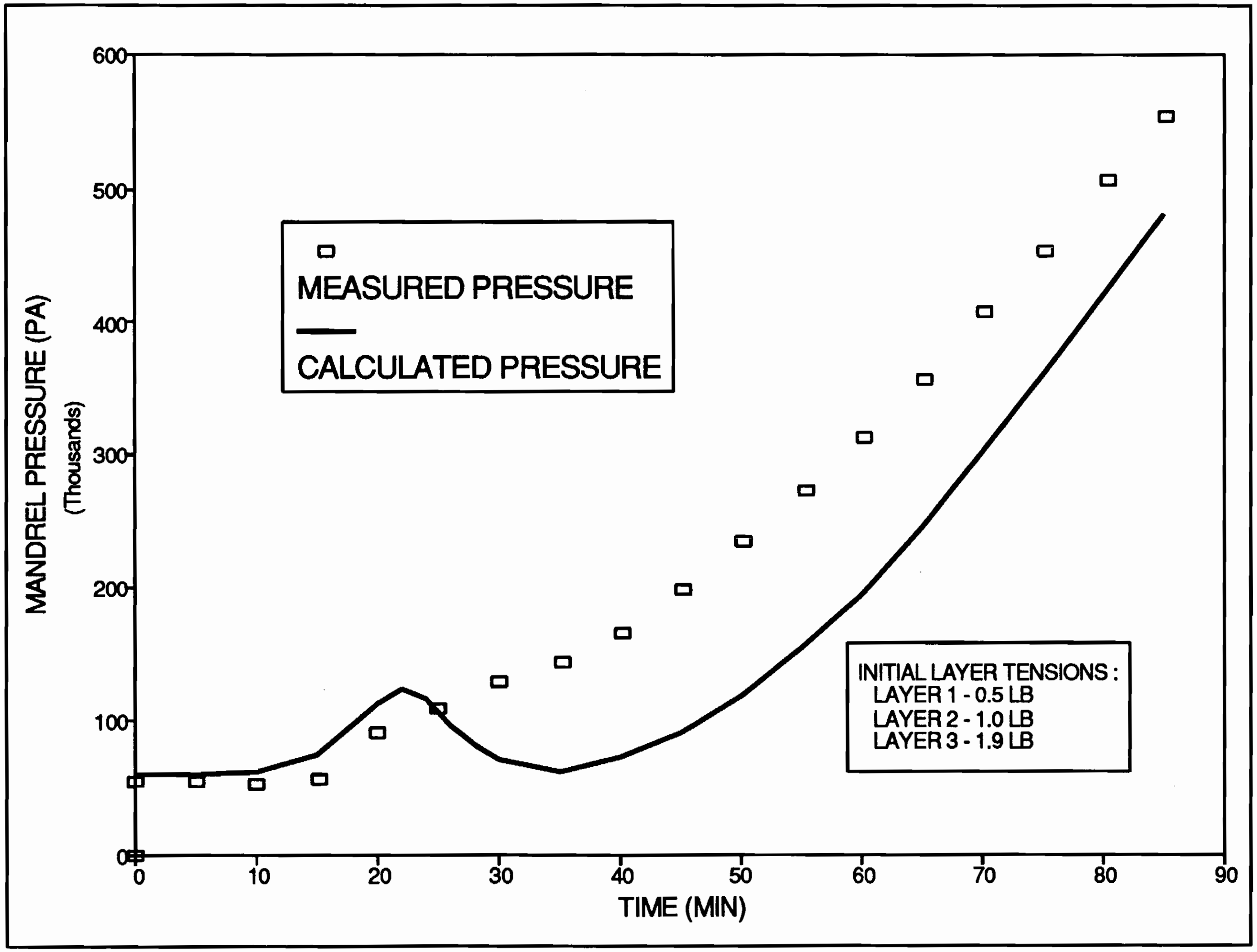

Figure 37. Measured and calculated mandrel pressures for a 3-layer wind of T40/1908 prepreg during the first ramp of the heatup (Wind 23)

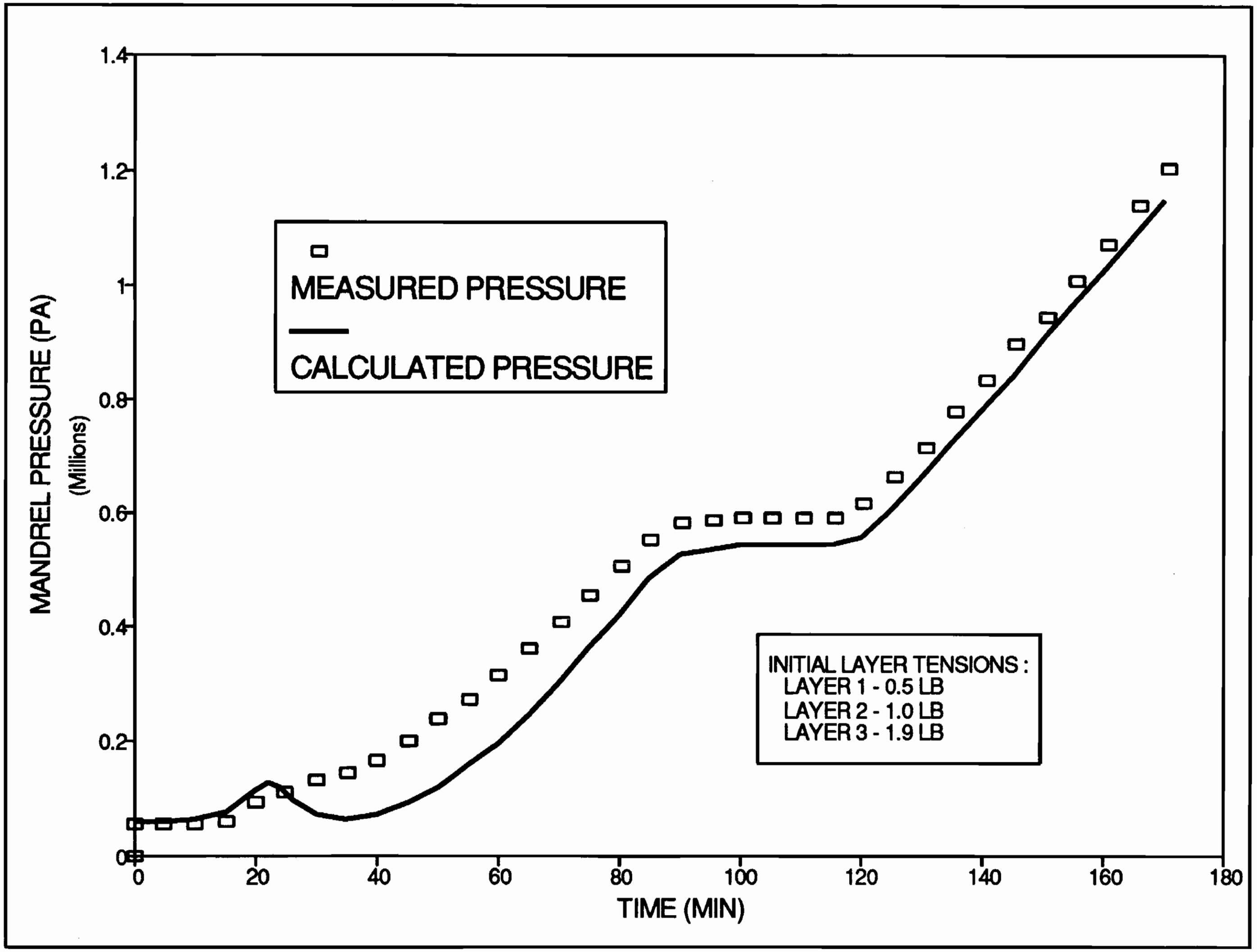

Figure 38. Measured and calculated mandrel pressures for a 3-layer wind of T40/1908 prepreg during the full heatup period (Wind 23)

in the permeability model (K_z) which scales the permeability, and 3) the maximum fiber volume fraction, V_{fmax} (a parameter in the permeability model which is defined as the fiber volume fraction at which resin flow stops). Before discussing the results of these studies, a description of the variation of simulated fiber tension of each layer is necessary.

Figure 39 shows the calculated fiber tension in each layer of the three-layer wind (Wind 23). The fiber tension is the sum of the thermally-induced tension and the tension loss due to resin flow (RFTL). The rate, duration and total amount of tension loss in the outermost layer (Layer 3) is greater than in the inner layers. The duration and total amount of tension loss are greater because the excess resin from the inner layers must flow through the third layer as well. The rate of loss is greater because the initial tension in the third layer is higher, producing a larger pressure gradient and more flow in this layer. Due to greater tension loss in the outer layer, the tension in this layer following compaction is significantly lower than the tension in the inner layers. Each layer has fully compacted when the tension curves are linear. Following compaction, all layer tensions increase equally because the change is thermally-induced.

One could conclude from Figure 39 that the layers which lose tension most rapidly are the ones which have the highest initial tension. Therefore, using lower initial tensions could reduce the excessive decrease in mandrel pressure. The lowest level of tension which could be used in all three layers, and still accurately simulate the initial experimental mandrel pressure was 1.0 lb (4.9 N). But, as shown in Figure 40, using these minimum levels of initial tension had little effect on the simulated mandrel pressure.

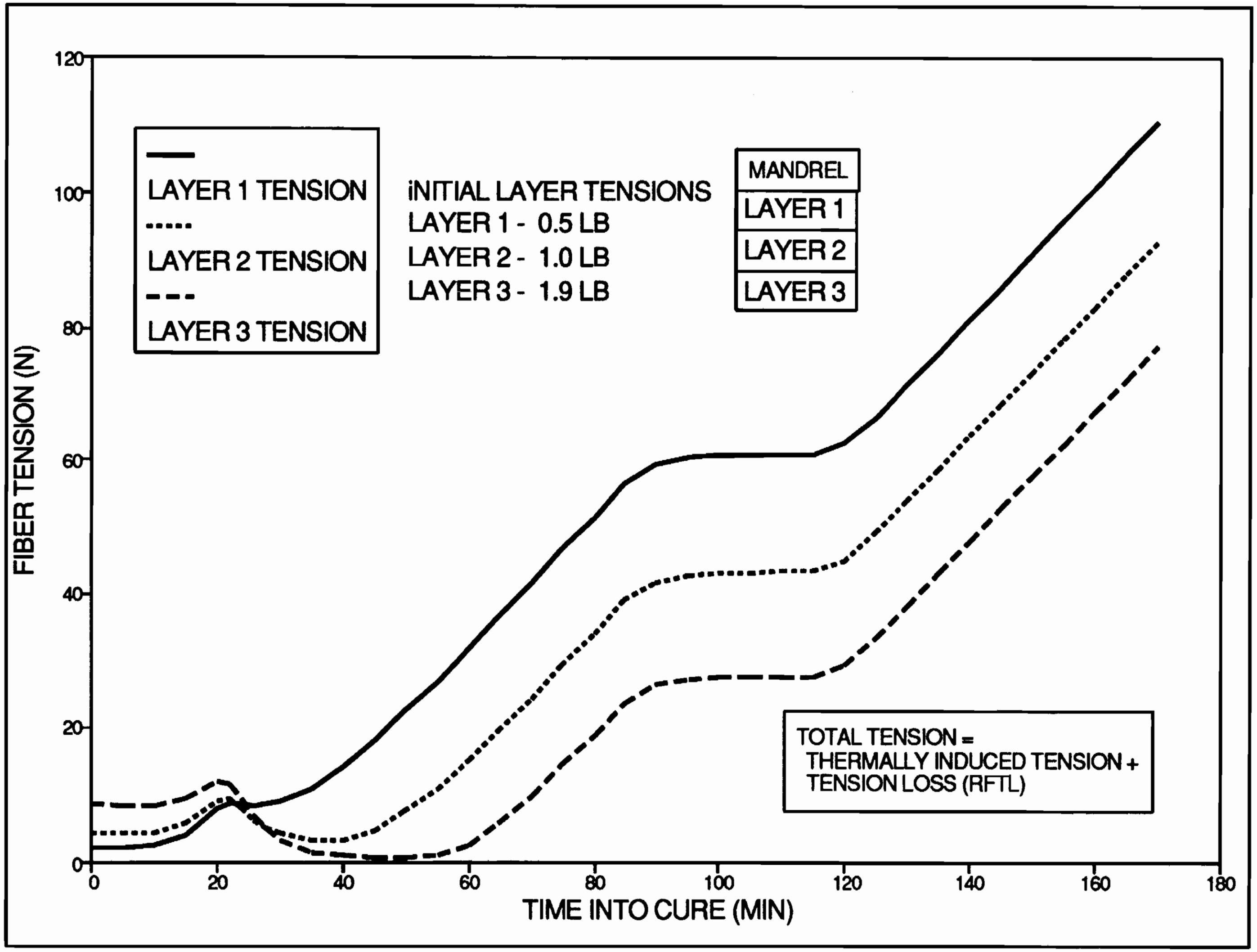

Figure 39. Calculated fiber tension in a 3-layer wind of T40/1908 prepreg (Wind 23)

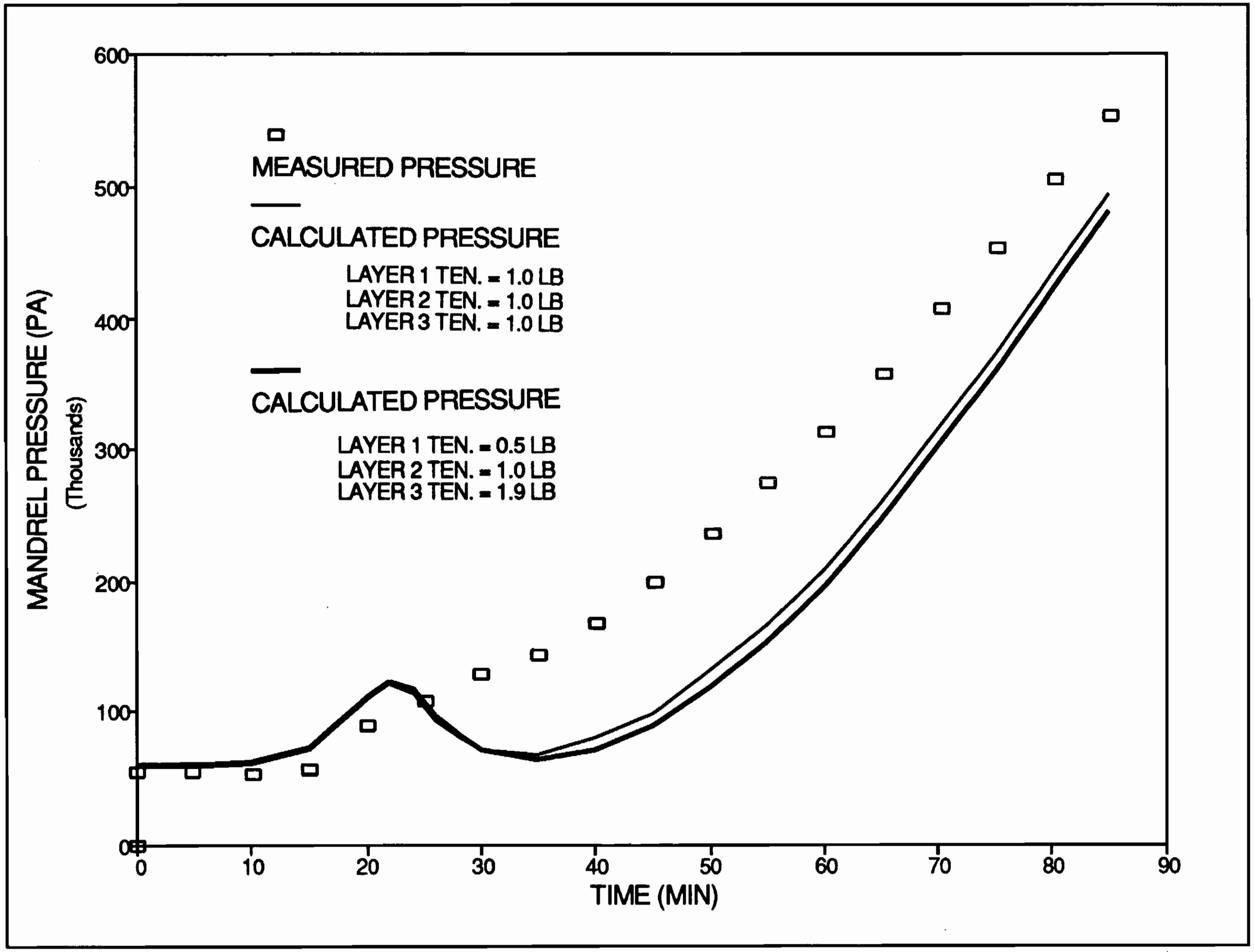

Figure 40. Effect of changing the distribution of initial tension in each layer on mandrel pressure for a 3-layer wind of T40/1908 prepreg (Wind 23)

The second sensitivity study involved varying K_z, an empirical constant in the permeability model (see Appendix B). Figure 41 shows the mandrel pressure curves using different values of K_z in the simulations. Increasing K_z decreases the permeability. In Figure 41, the permeability has been lowered by a factor of five from the level used to fit the single layer simulation. The reduction in permeability does slightly delay and lengthen the time period in which flow and tension loss occur. However, decreasing the permeability has no effect on the mandrel pressure beyond 80 minutes into cure, when compaction is complete. The rapid decline of the calculated mandrel pressure during the flow period (20-60 minutes) is not improved.

The third sensitivity study involved the parameter in the permeability model, V_{fmax}, defined as the fiber volume fraction beyond which flow cannot occur. In effect, the value of V_{fmax} sets an upper limit on the level of compaction and the amount of RFTL which can occur in the simulation. Figure 42 shows the results of lowering V_{fmax} from 0.70 to 0.66. The effect of reducing V_{fmax} is to reduce the total amount of tension loss which occurs before full compaction is reached. Decreasing V_{fmax} improves the calculated tension loss during the early part of heatup, but the reduced tension loss causes an overprediction of mandrel pressure following the flow period.

In summary, the sensitivity studies show that none of the three parameters investigated could be varied in a way that would produce an accurate simulation of the experimental mandrel pressure and tension loss. However, it must be pointed out that although the <u>rate</u> of tension loss is overpredicted by FWEXPAND, the <u>total amount</u> of

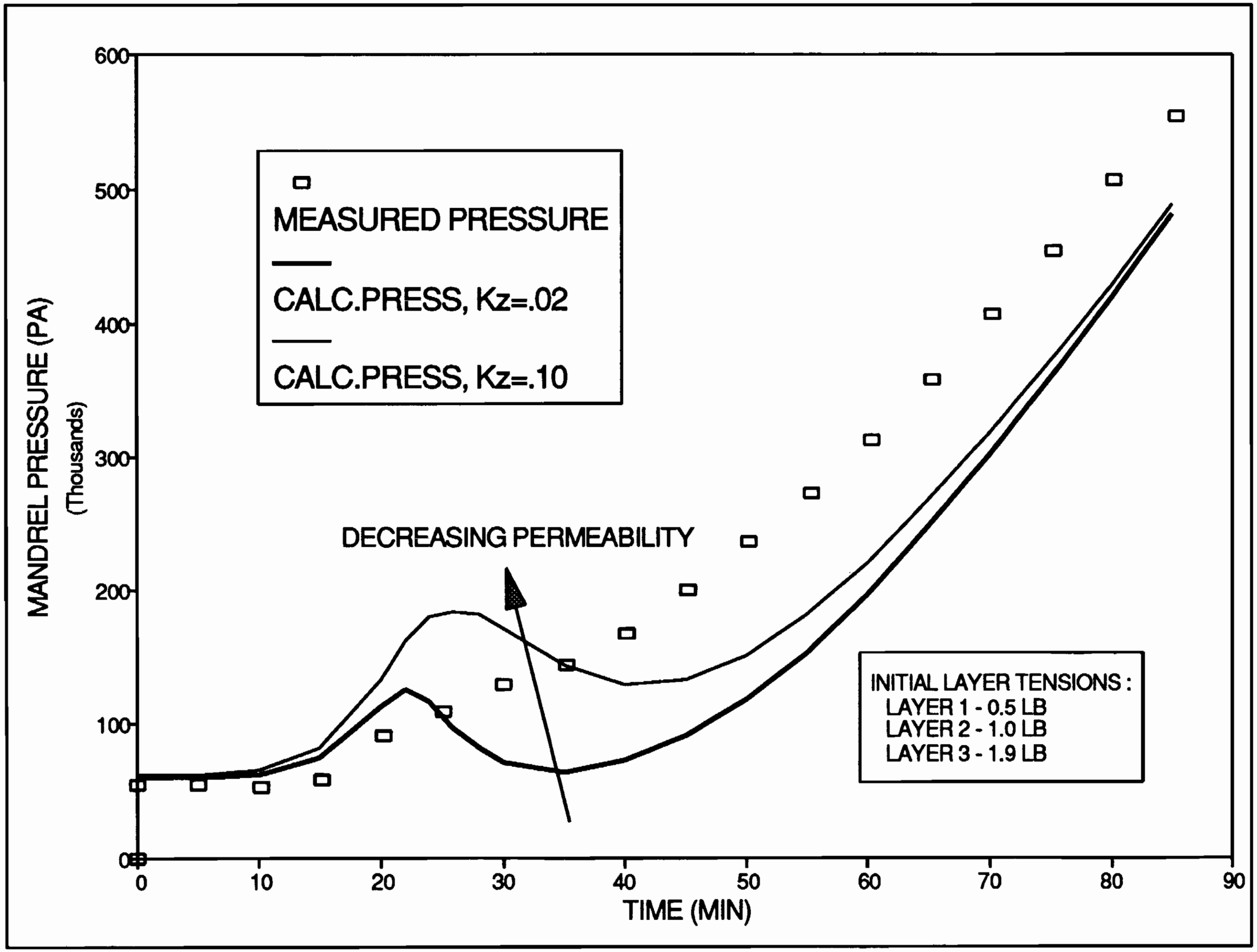

Figure 41. Effect of permeability on calculated mandrel pressure for a 3-layer wind of T40/1908 prepreg (Wind 23)

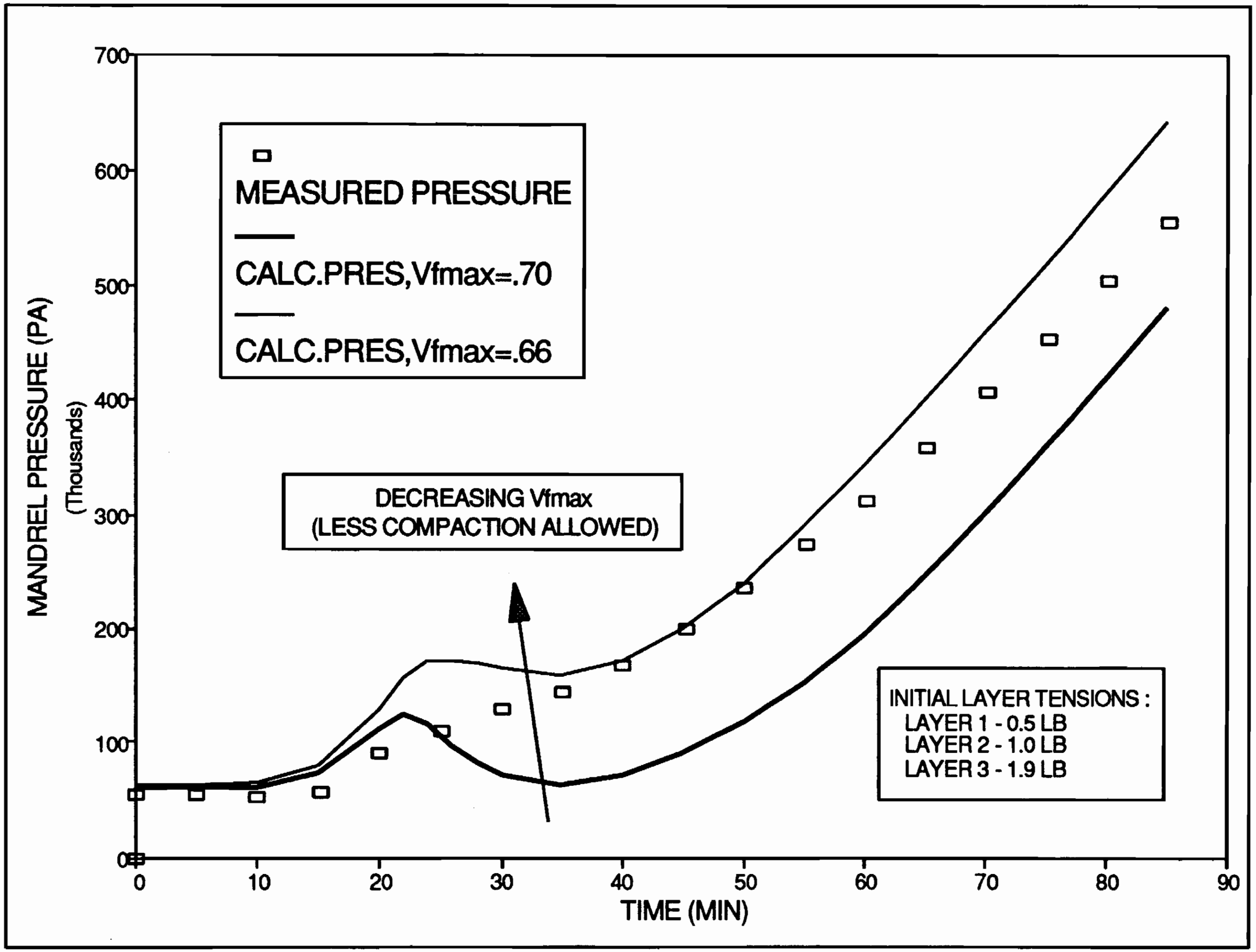

Figure 42. Effect of the maximum fiber volume fraction, V_{fmax}, on calculated mandrel pressure for a 3-layer wind of T40/1908 prepreg (Wind 23)

tension loss due to resin flow during the full heatup is predicted reasonably well.

6.0 Summary, Conclusions, and Future Research

6.1 Summary and Conclusions

The objectives of this study were 1) to experimentally quantify the variation of fiber tension in a prepreg-wound cylindrical composite case during the winding and cure stages of fabrication, and 2) to extend the cure simulation code FWCURE to include thermally-induced fiber tension due to mandrel expansion, and to simulate the permeability characteristics of the as-wound fiber network.

The experimental parameters used in this study were spool tension, oven ramp rate, and the number of layers wound. During the winding stage, it was found that the combined tension loss due to viscoplastic and side-by-side losses was approximately 50-60% of the spool tension for two different spool tensions. As a result of real time measurements of mandrel strain during winding, it is estimated that at least 30% of this loss is due to viscoplastic loss, with the remaining 20-30% resulting from side-by-side loss.

Two sets of experiments were performed to determine the repeatability of the experimental data. Within each set, the three experimental parameters (spool tension, oven ramp rate, and number of layers) were held constant. Overall, the repeatability of the measured mandrel strain was reasonably good.

Studies were also performed to determine the effect of each experimental parameter on the tension loss characteristics. The variation of spool tension and the number of layers was found to effect the mandrel strain during cure, while the variation of oven ramp rate had very little effect. This latter result is attributed to the low sensitivity of resin viscosity to heating rate during the flow period of cure. Low levels of spool tension resulted in larger amounts of RFTL than did higher levels of spool tension. The rate of tension loss was found to be fairly constant for the one, two and three layer winds. But the duration over which the loss occurred was longer for the multi-layer winds. This is consistent with the fact that the viscosity and permeability of the fiber network is the same in all three cases, so the flow rate would also be the same; but in the multi-layer winds more excess resin is flowing to the surface of the case, which takes more time. However, for all of the winds, the RFTL was complete during the heatup portion of cure while the resin viscosity was at a minimum.

An effort was made to experimentally measure RFTL by comparing the mandrel strains associated with sets of dry fiber and prepreg winds in which both winds were wound and cured identically. The assumption in this comparison was that the mandrel strain in the dry fiber wind would not be affected by RFTL and could therefore be subtracted from the prepreg wind strains. However, the compaction of the dry fiber prevented the measurement of RFTL.

A mandrel expansion model for thin shells was developed and integrated into FWCURE, and validated experimentally. In this experiment, the thermally-induced mandrel strain caused by a single layer of dry T40 fiber wound around the mandrel was measured during heatup. Dry fiber was used rather than prepreg because there would be no effect of resin flow. The resulting mandrel strain curve had a non-linear section at the beginning of heatup, reflecting the dry compaction of the filaments. The linear portion of the curve reflects only thermally-induced strain. The mandrel expansion model accurately simulated the measured thermally-induced strain, thereby verifying its accuracy.

The permeability model in FWCURE was adjusted by fitting the simulated mandrel strain for a single layer wind to the experimental data. The values of the maximum fiber volume fraction and the initial resin volume fraction used in the permeability model were corroborated by measurements of these values using photomicrographs.

Using this permeability model, other single and multi-layer winds were simulated. The high spool tension single layer winds were simulated accurately. At lower levels of spool tension, the measured mandrel strain was lower than the calculated strain, reflecting greater measured tension loss. The simulation was improved slightly by increasing the initial resin volume fraction, which increased both the duration and rate of flow.

The variable used for comparing multi-layer winds was the pressure at the mandrel surface. This quantity accounts for the cumulative effect of the tension in every layer. The calculated mandrel pressure revealed an accelerated tension loss relative to the experimental data. However, although the rate of tension loss was much greater than shown in the experimental data, the total amount of tension loss over the full heatup period was comparable.

In an effort to improve the multi-layer simulation, three parameters were varied: 1) the maximum fiber volume fraction, V_{fmax}, 2) the permeability, and 3) the initial tension used in each layer. Decreasing V_{fmax} was successful in reducing the early tension loss, but as a result the total tension loss was too low. Decreasing the permeability did not change the total loss of tension. It only increased the level of pressure at which the exaggerated flow occurred. Minimizing the initial tension in each layer had no effect on the pressure during the flow period, and only slightly changed the total loss of tension. The reason for this exaggerated loss of simulated tension is not known.

6.2 Future Research

Future efforts in this area of research should include the following improvements:

- Use thin-film, resistive pressure sensors between each layer to measure the pressure through the thickness of the case. These sensors will need to be modified so that they will respond to mechanically-imposed pressure as well as hydrostatic pressure. This modification may be accomplished by coating them with a thin film of compliant material, such as a silicone based material.
- Use lower levels of spool tension to more accurately simulate the lower pressures which occur in full scale articles. This will require increased mandrel strain sensitivity, so a mandrel which is less stiff (reduced thickness or made from a more compliant material) should be used.
- Improve the winding delivery system to avoid tow bandwidth narrowing.
- To study the side-by-side loss which occurs during winding, the mandrel

should be instrumented with micro-strain gages along the full length of the mandrel.

- A new displacement-based model should be developed. This model would calculate the effects of resin flow and thermal expansion on the displacement of each point in the wound assembly.
- The mandrel expansion model in FWEXPAND should be revised to allow a variation of strain through the thickness of a thick mandrel/composite assembly.

Bibliography

1. Spencer, B., "Modeling the Filament Winding Process," Proceedings of the 34th International SAMPE Symposium, May 1989, pp. 1556-1570.

2. Cai, Z., Gutowski, T. and Allen, S., "Winding and Consolidation Analysis for Cylindrical Composite Structures," paper submitted to the Journal of Composite Materials in November 1990.

3. Lee, S.Y. and Springer, G.S., "Filament Winding Cylinders: I. Process Model," Journal of Composite Materials, Vol.24, December 1990, pp. 1270-1298.

4. Calius, E.P., Lee, S.Y. and Springer, G.S., "Filament Winding Cylinders: II. Validation of the Process Model," Journal of Composite Materials, Vol.24, December 1990, pp. 1299-1343.

5. Lee, S.Y. and Springer, G.S., "Filament Winding Cylinders: III. Selection of the Process Variables," Journal of Composite Materials, Vol.24, December 1990, pp. 1344-1366.

6. Calius, E. and Springer, G.S., "Optimization of the Cure Window for a Large Filament Wound Case," Report to the Chemical Research Projects Office of NASA-Ames Research Center, November 1984.

7. Calius, E. and Springer, G.S., "Modeling the Filament Winding Process," Proceedings of the Fifth International Conference on Composite Materials, San Diego, CA, July 1985, pp. 1071-1088.

8. Tzeng, T.S., "A Model of the Winding and Cure Processes for Filament Wound Composites," Ph.D. Dissertation, Virginia Tech, October 1988.

9. Nguyen, V.D., "A Fabrication Stress Model for Filament Wound Composite Structures," Ph.D. Dissertation, Virginia Tech, February 1988.

10. Call, R.K., "Parameter Establishment and Verification of a Fabrication Stress Model and a Thermo-Kinetic Cure Model for Filament Wound Structures," Masters Thesis, Virginia Tech, September 1991.

11. Knight, C.E., "Residual Stress and Strength Loss in Filament-Wound Composites,"

Composite Materials: Testing and Design (Eighth Conference), ASTM STP 972, J.D. Whitcomb, Ed., American Society for Testing and Materials, Philadelphia, PA, 1988, pp. 413-422.

12. Faupel, J.H., *Engineering Design: A Synthesis of Stress Analysis and Materials Engineering*, John Wiley and Sons, New York, 1964.

13. Perry, C.C., "Practical Thermal Stress Analysis," Reprint from The VRE Technical Education Newsletter, No. 27, published by the Measurements Group, Inc., 1979.

14. Lundström, T.S., "Micromechanical Analysis of the Permeability of a Fibrous Preform," Swedish Institute of Composites (SICOMP), Technical Report 91-001, January 1991.

Appendix A: Calculation of Fiber Tension from Mandrel Hoop Strain

Consider a cylindrical mandrel wound with rovings of fiber having tension, T, and bandwidth, B. In Figure 43, the assembly has first been cut in half lengthwise, then sectioned radially into a width equal to the bandwidth of one roving. What remains is a free body diagram of the mandrel/composite assembly containing one layer of composite.

The force exerted on the mandrel by the roving, F_m, is the tension in the roving, T. This force acts on a cross-sectional area of the mandrel equal to the product of the mandrel thickness, t_m, and an arbitrary axial length, x, chosen to be equal to one bandwidth, B. The mandrel hoop stress produced by this force is:

$$\sigma_h = -\frac{T}{(B)(t_m)} \tag{A.1}$$

The negative sign designates compressive stress. The mandrel hoop strain produced by the stress in Equation (A.1) is:

$$\epsilon_h = \frac{\sigma_h}{E_m} = -\frac{T}{(E_m)(B)(t_m)} \tag{A.2}$$

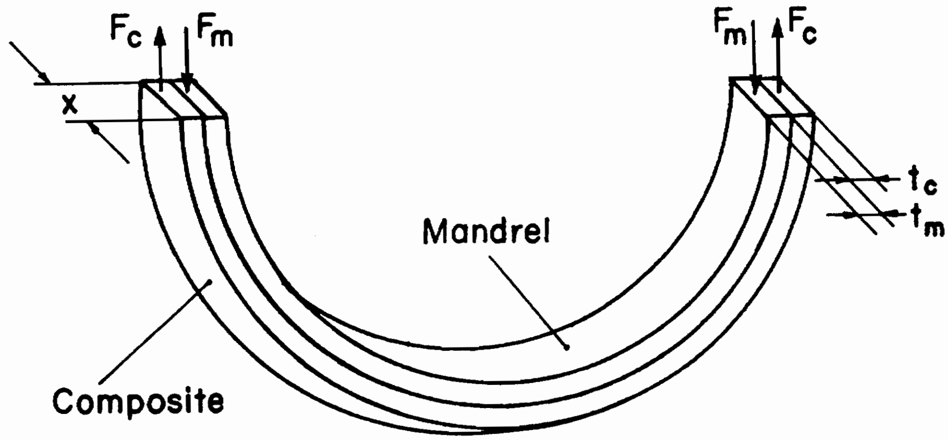

Figure 43. Free body diagram of the mandrel and one layer of composite

where E_m is the mandrel modulus of elasticity. Therefore, if the mandrel strain is known, the tension can be calculated from Equation (A.2) as:

$$T = -(\epsilon_h)(E_m)(B)(t_m) \tag{A.3}$$

Appendix B: Permeability Models

Four permeability models were investigated in this study. All relate the permeability to some or all of the following parameters:

1) the maximum fiber volume fraction, V_{fmax}, which is defined by either:

a) the physical geometric constraints associated with the assumed packing arrangement of the fibers (Lundström's models), or by

b) the fiber volume fraction at which resin flow ceases (Cai and Gutowski's model).

2) the instantaneous fiber volume fraction, V_f, which is expressed in terms of resin volume fraction or porosity in Tzeng's model

3) the radius of a single fiber

4) an empirical constant which is unique to each model

These models are listed below. In each case, 'K' is the permeability normal to the fiber direction.

Tzeng (hexagonal packing arrangement)

$$K = \frac{r^2 p^3}{4C''(1-p)^2} \tag{B.1}$$

The porosity, p, in Equation (B.1) is given by:

$$p = \frac{T - \frac{2r}{\cos(\frac{\pi}{6})}}{T} \tag{B.2}$$

where r is the fiber radius, C" is an empirical constant, and T is the distance between two adjacent fiber centers, which has the form:

$$T = \sqrt{\frac{\pi r^2}{(1-V_r)\sin(\frac{\pi}{3})}} \tag{B.3}$$

where V_r is the instantaneous resin volume fraction.

Cai and Gutowski (unspecified packing arrangement)

$$K = \frac{r^2 \left(\sqrt{\frac{V_{fmax}}{V_f}} - 1 \right)^3}{4K_z \left(\frac{V_{fmax}}{V_f} + 1 \right)} \tag{B.4}$$

where r is the fiber radius, V_{fmax} is the maximum fiber volume fraction at which resin flow ceases (empirically derived), V_f is the instantaneous fiber volume fraction, and K_z is an empirical constant.

Lundström (Quadratic packing arrangement)

$$K = \frac{16}{9\pi\sqrt{2}} \left(\sqrt{\frac{V_{fmax}}{V_f}} - 1 \right)^{5/2} (Ar)^2 \tag{B.5}$$

where r is the fiber radius, A is an empirical constant which is a fiber radius multiplier used to change the effective fiber radius, $V_{fmax} = \pi/4$ (0.785), and V_f is the instantaneous fiber volume fraction.

<u>**Lundström** (Hexagonal packing arrangement)</u>

$$K = \frac{16}{9\pi\sqrt{6}}\left(\sqrt{\frac{V_{fmax}}{V_f}} - 1\right)^{5/2}(Br)^2 \tag{B.6}$$

where r is the fiber raduis, $V_{fmax} = \pi/(2\sqrt{3})$ (0.907), and V_f is the instantaneous fiber volume fraction.

Appendix C: Experimental Data

This appendix contains the experimental data from the 24 winds performed using either dry T40 fiber or T40/1908 prepreg. The title block of each data set contains information concerning the type of material used (fiber or prepreg) as well as the spool tension, winding tension, stress retention factor, number of layers and oven ramp rate. Following the header, listed as a function of time are the oven and mandrel temperature, measured and apparent strain for gage 1 and gage 2, and the actual strain. The apparent strain was measured during heatup with no load (windings) on the mandrel, and the data was fit with curves with curves having the following form:

Gage 1

$$\epsilon_{a1} = -43.2 + 2.82T - 4.81x10^{-2}T^2 + 2.18x10^{-4}T^3 \qquad (C.1)$$

Gage 2

$$\epsilon_{a2} = -13.2 + 1.44T - 3.85x10^{-2}T^2 + 1.87x10^{-4}T^3 \qquad (C.2)$$

where ε_{a1} and ε_{a2} are the apparent strain in gage 1 and gage 2, respectively, and T is the mandrel temperature(°C).

The actual strain is calculated as:

$$\epsilon_{actual} = \frac{[(\epsilon_{m1} - \epsilon_{a1}) + (\epsilon_{m2} - \epsilon_{a2})]}{2} \qquad (C.3)$$

where ε_{m1} and ε_{m2} are the measured strain in gage 1 and gage 2, respectively.

With the exception of Wind 28, all winds had a circuit-to-circuit spacing (apparent bandwidth) of 0.12 inch and were wound using a 6.0 inch O.D., 0.05 inch thick aluminum mandrel. Wind 28 was wound with a circuit-to-circuit spacing of 0.087 inch to create an even, continuous layer of dry fiber for the purpose of verifying the mandrel expansion model. Wind 30 was aged for seven days at room temperature before being cured.

Wind #10 (Cure Data)

Material: T40/1908 prepreg — Spool Tension(lb): 5.0

Number of Layers: 1 — Winding Tension(lb): 2.4

Oven Ramp Rate(degC/m): 1.0 — Stress Retention Factor: 0.48

Cure Time (min)	Mand. Temp. (deg C)	Oven Temp. (deg C)	Measured Microstrain Gage 1	Measured Microstrain Gage 2	Apparent Microstrain Gage 1	Apparent Microstrain Gage 2	Actual Microstrain
0	23.75	23.75	-61.5	-43.4	-0.5	1.9	-53.1
2.1	24.06	24.02	-58.1	-37.8	-0.2	1.8	-48.8
4.1	23.99	24.02	-52.2	-34	-0.3	1.8	-43.9
6.2	24.28	24.15	-51.6	-30.2	-0.0	1.8	-41.8
8.3	24.01	24.21	-50.4	-31.8	-0.3	1.8	-41.9
10.3	24.26	24.74	-55.9	-33.8	-0.0	1.8	-45.7
12.4	24.56	25.16	-50.5	-32.3	0.2	1.8	-42.4
14.4	26.05	27.86	-54.7	-34.4	1.4	1.6	-46.0
16.5	28.82	31.44	-64.7	-45.9	3.3	0.9	-57.4
18.5	31.65	34.19	-73.7	-54.4	4.7	-0.2	-66.3
20.6	34.37	36.57	-82.5	-63.1	5.6	-1.5	-74.9
22.7	36.73	38.73	-88.1	-67.7	6.2	-2.8	-79.6
24.7	39.24	40.93	-97.4	-74.4	6.4	-4.5	-86.9
26.8	41.11	42.97	-104.9	-82.2	6.4	-5.9	-93.8
28.8	43.28	45.01	-110.4	-90.7	6.3	-7.6	-99.9
30.9	45.15	47.2	-121.3	-101.7	6.0	-9.3	-109.9
32.9	47.43	49.28	-130.4	-109.7	5.4	-11.3	-117.1
35	49.33	51.28	-134.6	-117.8	4.8	-13.2	-122.0
37.1	51.4	53.35	-149.4	-127.5	4.1	-15.2	-132.9
39.1	53.56	55.33	-158.9	-136.2	3.1	-17.5	-140.4
41.2	55.39	57.39	-168.8	-147.7	2.2	-19.5	-149.6
43.3	57.57	59.71	-179.3	-157.7	1.1	-21.9	-158.1
45.3	59.72	61.75	-189.9	-166	-0.2	-24.3	-165.7
47.4	61.53	63.69	-200.2	-177.6	-1.3	-26.4	-175.0
49.5	63.75	65.88	-210.9	-187.2	-2.7	-29.0	-183.2
51.5	65.92	67.97	-222	-197.7	-4.2	-31.6	-192.0
53.6	67.96	69.88	-232.4	-208	-5.6	-34.0	-200.4
55.6	70.04	72.09	-239.7	-218.4	-7.1	-36.5	-207.3
57.7	71.96	74.24	-257.3	-229.1	-8.5	-38.7	-219.6
59.8	74.11	76.09	-263	-237.4	-10.1	-41.3	-224.5
61.8	76.33	78.32	-276	-246.5	-11.7	-43.8	-233.5
63.9	78.2	80.4	-291.1	-257.5	-13.0	-46.0	-244.8
65.9	80.38	82.45	-300.4	-267.3	-14.5	-48.4	-252.4
68	82.34	84.54	-312.3	-277.4	-15.9	-50.6	-261.6
70.1	84.56	86.43	-324.3	-287.9	-17.4	-52.9	-271.0
72.1	86.48	88.65	-337.7	-299.4	-18.6	-54.9	-281.8
74.2	88.66	90.59	-347.8	-306.7	-19.9	-57.0	-288.8
76.3	90.86	92.89	-359	-316.6	-21.1	-59.1	-297.7
78.3	92.74	94.61	-368.1	-326.1	-22.1	-60.7	-305.7
80.4	94.69	96.62	-378.9	-335.5	-23.0	-62.3	-314.5
82.4	96.47	98.75	-392.5	-348.2	-23.7	-63.7	-326.6
84.5	98.56	100.49	-398.4	-355.4	-24.5	-65.2	-332.1

Wind #10 (Cure Data)

Material: T40/1908 prepreg | Spool Tension(lb): 5.0
Number of Layers: 1 | Winding Tension(lb): 2.4
Oven Ramp Rate(degC/m): 1.0 | Stress Retention Factor: 0.48

Cure Time (min)	Mand. Temp. (deg C)	Oven Temp. (deg C)	Measured Microstrain Gage 1	Measured Microstrain Gage 2	Apparent Microstrain Gage 1	Apparent Microstrain Gage 2	Actual Microstrain
86.5	99.74	100.87	-409.5	-360.6	-24.8	-65.9	-339.7
88.6	100.74	101.45	-412.8	-360.3	-25.1	-66.6	-340.7
90.7	100.86	101.47	-414.6	-363.3	-25.1	-66.6	-343.1
92.7	101.06	101.47	-412.1	-363.2	-25.2	-66.7	-341.7
94.8	100.9	101.51	-414.5	-365.8	-25.1	-66.7	-344.3
96.9	101.02	101.73	-415.5	-365.9	-25.2	-66.7	-344.8
98.9	101.31	101.7	-414.7	-365.1	-25.2	-66.9	-343.8
101	101.85	103.01	-419.6	-368.2	-25.4	-67.2	-347.6
103	102.94	104.48	-424.6	-373	-25.6	-67.8	-352.1
105.1	104.57	106.26	-430.1	-381.8	-25.8	-68.6	-358.8
107.2	106.63	108.3	-444.8	-389.3	-25.9	-69.4	-369.4
109.2	108.48	110.2	-452.5	-396.7	-25.9	-70.0	-376.7
111.3	110.23	112.05	-461.4	-406.3	-25.7	-70.4	-385.8
113.3	112.13	114.14	-471.3	-416.8	-25.3	-70.7	-396.0
115.4	114.42	116.34	-483.8	-424.1	-24.6	-70.9	-406.2
117.4	116.43	118.28	-490.4	-430	-23.8	-70.7	-412.9
119.5	118.36	120.14	-499.3	-439	-22.8	-70.4	-422.5
121.6	120.37	122.28	-510.7	-449	-21.5	-69.9	-434.2
123.6	122.34	124.35	-521.4	-458.9	-20.0	-69.1	-445.6
125.7	124.28	126.13	-531.2	-465.3	-18.3	-68.1	-455.0
127.7	126.36	128.24	-541	-472.2	-16.2	-66.8	-465.1
129.8	128.47	130.25	-549	-479.1	-13.8	-65.1	-474.6
131.9	130.52	132.39	-554.7	-486	-11.1	-63.3	-483.2
133.9	132.26	134.2	-565.2	-495.8	-8.5	-61.5	-495.5
136	134.25	136.35	-573.8	-503.2	-5.4	-59.1	-506.3
138.1	136.25	138.28	-583.9	-509.4	-1.9	-56.4	-517.5
140.1	138.34	140.3	-593.4	-515.7	2.1	-53.3	-528.9
142.2	140.35	142.31	-597.4	-521.4	6.3	-50.0	-537.5
144.2	142.51	144.22	-609	-527.4	11.2	-46.1	-550.8
146.3	144.46	146.55	-614.8	-533.9	16.0	-42.2	-561.2
148.4	146.51	148.37	-623.8	-539	21.4	-37.8	-573.2
150.4	148.43	150.36	-630.6	-545	26.9	-33.3	-584.6
152.5	150.38	152.4	-639.2	-551.9	32.8	-28.5	-597.7
154.5	152.29	154.12	-641.3	-556.2	38.9	-23.3	-606.5
156.6	153.79	154.92	-647.3	-558.3	44.0	-19.1	-615.3
158.7	154.28	155.22	-652.3	-563.4	45.7	-17.6	-621.9
160.7	154.7	155.37	-651.7	-561.5	47.2	-16.4	-622.0
162.8	154.93	155.72	-656.9	-562.7	48.0	-15.7	-626.0
164.9	155.19	155.85	-652.6	-561.5	48.9	-14.9	-624.1
166.9	155.47	155.95	-652.4	-560.5	50.0	-14.0	-624.4
169	155.3	154.92	-651.9	-560.2	49.3	-14.5	-623.4
171.1	152.16	149.16	-644.2	-547.8	38.5	-23.7	-603.4

Wind #10 (Cure Data)

Material: T40/1908 prepreg
Spool Tension(lb): 5.0
Number of Layers: 1
Winding Tension(lb): 2.4
Oven Ramp Rate(degC/m): 1.0
Stress Retention Factor: 0.48

Cure Time (min)	Mand. Temp. (deg C)	Oven Temp. (deg C)	Measured Microstrain Gage 1	Measured Microstrain Gage 2	Apparent Microstrain Gage 1	Apparent Microstrain Gage 2	Actual Microstrain
173.1	146.95	143.41	-628	-537.5	22.7	-36.8	-575.7
175.2	140.95	133.44	-603.6	-515.6	7.7	-49.0	-538.9
177.2	125.09	113.18	-533.9	-460.8	-17.5	-67.6	-454.8
179.3	111.43	101.86	-463.2	-409.5	-25.5	-70.6	-388.3
181.4	100.32	92.28	-406.1	-360.1	-25.0	-66.3	-337.5
183.4	88.37	73.25	-341.5	-298.5	-19.7	-56.7	-281.8
185.5	68.98	56.35	-227.8	-191.5	-6.3	-35.2	-188.9
187.6	51.55	31.82	-137.8	-107.2	4.0	-15.4	-116.8
189.6	41.15	28.15	-85.9	-67	6.4	-5.9	-76.7
191.7	35.52	27.05	-64.1	-49.6	5.9	-2.1	-58.8
193.7	32.59	26.55	-51.6	-36.5	5.1	-0.6	-46.3
195.8	30.5	26.37	-41.3	-28.5	4.2	0.3	-37.1
197.9	28.87	25.78	-39.8	-24.5	3.3	0.9	-34.2
199.9	28.07	25.65	-34.2	-22.4	2.8	1.1	-30.3
202	27.65	25.59	-35.4	-22.2	2.5	1.2	-30.7
204	27.09	25.31	-29.2	-19.4	2.2	1.4	-26.1

Wind #10a2 (Cure Data)

Material: T40/1908 prepreg — Spool Tension(lb): 5.5
Number of Layers: 1 — Winding Tension(lb): 3.7
Oven Ramp Rate(degC/m): 1.0 — Stress Retention Factor: 0.67

Cure Time (min)	Mand. Temp. (deg C)	Oven Temp. (deg C)	Measured Microstrain Gage 1	Measured Microstrain Gage 2	Apparent Microstrain Gage 1	Apparent Microstrain Gage 2	Actual Microstrain
2	23.24	23.45	-65.2	-67.3	-1.0	1.9	-66.7
6.1	23.38	23.89	-61.9	-62.7	-0.8	1.9	-62.8
10.2	24.85	26.96	-63.5	-64.1	0.5	1.7	-64.9
14.3	30.81	33.47	-82.2	-80.8	4.3	0.2	-83.7
18.3	35.75	37.97	-97.6	-96	6.0	-2.3	-98.7
22.4	40.04	42.08	-113.6	-110.5	6.4	-5.1	-112.7
26.4	44.34	46.35	-127.6	-125.7	6.1	-8.5	-125.4
30.5	48.59	50.49	-145.3	-141.7	5.1	-12.4	-139.8
34.6	52.57	54.52	-165.1	-160.1	3.6	-16.5	-156.2
38.6	56.73	58.72	-187.3	-181.3	1.5	-21.0	-174.6
42.7	60.82	62.85	-211.2	-202.3	-0.8	-25.6	-193.5
46.8	64.96	67.02	-234.8	-223.1	-3.5	-30.4	-212.0
50.9	69	71.09	-257.1	-245.7	-6.4	-35.2	-230.6
54.9	73.09	75.16	-281.4	-268.2	-9.3	-40.1	-250.1
59	77.29	79.38	-305.9	-291.1	-12.4	-44.9	-269.9
63.1	81.5	83.47	-330.8	-312.4	-15.3	-49.6	-289.1
67.2	85.56	87.59	-356.4	-334.5	-18.0	-53.9	-309.5
71.2	89.5	91.62	-379.8	-354.4	-20.4	-57.8	-328.0
75.3	93.75	95.77	-405.4	-375.4	-22.6	-61.6	-348.3
79.4	98.05	99.98	-431.9	-395.2	-24.3	-64.8	-369.0
83.4	100.71	101.6	-449.2	-407.7	-25.1	-66.5	-382.6
87.5	101.61	102.02	-453.3	-412.1	-25.3	-67.1	-386.5
91.6	101.79	102.14	-456.5	-412.1	-25.3	-67.2	-388.0
95.6	101.91	102.08	-459.1	-413.6	-25.4	-67.2	-390.1
99.7	102.15	102.26	-461.9	-413.7	-25.4	-67.4	-391.4
103.8	102.07	102.24	-462	-413.8	-25.4	-67.3	-391.5
107.8	102.13	102.26	-462.2	-413.7	-25.4	-67.4	-391.6
111.9	102.43	103.22	-464.9	-416.4	-25.5	-67.5	-394.2
115.9	105.03	106.59	-480.5	-428.4	-25.8	-68.8	-407.2
120	108.74	110.5	-500.6	-445.9	-25.8	-70.1	-425.3
124.1	112.8	114.54	-523.3	-463.9	-25.1	-70.8	-445.6
128.1	116.68	118.49	-544.4	-481.2	-23.7	-70.7	-465.6
132.2	120.81	122.64	-567.5	-498.8	-21.2	-69.7	-487.7
136.2	124.69	126.57	-590.1	-515	-17.9	-67.9	-509.7
140.3	128.77	130.61	-610.7	-531.8	-13.4	-64.9	-532.1
144.4	132.7	134.63	-631.3	-547.5	-7.9	-61.0	-555.0
148.4	136.74	138.82	-652	-561	-1.0	-55.8	-578.1
152.5	140.67	142.78	-670.7	-574.9	7.0	-49.5	-601.6
156.5	144.72	146.65	-689.5	-587.4	16.7	-41.7	-625.9
160.6	148.79	150.77	-705.2	-599.7	27.9	-32.5	-650.2
164.7	152.72	154.83	-724.7	-609.8	40.3	-22.1	-676.4
168.7	155.47	156.6	-736.7	-617	50.0	-14.0	-694.8

Wind #10a2 (Cure Data)

Material: T40/1908 prepreg — Spool Tension(lb): 5.5

Number of Layers: 1 — Winding Tension(lb): 3.7

Oven Ramp Rate(degC/m): 1.0 — Stress Retention Factor: 0.67

Cure Time (min)	Mand. Temp. (deg C)	Oven Temp. (deg C)	Measured Microstrain Gage 1	Measured Microstrain Gage 2	Apparent Microstrain Gage 1	Apparent Microstrain Gage 2	Actual Microstrain
172.8	156.28	156.96	-743	-618.2	52.9	-11.5	-701.3
176.9	156.71	157.25	-743.1	-620.1	54.6	-10.1	-703.8
180.9	156.72	157.19	-743.9	-620.3	54.6	-10.1	-704.3
185	156.91	157.4	-744.9	-620	55.3	-9.5	-705.4
189.1	156.93	157.39	-746.6	-620	55.4	-9.4	-706.3
193.1	156.97	157.4	-748.3	-619.3	55.5	-9.3	-706.9
197.2	153.07	149.51	-737	-607.9	41.5	-21.1	-682.6
201.2	140.99	136.45	-692.5	-570.6	7.7	-48.9	-611.0
205.3	129.49	125.34	-635.6	-528.5	-12.5	-64.3	-543.7
209.4	119.16	115.5	-585.2	-483.9	-22.3	-70.2	-488.3
213.4	110.08	106.83	-534.7	-442.9	-25.7	-70.4	-440.7
217.5	101.91	99.08	-486.9	-402.8	-25.4	-67.2	-398.6
221.6	94.73	92.03	-445.9	-367.4	-23.0	-62.3	-364.0
225.6	88.1	85.83	-378.7	-363	-19.6	-56.5	-332.8
229.7	82.23	80.21	-360.4	-328.6	-15.8	-50.4	-311.4
233.8	76.99	75.22	-305.8	-326.7	-12.1	-44.6	-287.9
237.8	72.28	70.67	-281.9	-269.1	-8.7	-39.1	-251.6
241.9	67.93	66.58	-261	-222.4	-5.6	-34.0	-221.9
245.9	63.98	62.83	-237.2	-197.9	-2.9	-29.3	-201.5
250	60.5	59.42	-220.5	-181.9	-0.7	-25.2	-188.3
254	57.46	56.45	-204.5	-166.1	1.1	-21.8	-175.0
258.1	54.47	53.74	-188.8	-150.3	2.7	-18.5	-161.7
262.2	51.85	51.15	-179.2	-140.2	3.9	-15.7	-153.8
266.2	49.59	48.93	-167	-128.3	4.7	-13.4	-143.3
270.3	47.68	47.32	-157.5	-118.4	5.3	-11.6	-134.8
274.4	47.27	47.27	-153	-115.4	5.5	-11.2	-131.3
278.4	46.84	46.75	-152.9	-112.8	5.6	-10.8	-130.2
282.5	46.2	46	-150.4	-110.1	5.7	-10.2	-128.0
286.6	45.52	45.19	-145.2	-107.8	5.9	-9.6	-124.7
290.6	44.81	44.43	-142.3	-102.6	6.0	-9.0	-121.0
294.7	43.86	43.45	-138.3	-97.3	6.2	-8.1	-116.8
298.8	42.85	42.4	-132.6	-92.6	6.3	-7.3	-112.1
302.8	41.92	41.31	-127.6	-88.5	6.4	-6.5	-108.0
306.9	40.95	40.34	-120.1	-83.7	6.4	-5.8	-102.2
311	39.95	39.38	-117.2	-79.9	6.4	-5.0	-99.3
315	39.12	38.48	-114.7	-76.3	6.4	-4.4	-96.5
319.1	38.15	37.58	-111.6	-72.7	6.3	-3.8	-93.4
323.2	37.45	36.8	-105.5	-68.4	6.3	-3.3	-88.4
327.3	36.38	35.82	-102.9	-65.3	6.1	-2.6	-85.8
331.3	35.61	35.07	-99.3	-61.5	6.0	-2.2	-82.3
335.4	34.78	34.27	-95.5	-59	5.8	-1.7	-79.3
339.5	34.06	33.54	-91.5	-55.3	5.6	-1.3	-75.5

Wind #10a2 (Cure Data)

Material: T40/1908 prepreg Spool Tension(lb): 5.5
Number of Layers: 1 Winding Tension(lb): 3.7
Oven Ramp Rate(degC/m): 1.0 Stress Retention Factor: 0.67

Cure Time (min)	Mand. Temp. (deg C)	Oven Temp. (deg C)	Measured Microstrain Gage 1	Measured Microstrain Gage 2	Apparent Microstrain Gage 1	Apparent Microstrain Gage 2	Actual Microstrain
343.6	33.34	32.91	-90	-52.9	5.3	-0.9	-73.6
347.6	32.7	32.26	-86.4	-49.9	5.1	-0.6	-70.4
351.7	31.97	31.63	-80.9	-47.6	4.8	-0.3	-66.5
355.8	31.46	31.1	-78.1	-45.4	4.6	-0.1	-64.0
359.9	30.89	30.57	-76.4	-42.5	4.3	0.2	-61.7
363.9	30.32	30.01	-76.8	-42.7	4.1	0.4	-62.0
367.9	29.81	29.58	-71.9	-40.2	3.8	0.6	-58.2
372	29.38	29.16	-70.4	-38.5	3.6	0.7	-56.6
376	28.87	28.66	-71.2	-36.1	3.3	0.9	-55.7
380.1	28.47	28.34	-67.7	-35.3	3.0	1.0	-53.5
384.2	28.06	27.97	-66.7	-34.1	2.8	1.1	-52.4
388.3	27.66	27.58	-63.9	-32.3	2.5	1.2	-50.0
392.3	27.48	27.45	-64	-31.8	2.4	1.3	-49.7
396.4	27.01	27.02	-61.8	-30.6	2.1	1.4	-47.9
400.5	26.78	26.78	-62.6	-28.5	1.9	1.4	-47.2
404.6	26.37	26.39	-62	-28.2	1.6	1.5	-46.7
408.6	26.17	26.21	-59.1	-26.8	1.5	1.5	-44.5
412.7	25.98	26.03	-58.1	-25.6	1.3	1.6	-43.3
416.8	25.75	25.72	-55.4	-24.7	1.2	1.6	-41.4
420.9	25.57	25.6	-55.9	-24.2	1.0	1.6	-41.4
425	25.29	25.35	-56.7	-23.7	0.8	1.7	-41.5
429	25.13	25.23	-53.6	-22.7	0.7	1.7	-39.3
433.1	25.02	25.13	-54.7	-20.7	0.6	1.7	-38.9
437.2	24.86	24.93	-55.3	-21.1	0.5	1.7	-39.3
441.2	24.71	24.8	-54.7	-20.5	0.3	1.8	-38.7
445.3	24.53	24.71	-53.3	-19	0.2	1.8	-37.1
449.4	24.45	24.59	-53.5	-18.6	0.1	1.8	-37.0
453.5	24.17	24.34	-51.9	-18.4	-0.1	1.8	-36.0
457.5	24.11	24.31	-50.4	-18.1	-0.2	1.8	-35.1
461.6	24	24.2	-52.1	-18.4	-0.3	1.8	-36.0
465.7	24.01	24.18	-49.7	-17.9	-0.3	1.8	-34.6
469.7	23.78	23.96	-50.8	-18	-0.5	1.9	-35.1
473.8	23.85	24	-49.7	-17.8	-0.4	1.8	-34.5
477.9	23.7	23.93	-51.1	-17.7	-0.5	1.9	-35.1
481.9	23.58	23.78	-51	-16.9	-0.7	1.9	-34.6
486	23.6	23.74	-49.2	-16.7	-0.6	1.9	-33.6
490.1	23.51	23.72	-50.5	-15.5	-0.7	1.9	-33.6
494.1	23.36	23.61	-48.4	-15.4	-0.9	1.9	-32.4
498.2	23.49	23.66	-48	-15.8	-0.7	1.9	-32.5
502.3	23.29	23.49	-47.7	-15.2	-0.9	1.9	-31.9
506.4	23.13	23.41	-47.8	-15.5	-1.1	1.9	-32.1
510.4	23.08	23.33	-48.2	-14.5	-1.1	1.9	-31.7

Wind #11 (Cure Data)

Material: T40 fiber — Spool Tension(lb): 5.1
Number of Layers: 1 — Winding Tension(lb): 4.1
Oven Ramp Rate(degC/m): 1.0 — Stress Retention Factor: 0.80

Cure Time (min)	Mand. Temp. (deg C)	Oven Temp. (deg C)	Measured Microstrain Gage 1	Measured Microstrain Gage 2	Apparent Microstrain Gage 1	Apparent Microstrain Gage 2	Actual Microstrain
0	24.26	24.26	-84.6	-70.2	-0.0	1.8	-78.3
2.1	24.54	24.41	-70.7	-66.6	0.2	1.8	-69.6
4.2	24.6	24.91	-66.5	-64.7	0.2	1.8	-66.6
6.2	24.88	25.35	-73.7	-64.6	0.5	1.7	-70.3
8.3	25.03	25.54	-69.2	-66.2	0.6	1.7	-68.9
10.4	27.09	28.94	-75.6	-71	2.2	1.4	-75.1
12.4	29.94	32.29	-85.5	-81.4	3.9	0.5	-85.6
14.5	32.68	34.82	-90.9	-88.5	5.1	-0.6	-91.9
16.6	35.15	37.02	-102	-95.5	5.8	-1.9	-100.7
18.7	37.17	39.13	-108.7	-102.3	6.2	-3.1	-107.1
20.7	39.44	41.53	-112.7	-109.4	6.4	-4.7	-111.9
22.8	41.72	43.51	-116.3	-114.7	6.4	-6.4	-115.5
24.9	43.73	45.46	-123.8	-120.8	6.2	-8.0	-121.4
27	45.85	47.64	-129.8	-128.1	5.8	-9.9	-126.9
29	48.01	49.8	-142.8	-134.9	5.3	-11.9	-135.5
31.1	49.93	51.74	-148.8	-142.8	4.6	-13.8	-141.2
33.2	52.04	53.82	-157.3	-150.1	3.8	-15.9	-147.6
35.3	54.01	55.88	-160.1	-158.6	2.9	-18.0	-151.8
37.3	56.14	57.98	-173.6	-167.8	1.8	-20.3	-161.5
39.4	58.28	60.05	-179	-177.1	0.7	-22.7	-167.0
41.5	60.44	62.28	-193.7	-185.7	-0.6	-25.2	-176.8
43.6	62.53	64.46	-205	-195.9	-1.9	-27.6	-185.7
45.6	64.65	66.54	-211.8	-205.4	-3.3	-30.1	-191.9
47.7	66.65	68.51	-225.5	-216	-4.7	-32.4	-202.2
49.8	68.75	70.71	-240.9	-226	-6.2	-34.9	-212.9
51.9	70.88	72.74	-244.6	-234.9	-7.7	-37.5	-217.2
53.9	72.87	74.78	-254.9	-246.6	-9.2	-39.8	-226.3
56	74.87	76.85	-270.5	-255.5	-10.6	-42.1	-236.6
58.1	77.1	78.82	-278.9	-264.4	-12.2	-44.7	-243.2
60.2	79.16	80.85	-288.4	-274.3	-13.7	-47.1	-251.0
62.2	81.15	82.89	-303.9	-284.9	-15.1	-49.3	-262.2
64.3	83.37	85.31	-316	-295.1	-16.6	-51.7	-271.4
66.4	85.21	87.21	-326.1	-304.6	-17.8	-53.6	-279.7
68.5	87.2	89.17	-336	-315.6	-19.0	-55.6	-288.5
70.5	89.47	91.27	-343.1	-324.3	-20.4	-57.8	-294.6
72.6	91.39	93.42	-358.3	-333.1	-21.4	-59.5	-305.2
74.7	93.55	95.45	-370.3	-342.3	-22.5	-61.4	-314.4
76.8	95.45	97.28	-379.3	-352.2	-23.3	-62.9	-322.6
78.8	97.75	99.48	-387.5	-360.3	-24.2	-64.6	-329.5
80.9	99.28	100.53	-403	-367.7	-24.7	-65.6	-340.2
83	99.99	100.86	-410.9	-371.3	-24.9	-66.1	-345.6
85	100.69	101.23	-406.3	-374.1	-25.1	-66.5	-344.4

Wind #11 (Cure Data)

Material: T40 fiber — Spool Tension(lb): 5.1
Number of Layers: 1 — Winding Tension(lb): 4.1
Oven Ramp Rate(degC/m): 1.0 — Stress Retention Factor: 0.80

Cure Time (min)	Mand. Temp. (deg C)	Oven Temp. (deg C)	Measured Microstrain Gage 1	Measured Microstrain Gage 2	Apparent Microstrain Gage 1	Apparent Microstrain Gage 2	Actual Microstrain
87.1	100.91	101.42	-409.2	-373.9	-25.1	-66.7	-345.6
89.2	100.82	101.37	-407.2	-373.9	-25.1	-66.6	-344.7
91.2	100.9	101.35	-409.9	-375	-25.1	-66.7	-346.6
93.3	101.26	101.42	-408.7	-373.7	-25.2	-66.9	-345.2
95.4	101.21	101.91	-411.6	-376.2	-25.2	-66.8	-347.9
97.5	102.44	103.53	-415.8	-380.5	-25.5	-67.5	-351.7
99.5	103.64	105.28	-426.6	-387.5	-25.7	-68.1	-360.1
101.6	105.45	107.08	-433.9	-396.1	-25.9	-69.0	-367.6
103.7	107.57	109.17	-443.9	-404	-25.9	-69.7	-376.1
105.8	109.48	111.02	-456.9	-412.6	-25.8	-70.3	-386.7
107.8	111.53	113.29	-465.1	-421.1	-25.4	-70.7	-395.0
109.9	113.63	115.16	-472.8	-428.7	-24.9	-70.8	-402.9
112	115.48	117.17	-489.1	-438.3	-24.2	-70.8	-416.2
114	117.51	119.14	-493	-445.7	-23.3	-70.6	-422.4
116.1	119.42	121.07	-499.8	-454.3	-22.2	-70.2	-430.9
118.2	121.62	123.24	-514.1	-462.2	-20.6	-69.4	-443.1
120.3	123.67	125.45	-527.7	-469.9	-18.9	-68.4	-455.1
122.3	125.47	127.25	-529.7	-477.4	-17.1	-67.4	-461.3
124.4	127.7	129.32	-541.8	-484.2	-14.7	-65.8	-472.8
126.5	129.78	131.4	-551.7	-491.3	-12.1	-64.0	-483.5
128.6	131.65	133.27	-564	-500.4	-9.5	-62.1	-496.4
130.6	133.75	135.36	-567.7	-506.6	-6.2	-59.7	-504.2
132.7	135.76	137.41	-577.5	-515	-2.8	-57.1	-516.3
134.7	137.71	139.36	-589.2	-520.8	0.9	-54.3	-528.3
136.8	139.62	141.33	-594	-528.6	4.8	-51.3	-538.0
138.9	141.79	143.44	-602.2	-533.1	9.6	-47.5	-548.7
141	143.82	145.56	-609.3	-539.9	14.4	-43.6	-560.0
143.1	145.95	147.47	-618.4	-545.4	19.9	-39.1	-572.3
145.1	147.7	149.4	-627.3	-552.6	24.8	-35.1	-584.8
147.2	149.79	151.46	-634.3	-558.7	30.9	-30.0	-597.0
149.3	151.87	153.61	-639.6	-564.9	37.5	-24.5	-608.8
151.4	153.55	154.57	-644.9	-569.1	43.2	-19.8	-618.7
153.4	154.48	155.05	-652.3	-572.6	46.4	-17.0	-627.1
155.5	154.77	155.09	-650.3	-574.7	47.4	-16.2	-628.1
157.6	155.24	155.37	-653	-575.2	49.1	-14.7	-631.3
159.7	155.31	155.34	-657.5	-577.1	49.4	-14.5	-634.7
161.7	155.3	155.62	-653.8	-578.8	49.3	-14.5	-633.7
163.8	155.39	155.49	-652.3	-579.9	49.7	-14.3	-633.8
165.9	153.18	150.33	-647.7	-574.6	41.9	-20.8	-621.7
168	148.13	144.11	-629.7	-561.2	26.0	-34.1	-591.4
170	142.71	138.53	-607.3	-546.7	11.7	-45.7	-560.0
172.1	137.44	133.32	-583.7	-528.5	0.4	-54.7	-528.9

Wind #11 (Cure Data)

Material: T40 fiber — Spool Tension(lb): 5.1
Number of Layers: 1 — Winding Tension(lb): 4.1
Oven Ramp Rate(degC/m): 1.0 — Stress Retention Factor: 0.80

Cure Time (min)	Mand. Temp. (deg C)	Oven Temp. (deg C)	Measured Microstrain Gage 1	Measured Microstrain Gage 2	Apparent Microstrain Gage 1	Apparent Microstrain Gage 2	Actual Microstrain
174.2	132.28	128.47	-570	-511	-8.5	-61.4	-505.5
176.3	127.58	123.89	-539.2	-492.4	-14.8	-65.9	-475.5
178.3	122.86	119.33	-517.4	-474.3	-19.6	-68.9	-451.6
180.4	118.76	115.25	-496.1	-458.2	-22.6	-70.3	-430.7
182.5	114.65	111.55	-477	-439.9	-24.5	-70.9	-410.7
184.5	108.43	100.96	-447.2	-412.5	-25.9	-70.0	-381.9
186.6	99.1	91.38	-399.2	-368.5	-24.6	-65.5	-338.8
188.7	90.45	83.9	-349.6	-327.9	-20.9	-58.7	-299.0
190.7	83.12	77.18	-306.4	-290.2	-16.4	-51.4	-264.4
192.8	70.57	53.91	-231.2	-215.6	-7.5	-37.1	-201.1
194.9	54.13	42.4	-132.1	-131	2.9	-18.1	-123.9
197	41.67	28.2	-87.4	-83.1	6.4	-6.3	-85.3
199.1	35.45	26.6	-59.7	-56.7	5.9	-2.1	-60.1
201.1	31.62	25.94	-53.5	-42.8	4.7	-0.1	-50.4
203.2	29.45	25.52	-44.3	-36	3.6	0.7	-42.3
205.3	27.76	25.31	-37	-35.2	2.6	1.2	-38.0
207.4	27.14	25.02	-34.6	-30.9	2.2	1.3	-34.5
209.4	26.47	24.99	-35	-29.6	1.7	1.5	-33.9
211.5	26.03	25.02	-37.1	-29.6	1.4	1.6	-34.8
213.6	25.58	24.37	-34.5	-27.8	1.0	1.6	-32.5
215.7	25.65	24.77	-35.1	-26.6	1.1	1.6	-32.2
217.7	25.52	24.4	-31.4	-26.4	1.0	1.7	-30.2
219.8	25.52	25.29	-13.9	-42.6	1.0	1.7	-29.6
221.9	26.22	25.47	-6.1	-2.2	1.5	1.5	-5.7
224	26.09	24.92	-7.7	-2.3	1.4	1.6	-6.5

Wind #11a (Cure Data)

Material: T40 fiber
Number of Layers: 1
Oven Ramp Rate(degC/m): 1.0
Spool Tension(lb): 5.0
Winding Tension(lb): 4.3
Stress Retention Factor: 0.86

Cure Time (min)	Mand. Temp. (deg C)	Oven Temp. (deg C)	Measured Microstrain Gage 1	Measured Microstrain Gage 2	Apparent Microstrain Gage 1	Apparent Microstrain Gage 2	Actual Microstrain
2	22.88	23.13	-74.4	-77.3	-1.3	1.9	-76.1
4.1	22.97	23.41	-71.5	-73.2	-1.2	1.9	-72.7
6.1	23.13	23.73	-71.4	-71.6	-1.1	1.9	-71.9
8.1	23.41	24	-69.9	-71.9	-0.8	1.9	-71.4
10.2	24.05	25.19	-73	-72.5	-0.2	1.8	-73.5
12.2	26.2	28.8	-79.8	-78.2	1.5	1.5	-80.5
14.3	29.19	31.89	-89.6	-86.9	3.5	0.8	-90.4
16.3	32.02	34.43	-98.5	-93.6	4.8	-0.3	-98.3
18.3	34.51	36.74	-106.9	-100.5	5.7	-1.5	-105.8
20.4	36.73	38.86	-115.3	-106.6	6.2	-2.8	-112.6
22.4	38.94	41.08	-122.1	-112	6.4	-4.3	-118.1
24.4	40.97	43.07	-128.6	-118.3	6.4	-5.8	-123.8
26.4	43.02	45.05	-135.6	-124.6	6.3	-7.4	-129.5
28.5	45.1	47.14	-141.6	-130.2	6.0	-9.2	-134.3
30.5	47.16	49.18	-150.6	-138	5.5	-11.1	-141.5
32.5	49.22	51.27	-158.7	-144.9	4.9	-13.1	-147.7
34.6	51.33	53.35	-166.6	-153.4	4.1	-15.2	-154.5
36.6	53.39	55.41	-174.4	-161.9	3.2	-17.3	-161.1
38.6	55.47	57.5	-184	-171.5	2.2	-19.6	-169.1
40.7	57.54	59.6	-195	-180	1.1	-21.9	-177.1
42.7	59.56	61.63	-205.1	-188.9	-0.1	-24.1	-184.9
44.7	61.6	63.7	-215.4	-199.6	-1.3	-26.5	-193.6
46.8	63.71	65.79	-226.8	-209.1	-2.7	-29.0	-202.1
48.8	65.73	67.82	-238.6	-218.9	-4.1	-31.3	-211.0
50.9	67.76	69.87	-249.8	-228.5	-5.5	-33.8	-219.5
52.9	69.85	71.93	-260.9	-239.4	-7.0	-36.2	-228.5
54.9	71.8	73.94	-272.5	-249.3	-8.4	-38.5	-237.4
56.9	74.01	76.11	-284.5	-259.2	-10.0	-41.1	-246.3
58.9	76.05	78.22	-296.8	-268.4	-11.5	-43.5	-255.1
61	78.04	80.07	-308	-277.9	-12.9	-45.8	-263.6
63	80.06	82.17	-319.6	-287.6	-14.3	-48.1	-272.4
65.1	82.13	84.26	-331	-298.2	-15.8	-50.3	-281.6
67.1	84.15	86.39	-344.3	-308	-17.1	-52.5	-291.4
69.1	86.22	88.37	-356.6	-318.3	-18.4	-54.6	-300.9
71.2	88.32	90.43	-367.3	-327.2	-19.7	-56.7	-309.1
73.2	90.32	92.48	-379.3	-337.2	-20.8	-58.6	-318.6
75.2	92.47	94.58	-391.3	-346.7	-22.0	-60.5	-327.8
77.3	94.47	96.69	-401.9	-356	-22.9	-62.1	-336.4
79.3	96.5	98.65	-414.2	-365.6	-23.7	-63.7	-346.2
81.3	98.38	100.46	-425.2	-375.6	-24.4	-65.0	-355.7
83.4	99.83	101.32	-433.6	-382	-24.9	-66.0	-362.4
85.4	100.51	101.65	-438.3	-385.7	-25.0	-66.4	-366.3

Wind #11a (Cure Data)

Material: T40 fiber
Spool Tension(lb): 5.0
Number of Layers: 1
Winding Tension(lb): 4.3
Oven Ramp Rate(degC/m): 1.0
Stress Retention Factor: 0.86

Cure Time (min)	Mand. Temp. (deg C)	Oven Temp. (deg C)	Measured Microstrain Gage 1	Measured Microstrain Gage 2	Apparent Microstrain Gage 1	Apparent Microstrain Gage 2	Actual Microstrain
87.5	101	101.91	-438.7	-386.9	-25.2	-66.7	-366.9
89.5	101.23	101.97	-440.6	-391.3	-25.2	-66.8	-369.9
91.5	101.27	102	-440	-388.5	-25.2	-66.9	-368.2
93.5	101.39	102.06	-441.2	-388.6	-25.3	-66.9	-368.8
95.6	101.49	102.19	-440.5	-388.7	-25.3	-67.0	-368.5
97.6	101.49	102.13	-440.1	-388.1	-25.3	-67.0	-368.0
99.6	101.48	102.12	-440.6	-388.8	-25.3	-67.0	-368.6
101.7	101.46	102.16	-440.4	-388.2	-25.3	-67.0	-368.2
103.7	101.68	102.28	-441.4	-387.3	-25.3	-67.1	-368.1
105.7	101.59	102.2	-440.8	-387.7	-25.3	-67.1	-368.1
107.8	101.57	102.19	-439.9	-387.3	-25.3	-67.0	-367.4
109.8	101.63	102.23	-439.2	-387.7	-25.3	-67.1	-367.3
111.8	101.67	102.43	-440.4	-387.7	-25.3	-67.1	-367.8
113.9	102.4	103.73	-443.6	-390	-25.5	-67.5	-370.3
115.9	103.65	105.36	-451.8	-396.3	-25.7	-68.1	-377.1
117.9	105.3	107.22	-459.5	-403.2	-25.8	-68.9	-384.0
119.9	107.14	109.16	-470.5	-411.9	-25.9	-69.6	-393.4
122	109	111.04	-479.9	-420.5	-25.8	-70.2	-402.2
124	110.88	112.98	-489.8	-428.3	-25.6	-70.6	-411.0
126	112.93	115.06	-500.1	-437.1	-25.1	-70.8	-420.6
128.1	114.8	117.02	-510.4	-445.8	-24.5	-70.8	-430.4
130.1	116.89	119.02	-521.2	-452.6	-23.6	-70.7	-439.8
132.1	118.79	121	-531.9	-461.9	-22.5	-70.3	-450.5
134.2	120.81	123.02	-540.7	-468.8	-21.2	-69.7	-459.3
136.2	122.85	125.05	-551.2	-476.6	-19.6	-68.9	-469.7
138.2	125.17	127.17	-560.8	-484.1	-17.4	-67.6	-479.9
140.3	127.12	129.13	-570.5	-491.8	-15.4	-66.2	-490.4
142.3	129.01	131.09	-578.3	-498.5	-13.1	-64.7	-499.5
144.3	131.16	133.26	-588.1	-505.6	-10.2	-62.6	-510.5
146.4	133.11	135.13	-596.8	-511.9	-7.2	-60.5	-520.5
148.4	135.07	137.08	-606.1	-517.6	-4.0	-58.1	-530.8
150.4	137.02	139.17	-614.6	-524.2	-0.4	-55.3	-541.5
152.5	139.01	141.17	-623.3	-530.3	3.5	-52.3	-552.4
154.5	141.02	143.17	-631.4	-537.5	7.8	-48.9	-563.9
156.5	143.14	145.24	-640.5	-543.3	12.7	-44.9	-575.8
158.6	145.07	147.21	-648.2	-548.6	17.6	-41.0	-586.7
160.6	146.98	149.18	-657	-554.3	22.7	-36.8	-598.6
162.6	149	151.19	-663.5	-559.3	28.6	-32.0	-609.7
164.7	150.88	153.06	-669.9	-564.1	34.3	-27.1	-620.6
166.7	152.97	155.06	-678	-569.5	41.2	-21.4	-633.6
168.7	154.36	155.91	-683	-571.6	46.0	-17.4	-641.6
170.7	155.18	156.38	-685.5	-574	48.9	-14.9	-646.7

Wind #11a (Cure Data)

Material: T40 fiber
Number of Layers: 1
Oven Ramp Rate(degC/m): 1.0

Spool Tension(lb): 5.0
Winding Tension(lb): 4.3
Stress Retention Factor: 0.86

Cure Time (min)	Mand. Temp. (deg C)	Oven Temp. (deg C)	Measured Microstrain Gage 1	Measured Microstrain Gage 2	Apparent Microstrain Gage 1	Apparent Microstrain Gage 2	Actual Microstrain
172.8	155.57	156.6	-686.1	-575.5	50.3	-13.7	-649.1
174.8	155.87	156.79	-688.6	-576.6	51.4	-12.8	-651.9
176.9	156.07	156.97	-688.4	-576.4	52.2	-12.2	-652.4
178.9	156.24	157.05	-687	-577.5	52.8	-11.6	-652.8
180.9	156.26	157.08	-688.4	-577.3	52.9	-11.6	-653.5
183	156.29	157.1	-688	-577	53.0	-11.5	-653.3
185	156.26	157.03	-689.7	-576.8	52.9	-11.6	-653.9
187	156.41	157.19	-688.2	-576.9	53.4	-11.1	-653.7
189	156.42	157.17	-688.3	-576.7	53.5	-11.1	-653.7
191.1	156.36	157.11	-688.4	-576.2	53.2	-11.2	-653.3
193.1	156.46	157.26	-687.6	-576.3	53.6	-10.9	-653.3
195.1	156.49	157.19	-687.5	-576.9	53.7	-10.8	-653.6
197.2	155.12	153.72	-683.8	-574	48.7	-15.1	-645.7
199.2	150.25	146.9	-666.6	-561	32.4	-28.8	-615.6
201.3	144.06	140.12	-641.8	-544.3	15.0	-43.1	-579.0
203.3	137.82	133.85	-616.2	-523.6	1.1	-54.1	-543.4
205.3	131.9	128.06	-588.8	-502.3	-9.1	-61.8	-510.1
207.4	126.22	122.56	-561.7	-480.4	-16.4	-66.9	-479.4
209.4	121.01	117.51	-533.7	-458.4	-21.1	-69.6	-450.7
211.4	116.07	112.74	-508.7	-436.8	-24.0	-70.8	-425.4
213.5	111.16	106.75	-482.5	-414.7	-25.5	-70.6	-400.5
215.5	100.36	89.66	-421.8	-364	-25.0	-66.3	-347.2
217.5	88.57	79.5	-350.8	-305.1	-19.8	-56.9	-289.6
219.5	79.21	71.69	-292.5	-255.8	-13.7	-47.1	-243.7
221.6	71.45	65.33	-245.1	-213	-8.1	-38.1	-205.9
223.6	65.2	60.23	-208.3	-179.4	-3.7	-30.7	-176.6
225.7	59.89	55.79	-178.4	-151.9	-0.3	-24.5	-152.7
227.7	55.64	52.25	-152.8	-128.6	2.1	-19.7	-131.9
229.7	51.92	49.13	-132.7	-110.5	3.8	-15.8	-115.6
231.8	48.9	46.6	-115.6	-95.9	5.0	-12.7	-101.9
233.8	46.55	44.46	-103.1	-83.6	5.7	-10.5	-90.9
235.8	45.16	41.84	-96.7	-76.1	6.0	-9.3	-84.7
237.8	43.27	38.48	-88.4	-67.6	6.3	-7.6	-77.3
239.9	38.68	29.83	-66	-47.4	6.4	-4.1	-57.8
241.9	34.81	28.18	-47.5	-32.3	5.8	-1.7	-41.9
243.9	32.23	27.4	-36	-22.3	4.9	-0.4	-31.4
246	30.19	26.44	-27.6	-15	4.0	0.4	-23.5
248	28.96	26.15	-22.8	-10.9	3.3	0.8	-18.9
250	28.15	26.27	-19.3	-8.5	2.8	1.1	-15.9
252.1	27.44	25.78	-17.7	-6.1	2.4	1.3	-13.7
254.1	26.96	25.77	-14.9	-3.8	2.1	1.4	-11.1
256.1	26.64	25.43	-14.5	-2.9	1.8	1.5	-10.3

Wind #11a (Cure Data)

Material: T40 fiber | Spool Tension(lb): 5.0
Number of Layers: 1 | Winding Tension(lb): 4.3
Oven Ramp Rate(degC/m): 1.0 | Stress Retention Factor: 0.86

Cure Time (min)	Mand. Temp. (deg C)	Oven Temp. (deg C)	Measured Microstrain Gage 1	Measured Microstrain Gage 2	Apparent Microstrain Gage 1	Apparent Microstrain Gage 2	Actual Microstrain
258.2	26.26	25.32	-12.1	-1.1	1.6	1.5	-8.1
260.2	25.93	25.17	-11.6	-0.6	1.3	1.6	-7.5
262.3	25.85	25.07	-10.5	0.3	1.3	1.6	-6.5
264.3	25.62	25.06	-9.3	1	1.1	1.6	-5.5
266.3	25.36	24.91	-8.5	1.3	0.9	1.7	-4.9
268.3	25.3	24.91	-9.3	2.7	0.8	1.7	-4.6
270.4	25.24	24.76	-9	3.8	0.8	1.7	-3.8
272.4	24.96	24.3	-7.8	4.3	0.5	1.7	-2.9
274.4	24.49	23.82	-7.1	5.7	0.2	1.8	-1.7

Wind #12 (Cure Data)

Material: T40 fiber | Spool Tension(lb): 5.0

Number of Layers: 3 | Winding Tension(lb): 4.1

Oven Ramp Rate(degC/m): 2.0 | Stress Retention Factor: 0.82

Cure Time (min)	Mand. Temp. (deg C)	Oven Temp. (deg C)	Measured Microstrain Gage 1	Measured Microstrain Gage 2	Apparent Microstrain Gage 1	Apparent Microstrain Gage 2	Actual Microstrain
0.7	23.32	23.72	-138.8	-120	-0.9	1.9	-129.9
4.9	23.81	24.35	-140.6	-123.4	-0.4	1.8	-132.7
9	30.04	34.16	-178.1	-156	3.9	0.5	-169.3
13.2	39.8	43.54	-235	-209.5	6.4	-4.9	-223.0
17.4	48.71	52.27	-302.6	-269.5	5.0	-12.6	-282.3
21.5	57.15	60.61	-377.2	-341	1.3	-21.4	-349.0
25.6	65.22	68.8	-459	-412.5	-3.7	-30.7	-418.5
29.7	73.68	77.12	-545	-489.2	-9.7	-40.8	-491.9
33.7	81.58	85.14	-633.5	-563	-15.4	-49.7	-565.7
37.8	89.62	93.29	-722.7	-641.1	-20.4	-57.9	-642.7
41.9	97.24	99.85	-804.4	-709.8	-24.0	-64.3	-713.0
46	100.46	101.6	-840.7	-740.4	-25.0	-66.4	-744.8
50.2	101.54	102.05	-850.5	-753.1	-25.3	-67.0	-755.6
54.3	101.77	102.17	-856	-754.2	-25.3	-67.2	-758.9
58.5	102.05	102.5	-858.3	-755.3	-25.4	-67.3	-760.4
62.6	102.09	102.33	-854.9	-756.8	-25.4	-67.3	-759.5
66.8	102.15	102.45	-857.7	-754	-25.4	-67.4	-759.5
71	102.46	103.02	-860	-757.5	-25.5	-67.5	-762.2
75.1	106.17	108.76	-900.5	-791.3	-25.9	-69.2	-798.3
79.3	113.21	116.53	-977.8	-856.4	-25.0	-70.8	-869.2
83.4	121.01	124.48	-1062.1	-922.3	-21.1	-69.6	-946.8
87.6	129.01	132.47	-1146.6	-993.1	-13.1	-64.7	-1031.0
91.7	137.04	140.73	-1232.4	-1067.3	-0.4	-55.3	-1122.0
95.9	145.1	148.76	-1316.5	-1132.3	17.7	-40.9	-1212.8
100	152.36	155	-1391.8	-1192.6	39.1	-23.1	-1300.2
104.1	155.09	156.54	-1420.4	-1218.8	48.6	-15.2	-1336.3
108.3	156.1	157.04	-1431.7	-1222	52.3	-12.1	-1346.9
112.4	156.37	157.19	-1441.6	-1230.8	53.3	-11.2	-1357.2
116.5	156.75	157.53	-1450.4	-1233.1	54.7	-10.0	-1364.1
120.7	156.86	157.58	-1453	-1236.5	55.1	-9.7	-1367.5
124.8	156.88	157.48	-1456.5	-1238.8	55.2	-9.6	-1370.5
128.9	155.8	154.16	-1449	-1229.5	51.2	-13.0	-1358.3
133.1	144.64	140.42	-1339.6	-1141.8	16.5	-41.9	-1228.0
137.2	132.1	128.21	-1211.6	-1042.7	-8.8	-61.6	-1091.9
141.4	120.91	117.38	-1093.8	-934.1	-21.1	-69.7	-968.5
145.5	111.25	108.12	-983.2	-851	-25.5	-70.6	-869.0
149.7	102.65	99.87	-888.8	-768.7	-25.5	-67.6	-782.2
154.8	93.45	90.92	-779.5	-674.4	-22.4	-61.3	-685.1
158.9	86.96	84.67	-709	-610	-18.9	-55.4	-622.4
162.9	81.22	79.09	-641.1	-553.3	-15.1	-49.3	-565.0
167	76.03	74.11	-585.4	-503.2	-11.4	-43.5	-516.8
171.1	71.35	69.63	-535.1	-459.1	-8.0	-38.0	-474.1

Wind #12 (Cure Data)

Material: T40 fiber
Number of Layers: 3
Oven Ramp Rate(degC/m): 2.0
Spool Tension(lb): 5.0
Winding Tension(lb): 4.1
Stress Retention Factor: 0.82

Cure Time (min)	Mand. Temp. (deg C)	Oven Temp. (deg C)	Measured Microstrain Gage 1	Measured Microstrain Gage 2	Apparent Microstrain Gage 1	Apparent Microstrain Gage 2	Actual Microstrain
175.1	67.17	65.61	-487.4	-420.4	-5.1	-33.1	-434.8
179.2	63.34	61.94	-448.5	-386.4	-2.5	-28.5	-402.0
183.4	59.86	58.67	-411	-348.5	-0.3	-24.5	-367.4
187.5	56.78	55.66	-381.4	-327.5	1.5	-21.0	-344.7
191.7	53.89	52.93	-354.7	-296.2	3.0	-17.9	-318.0
195.8	51.47	50.57	-332.8	-277.9	4.0	-15.3	-299.7
200	49.13	48.33	-309.6	-258.7	4.9	-13.0	-280.1
204.2	47.9	47.67	-299.3	-250.1	5.3	-11.8	-271.5
208.3	47.4	47.31	-298.4	-248.1	5.4	-11.3	-270.3
212.5	46.89	46.91	-291	-243.5	5.6	-10.8	-264.6
216.7	46.26	46.26	-289.5	-239.4	5.7	-10.2	-262.2
220.8	45.51	45.37	-283.3	-234.3	5.9	-9.6	-257.0
225	44.78	44.45	-276.6	-228	6.0	-8.9	-250.9
229.1	44.07	43.62	-268.3	-219.7	6.2	-8.3	-242.9
233.3	43.13	42.77	-259.3	-214.9	6.3	-7.5	-236.5
237.4	42.2	41.75	-254.9	-208.1	6.4	-6.8	-231.3
241.6	41.41	40.9	-246.6	-202.4	6.4	-6.1	-224.6
245.7	40.22	39.9	-241	-195.1	6.5	-5.2	-218.7
249.9	39.47	39.06	-235	-190.7	6.4	-4.7	-213.7
254.1	38.48	38.06	-227.5	-180.2	6.4	-4.0	-205.0
258.2	37.72	37.26	-219.5	-179.3	6.3	-3.5	-200.8
262.4	36.99	36.55	-215.8	-175.6	6.2	-3.0	-197.3
266.6	36.11	35.75	-211.3	-167.2	6.1	-2.5	-191.0
270.7	35.34	34.9	-207.1	-167.6	5.9	-2.0	-189.3
274.9	34.56	34.18	-201.5	-161.4	5.7	-1.6	-183.5
279	33.91	33.49	-197.8	-159.2	5.5	-1.2	-180.6
283.2	33.19	32.82	-191.9	-156.7	5.3	-0.9	-176.5
287.3	32.52	32.22	-192.1	-152.8	5.0	-0.5	-174.7
291.5	32.01	31.67	-186.4	-149.4	4.8	-0.3	-170.2
295.7	31.58	31.23	-187.9	-149.2	4.7	-0.1	-170.8
299.8	30.81	30.64	-182.1	-142.9	4.3	0.2	-164.7
304	30.54	30.19	-177.7	-141.3	4.2	0.3	-161.7
311.2	29.65	29.35	-175.9	-140.8	3.7	0.6	-160.5
315.4	29.23	28.97	-175	-140.7	3.5	0.8	-160.0
319.6	28.72	28.51	-173.2	-137.3	3.2	0.9	-157.3
323.7	28.35	28.16	-170.6	-135.8	3.0	1.0	-155.2
327.9	28.12	27.9	-171.5	-137.1	2.8	1.1	-156.3
332.1	27.87	27.6	-171.5	-135.8	2.7	1.2	-155.6
336.2	27.52	27.37	-168.3	-133.1	2.4	1.3	-152.5
340.4	27.14	26.98	-166.9	-134.9	2.2	1.3	-152.7
344.5	26.89	26.7	-164.4	-133.1	2.0	1.4	-150.5
348.7	26.68	26.53	-166.7	-134.6	1.9	1.4	-152.3

Wind #12 (Cure Data)

Material: T40 fiber
Number of Layers: 3
Oven Ramp Rate(degC/m): 2.0

Spool Tension(lb): 5.0
Winding Tension(lb): 4.1
Stress Retention Factor: 0.82

Cure Time (min)	Mand. Temp. (deg C)	Oven Temp. (deg C)	Measured Microstrain Gage 1	Measured Microstrain Gage 2	Apparent Microstrain Gage 1	Apparent Microstrain Gage 2	Actual Microstrain
352.8	26.41	26.3	-165.8	-130.8	1.7	1.5	-149.9
357	26.3	26.14	-164.1	-132.3	1.6	1.5	-149.8
361.2	26.12	25.99	-164.2	-130.3	1.5	1.6	-148.8
365.3	25.74	25.61	-163.3	-131	1.2	1.6	-148.5
369.5	25.57	25.39	-162.2	-130.2	1.0	1.6	-147.5
373.6	25.51	25.32	-162.5	-127.7	1.0	1.7	-146.4
377.8	25.32	25.18	-159.5	-130.5	0.8	1.7	-146.3
382	25.16	25.01	-164.4	-127.6	0.7	1.7	-147.2
386.1	24.92	24.82	-159.9	-130	0.5	1.7	-146.1
390.3	24.78	24.68	-162.5	-127.9	0.4	1.8	-146.3
394.4	24.74	24.59	-159.3	-129.1	0.4	1.8	-145.3
398.6	24.49	24.43	-160.5	-129.3	0.2	1.8	-145.9
402.7	24.55	24.38	-159.2	-127.3	0.2	1.8	-144.2
406.9	24.39	24.31	-159.8	-127.2	0.1	1.8	-144.4
411.1	24.2	24.1	-159.5	-129.4	-0.1	1.8	-145.3
415.2	24.09	24.03	-159.4	-128.1	-0.2	1.8	-144.6
419.4	24.06	23.94	-160	-126.3	-0.2	1.8	-144.0
423.6	23.75	23.88	-157.4	-126.4	-0.5	1.9	-142.6
427.7	23.84	23.75	-158.8	-125.7	-0.4	1.8	-143.0

Wind #13 (Cure Data)

Material: T40/1908 prepreg — Spool Tension(lb): 5.0

Number of Layers: 3 — Winding Tension(lb): 2.5

Oven Ramp Rate(degC/m): 2.0 — Stress Retention Factor: 0.50

Cure Time (min)	Mand. Temp. (deg C)	Oven Temp. (deg C)	Measured Microstrain Gage 1	Measured Microstrain Gage 2	Apparent Microstrain Gage 1	Apparent Microstrain Gage 2	Actual Microstrain
0.7	23.12	23.13	-67.5	-81.5	-1.1	1.9	-74.9
2.8	23.22	23.48	-66.6	-81.8	-1.0	1.9	-74.6
4.9	23.54	23.82	-66.5	-83.4	-0.7	1.9	-75.5
6.9	24.78	27.77	-78	-91.9	0.4	1.8	-86.0
9	28.93	33.73	-102.1	-115.8	3.3	0.9	-111.0
11.1	33.77	38.6	-131.8	-140.4	5.5	-1.2	-138.3
13.1	38.44	43.08	-153.8	-160	6.4	-4.0	-158.1
15.2	43.01	47.57	-174	-178.9	6.3	-7.4	-175.9
17.3	47.37	51.72	-193.7	-197.5	5.4	-11.3	-192.7
19.4	51.47	55.82	-216	-217.5	4.0	-15.3	-211.1
21.4	55.68	59.94	-240.5	-241	2.1	-19.8	-231.9
23.5	59.93	64.29	-270	-269.4	-0.3	-24.6	-257.3
25.6	64.18	68.55	-304.8	-300.4	-3.0	-29.5	-286.3
27.6	68.08	72.41	-338.1	-333.2	-5.7	-34.1	-315.7
29.7	72.16	76.48	-374.7	-366.4	-8.6	-39.0	-346.7
31.7	76.29	80.56	-412.4	-400.3	-11.6	-43.8	-378.6
33.7	80.28	84.66	-451	-435.2	-14.5	-48.3	-411.7
35.7	84.36	88.59	-490.9	-468.9	-17.2	-52.7	-444.9
37.8	88.34	92.69	-532	-503.9	-19.7	-56.7	-479.7
39.9	92.55	96.83	-571	-539.5	-22.0	-60.5	-514.0
41.9	96.33	99.7	-608.3	-571.2	-23.7	-63.6	-546.1
43.9	98.83	100.84	-630.8	-591.5	-24.6	-65.4	-566.2
46	100.24	101.45	-642.9	-602.2	-25.0	-66.3	-576.9
48.1	101.11	101.88	-653	-606.8	-25.2	-66.8	-583.9
50.2	101.46	102.03	-655.6	-611.4	-25.3	-67.0	-587.4
52.2	101.78	102.21	-658.3	-613.9	-25.3	-67.2	-589.8
54.3	101.95	102.24	-659.4	-616.6	-25.4	-67.3	-591.7
56.4	102.11	102.34	-659.7	-616.2	-25.4	-67.3	-591.6
58.5	102.24	102.36	-661.2	-617.3	-25.4	-67.4	-592.8
60.6	102.27	102.43	-661.4	-616	-25.4	-67.4	-592.3
62.6	102.39	102.45	-662.7	-618.2	-25.5	-67.5	-594.0
64.7	102.34	102.48	-662	-617.9	-25.5	-67.5	-593.5
66.8	102.41	102.53	-662.7	-618.5	-25.5	-67.5	-594.1
68.9	102.44	102.47	-663.2	-618.1	-25.5	-67.5	-594.2
70.9	102.6	102.69	-663.7	-617.1	-25.5	-67.6	-593.8
73	103.4	104.92	-674	-627	-25.6	-68.0	-603.7
75.1	105.69	108.22	-696.9	-649.6	-25.9	-69.1	-625.8
77.2	108.69	111.8	-732.4	-678	-25.8	-70.1	-657.2
79.3	112.18	115.65	-767	-709.9	-25.3	-70.7	-690.4
81.3	116.08	119.8	-805.5	-742.7	-24.0	-70.8	-726.7
83.4	120.09	123.7	-846.9	-777.9	-21.7	-70.0	-766.6
85.5	124.05	127.78	-886.8	-812.5	-18.5	-68.2	-806.3

Wind #13 (Cure Data)

Material: T40/1908 prepreg — Spool Tension(lb): 5.0
Number of Layers: 3 — Winding Tension(lb): 2.5
Oven Ramp Rate(degC/m): 2.0 — Stress Retention Factor: 0.50

Cure Time (min)	Mand. Temp. (deg C)	Oven Temp. (deg C)	Measured Microstrain Gage 1	Measured Microstrain Gage 2	Apparent Microstrain Gage 1	Apparent Microstrain Gage 2	Actual Microstrain
87.6	128.14	131.98	-924.4	-846.7	-14.2	-65.4	-845.8
89.7	132.14	135.96	-967.4	-881	-8.7	-61.6	-889.0
91.7	136.12	139.91	-1007	-916	-2.1	-56.6	-932.1
93.8	140.17	143.91	-1046.9	-950.7	5.9	-50.3	-976.6
95.9	144.23	147.99	-1086	-983.6	15.4	-42.7	-1021.2
98	148.36	151.98	-1126.5	-1015.8	26.7	-33.5	-1067.7
100	152.03	154.64	-1159.9	-1042.8	38.0	-24.0	-1108.3
102.1	154.12	155.75	-1181.1	-1058.9	45.1	-18.1	-1133.5
104.2	155.32	156.32	-1191.1	-1068.2	49.4	-14.5	-1147.1
106.2	156.05	156.75	-1197.6	-1071.7	52.1	-12.2	-1154.6
108.3	156.55	157.07	-1203.2	-1075.3	53.9	-10.6	-1160.9
110.4	156.61	157.02	-1204.5	-1077.8	54.2	-10.5	-1163.0
112.4	156.77	157.15	-1208.2	-1080.3	54.8	-9.9	-1166.7
114.5	156.93	157.25	-1209	-1080.5	55.4	-9.4	-1167.7
116.6	156.99	157.32	-1209.7	-1082.8	55.6	-9.2	-1169.4
118.6	156.94	157.35	-1210.4	-1081.5	55.4	-9.4	-1169.0
120.7	157.07	157.45	-1210.3	-1082	55.9	-9.0	-1169.6
122.8	157.32	157.6	-1214.3	-1083.7	56.9	-8.2	-1173.4
124.9	157.17	157.5	-1213.2	-1083.1	56.3	-8.7	-1172.0
126.9	157.19	157.52	-1214.3	-1083.3	56.4	-8.6	-1172.7
129	156.9	155.35	-1209.4	-1079.5	55.3	-9.5	-1167.3
131.1	152.6	148.23	-1167	-1042.7	39.9	-22.5	-1113.6
133.2	146.64	141.43	-1105.6	-989	21.8	-37.5	-1039.4
135.2	140.27	134.97	-1040	-933.6	6.2	-50.2	-964.8
137.3	134.1	128.95	-973.7	-878.1	-5.6	-59.3	-893.4
139.4	128.4	123.48	-911.4	-825.4	-13.8	-65.2	-828.9
141.5	123.01	118.22	-850.2	-774.4	-19.5	-68.8	-768.2
143.5	117.85	113.27	-793.8	-725.5	-23.1	-70.5	-712.8
145.6	112.98	108.7	-739.8	-678.4	-25.1	-70.8	-661.1
149.8	104.18	100.38	-636.7	-589.6	-25.7	-68.4	-566.1
154.9	94.65	91.15	-525.3	-493.2	-23.0	-62.3	-466.6
158.9	87.96	84.82	-450	-427.5	-19.5	-56.3	-400.8
163	81.89	79.1	-380.1	-366.2	-15.6	-50.1	-340.3
167.1	76.61	74.1	-320	-312.5	-11.9	-44.2	-288.2
171.1	71.9	69.62	-264	-261.4	-8.4	-38.7	-239.1
175.2	67.31	65.22	-216.6	-216.7	-5.2	-33.2	-197.5
179.3	63.55	61.64	-172.8	-176.8	-2.6	-28.8	-159.1
183.4	59.99	58.26	-133.6	-141	-0.3	-24.6	-124.8
187.6	56.85	55.24	-99	-113.2	1.5	-21.1	-96.3
191.7	54.06	52.63	-66.4	-85.8	2.9	-18.0	-68.5
195.8	51.35	50.18	-38.7	-62.9	4.1	-15.2	-45.2
200	49.07	47.91	-13.7	-42.1	4.9	-12.9	-23.9

Wind #13 (Cure Data)

Material: T40/1908 prepreg — Spool Tension(lb): 5.0
Number of Layers: 3 — Winding Tension(lb): 2.5
Oven Ramp Rate(degC/m): 2.0 — Stress Retention Factor: 0.50

Cure Time (min)	Mand. Temp. (deg C)	Oven Temp. (deg C)	Measured Microstrain Gage 1	Measured Microstrain Gage 2	Apparent Microstrain Gage 1	Apparent Microstrain Gage 2	Actual Microstrain
204	48.17	47.77	-5.4	-35.3	5.2	-12.0	-16.9
208.1	47.59	47.42	0.1	-30.4	5.4	-11.5	-12.1
212.2	47.07	46.76	5.9	-25.7	5.5	-11.0	-7.2
216.3	46.52	46.26	12.1	-19.1	5.7	-10.5	-1.1
220.4	45.78	45.35	22.3	-11.2	5.8	-9.8	7.5
224.5	44.97	44.47	29	-3.4	6.0	-9.1	14.3
228.5	44.01	43.44	39.3	5.1	6.2	-8.3	23.3
232.7	43.08	42.58	48.1	14.6	6.3	-7.5	31.9
236.8	42.05	41.65	57.9	24.1	6.4	-6.6	41.1
240.9	40.95	40.59	69.5	33	6.4	-5.8	50.9
245	40.19	39.56	72.7	40.9	6.5	-5.2	56.2
249.1	38.97	38.64	82.6	49.2	6.4	-4.3	64.9
253.2	38.25	37.71	105.8	55.3	6.4	-3.8	79.3
257.4	37.1	36.74	117.7	62.3	6.2	-3.1	88.4
261.5	36.26	35.94	127.3	69.4	6.1	-2.6	96.6
265.7	35.41	35.1	130.9	65.7	5.9	-2.1	96.4
269.8	34.71	34.33	139.7	71.8	5.7	-1.7	103.7
273.9	33.92	33.6	147.1	76.8	5.5	-1.2	109.8
278.1	33.31	32.94	153.2	80.3	5.3	-0.9	114.6
282.2	32.48	32.26	162.1	85.9	5.0	-0.5	121.8
286.4	32.05	31.75	169.9	89.2	4.8	-0.3	127.3
290.5	31.53	31.27	178.1	96.1	4.6	-0.1	134.8
294.7	30.93	30.55	157.2	104.6	4.4	0.1	128.6
298.8	30.35	30.04	159.9	107.7	4.1	0.4	131.6
303	30.02	29.65	165.2	111	3.9	0.5	135.9
307.2	29.51	29.19	168.2	114.8	3.6	0.7	139.3
311.3	28.81	28.71	166.9	127.6	3.2	0.9	145.2
315.5	28.35	28.3	170.6	132.7	3.0	1.0	149.6
319.6	28.07	27.98	173	136.3	2.8	1.1	152.7
323.8	27.72	27.63	173.4	138.7	2.6	1.2	154.2
327.9	27.36	27.36	177.3	141.2	2.3	1.3	157.4
332.1	27.19	27.1	179.5	142.9	2.2	1.3	159.4
336.3	26.78	26.73	183	144.4	1.9	1.4	162.0
340.4	26.44	26.31	185.3	145.4	1.7	1.5	163.8
344.6	26.27	26.16	192.2	146	1.6	1.5	167.6
348.7	25.86	25.91	200.3	131	1.3	1.6	164.2
352.9	25.79	25.75	200.2	126.2	1.2	1.6	161.8
357.1	25.47	25.55	202.1	127.1	1.0	1.7	163.3
361.2	25.38	25.38	202.3	128.1	0.9	1.7	163.9
365.3	25.12	25.14	97.6	110.5	0.7	1.7	102.9
369.4	25.03	25.07	177.4	53.4	0.6	1.7	114.2
373.5	24.78	24.81	176.1	53	0.4	1.8	113.5

Wind #14a (Cure Data)

Material: T40/1908 prepreg | Spool Tension(lb): 5.0
Number of Layers: 1 | Winding Tension(lb): 1.5
Oven Ramp Rate(degC/m): 1.0 | Stress Retention Factor: 0.30

Cure Time (min)	Mand. Temp. (deg C)	Oven Temp. (deg C)	Measured Microstrain Gage 1	Measured Microstrain Gage 2	Apparent Microstrain Gage 1	Apparent Microstrain Gage 2	Actual Microstrain
5.0	23.6	23.8	-34.6	-13.8	-0.6	1.9	-24.8
10.0	29.6	31.5	-39.4	-28.4	3.7	0.6	-36.1
15.1	34.3	35.7	-55.1	-45.4	5.6	-1.4	-52.3
20.1	38.5	40.1	-66.0	-55.4	6.4	-4.0	-61.9
25.1	43.4	45.0	-82.9	-72.2	6.3	-7.7	-76.8
30.1	48.5	50.2	-95.8	-95.1	5.1	-12.4	-91.8
35.2	53.6	55.3	-121.9	-111.9	3.1	-17.5	-109.7
40.2	59.0	60.4	-146.8	-142.3	0.3	-23.4	-133.0
45.2	64.1	65.5	-188.4	-165.0	-3.0	-29.4	-160.5
50.3	69.4	70.8	-204.1	-198.4	-6.6	-35.6	-180.1
55.3	74.4	75.8	-229.2	-217.0	-10.2	-41.6	-197.2
60.3	79.1	80.6	-265.6	-243.7	-13.6	-46.9	-224.4
65.3	84.3	85.8	-288.9	-271.1	-17.2	-52.6	-245.1
70.3	89.4	90.9	-326.8	-294.8	-20.3	-57.7	-271.8
75.4	94.5	96.1	-356.7	-321.8	-22.9	-62.2	-296.7
80.4	99.4	100.5	-377.7	-347.6	-24.7	-65.7	-317.4
85.4	101.3	101.6	-390.5	-351.9	-25.2	-66.9	-325.2
90.5	101.8	101.8	-396.0	-357.3	-25.3	-67.1	-330.4
95.5	101.9	101.7	-397.5	-352.0	-25.4	-67.2	-328.5
100.5	101.8	101.6	-396.6	-358.0	-25.3	-67.2	-331.0
105.6	101.8	101.7	-403.7	-359.3	-25.3	-67.2	-335.2
110.6	101.9	102.1	-401.1	-357.7	-25.4	-67.3	-333.1
115.6	105.1	106.3	-422.1	-375.1	-25.8	-68.8	-351.3
120.7	109.7	111.2	-441.7	-400.3	-25.7	-70.3	-373.0
125.7	114.6	116.3	-473.5	-418.5	-24.6	-70.9	-398.3
130.7	119.8	121.4	-497.6	-445.6	-21.9	-70.1	-425.6
135.7	124.9	126.4	-525.2	-465.4	-17.7	-67.8	-452.6
140.8	129.9	131.5	-543.5	-486.2	-11.9	-63.9	-476.9
145.8	134.8	136.4	-580.4	-507.6	-4.5	-58.4	-512.6
150.8	140.0	142.0	-603.2	-525.8	5.6	-50.7	-541.9
155.9	144.5	146.1	-624.3	-547.3	16.0	-42.3	-572.7
160.9	149.6	151.2	-641.9	-563.6	30.3	-30.5	-602.7
165.9	154.5	155.8	-665.6	-577.3	46.4	-17.1	-636.1
171.0	156.4	156.7	-674.4	-582.5	53.3	-11.2	-649.5
176.0	156.8	157.0	-682.7	-585.8	54.9	-9.9	-656.7
181.1	157.0	157.1	-674.4	-591.9	55.6	-9.3	-656.3
186.1	157.1	157.3	-675.9	-584.5	56.0	-8.9	-653.8
191.2	157.1	157.2	-681.3	-588.3	56.0	-8.9	-658.3
196.2	153.8	149.7	-670.5	-579.0	44.1	-18.9	-637.3
201.2	138.0	133.0	-606.4	-529.0	1.4	-53.9	-541.4
206.2	125.1	120.6	-554.5	-473.2	-17.5	-67.6	-471.3
211.3	112.5	108.5	-484.3	-421.0	-25.2	-70.8	-404.7

Wind #14a (Cure Data)

Material: T40/1908 prepreg — Spool Tension(lb): 5.0
Number of Layers: 1 — Winding Tension(lb): 1.5
Oven Ramp Rate(degC/m): 1.0 — Stress Retention Factor: 0.30

Cure Time (min)	Mand. Temp. (deg C)	Oven Temp. (deg C)	Measured Microstrain Gage 1	Measured Microstrain Gage 2	Apparent Microstrain Gage 1	Apparent Microstrain Gage 2	Actual Microstrain
216.3	101.6	98.4	-428.6	-368.9	-25.3	-67.0	-352.6
221.3	92.4	89.5	-366.5	-319.0	-21.9	-60.4	-301.6
226.3	84.4	81.9	-313.7	-280.0	-17.2	-52.7	-261.9
231.3	77.2	75.1	-263.3	-243.8	-12.3	-44.8	-225.0
236.4	71.2	69.1	-226.9	-208.1	-7.9	-37.8	-194.7
241.4	65.8	64.1	-199.1	-175.5	-4.1	-31.4	-169.5
246.5	60.8	59.6	-156.9	-156.5	-0.8	-25.6	-143.5
251.5	57.1	55.8	-145.4	-131.0	1.3	-21.4	-128.2
256.5	53.6	52.5	-131.9	-108.5	3.1	-17.5	-113.0
261.6	50.4	49.4	-110.8	-94.1	4.4	-14.3	-97.5
266.6	47.4	46.6	-94.3	-80.6	5.4	-11.3	-84.5
271.6	47.0	46.8	-120.0	-65.6	5.5	-10.9	-90.1
276.7	46.6	46.3	-116.1	-61.9	5.6	-10.5	-86.6
281.7	45.8	45.5	-114.0	-59.1	5.8	-9.9	-84.5
286.7	44.8	44.3	-109.8	-51.9	6.0	-8.9	-79.4
291.7	43.7	43.2	-110.6	-46.3	6.2	-8.0	-77.6
296.7	42.6	42.1	-97.2	-39.8	6.3	-7.1	-68.1
301.7	41.5	40.7	-97.8	-32.9	6.4	-6.2	-65.5
306.8	40.4	39.5	-79.6	-29.3	6.5	-5.4	-55.0
311.8	39.1	38.6	-80.2	-15.1	6.4	-4.5	-48.6
316.8	38.0	37.5	-82.1	-12.1	6.3	-3.6	-48.4
321.8	37.1	36.0	-95.1	-7.2	6.2	-3.1	-52.7
326.9	36.1	35.4	-72.2	-9.1	6.1	-2.5	-42.4
331.9	35.0	34.3	-55.3	-5.4	5.8	-1.8	-32.3
336.9	34.1	33.5	-8.9	-27.5	5.6	-1.3	-20.3
341.9	33.2	32.7	-7.2	-24.1	5.3	-0.9	-17.9
346.9	32.5	31.9	7.2	-9.7	5.0	-0.5	-3.5
352.0	31.9	31.3	6.9	-5.1	4.8	-0.2	-1.4
357.0	31.0	30.6	18.7	4.8	4.4	0.1	9.5
362.0	30.4	30.0	26.8	7.4	4.1	0.4	14.9
367.0	29.8	29.5	22.3	12.4	3.8	0.6	15.2
372.0	29.2	28.7	11.2	29.1	3.5	0.8	18.0
377.1	28.7	28.4	20.7	32.2	3.2	0.9	24.4
382.1	28.3	27.9	19.6	32.0	2.9	1.0	23.8
387.1	27.8	27.6	17.9	32.3	2.6	1.2	23.2
392.1	27.4	27.3	20.3	36.9	2.4	1.3	26.8
397.2	27.2	26.9	24.7	37.3	2.2	1.3	29.2
402.2	26.7	26.3	29.1	37.4	1.9	1.4	31.6
407.2	26.2	26.1	31.4	39.1	1.5	1.5	33.7
412.2	26.1	25.9	33.9	41.2	1.5	1.5	36.0
417.3	25.9	25.6	30.4	43.2	1.3	1.6	35.4
422.3	25.4	25.3	27.2	39.9	0.9	1.7	32.3

Wind #14a (Cure Data)

Material: T40/1908 prepreg   Spool Tension(lb): 5.0
Number of Layers: 1   Winding Tension(lb): 1.5
Oven Ramp Rate(degC/m): 1.0   Stress Retention Factor: 0.30

Cure Time (min)	Mand. Temp. (deg C)	Oven Temp. (deg C)	Measured Microstrain Gage 1	Measured Microstrain Gage 2	Apparent Microstrain Gage 1	Apparent Microstrain Gage 2	Actual Microstrain
427.3	25.0	24.8	32.1	43.0	0.6	1.7	36.4
432.3	25.0	24.8	37.1	50.6	0.6	1.7	42.7
437.3	24.8	24.8	39.8	44.7	0.4	1.7	41.2
442.4	24.6	24.6	24.6	48.7	0.3	1.8	35.6
447.4	24.6	24.6	39.0	49.2	0.2	1.8	43.1
452.4	24.3	24.3	32.6	46.6	-0.0	1.8	38.7
457.4	24.1	24.1	44.5	45.5	-0.2	1.8	44.2
462.5	24.1	24.0	44.0	51.6	-0.2	1.8	47.0
467.5	24.1	24.0	41.8	52.2	-0.2	1.8	46.2
472.5	23.7	23.8	41.2	57.3	-0.5	1.9	48.6
477.5	23.6	23.6	37.8	54.1	-0.6	1.9	45.3
482.5	23.5	23.5	39.0	55.7	-0.7	1.9	46.8
487.5	23.5	23.5	35.4	57.8	-0.8	1.9	46.0
492.6	23.3	23.5	41.0	52.1	-0.9	1.9	46.1
497.6	23.3	23.2	39.5	54.8	-0.9	1.9	46.6
502.6	23.2	23.3	36.8	49.4	-1.0	1.9	42.7
507.6	23.3	23.4	41.5	55.6	-0.9	1.9	48.1
512.6	22.9	23.0	32.0	62.5	-1.3	1.9	46.9
517.7	23.2	23.0	34.0	55.7	-1.0	1.9	44.4
522.7	22.9	22.9	47.4	56.6	-1.3	1.9	51.7
527.7	23.0	22.9	46.4	55.8	-1.2	1.9	50.7
532.7	23.0	22.9	44.6	57.3	-1.2	1.9	50.6
537.8	22.9	22.9	49.6	56.1	-1.3	1.9	52.6
542.8	22.8	22.8	46.2	56.1	-1.4	1.9	50.9
547.8	22.7	22.8	48.2	54.7	-1.5	1.9	51.2
552.8	22.8	22.8	48.3	54.1	-1.4	1.9	51.0
557.8	22.8	22.8	49.0	53.5	-1.4	1.9	51.0
562.9	22.7	22.7	44.8	58.5	-1.5	1.9	51.5
567.9	22.6	22.6	48.3	54.2	-1.6	1.9	51.1

Wind #15 (Cure Data)

Material: T40 fiber — Spool Tension(lb): 5.0

Number of Layers: 1 — Winding Tension(lb): 4.6

Oven Ramp Rate(degC/m): 1.0 — Stress Retention Factor: 0.92

Cure Time (min)	Mand. Temp. (deg C)	Oven Temp. (deg C)	Measured Microstrain Gage 1	Measured Microstrain Gage 2	Apparent Microstrain Gage 1	Apparent Microstrain Gage 2	Actual Microstrain
5	23.3	23.48	-84.7	-62.8	-0.9	1.9	-74.2
10.1	24.19	24.93	-72.4	-62.8	-0.1	1.8	-68.5
15.1	29.72	31.96	-91.5	-79.4	3.8	0.6	-87.6
20.1	36.1	37.86	-112.2	-96.2	6.1	-2.5	-106.0
25.1	41.38	43.01	-128.9	-110.9	6.4	-6.1	-120.1
30.2	46.58	48.2	-148	-126.7	5.6	-10.5	-134.9
35.2	51.64	53.2	-169.1	-145.9	4.0	-15.5	-151.7
40.2	56.92	58.4	-193.1	-168.4	1.4	-21.2	-170.9
45.3	62.09	63.56	-219.5	-192.6	-1.6	-27.1	-191.7
50.3	67.12	68.55	-247.7	-217.8	-5.0	-33.0	-213.7
55.3	72.22	73.67	-277	-244.1	-8.7	-39.0	-236.7
60.3	77.34	78.65	-307.1	-271.1	-12.4	-45.0	-260.4
65.3	82.46	83.71	-336.5	-298.1	-16.0	-50.7	-284.0
70.4	87.4	88.79	-366.2	-323.9	-19.2	-55.8	-307.6
75.4	92.59	93.87	-396.1	-349.3	-22.0	-60.6	-331.4
80.4	97.47	98.81	-426.2	-373.6	-24.1	-64.4	-355.6
85.4	100.85	101.3	-445.6	-389.6	-25.1	-66.6	-371.7
90.4	101.88	101.83	-451.2	-393.9	-25.4	-67.2	-376.3
95.5	102.06	101.93	-453.2	-395.5	-25.4	-67.3	-378.0
100.5	102.03	101.89	-452.3	-396.2	-25.4	-67.3	-377.9
105.5	102.1	102.01	-452.2	-395.3	-25.4	-67.3	-377.4
110.6	102.09	102.02	-453.2	-395.2	-25.4	-67.3	-377.8
115.6	103.64	104.42	-462.1	-403.3	-25.7	-68.1	-385.8
120.6	107.69	108.87	-486.5	-422.8	-25.9	-69.8	-406.8
125.7	112.44	113.83	-512.7	-444.9	-25.2	-70.8	-430.8
130.7	117.49	118.8	-539.6	-466.5	-23.3	-70.6	-456.1
135.7	122.58	123.8	-565.8	-487.4	-19.8	-69.0	-482.2
140.8	127.56	128.74	-590.4	-507.1	-14.8	-65.9	-508.4
145.8	132.52	133.68	-614.9	-526.1	-8.2	-61.2	-535.8
150.8	137.5	138.68	-638.7	-543.6	0.5	-54.6	-564.1
155.9	142.48	143.69	-660.4	-559.3	11.2	-46.2	-592.3
160.9	147.43	148.7	-681.3	-575.2	24.0	-35.7	-622.4
165.9	152.37	153.51	-701.5	-590.4	39.2	-23.1	-654.0
171	155.56	155.99	-713.2	-597.6	50.3	-13.8	-673.7
176	156.47	156.57	-717.3	-599.6	53.6	-10.9	-679.8
181	156.76	156.81	-719.4	-598.3	54.7	-10.0	-681.2
186.1	156.91	156.89	-719.4	-599.7	55.3	-9.5	-682.5
191.1	156.94	156.96	-719.9	-600	55.4	-9.4	-683.0
196.1	156.51	155.79	-718.5	-598.2	53.8	-10.8	-679.9
201.2	146.12	142.79	-679.6	-570.1	20.4	-38.7	-615.7
206.2	131.32	128.04	-612.1	-520.1	-9.9	-62.5	-529.9
211.2	118.34	115.46	-545.9	-466.4	-22.8	-70.4	-459.5

Wind #15 (Cure Data)

Material: T40 fiber

Number of Layers: 1

Oven Ramp Rate(degC/m): 1.0

Spool Tension(lb): 5.0

Winding Tension(lb): 4.6

Stress Retention Factor: 0.92

Cure Time (min)	Mand. Temp. (deg C)	Oven Temp. (deg C)	Measured Microstrain Gage 1	Measured Microstrain Gage 2	Apparent Microstrain Gage 1	Apparent Microstrain Gage 2	Actual Microstrain
216.2	107.14	104.76	-483.4	-417	-25.9	-69.6	-402.4
221.3	97.47	95.41	-426.4	-369.1	-24.1	-64.4	-353.5
226.3	89.12	87.2	-374.7	-326.5	-20.2	-57.4	-311.8
231.3	81.89	80.16	-330.2	-287.5	-15.6	-50.1	-276.0
236.3	75.49	73.9	-290.1	-252.9	-11.1	-42.9	-244.5
241.3	69.9	68.48	-256.3	-222.5	-7.0	-36.3	-217.8
246.4	65.04	63.72	-227	-195.2	-3.6	-30.5	-194.0
251.4	60.52	59.37	-201.5	-171.3	-0.7	-25.2	-173.4
256.4	56.78	55.68	-179.4	-151.2	1.5	-21.0	-155.5
261.5	53.4	52.46	-160.9	-133.7	3.2	-17.3	-140.2
266.5	50.34	49.58	-144.6	-119.2	4.5	-14.2	-127.1
271.6	48	47.41	-132.4	-107.8	5.3	-11.9	-116.8
276.6	47.37	47.09	-129.6	-104.6	5.4	-11.3	-114.2
281.6	46.65	46.36	-126.4	-102	5.6	-10.6	-111.7
286.6	45.93	45.53	-122.7	-98.5	5.8	-10.0	-108.5
291.7	44.93	44.5	-118.4	-92.9	6.0	-9.1	-104.1
296.7	43.95	43.45	-112.4	-88.3	6.2	-8.2	-99.3
301.7	42.8	42.26	-106.8	-83.1	6.3	-7.2	-94.5
306.7	41.68	41.09	-101.5	-77.7	6.4	-6.3	-89.6
311.7	40.43	39.98	-96.3	-72.3	6.5	-5.4	-84.8
316.7	39.24	38.78	-91.1	-67.3	6.4	-4.5	-80.2
321.8	38.04	37.68	-87.3	-62.6	6.3	-3.7	-76.3
326.8	37	36.67	-81.2	-58.8	6.2	-3.0	-71.6
331.8	36.18	35.68	-77.5	-54.7	6.1	-2.5	-67.9
336.8	35.27	34.8	-73.6	-50.9	5.9	-2.0	-64.2
341.8	34.25	33.83	-69.9	-47.3	5.6	-1.4	-60.7
346.8	33.48	33.11	-66.3	-44.2	5.4	-1.0	-57.4
351.9	32.68	32.42	-63.1	-41.2	5.1	-0.6	-54.4
356.9	31.93	31.55	-60.2	-38.6	4.8	-0.3	-51.7
361.9	31.12	30.87	-57.5	-35.7	4.5	0.1	-48.9
366.9	30.66	30.34	-55.6	-33.8	4.2	0.2	-46.9
371.9	30.05	29.72	-53	-31.9	3.9	0.5	-44.7
376.9	29.59	29.29	-50.8	-30	3.7	0.6	-42.6
381.9	28.98	28.6	-49.1	-28.3	3.3	0.8	-40.8
387	28.49	28.18	-47.7	-26.4	3.1	1.0	-39.1
392	28.08	27.8	-46	-25.7	2.8	1.1	-37.8
397	27.61	27.35	-45.1	-24	2.5	1.2	-36.4
402	27.26	27.02	-43.5	-23.4	2.3	1.3	-35.2
407	26.88	26.64	-43.4	-21.8	2.0	1.4	-34.3
412	26.56	26.31	-41.3	-21.3	1.8	1.5	-32.9
417.1	26.27	26.06	-41.1	-19.8	1.6	1.5	-32.0
422.1	25.98	25.8	-39.5	-19	1.3	1.6	-30.7

Wind #15 (Cure Data)

Material: T40 fiber | Spool Tension(lb): 5.0
Number of Layers: 1 | Winding Tension(lb): 4.6
Oven Ramp Rate(degC/m): 1.0 | Stress Retention Factor: 0.92

Cure Time (min)	Mand. Temp. (deg C)	Oven Temp. (deg C)	Measured Microstrain Gage 1	Measured Microstrain Gage 2	Apparent Microstrain Gage 1	Apparent Microstrain Gage 2	Actual Microstrain
427.1	25.69	25.55	-38.8	-18.9	1.1	1.6	-30.2
432.1	25.44	25.37	-38.6	-18.2	0.9	1.7	-29.7
437.1	25.24	25.15	-37.6	-17.6	0.8	1.7	-28.8
442.1	25.07	24.95	-37.1	-16.7	0.6	1.7	-28.1
447.1	24.86	24.67	-37	-16.2	0.5	1.7	-27.7
452.2	24.71	24.56	-36.4	-16.2	0.3	1.8	-27.4
457.2	24.64	24.44	-36.5	-16.6	0.3	1.8	-27.6
462.2	24.45	24.29	-36.1	-15.9	0.1	1.8	-27.0
467.2	24.34	24.17	-35.3	-15.7	0.0	1.8	-26.4
472.2	24.16	23.96	-34.8	-15.3	-0.1	1.8	-25.9
477.2	24.08	23.93	-34.6	-14.8	-0.2	1.8	-25.5
482.3	24.02	23.87	-34.3	-13.7	-0.3	1.8	-24.8
487.3	23.86	23.71	-33.6	-13.2	-0.4	1.8	-24.1
492.3	23.74	23.59	-33.3	-12.8	-0.5	1.9	-23.7
497.3	23.66	23.53	-33.5	-13.5	-0.6	1.9	-24.1
502.3	23.46	23.36	-32.9	-13.1	-0.8	1.9	-23.6
507.3	23.41	23.32	-33.8	-12.1	-0.8	1.9	-23.5
512.4	23.39	23.29	-33.3	-12.4	-0.8	1.9	-23.4
517.4	23.35	23.24	-32.6	-13	-0.9	1.9	-23.3
522.4	23.18	23.07	-32.8	-13.1	-1.0	1.9	-23.4
527.4	23.13	23	-32.7	-13.1	-1.1	1.9	-23.3

Wind #16 (Cure Data)

Material: T40 fiber
Spool Tension(lb): 2.4
Number of Layers: 1
Winding Tension(lb): 1.3
Oven Ramp Rate(degC/m): 1.0
Stress Retention Factor: 0.54

Cure Time (min)	Mand. Temp. (deg C)	Oven Temp. (deg C)	Measured Microstrain Gage 1	Measured Microstrain Gage 2	Apparent Microstrain Gage 1	Apparent Microstrain Gage 2	Actual Microstrain
5	22.39	22.34	-18.9	-19.3	-1.8	1.9	-19.2
10	22.72	23.02	-17.5	-21	-1.5	1.9	-19.5
15.1	23.86	25.19	-21.7	-20.1	-0.4	1.8	-21.6
20.1	31.05	33.3	-35.4	-37.6	4.4	0.1	-38.8
25.1	36.8	38.59	-44.5	-49.9	6.2	-2.9	-48.8
30.1	42.09	43.85	-58.1	-66.1	6.4	-6.7	-62.0
35.1	47.13	48.85	-73.7	-79.5	5.5	-11.1	-73.8
40.2	52.52	54.24	-90.3	-94.2	3.6	-16.4	-85.8
45.2	57.67	59.32	-111	-113.5	1.0	-22.0	-101.8
50.2	62.62	64.16	-135.1	-130.8	-2.0	-27.7	-118.1
55.3	67.81	69.58	-157.7	-160.9	-5.5	-33.8	-139.6
60.3	72.83	74.65	-184.5	-179.5	-9.1	-39.8	-157.6
65.3	77.58	79.31	-209.6	-201.9	-12.6	-45.3	-176.8
70.3	82.67	84.41	-235.9	-224.2	-16.1	-50.9	-196.5
75.3	87.87	89.62	-264.8	-246.9	-19.4	-56.2	-218.0
80.3	93.12	94.82	-290.6	-271.1	-22.3	-61.0	-239.2
85.4	98.43	99.93	-317.3	-292.4	-24.4	-65.1	-260.1
90.4	101.19	101.57	-332.2	-305.7	-25.2	-66.8	-272.9
95.4	101.73	101.83	-337.4	-306.6	-25.3	-67.1	-275.8
100.5	101.91	101.99	-334.6	-309.8	-25.4	-67.2	-275.9
105.5	102.38	102.11	-336.5	-312.4	-25.5	-67.5	-278.0
110.6	101.94	102.12	-345.8	-298.7	-25.4	-67.3	-275.9
115.6	102.05	102	-335.6	-307.9	-25.4	-67.3	-275.4
120.6	104.08	105.21	-348.8	-314.2	-25.7	-68.3	-284.5
125.6	108.48	109.89	-371.6	-333.9	-25.9	-70.0	-304.8
130.7	113.54	114.97	-395.7	-358.5	-24.9	-70.8	-329.2
135.7	118.3	119.95	-419.1	-378.1	-22.8	-70.4	-352.0
140.7	123.47	125.13	-444.9	-397.8	-19.1	-68.5	-377.5
145.8	128.57	130.12	-472.4	-416	-13.6	-65.1	-404.9
150.8	133.67	135.18	-493.3	-429.9	-6.3	-59.8	-428.5
155.8	138.64	140.2	-510.3	-453.1	2.7	-52.9	-456.6
160.9	143.77	145.01	-531.9	-467.7	14.3	-43.7	-485.1
165.9	148.22	149.85	-550.2	-476.2	26.3	-33.8	-509.4
170.9	153.13	154.9	-568.1	-488.2	41.7	-21.0	-538.5
176	156.19	156.83	-577.5	-495.7	52.6	-11.8	-557.0
181	156.9	157.24	-581.3	-496	55.3	-9.5	-561.5
186	157.11	157.3	-579.3	-493.6	56.1	-8.8	-560.1
191.1	157.26	157.39	-580	-495.3	56.6	-8.4	-561.8
196.1	157.32	157.49	-580.8	-499.4	56.9	-8.2	-564.5
201.1	156.8	155.62	-581	-493	54.9	-9.8	-559.5
206.1	143.16	138.52	-527.2	-456.5	12.8	-44.9	-475.8
211.2	127.93	123.71	-461.8	-406.9	-14.4	-65.6	-394.3

Wind #16 (Cure Data)

Material: T40 fiber
Number of Layers: 1
Oven Ramp Rate(degC/m): 1.0
Spool Tension(lb): 2.4
Winding Tension(lb): 1.3
Stress Retention Factor: 0.54

Cure Time (min)	Mand. Temp. (deg C)	Oven Temp. (deg C)	Measured Microstrain Gage 1	Measured Microstrain Gage 2	Apparent Microstrain Gage 1	Apparent Microstrain Gage 2	Actual Microstrain
216.2	116.1	112.31	-398	-358.6	-24.0	-70.8	-330.9
221.2	104.81	101.3	-333.8	-306.1	-25.8	-68.7	-272.7
226.3	94.79	91.89	-280.8	-259.6	-23.0	-62.4	-227.5
231.3	86.23	83.67	-232.3	-219.6	-18.4	-54.6	-189.4
236.3	79	76.76	-191.3	-177.7	-13.6	-46.9	-154.3
241.3	72.45	70.57	-156.9	-145.4	-8.8	-39.3	-127.1
246.3	66.82	65.13	-122	-118.9	-4.8	-32.6	-101.7
251.3	61.93	60.44	-95.4	-93.1	-1.5	-26.9	-80.0
256.4	57.47	56.2	-74.1	-69	1.1	-21.8	-61.2
261.4	53.61	52.46	-61	-58.1	3.1	-17.6	-52.3
266.4	50.49	49.33	-49	-42.7	4.4	-14.3	-40.9
271.4	47.75	47.29	-37	-35.1	5.3	-11.6	-32.9
276.5	47.27	46.85	-33.8	-35.5	5.5	-11.2	-31.8
281.5	46.58	46.1	-32.2	-30.9	5.6	-10.5	-29.1
286.5	45.99	45.22	-28.9	-26.3	5.8	-10.0	-25.5
291.5	44.68	43.8	-25.8	-28.1	6.1	-8.8	-25.6
296.5	43.79	42.8	-23.3	-22	6.2	-8.1	-21.7
301.6	42.39	41.35	-16.6	-11.5	6.4	-6.9	-13.8
306.6	41.15	40.22	-14.3	-7.5	6.4	-5.9	-11.1
311.6	40.39	38.9	-11	-11.6	6.5	-5.4	-11.8
316.6	38.87	37.94	-7.7	-6.3	6.4	-4.3	-8.1
321.6	37.82	36.86	-5.2	-4.1	6.3	-3.5	-6.0
326.7	36.67	35.71	-3.1	-0.3	6.2	-2.8	-3.4
331.7	35.7	34.81	-1.1	1.6	6.0	-2.2	-1.6
336.7	34.81	33.91	0.2	1.8	5.8	-1.7	-1.0
341.7	33.77	32.87	3.3	4.5	5.5	-1.2	1.7
346.8	32.93	32.11	3.9	4.8	5.2	-0.7	2.1
351.8	32.12	31.41	5.3	6.8	4.9	-0.4	3.8
356.8	31.37	30.75	7.8	7.1	4.6	-0.0	5.2
361.8	30.46	29.89	7.7	10.2	4.1	0.3	6.7
366.9	30.09	29.43	5.1	7.5	4.0	0.5	4.1
371.9	29.32	28.84	6	9.4	3.5	0.7	5.6
376.9	28.78	28.23	8.6	7.8	3.2	0.9	6.1
381.9	28.37	27.89	7.1	10.2	3.0	1.0	6.6
387	27.65	27.19	6.5	9.2	2.5	1.2	6.0
392	27.42	27	6.1	10	2.4	1.3	6.2
397	27.01	26.5	5.7	11.7	2.1	1.4	7.0
402	26.67	26.27	5.6	10.8	1.9	1.4	6.5
407.1	26.34	25.84	9.4	13.9	1.6	1.5	10.1
412.1	26	25.71	10	9.3	1.4	1.6	8.2
417.1	25.69	25.44	6.9	11.2	1.1	1.6	7.7
422.1	25.5	25.14	10	10.6	1.0	1.7	9.0

Wind #17 (Cure Data)

Material: T40/1908 prepreg — Spool Tension(lb): 2.5
Number of Layers: 1 — Winding Tension(lb): 0.8
Oven Ramp Rate(degC/m): 1.0 — Stress Retention Factor: 0.32

Cure Time (min)	Mand. Temp. (deg C)	Oven Temp. (deg C)	Measured Microstrain Gage 1	Measured Microstrain Gage 2	Apparent Microstrain Gage 1	Apparent Microstrain Gage 2	Actual Microstrain
5	23.12	23.17	-11.1	-12.2	-1.1	1.9	-12.1
10.1	25.09	26.48	-9.6	-10.8	0.7	1.7	-11.4
15.1	32.32	34.15	-16.9	-21.2	5.0	-0.5	-21.3
20.1	37.97	39.46	-26.1	-30.7	6.3	-3.6	-29.7
25.1	43.27	44.75	-34.7	-41.6	6.3	-7.6	-37.5
30.1	48.33	49.84	-52.8	-57.8	5.2	-12.2	-51.8
35.2	53.55	55.12	-72	-78.7	3.1	-17.5	-68.2
40.2	58.63	60.05	-92.7	-98.9	0.5	-23.1	-84.5
45.2	63.81	65.33	-119.2	-121.7	-2.8	-29.1	-104.5
50.3	69.02	70.5	-146.6	-149	-6.4	-35.3	-127.0
55.3	74.02	75.48	-170.4	-173.1	-10.0	-41.2	-146.2
60.3	79.37	80.87	-199.6	-200.1	-13.8	-47.3	-169.3
65.3	83.95	85.29	-223.6	-220.9	-17.0	-52.3	-187.6
70.3	89.15	90.52	-252.2	-244.2	-20.2	-57.5	-209.4
75.4	94.19	95.64	-278.5	-266.7	-22.8	-61.9	-230.3
80.4	99.11	100.34	-306.4	-289.7	-24.6	-65.5	-253.0
85.4	101	101.49	-314.2	-296.7	-25.2	-66.7	-259.5
90.4	101.41	101.7	-316.6	-297.7	-25.3	-67.0	-261.0
95.5	101.75	101.87	-320.5	-300.1	-25.3	-67.1	-264.1
100.5	101.84	101.93	-314.8	-299.9	-25.4	-67.2	-261.1
105.5	101.71	101.95	-314.4	-299.1	-25.3	-67.1	-260.5
110.6	101.85	102.22	-318.1	-300.2	-25.4	-67.2	-262.9
115.6	105.03	105.97	-333.6	-313.4	-25.8	-68.8	-276.2
120.6	109.77	110.8	-357.5	-335.2	-25.7	-70.3	-298.3
125.7	114.68	115.76	-383.4	-355.1	-24.5	-70.9	-321.6
130.7	119.86	120.88	-405.8	-373.8	-21.9	-70.0	-343.9
135.7	124.78	125.88	-431.8	-393.8	-17.8	-67.8	-370.0
140.8	129.91	130.96	-451.5	-410.5	-11.9	-63.9	-393.1
145.8	134.97	135.88	-474.5	-428.6	-4.2	-58.2	-420.4
150.8	140.12	141.18	-496.4	-447.2	5.8	-50.4	-449.5
155.8	145.05	146.05	-514.4	-459.3	17.5	-41.0	-475.1
160.9	149.44	150.49	-528.5	-471.7	29.9	-30.9	-499.6
165.9	154.24	155.04	-545.2	-482.8	45.6	-17.7	-527.9
171	156.28	156.5	-550.5	-486.1	52.9	-11.5	-539.0
176	156.7	156.8	-550.8	-485.5	54.5	-10.2	-540.3
181	156.98	157	-552	-484.3	55.6	-9.3	-541.3
186	157.06	157.01	-551.4	-485.4	55.9	-9.0	-541.8
191.1	157.15	157.06	-551.8	-485.4	56.2	-8.7	-542.4
196.1	153.64	151.07	-543.3	-475.6	43.5	-19.5	-521.4
201.1	138.1	134.37	-484.5	-431.5	1.6	-53.7	-432.0
206.2	123.69	120.39	-419.1	-377.4	-18.9	-68.4	-354.6
211.2	112.63	109.65	-362.5	-334.8	-25.2	-70.8	-300.7

Wind #17 (Cure Data)

Material: T40/1908 prepreg — Spool Tension(lb): 2.5
Number of Layers: 1 — Winding Tension(lb): 0.8
Oven Ramp Rate(degC/m): 1.0 — Stress Retention Factor: 0.32

Cure Time (min)	Mand. Temp. (deg C)	Oven Temp. (deg C)	Measured Microstrain Gage 1	Measured Microstrain Gage 2	Apparent Microstrain Gage 1	Apparent Microstrain Gage 2	Actual Microstrain
216.2	101.61	99.18	-304.3	-284.2	-25.3	-67.1	-248.1
221.2	92.22	90.21	-253.6	-239.1	-21.8	-60.3	-205.3
226.2	84.14	82.36	-205.8	-199.9	-17.1	-52.5	-168.1
231.3	77.02	75.46	-165.3	-164.9	-12.2	-44.6	-136.7
236.3	70.96	69.5	-128.3	-130.6	-7.8	-37.6	-106.8
241.3	65.58	64.25	-97.9	-100.7	-4.0	-31.2	-81.7
246.3	60.8	59.63	-71.3	-81.4	-0.8	-25.6	-63.1
251.4	56.78	55.77	-47.2	-56.6	1.5	-21.0	-42.1
256.4	53.24	52.39	-27.8	-36.3	3.3	-17.2	-25.1
261.4	49.98	49.28	-10.8	-24.3	4.6	-13.8	-12.9
266.4	47.62	47.23	1.3	-12.7	5.4	-11.5	-2.6
271.4	47.01	46.71	1.4	-9	5.5	-10.9	-1.1
276.5	46.51	46.18	9	-8.6	5.7	-10.5	2.6
281.5	45.53	45.01	-1.4	5.6	5.9	-9.6	4.0
286.5	44.6	44.05	6	13.2	6.1	-8.8	11.0
291.6	43.55	42.95	12.8	17.5	6.2	-7.9	16.0
296.6	42.53	41.91	20.7	21.6	6.3	-7.0	21.5
301.6	41.29	40.74	20.9	25.8	6.4	-6.0	23.2
306.6	40.23	39.63	27.3	31.7	6.5	-5.2	28.9
311.6	39.01	38.5	33.6	37	6.4	-4.4	34.3
316.7	38.01	37.44	38.9	40.9	6.3	-3.7	38.6
321.7	37.04	36.44	43.3	44.4	6.2	-3.0	42.3
326.7	35.97	35.51	48.7	50.4	6.0	-2.4	47.7
331.7	34.97	34.52	52.2	52.7	5.8	-1.8	50.5
336.8	34.12	33.57	56.1	57.1	5.6	-1.3	54.5
341.8	33.3	32.83	60	61.4	5.3	-0.9	58.5
346.8	32.25	31.87	64.1	63.5	4.9	-0.4	61.5
351.9	31.74	31.34	66.7	66.1	4.7	-0.2	64.1
356.9	30.99	30.64	71.4	68.1	4.4	0.1	67.5
361.9	30.45	30.13	72	68.3	4.1	0.3	67.9
366.9	29.86	29.52	73.3	72.2	3.8	0.5	70.6
372	29.26	28.97	79	74.3	3.5	0.7	74.5
377	28.78	28.5	80.1	75	3.2	0.9	75.5
382	28.33	28.05	82.4	79.8	3.0	1.0	79.1
387	27.82	27.65	85	79.7	2.6	1.2	80.4
392.1	27.5	27.27	85.6	80.3	2.4	1.3	81.1
397.1	27.18	26.98	87.9	81.6	2.2	1.3	83.0
402.1	26.67	26.54	88.1	83.6	1.9	1.4	84.2
407.2	26.5	26.35	89.6	81.9	1.7	1.5	84.1
412.2	26.29	26.08	90.8	83.3	1.6	1.5	85.5
417.2	25.89	25.7	92	86.4	1.3	1.6	87.8
422.2	25.66	25.46	93.7	85.5	1.1	1.6	88.2

Wind #17 (Cure Data)

Material: T40/1908 prepreg | Spool Tension(lb): 2.5
Number of Layers: 1 | Winding Tension(lb): 0.8
Oven Ramp Rate(degC/m): 1.0 | Stress Retention Factor: 0.32

Cure Time (min)	Mand. Temp. (deg C)	Oven Temp. (deg C)	Measured Microstrain Gage 1	Measured Microstrain Gage 2	Apparent Microstrain Gage 1	Apparent Microstrain Gage 2	Actual Microstrain
427.3	25.42	25.25	92.9	86.2	0.9	1.7	88.3
432.3	25.26	25.04	93.9	89.1	0.8	1.7	90.3
437.3	24.91	24.88	94.6	87.5	0.5	1.7	89.9
442.3	24.89	24.77	95.7	88.6	0.5	1.7	91.0
447.4	24.71	24.63	96.9	89.9	0.3	1.8	92.3
452.4	24.35	24.22	96.9	91.2	0.0	1.8	93.1
457.4	24.32	24.28	97.8	88.9	0.0	1.8	92.4
462.5	24.07	24.05	97.8	90.3	-0.2	1.8	93.2
467.5	24.05	23.98	97.3	93	-0.2	1.8	94.4
472.5	23.89	23.86	98	89.6	-0.4	1.8	93.1
477.5	23.85	23.84	97.6	91.5	-0.4	1.8	93.8
482.5	23.74	23.69	98.2	92.6	-0.5	1.9	94.7
487.6	23.59	23.54	100.9	93.4	-0.6	1.9	96.5
492.6	23.45	23.46	101.1	92.4	-0.8	1.9	96.2
497.6	23.54	23.47	101.1	93.1	-0.7	1.9	96.5
502.6	23.17	23.38	101.5	91.7	-1.0	1.9	96.2
507.6	23.13	23.28	98.7	94.1	-1.1	1.9	96.0
512.7	23.19	23.12	103.7	93.2	-1.0	1.9	98.0

Wind #18 (Cure Data)

Material: T40 fiber — Spool Tension(lb): 7.5
Number of Layers: 1 — Winding Tension(lb): 5.4
Oven Ramp Rate(degC/m): 1.0 — Stress Retention Factor: 0.72

Cure Time (min)	Mand. Temp. (deg C)	Oven Temp. (deg C)	Measured Microstrain Gage 1	Measured Microstrain Gage 2	Apparent Microstrain Gage 1	Apparent Microstrain Gage 2	Actual Microstrain
5	21.59	21.84	-99	-78.5	-2.6	1.9	-88.4
10	22.91	24.15	-99.4	-77	-1.3	1.9	-88.5
15	27.43	29.05	-109.1	-97.7	2.4	1.3	-105.2
20.1	32.33	34.07	-126	-110.6	5.0	-0.5	-120.6
25.1	37.66	39.32	-153	-132.9	6.3	-3.4	-144.4
30.1	42.73	44.38	-170.2	-151.9	6.3	-7.2	-160.6
35.2	47.64	49.45	-189.3	-160.2	5.4	-11.5	-171.7
40.2	53.09	54.94	-216.7	-179.3	3.3	-17.0	-191.2
45.2	58.51	59.8	-243	-202.9	0.5	-23.0	-211.7
50.3	63.07	64.68	-268.7	-228.1	-2.3	-28.2	-233.2
55.3	68.28	70	-293.2	-259.6	-5.8	-34.4	-256.3
60.3	73.23	75.04	-325.2	-275.5	-9.4	-40.2	-275.5
65.3	78.39	80.29	-354	-313.6	-13.1	-46.2	-304.1
70.3	83.51	85.38	-389.1	-332	-16.7	-51.8	-326.3
75.3	88.66	90.47	-413.4	-363.1	-19.9	-57.0	-349.8
80.4	93.86	95.77	-441.5	-385.9	-22.6	-61.6	-371.6
85.4	99.08	100.7	-476.2	-403	-24.6	-65.5	-394.5
90.4	101.3	102.02	-483.4	-382.7	-25.2	-66.9	-387.0
95.4	101.8	102.27	-493.6	-417.2	-25.3	-67.2	-409.1
100.5	102	102.33	-494.1	-433.3	-25.4	-67.3	-417.4
105.5	101.82	102.15	-497.8	-423.9	-25.3	-67.2	-414.6
110.5	102.09	102.46	-498	-423.6	-25.4	-67.3	-414.4
115.6	101.98	102.24	-496.8	-422.9	-25.4	-67.3	-413.5
120.6	104.65	106.08	-508.8	-445.1	-25.8	-68.6	-429.8
125.6	109.24	110.81	-531.8	-467	-25.8	-70.2	-451.4
130.7	114.15	115.85	-569.7	-476.4	-24.7	-70.9	-475.3
135.7	119.23	120.87	-593.2	-483.5	-22.3	-70.2	-492.1
140.7	124.37	125.8	-609.7	-536.9	-18.2	-68.1	-530.2
145.7	128.76	130.63	-640.9	-543.1	-13.4	-64.9	-552.9
150.8	133.82	135.68	-663.6	-559.3	-6.1	-59.6	-578.6
155.8	138.84	140.68	-686.9	-577.3	3.1	-52.6	-607.4
160.8	143.82	145.76	-712.9	-601.4	14.4	-43.6	-642.6
165.8	148.88	150.89	-729.3	-621.2	28.2	-32.2	-673.2
170.8	153.91	155.82	-751.5	-612.1	44.4	-18.7	-694.6
175.8	156.41	157.33	-765.5	-621.1	53.4	-11.1	-714.5
180.9	156.91	157.53	-757.6	-643.6	55.3	-9.5	-723.5
185.9	157.38	157.82	-765.6	-633.6	57.1	-8.0	-724.2
190.9	157.51	157.91	-769.6	-637	57.6	-7.5	-728.3
196	157.51	158.01	-771	-627.8	57.6	-7.5	-724.4
201	156.98	155.55	-766.9	-629.4	55.6	-9.3	-721.3
206	143.05	137.88	-708.1	-578.5	12.5	-45.1	-627.0
211	127.69	123.04	-638.6	-545.8	-14.7	-65.8	-552.0

Wind #18 (Cure Data)

Material: T40 fiber — Spool Tension(lb): 7.5

Number of Layers: 1 — Winding Tension(lb): 5.4

Oven Ramp Rate(degC/m): 1.0 — Stress Retention Factor: 0.72

Cure Time (min)	Mand. Temp. (deg C)	Oven Temp. (deg C)	Measured Microstrain Gage 1	Measured Microstrain Gage 2	Apparent Microstrain Gage 1	Apparent Microstrain Gage 2	Actual Microstrain
216	114.82	110.55	-574.9	-475.1	-24.5	-70.8	-477.3
221.1	103.65	99.91	-504.2	-436.7	-25.7	-68.1	-423.5
226.1	94.06	90.73	-457.3	-387.3	-22.7	-61.8	-380.0
231.1	86.35	83.76	-406.7	-342.5	-18.5	-54.7	-338.0
236.1	79.01	76.64	-357.1	-316.2	-13.6	-46.9	-306.4
241.2	72.61	70.69	-322.3	-276.3	-9.0	-39.5	-275.1
246.2	67.03	65.39	-287	-234.2	-5.0	-32.9	-241.7
251.2	61.96	60.6	-255	-225.3	-1.6	-26.9	-225.9
256.2	57.64	56.5	-237.3	-195.7	1.0	-22.0	-206.0
261.3	53.89	52.83	-212	-173.6	3.0	-17.9	-185.4
266.3	50.72	49.79	-189.6	-154.7	4.3	-14.6	-167.0
271.4	47.58	47.12	-181.9	-136.1	5.4	-11.5	-156.0
276.4	47.35	47.13	-175.3	-139.3	5.4	-11.3	-154.4
281.4	46.83	46.58	-175.5	-134.7	5.6	-10.8	-152.5
286.4	45.88	45.6	-169.6	-130.9	5.8	-9.9	-148.2
291.5	44.9	44.51	-168.8	-129.7	6.0	-9.0	-147.7
296.5	43.92	43.51	-158.5	-120.4	6.2	-8.2	-138.4
301.5	42.8	42.32	-158.7	-124.5	6.3	-7.2	-141.1
306.6	41.46	40.84	-154.2	-115	6.4	-6.2	-134.7
311.6	40.12	39.63	-141.7	-112.5	6.5	-5.2	-127.7
316.6	39.13	38.63	-133.1	-107.8	6.4	-4.4	-121.4
321.7	37.97	37.58	-130.4	-99.9	6.3	-3.6	-116.5
326.7	36.9	36.46	-129.5	-100.5	6.2	-3.0	-116.6
331.8	35.71	35.32	-125.2	-87.4	6.0	-2.2	-108.2
336.8	34.65	34.4	-116.1	-89.1	5.7	-1.6	-104.6
341.8	33.81	33.47	-112.3	-90.4	5.5	-1.2	-103.5
346.8	32.94	32.65	-111.3	-72.7	5.2	-0.7	-94.2
351.9	31.99	31.75	-113.3	-73.3	4.8	-0.3	-95.6
356.9	31.55	31.28	-104.3	-71.6	4.6	-0.1	-90.2
361.9	30.72	30.37	-100.2	-64.7	4.3	0.2	-84.7
366.9	29.88	29.69	-99.6	-59.4	3.8	0.5	-81.7
371.9	29.54	29.28	-97.4	-67.7	3.7	0.7	-84.7
377	28.84	28.66	-90.1	-54	3.3	0.9	-74.1
382	28.56	28.18	-92.4	-65.1	3.1	1.0	-80.8
387	27.81	27.56	-89.5	-68.5	2.6	1.2	-80.9
392	27.45	27.3	-82.1	-52.8	2.4	1.3	-69.3
397.1	27	26.84	-83.6	-55.2	2.1	1.4	-71.1
402.1	26.64	26.51	-79	-63.8	1.8	1.5	-73.0
407.1	26.3	26.27	-84.7	-66	1.6	1.5	-76.9
412.1	26.08	25.95	-78.5	-50.5	1.4	1.6	-66.0
417.2	25.65	25.75	-79.4	-49.6	1.1	1.6	-65.9
422.2	25.64	25.42	-81.5	-49	1.1	1.6	-66.6

Wind #19 (Cure Data)

Material: T40/1908 prepreg
Spool Tension(lb): 8.1
Number of Layers: 1
Winding Tension(lb): 3.8
Oven Ramp Rate(degC/m): 1.0
Stress Retention Factor: 0.47

Cure Time (min)	Mand. Temp. (deg C)	Oven Temp. (deg C)	Measured Microstrain Gage 1	Measured Microstrain Gage 2	Apparent Microstrain Gage 1	Apparent Microstrain Gage 2	Actual Microstrain
5	22.38	22.44	-71	-51.6	-1.8	1.9	-61.4
10	22.82	23.13	-70.1	-53.9	-1.4	1.9	-62.3
15.1	24.17	25.53	-69.5	-58.6	-0.1	1.8	-64.9
20.1	31.43	33.53	-81.9	-75.8	4.6	-0.1	-81.1
25.1	37.26	38.86	-101.1	-84.4	6.2	-3.2	-94.3
30.1	42.3	44.02	-113.3	-108	6.4	-6.8	-110.4
35.2	47.52	49.16	-131.6	-129.1	5.4	-11.4	-127.3
40.2	52.86	54.4	-157.3	-151.8	3.4	-16.8	-147.9
45.2	57.91	59.59	-186.6	-177.4	0.9	-22.3	-171.3
50.3	63.32	64.6	-216.8	-199.3	-2.4	-28.5	-192.6
55.3	68.43	69.89	-235.4	-231.1	-6.0	-34.6	-213.0
60.3	73.67	75.12	-286.7	-246.6	-9.7	-40.7	-241.4
65.3	77.8	79.65	-291	-268.4	-12.7	-45.5	-250.6
70.3	82.92	84.86	-322.6	-295.7	-16.3	-51.2	-275.4
75.4	88.11	90.06	-353.4	-321.9	-19.6	-56.5	-299.6
80.4	93.53	95.27	-381.1	-349.1	-22.5	-61.4	-323.2
85.4	98.63	100.2	-408.1	-368.5	-24.5	-65.2	-343.4
90.4	101.12	101.41	-425.9	-387.2	-25.2	-66.8	-360.6
95.5	101.83	101.78	-422.5	-377.9	-25.3	-67.2	-353.9
100.5	102.1	101.92	-421.3	-392.3	-25.4	-67.3	-360.4
105.5	102.13	101.95	-428.3	-403.5	-25.4	-67.4	-369.5
110.6	102.22	102.02	-427.6	-389.9	-25.4	-67.4	-362.3
115.6	102.39	102.23	-423.8	-384.5	-25.5	-67.5	-357.7
120.6	104.4	105.58	-439.5	-399.6	-25.8	-68.5	-372.4
125.6	108.93	110.36	-467.6	-419.3	-25.8	-70.1	-395.5
130.7	113.81	115.39	-488.7	-442.8	-24.8	-70.8	-417.9
135.7	118.57	120.29	-511.2	-467	-22.7	-70.4	-442.6
140.7	123.79	125.48	-542.6	-486.9	-18.8	-68.4	-471.2
145.8	128.8	130.47	-564.7	-498	-13.3	-64.9	-492.2
150.8	134.19	135.57	-584.8	-516.3	-5.5	-59.2	-518.2
155.8	138.8	140.57	-625.2	-551.4	3.1	-52.6	-563.5
160.9	143.34	145.1	-627.8	-553.8	13.2	-44.5	-575.2
165.9	148.36	149.94	-646.3	-567.1	26.7	-33.5	-603.3
171	153.41	155.05	-665.9	-585	42.7	-20.2	-636.7
176	155.98	156.57	-674.3	-590.2	51.8	-12.4	-651.9
181	156.77	157.02	-677	-587.5	54.8	-9.9	-654.7
186.1	157.04	157.24	-672.6	-590.1	55.8	-9.1	-654.7
191.1	157.08	157.23	-674.6	-581.8	56.0	-8.9	-651.7
196.2	157.14	157.4	-682.8	-592.9	56.2	-8.7	-661.6
201.2	156.48	153.98	-672.4	-586.3	53.7	-10.9	-650.8
206.2	142.21	137.01	-610.6	-542.2	10.5	-46.7	-558.3
211.3	129.08	124.09	-558.2	-499	-13.0	-64.6	-489.8

Wind #19 (Cure Data)

Material: T40/1908 prepreg — Spool Tension(lb): 8.1
Number of Layers: 1 — Winding Tension(lb): 3.8
Oven Ramp Rate(degC/m): 1.0 — Stress Retention Factor: 0.47

Cure Time (min)	Mand. Temp. (deg C)	Oven Temp. (deg C)	Measured Microstrain Gage 1	Measured Microstrain Gage 2	Apparent Microstrain Gage 1	Apparent Microstrain Gage 2	Actual Microstrain
216.3	115.99	111.56	-493.1	-444.4	-24.0	-70.8	-421.4
221.3	104.85	100.89	-425	-390	-25.8	-68.7	-360.2
226.3	95.1	91.6	-368.2	-348.6	-23.2	-62.6	-315.5
231.4	86.83	83.66	-322.1	-310	-18.8	-55.2	-279.0
236.4	79.32	76.58	-274.5	-269.7	-13.8	-47.2	-241.6
241.4	72.94	70.51	-245.7	-230.1	-9.2	-39.9	-213.4
246.4	66.93	64.89	-210.6	-196.3	-4.9	-32.8	-184.6
251.5	62	60.41	-171.5	-179.1	-1.6	-27.0	-161.0
256.5	58.27	56.59	-155	-156.8	0.7	-22.7	-144.9
261.5	54.42	52.98	-137.6	-136.2	2.7	-18.4	-129.0
266.6	50.93	49.61	-111.1	-123.7	4.2	-14.8	-112.1
271.6	48.16	46.96	-99.3	-111.8	5.2	-12.0	-102.1
276.6	47.56	47.21	-96.3	-107.4	5.4	-11.5	-98.8
281.6	46.84	46.56	-94	-102.7	5.6	-10.8	-95.7
286.7	46.06	45.66	-86.2	-98.3	5.8	-10.1	-90.1
291.7	45.03	44.6	-83.2	-95.7	6.0	-9.1	-87.9
296.7	43.98	43.32	-54.5	-117	6.2	-8.2	-84.7
301.7	42.95	42.27	-24.9	-149.4	6.3	-7.4	-86.6
306.7	41.59	40.94	-29	-124.8	6.4	-6.3	-77.0
311.7	40.51	39.8	-16.9	-144	6.5	-5.4	-81.0
316.7	39.12	38.61	-7.3	-139.7	6.4	-4.4	-74.5
321.8	37.96	37.35	-5.9	-135.8	6.3	-3.6	-72.2
326.8	36.83	36.28	5.9	-125.2	6.2	-2.9	-61.3
331.8	35.79	35.23	7.9	-128.4	6.0	-2.3	-62.1
336.8	34.76	34.29	19.9	-122.9	5.7	-1.7	-53.5
341.8	34.1	33.35	27.1	-124.3	5.6	-1.3	-50.7
346.9	32.96	32.61	21.7	-96.5	5.2	-0.8	-39.6
351.9	32.03	31.85	30.5	-77.5	4.8	-0.3	-25.8
356.9	31.34	30.96	26	-76.7	4.5	-0.0	-27.6
361.9	30.49	30.17	40.5	-68.7	4.2	0.3	-16.3
367	29.88	29.64	39.2	-69.3	3.8	0.5	-17.2
372	29.37	29.15	46.6	-65.8	3.6	0.7	-11.7
377	28.82	28.49	42.5	-62.5	3.3	0.9	-12.1
382	28.13	27.82	51.5	-62.8	2.8	1.1	-7.6
387.1	27.8	27.61	45	-69.3	2.6	1.2	-14.1
392.1	27.46	27.33	52.7	-44.4	2.4	1.3	2.3
397.1	26.76	26.64	61.4	-56.2	1.9	1.4	0.9
402.1	26.55	26.42	58.9	-60.4	1.8	1.5	-2.4
407.2	26.2	26.05	60.5	-50.8	1.5	1.5	3.3
412.2	25.87	25.87	60	-48.6	1.3	1.6	4.3
417.2	25.55	25.61	64.9	-56.7	1.0	1.7	2.8
422.2	25.32	25.23	60.1	-48.8	0.8	1.7	4.4

Wind #19 (Cure Data)

Material: T40/1908 prepreg
Number of Layers: 1
Oven Ramp Rate(degC/m): 1.0
Spool Tension(lb): 8.1
Winding Tension(lb): 3.8
Stress Retention Factor: 0.47

Cure Time (min)	Mand. Temp. (deg C)	Oven Temp. (deg C)	Measured Microstrain Gage 1	Measured Microstrain Gage 2	Apparent Microstrain Gage 1	Apparent Microstrain Gage 2	Actual Microstrain
427.3	25.02	25.02	60.4	-59.7	0.6	1.7	-0.8
432.3	24.86	24.83	71.6	-55.1	0.5	1.7	7.1
437.3	24.62	24.55	58.5	-59.8	0.3	1.8	-1.7
442.3	24.3	24.39	65.4	-53.8	-0.0	1.8	4.9
447.4	24.35	24.22	71.9	-53.7	0.0	1.8	8.2
452.4	23.91	24.07	66.8	-43.6	-0.4	1.8	10.9
457.4	23.87	23.9	69	-50	-0.4	1.8	8.8
462.4	23.84	23.78	73.5	-38.4	-0.4	1.8	16.8
467.5	23.62	23.75	63.1	-39	-0.6	1.9	11.4
472.5	23.32	23.58	68.5	-43.8	-0.9	1.9	11.9
477.5	23.35	23.35	65.7	-50.1	-0.9	1.9	7.3
482.5	23.26	23.35	68.9	-47.1	-0.9	1.9	10.4
487.6	23.18	23.18	73.6	-37.2	-1.0	1.9	17.8
492.6	22.88	23.11	69.4	-38.9	-1.3	1.9	15.0
497.6	23.16	23.07	62.5	-31.5	-1.0	1.9	15.1
502.6	22.64	22.87	59.3	-29.3	-1.5	1.9	14.8
507.6	22.39	22.77	48.5	-29.4	-1.8	1.9	9.5

Wind #20 (Cure Data)

Material: T40 fiber | Spool Tension(lb): 5.0
Number of Layers: 2 | Winding Tension(lb): 4.8
Oven Ramp Rate(degC/m): 1.0 | Stress Retention Factor: 0.96

Cure Time (min)	Mand. Temp. (deg C)	Oven Temp. (deg C)	Measured Microstrain Gage 1	Measured Microstrain Gage 2	Apparent Microstrain Gage 1	Apparent Microstrain Gage 2	Actual Microstrain
5	22.68	22.75	-118.7	-126.6	-1.5	1.9	-122.8
10	23.01	23.27	-119.6	-128.6	-1.2	1.9	-124.5
15.1	25.16	27.04	-129.7	-136.9	0.7	1.7	-134.5
20.1	32.39	34.42	-171.5	-171.1	5.0	-0.5	-173.5
25.1	38.09	39.75	-202.6	-188.6	6.3	-3.7	-196.9
30.2	43.2	45.04	-227.2	-214.9	6.3	-7.6	-220.4
35.2	48.43	50.02	-252.4	-230.5	5.1	-12.3	-237.9
40.2	53.62	55.37	-275.2	-254.3	3.1	-17.6	-257.5
45.2	58.83	60.61	-308.4	-282.5	0.3	-23.3	-284.0
50.3	63.59	65.23	-343.7	-315	-2.6	-28.8	-313.6
55.3	68.74	70.46	-385.3	-350.9	-6.2	-34.9	-347.6
60.3	73.88	75.49	-428.9	-393.3	-9.9	-41.0	-385.7
65.3	79.12	80.83	-474.4	-427.4	-13.7	-47.0	-420.6
70.3	84.04	85.78	-521.1	-468.3	-17.0	-52.4	-460.0
75.3	89.21	90.98	-568.1	-507.7	-20.2	-57.5	-499.0
80.4	94.26	96.11	-614.3	-549.5	-22.8	-62.0	-539.5
85.4	98.99	100.37	-660.3	-583.4	-24.6	-65.5	-576.8
90.4	100.75	101.14	-682.8	-595.6	-25.1	-66.6	-593.4
95.4	101.09	101.45	-696.5	-604.5	-25.2	-66.8	-604.5
100.4	101.52	101.67	-689.9	-606.4	-25.3	-67.0	-602.0
105.5	101.41	101.65	-692.6	-610	-25.3	-67.0	-605.2
110.5	101.6	101.78	-690.2	-611.7	-25.3	-67.1	-604.8
115.5	101.71	102.11	-692.2	-610.7	-25.3	-67.1	-605.2
120.5	104.62	106.28	-722	-638.3	-25.8	-68.6	-633.0
125.5	109.37	111.16	-763.6	-668.9	-25.8	-70.2	-668.2
130.5	114.43	116.13	-810.5	-709.5	-24.6	-70.9	-712.3
135.6	119.56	121.28	-856.3	-746	-22.1	-70.1	-755.1
140.6	123.9	125.76	-898	-781.8	-18.7	-68.3	-796.4
145.6	129.17	130.83	-944.5	-824.9	-12.9	-64.5	-846.0
150.6	133.98	135.9	-989.8	-852.5	-5.8	-59.4	-888.5
155.7	139.4	140.99	-1035.8	-893.6	4.3	-51.6	-941.0
160.7	144.28	145.84	-1079.6	-926.7	15.6	-42.6	-989.6
165.7	149.24	150.82	-1127.4	-959	29.3	-31.4	-1042.2
170.7	154.08	155.49	-1171.4	-995.7	45.0	-18.2	-1096.9
175.7	156.31	156.48	-1186.6	-1008.7	53.0	-11.4	-1118.5
180.8	156.55	156.72	-1194.6	-1006.3	53.9	-10.6	-1122.1
185.8	156.77	156.77	-1195.9	-1018.4	54.8	-9.9	-1129.6
190.8	156.81	157.02	-1205.9	-1013.4	54.9	-9.8	-1132.2
195.8	156.96	157.04	-1213.2	-1018.9	55.5	-9.3	-1139.1
200.8	155.36	152.44	-1204.6	-1009.5	49.6	-14.4	-1124.6
205.8	140.69	135.68	-1097.3	-918.4	7.1	-49.4	-986.7
210.9	125.76	121.36	-971	-818.5	-16.8	-67.2	-852.7

Wind #20 (Cure Data)

Material: T40 fiber
Number of Layers: 2
Oven Ramp Rate(degC/m): 1.0
Spool Tension(lb): 5.0
Winding Tension(lb): 4.8
Stress Retention Factor: 0.96

Cure Time (min)	Mand. Temp. (deg C)	Oven Temp. (deg C)	Measured Microstrain Gage 1	Measured Microstrain Gage 2	Apparent Microstrain Gage 1	Apparent Microstrain Gage 2	Actual Microstrain
215.9	113.25	109.39	-863	-729.6	-25.0	-70.8	-748.4
221	102.42	99.11	-762.1	-643.2	-25.5	-67.5	-656.2
226	92.91	90.02	-675.9	-577.3	-22.2	-60.8	-585.1
231	84.99	82.37	-601.2	-512.7	-17.6	-53.4	-521.4
236	77.84	75.64	-537.5	-451.9	-12.8	-45.6	-465.5
241	71.47	69.43	-476.2	-400	-8.1	-38.2	-415.0
246.1	66.1	64.09	-443.3	-362.9	-4.3	-31.8	-385.0
251.1	61.75	60.2	-392.4	-328	-1.4	-26.7	-346.1
256.1	57.57	56.22	-357.4	-293	1.1	-21.9	-314.8
261.1	53.73	52.72	-326.8	-267	3.0	-17.7	-289.6
266.2	50.7	49.63	-301	-244.7	4.3	-14.5	-267.8
271.2	47.7	46.89	-281.5	-224.4	5.3	-11.6	-249.8
276.3	46.85	46.62	-274.6	-219.8	5.6	-10.8	-244.6
281.3	46.36	46.1	-271.8	-218.7	5.7	-10.3	-242.9
286.3	45.82	45.35	-267.5	-210.1	5.8	-9.9	-236.8
291.4	44.75	44.43	-253.6	-203.8	6.0	-8.9	-227.3
296.4	43.84	43.1	-260.2	-208.5	6.2	-8.1	-233.4
301.4	42.7	42.26	-243.9	-191.5	6.3	-7.2	-217.3
306.5	41.53	40.99	-237.8	-187.1	6.4	-6.2	-212.5
311.5	40.4	39.85	-225.6	-179.4	6.5	-5.4	-203.0
316.5	39.18	38.75	-220.1	-171.4	6.4	-4.5	-196.7
321.6	38.01	37.63	-214.8	-167.6	6.3	-3.7	-192.5
326.6	37.04	36.53	-207.2	-157.4	6.2	-3.0	-183.9
331.7	36.05	35.63	-197.5	-155.7	6.0	-2.4	-178.4
336.7	35.01	34.63	-193.1	-147.4	5.8	-1.8	-172.2
341.7	34.05	33.96	-184.8	-143.6	5.5	-1.3	-166.3
346.7	32.91	32.53	-177.1	-134.7	5.2	-0.7	-158.1
351.8	32.53	32.13	-177.5	-134.9	5.0	-0.6	-158.4
356.8	31.78	31.5	-175.5	-130.4	4.7	-0.2	-155.2
361.8	31.06	30.78	-169.5	-125.9	4.4	0.1	-150.0
366.9	30.38	30.16	-170.3	-122.1	4.1	0.4	-148.4
371.9	29.81	29.52	-162.9	-122.2	3.8	0.6	-144.7
377	29.19	28.93	-163	-115.6	3.5	0.8	-141.4
382	28.76	28.63	-162.4	-114.5	3.2	0.9	-140.5
387	28.14	28.14	-158.3	-114.5	2.8	1.1	-138.4
392.1	28.01	27.68	-150.6	-113.9	2.8	1.1	-134.2
397.1	27.99	27.42	-147.6	-106.7	2.7	1.1	-129.1
402.2	26.95	26.81	-152	-107.3	2.1	1.4	-131.4
407.2	26.62	26.56	-150.5	-107.2	1.8	1.5	-130.5
412.2	26.32	26.23	-153.1	-107	1.6	1.5	-131.6
417.3	26.08	25.97	-148.3	-103.4	1.4	1.6	-127.3
422.3	25.91	25.8	-146.3	-103	1.3	1.6	-126.1

Wind #20 (Cure Data)

Material: T40 fiber — Spool Tension(lb): 5.0

Number of Layers: 2 — Winding Tension(lb): 4.8

Oven Ramp Rate(degC/m): 1.0 — Stress Retention Factor: 0.96

Cure Time (min)	Mand. Temp. (deg C)	Oven Temp. (deg C)	Measured Microstrain Gage 1	Measured Microstrain Gage 2	Apparent Microstrain Gage 1	Apparent Microstrain Gage 2	Actual Microstrain
427.3	25.64	25.47	-145.8	-101.8	1.1	1.6	-125.2
432.3	25.28	25.33	-147.9	-99.8	0.8	1.7	-125.1
437.3	25.09	25.04	-141.7	-101.7	0.7	1.7	-122.9
442.3	24.82	24.85	-145	-99.4	0.4	1.8	-123.3
447.4	24.68	24.7	-144.3	-98.3	0.3	1.8	-122.3
452.4	24.46	24.46	-143.9	-99.9	0.1	1.8	-122.9
457.4	24.29	24.3	-142.6	-99.5	-0.0	1.8	-121.9
462.4	24.17	24.12	-140.8	-99.1	-0.1	1.8	-120.8
467.4	24.17	24.17	-141.9	-99.3	-0.1	1.8	-121.4
472.4	23.97	24	-138.5	-99.2	-0.3	1.8	-119.6
477.4	24.11	23.82	-141.9	-98.5	-0.2	1.8	-121.0
482.5	23.7	23.74	-141	-96.8	-0.5	1.9	-119.6
487.5	23.57	23.65	-141.8	-97	-0.7	1.9	-120.0
492.5	23.52	23.58	-143	-96.6	-0.7	1.9	-120.4
497.5	23.52	23.58	-138.6	-95.6	-0.7	1.9	-117.7
502.5	23.28	23.37	-141.3	-96.3	-0.9	1.9	-119.3
507.5	23.29	23.35	-139.9	-94.9	-0.9	1.9	-117.9
512.5	23.24	23.27	-142.3	-95	-1.0	1.9	-119.1
517.6	23.27	23.4	-138.4	-94.8	-0.9	1.9	-117.1
522.6	23.01	23.08	-140.1	-96	-1.2	1.9	-118.4
527.6	23.08	23.09	-141.3	-96	-1.1	1.9	-119.0
532.6	22.93	23.01	-139	-94.6	-1.3	1.9	-117.1
537.6	22.74	22.88	-139.8	-94.4	-1.4	1.9	-117.3
542.6	22.93	23.03	-137.4	-95.1	-1.3	1.9	-116.6
547.7	22.79	22.85	-142.4	-91.6	-1.4	1.9	-117.3
552.7	22.85	22.79	-140.1	-95.1	-1.3	1.9	-117.9

Wind #21 (Cure Data)

Material: T40/1908 prepreg | Spool Tension(lb): 5.3

Number of Layers: 2 | Winding Tension(lb): 3.3

Oven Ramp Rate(degC/m): 1.0 | Stress Retention Factor: 0.62

Cure Time (min)	Mand. Temp. (deg C)	Oven Temp. (deg C)	Measured Microstrain Gage 1	Measured Microstrain Gage 2	Apparent Microstrain Gage 1	Apparent Microstrain Gage 2	Actual Microstrain
5	22.81	22.77	-58.2	-54.3	-1.4	1.9	-56.5
10.1	23.2	23.41	-57.6	-53.9	-1.0	1.9	-56.2
15.1	24.99	27.01	-72.5	-61.1	0.6	1.7	-67.9
20.1	32.15	34.17	-103.2	-91.6	4.9	-0.4	-99.7
25.1	38.03	39.97	-127.5	-112.3	6.3	-3.7	-121.2
30.2	43.12	44.75	-152.6	-132.4	6.3	-7.5	-141.9
35.2	48.46	50.44	-172.4	-155.6	5.1	-12.3	-160.4
40.2	53.45	55.31	-201.5	-181.8	3.2	-17.4	-184.5
45.2	58.78	60.74	-231.9	-224.3	0.4	-23.3	-216.7
50.3	63.81	65.82	-282.9	-259.3	-2.8	-29.1	-255.2
55.3	68.31	70.55	-313.3	-292.8	-5.9	-34.4	-282.9
60.3	73.62	75.71	-362	-331.1	-9.7	-40.7	-321.4
65.3	78.65	80.64	-402.5	-368.7	-13.3	-46.5	-355.7
70.4	83.84	85.88	-450.1	-407	-16.9	-52.2	-394.0
75.4	89.01	91.19	-493.6	-445.7	-20.1	-57.3	-430.9
80.4	94.14	96.36	-542.8	-482.6	-22.8	-61.9	-470.4
85.4	98.99	100.9	-589.3	-520.8	-24.6	-65.5	-510.0
90.5	100.92	101.76	-601.2	-533.6	-25.1	-66.7	-521.5
95.5	101.23	101.84	-603.3	-536.5	-25.2	-66.8	-523.9
100.5	101.34	101.79	-600.7	-531.4	-25.2	-66.9	-520.0
105.6	101.68	102.25	-602.5	-539.2	-25.3	-67.1	-524.6
110.6	101.63	102.38	-605.3	-537.4	-25.3	-67.1	-525.2
115.7	101.64	102.48	-605.4	-539.4	-25.3	-67.1	-526.2
120.7	104.59	106.46	-632.9	-561.1	-25.8	-68.6	-549.8
125.7	109.47	111.46	-673.8	-594.7	-25.8	-70.3	-586.2
130.8	114.36	116.65	-718.9	-629	-24.7	-70.9	-626.2
135.8	119.38	121.46	-762.5	-664.5	-22.2	-70.2	-667.3
140.9	124.47	126.7	-802.7	-700.1	-18.1	-68.0	-708.3
145.9	129.36	131.46	-847.5	-733.1	-12.6	-64.4	-751.8
150.9	134.55	135.79	-888.2	-765.5	-4.9	-58.7	-795.0
155.9	138.99	141.25	-920.8	-795.4	3.4	-52.3	-833.7
161	144.23	146.34	-961.7	-825.9	15.4	-42.7	-880.2
166	149.04	151.48	-1000.3	-853.8	28.7	-31.9	-925.5
171	153.98	155.96	-1034.8	-879.6	44.6	-18.5	-970.3
176	155.85	157.22	-1049.3	-891.7	51.3	-12.9	-989.7
181	156.32	157.47	-1055.4	-895.6	53.1	-11.4	-996.4
186.1	156.52	157.7	-1057.6	-895.9	53.8	-10.7	-998.3
191.1	156.5	157.14	-1061.4	-898.9	53.8	-10.8	-1001.6
196.1	156.5	157.88	-1061.8	-897.7	53.8	-10.8	-1001.2
201.1	153.72	150.89	-1045.8	-883.2	43.7	-19.3	-976.7
206.2	139.98	136.57	-938	-803.6	5.5	-50.7	-848.2
211.2	125.38	122.04	-812.6	-707.5	-17.2	-67.4	-717.7

Wind #21 (Cure Data)

Material: T40/1908 prepreg   Spool Tension(lb): 5.3
Number of Layers: 2   Winding Tension(lb): 3.3
Oven Ramp Rate(degC/m): 1.0   Stress Retention Factor: 0.62

Cure Time (min)	Mand. Temp. (deg C)	Oven Temp. (deg C)	Measured Microstrain Gage 1	Measured Microstrain Gage 2	Apparent Microstrain Gage 1	Apparent Microstrain Gage 2	Actual Microstrain
216.2	112.67	109.85	-702	-617.5	-25.2	-70.8	-611.8
221.2	102.08	99.31	-600.6	-536.7	-25.4	-67.3	-522.3
226.2	92.72	90.57	-513.2	-466.7	-22.1	-60.7	-448.6
231.3	84.44	82.56	-440.8	-401.4	-17.3	-52.8	-386.1
236.3	77.49	75.72	-369.8	-341.8	-12.5	-45.2	-327.0
241.3	71.55	69.42	-310.9	-290.5	-8.2	-38.2	-277.5
246.3	66.44	65.2	-266.8	-250.5	-4.6	-32.2	-240.3
251.4	61.62	60.5	-218.6	-210.5	-1.4	-26.5	-200.6
256.4	57.32	56.14	-184.1	-177.8	1.2	-21.6	-170.7
261.4	53.64	52.86	-148.7	-150.1	3.1	-17.6	-142.1
266.5	50.31	49.4	-117.5	-125.1	4.5	-14.1	-116.5
271.5	47.54	46.9	-98	-105.6	5.4	-11.4	-98.8
276.5	46.99	46.74	-88.4	-101.1	5.5	-10.9	-92.1
281.6	46.57	46.47	-81	-97.8	5.6	-10.5	-87.0
286.6	45.6	45.33	-74.1	-90.8	5.9	-9.7	-80.6
291.6	44.55	44.2	-64.3	-83.7	6.1	-8.7	-72.7
296.6	43.52	43.25	-59.4	-67.5	6.2	-7.8	-62.6
301.7	42.46	41.96	-54.3	-59.3	6.4	-7.0	-56.5
306.7	41.29	40.67	-36.9	-52	6.4	-6.0	-44.6
311.7	40.1	39.49	-28.2	-45	6.5	-5.1	-37.3
316.7	38.94	38.25	-19.2	-36.1	6.4	-4.3	-28.7
321.7	37.85	37.36	-12.6	-27.3	6.3	-3.6	-21.3
326.8	36.77	36.12	-5.2	-20.1	6.2	-2.9	-14.3
331.8	35.85	35.42	7.7	-47.9	6.0	-2.3	-21.9
336.8	34.96	34.59	22	-43	5.8	-1.8	-12.5
341.8	33.97	33.41	63.8	-53.3	5.5	-1.3	3.1
346.9	33.07	32.98	79.6	-45.6	5.2	-0.8	14.8
351.9	32.09	31.15	71.1	-40.3	4.9	-0.3	13.1
356.9	31.66	30.91	83.1	-36.7	4.7	-0.2	20.9
361.9	30.95	30.67	89.8	-33.8	4.4	0.1	25.7
366.9	30.13	30.5	98.1	-24.1	4.0	0.4	34.8
372	29.65	29.41	100.6	-25.8	3.7	0.6	35.2
377	29.14	29.03	104.4	-22.5	3.4	0.8	38.8
382	28.48	28.2	108.7	-22	3.1	1.0	41.3
387	28.06	27.98	113.1	-17.6	2.8	1.1	45.8
392.1	27.68	27.54	117.6	-14.6	2.5	1.2	49.6
397.1	27.44	27.11	118.5	-13.9	2.4	1.3	50.5
402.1	27.02	27.05	121.4	-9.6	2.1	1.4	54.2
407.1	26.24	26.24	121.6	-8.5	1.5	1.5	55.0
412.1	26.24	26.38	129.7	-8	1.5	1.5	59.3
417.2	26	25.88	134	-5.4	1.4	1.6	62.8
422.2	25.66	25.6	130.3	-5.4	1.1	1.6	61.1

Wind #21 (Cure Data)

Material: T40/1908 prepreg Spool Tension(lb): 5.3
Number of Layers: 2 Winding Tension(lb): 3.3
Oven Ramp Rate(degC/m): 1.0 Stress Retention Factor: 0.62

Cure Time (min)	Mand. Temp. (deg C)	Oven Temp. (deg C)	Measured Microstrain Gage 1	Measured Microstrain Gage 2	Apparent Microstrain Gage 1	Apparent Microstrain Gage 2	Actual Microstrain
427.2	25.45	25.41	135.7	-5.6	0.9	1.7	63.7
432.2	25.11	25.13	139.7	-2.5	0.7	1.7	67.4
437.2	25.06	24.95	138.6	-0.5	0.6	1.7	67.9
442.2	24.91	24.84	137	5.3	0.5	1.7	70.0
447.3	24.64	24.62	135.1	7.2	0.3	1.8	70.1
452.3	24.69	24.34	139.8	7.6	0.3	1.8	72.7
457.3	24.31	24.17	141.1	8.2	-0.0	1.8	73.7
462.3	24.2	24.36	141	9.8	-0.1	1.8	74.5
467.3	24.07	24.31	140.4	10.4	-0.2	1.8	74.6
472.3	23.85	23.8	140.9	11.1	-0.4	1.8	75.3
477.3	23.92	23.98	141.6	12.5	-0.3	1.8	76.3
482.4	23.53	23.76	129.6	75.5	-0.7	1.9	102.0
487.4	23.76	23.68	127.6	75	-0.5	1.9	100.6
492.4	23.41	23.63	126.5	75.4	-0.8	1.9	100.4
497.4	23.39	23.39	131.3	75.1	-0.8	1.9	102.7
502.4	23.38	23.59	131.5	78.2	-0.8	1.9	104.3
507.4	23.35	23.57	130	79.8	-0.9	1.9	104.4
512.4	23.19	23.52	131.6	80.4	-1.0	1.9	105.6
517.5	23.08	23.45	130.4	80.3	-1.1	1.9	105.0
522.5	22.99	23.45	133	80.3	-1.2	1.9	106.3
527.5	23.11	23.15	130.2	79.4	-1.1	1.9	104.4
532.5	23.03	22.97	131.1	80.7	-1.2	1.9	105.5
537.5	22.95	23.14	129.8	80.5	-1.2	1.9	104.8
542.6	22.89	23.46	129.2	80.6	-1.3	1.9	104.6
547.6	22.89	22.52	137.1	80.4	-1.3	1.9	108.5
552.6	22.81	23.02	133.7	81.2	-1.4	1.9	107.2
557.6	22.7	22.93	136.7	82.3	-1.5	1.9	109.3
562.6	22.73	22.94	133.8	81.5	-1.4	1.9	107.4
567.7	22.8	22.95	133.6	82.6	-1.4	1.9	107.8
572.7	22.65	22.83	134.4	82.6	-1.5	1.9	108.3
577.7	22.78	22.83	135	83.9	-1.4	1.9	109.2
582.7	22.51	22.57	134.6	82.2	-1.7	1.9	108.3
587.7	22.72	23.39	130.1	83.2	-1.5	1.9	106.4
592.7	22.6	22.76	137.5	83.5	-1.6	1.9	110.3
597.8	22.63	22.82	136.9	83	-1.5	1.9	109.8
602.8	22.53	22.86	138.8	84.5	-1.6	1.9	111.5
607.8	22.67	22.78	137.2	84.4	-1.5	1.9	110.6

Wind #22 (Cure Data)

Material: T40 fiber
Number of Layers: 3
Oven Ramp Rate(degC/m): 1.0

Spool Tension(lb): 5.2
Winding Tension(lb): 4.6
Stress Retention Factor: 0.88

Cure Time (min)	Mand. Temp. (deg C)	Oven Temp. (deg C)	Measured Microstrain Gage 1	Measured Microstrain Gage 2	Apparent Microstrain Gage 1	Apparent Microstrain Gage 2	Actual Microstrain
5	23.13	23.21	-165.4	-163.8	-1.1	1.9	-165.0
10	24.31	25.11	-176.9	-173.5	-0.0	1.8	-176.1
15.1	28.41	29.91	-208.2	-197.5	3.0	1.0	-204.9
20.1	33.13	34.93	-238.3	-221.8	5.3	-0.8	-232.3
25.1	38.24	40.06	-270	-244.1	6.4	-3.8	-258.3
30.2	43.39	45.18	-293.6	-265	6.2	-7.7	-278.6
35.2	48.49	50.38	-328.1	-283.6	5.1	-12.3	-302.2
40.2	53.75	55.53	-359.9	-315.3	3.0	-17.7	-330.3
45.3	58.85	60.74	-399.6	-342.7	0.3	-23.3	-359.7
50.3	63.55	65.48	-444	-393.8	-2.6	-28.8	-403.2
55.3	68.61	70.51	-501.3	-440.2	-6.1	-34.8	-450.3
60.3	73.82	75.81	-553.1	-487.2	-9.8	-40.9	-494.8
65.3	78.89	80.76	-609.7	-535.8	-13.5	-46.8	-542.6
70.4	83.88	85.86	-673	-585.1	-16.9	-52.2	-594.5
75.4	89.1	91.14	-731.6	-636.9	-20.2	-57.4	-645.5
80.4	94.15	96.05	-787.8	-684.8	-22.8	-61.9	-694.0
85.4	99.22	100.81	-849.1	-732.2	-24.7	-65.6	-745.5
90.5	101.31	101.85	-876	-751.3	-25.2	-66.9	-767.6
95.5	101.53	101.8	-882.9	-754.4	-25.3	-67.0	-772.5
100.5	101.59	102.05	-885.1	-759.6	-25.3	-67.1	-776.2
105.5	102.06	102.29	-883.4	-757.7	-25.4	-67.3	-774.2
110.5	101.85	102.27	-887.3	-770.3	-25.4	-67.2	-782.5
115.6	102.18	102.59	-887.1	-761.7	-25.4	-67.4	-778.0
120.6	104.67	106.23	-924.7	-791	-25.8	-68.6	-810.6
125.6	109.34	111.1	-978.9	-834.1	-25.8	-70.2	-858.5
130.7	114.31	116.07	-1037.9	-884.1	-24.7	-70.9	-913.2
135.7	119.24	120.98	-1091.9	-933.1	-22.3	-70.2	-966.3
140.7	124.25	125.93	-1150.9	-976.8	-18.3	-68.1	-1020.6
145.7	129.25	131.01	-1215.1	-1027.2	-12.8	-64.5	-1082.5
150.7	134.38	136.07	-1275.4	-1069.8	-5.2	-58.9	-1140.5
155.8	139.12	140.84	-1336	-1119.7	3.7	-52.1	-1203.7
160.8	144.22	145.88	-1386	-1158.3	15.4	-42.7	-1258.5
165.8	148.99	150.4	-1442.8	-1199.9	28.5	-32.0	-1319.6
170.8	153.88	155.12	-1501.3	-1246.4	44.3	-18.8	-1386.6
175.8	155.95	156.39	-1536.1	-1266.9	51.7	-12.5	-1421.1
180.9	156.49	156.64	-1548.3	-1274.1	53.7	-10.8	-1432.6
185.9	156.66	156.77	-1557.8	-1278.4	54.4	-10.3	-1440.1
190.9	156.81	157.05	-1567.2	-1281.2	54.9	-9.8	-1446.8
195.9	156.94	157.1	-1573.3	-1284.6	55.4	-9.4	-1452.0
200.9	154.74	152.64	-1552.8	-1267.2	47.3	-16.2	-1425.5
205.9	140.24	136.28	-1397.7	-1139.8	6.1	-50.2	-1246.7
211	125.73	122.17	-1219.2	-1013.5	-16.9	-67.2	-1074.3

Wind #22 (Cure Data)

Material: T40 fiber
Number of Layers: 3
Oven Ramp Rate(degC/m): 1.0

Spool Tension(lb): 5.2
Winding Tension(lb): 4.6
Stress Retention Factor: 0.88

Cure Time (min)	Mand. Temp. (deg C)	Oven Temp. (deg C)	Measured Microstrain Gage 1	Measured Microstrain Gage 2	Apparent Microstrain Gage 1	Apparent Microstrain Gage 2	Actual Microstrain
216	114.47	111.34	-1094.4	-905.5	-24.6	-70.9	-952.2
221	103.6	100.69	-965.6	-797.2	-25.7	-68.1	-834.5
226	94.16	91.67	-852.5	-705	-22.8	-61.9	-736.4
231.1	85.91	83.82	-755.8	-620.6	-18.2	-54.3	-651.9
236.1	78.67	76.88	-670.3	-552.2	-13.3	-46.5	-581.3
241.1	72.55	70.77	-596.5	-488	-8.9	-39.4	-518.1
246.1	67.19	65.58	-534.9	-433	-5.1	-33.1	-464.9
251.2	62.12	60.82	-479.2	-388.5	-1.7	-27.1	-419.5
256.2	57.78	56.55	-432.4	-345.5	1.0	-22.1	-378.4
261.2	54.29	53.11	-397.9	-315.2	2.8	-18.3	-348.8
266.3	51.01	49.93	-367.1	-286.9	4.2	-14.8	-321.7
271.3	48.11	47.21	-335.2	-263	5.2	-12.0	-295.7
276.3	47.26	46.7	-323.4	-252.1	5.5	-11.2	-284.9
281.3	46.73	46.44	-325.5	-254.6	5.6	-10.7	-287.5
286.4	46.02	45.63	-316.3	-246	5.8	-10.0	-279.0
291.4	45	44.55	-311	-239.6	6.0	-9.1	-273.7
296.4	44.11	43.61	-302.3	-228.5	6.1	-8.3	-264.3
301.5	43.14	42.52	-293.2	-221.3	6.3	-7.5	-256.6
306.5	41.94	41.25	-281.4	-213.1	6.4	-6.6	-247.2
311.6	40.72	40.07	-269.7	-204.2	6.4	-5.6	-237.4
316.6	39.49	38.91	-264.7	-197.7	6.4	-4.7	-232.1
321.6	38.27	37.67	-248.3	-185.1	6.4	-3.8	-218.0
326.7	37.32	36.82	-241.8	-175.4	6.3	-3.2	-210.1
331.7	36.4	35.92	-234.9	-171.2	6.1	-2.6	-204.8
336.7	35.37	34.87	-227.7	-165.1	5.9	-2.0	-198.3
341.7	34.54	34.11	-218.2	-159.8	5.7	-1.6	-191.1
346.8	33.63	33.25	-209.9	-153.3	5.4	-1.1	-183.8
351.8	32.93	32.53	-203.4	-146.2	5.2	-0.7	-177.0
356.9	32.26	31.94	-198.1	-143.8	4.9	-0.4	-173.2
361.9	31.54	31.2	-189.8	-139	4.6	-0.1	-166.7
366.9	30.71	30.48	-189.2	-130.6	4.3	0.2	-162.1
372	30.22	29.66	-194.1	-130.3	4.0	0.4	-164.4
377	29.71	29.43	-185.6	-129.6	3.8	0.6	-159.8
382.1	29.15	28.83	-176	-121.2	3.4	0.8	-150.7
387.1	28.61	28.33	-170.8	-119.3	3.1	1.0	-147.1
392.2	28.1	27.85	-167.7	-118.7	2.8	1.1	-145.2
397.2	27.51	27.26	-165.1	-116.8	2.4	1.3	-142.8
402.2	27.36	27.02	-166.7	-111.9	2.3	1.3	-141.1
407.2	26.95	26.68	-159.5	-111.1	2.1	1.4	-137.0
412.3	26.44	26.11	-163.2	-107.6	1.7	1.5	-137.0
417.3	26.24	25.98	-158.1	-105.8	1.5	1.5	-133.5
422.4	25.85	25.51	-153.8	-104.8	1.3	1.6	-130.7

Wind #23 (Cure Data)

Material: T40/1908 prepreg   Spool Tension(lb): 5.1
Number of Layers: 3   Winding Tension(lb): 1.9
Oven Ramp Rate(degC/m): 1.0   Stress Retention Factor: 0.37

Cure Time (min)	Mand. Temp. (deg C)	Oven Temp. (deg C)	Measured Microstrain Gage 1	Measured Microstrain Gage 2	Apparent Microstrain Gage 1	Apparent Microstrain Gage 2	Actual Microstrain
5	22.4	22.4	-45.2	-47.1	-1.8	1.9	-46.2
10.1	22.75	23.1	-40.1	-43.6	-1.4	1.9	-42.1
15.1	24	25.57	-47.3	-50	-0.3	1.8	-49.4
20.1	30.73	33.22	-78.5	-74.2	4.3	0.2	-78.6
25.1	36.87	38.86	-97.7	-88.3	6.2	-2.9	-94.6
30.1	42.16	43.94	-118	-106.6	6.4	-6.7	-112.1
35.2	47.24	49.04	-132.5	-122.8	5.5	-11.2	-124.8
40.2	52.36	54.27	-155.8	-146	3.7	-16.2	-144.6
45.2	57.44	59.37	-190.6	-176.4	1.1	-21.7	-173.2
50.2	62.71	64.51	-231.3	-208.5	-2.0	-27.8	-205.0
55.3	68.21	69.86	-275.2	-240.8	-5.8	-34.3	-238.0
60.3	72.44	74.33	-309.8	-282	-8.8	-39.3	-271.8
65.3	77.4	79.32	-357.6	-323.4	-12.4	-45.1	-311.8
70.3	82.59	84.51	-409.6	-366.8	-16.1	-50.8	-354.8
75.3	87.85	89.69	-455.4	-409.3	-19.4	-56.2	-394.5
80.3	92.9	94.75	-511.7	-452.2	-22.2	-60.8	-440.4
85.3	98.07	99.82	-559.6	-495.5	-24.3	-64.8	-483.0
90.4	100.59	101.22	-591.9	-512.4	-25.1	-66.5	-506.4
95.4	101.18	101.6	-596.8	-519.6	-25.2	-66.8	-512.2
100.4	101.49	101.7	-595.7	-522.2	-25.3	-67.0	-512.8
105.5	101.65	101.78	-595.1	-522.9	-25.3	-67.1	-512.8
110.5	101.7	101.87	-595.4	-525.6	-25.3	-67.1	-514.3
115.6	101.79	101.91	-597.7	-522.1	-25.3	-67.2	-513.6
120.6	103.87	105.26	-620.5	-543.5	-25.7	-68.2	-535.0
125.6	108.22	109.96	-668.1	-580.4	-25.9	-69.9	-576.3
130.7	113.12	114.96	-717	-626.1	-25.1	-70.8	-623.6
135.7	118.34	120.12	-779.1	-665.1	-22.8	-70.4	-675.5
140.8	123.3	125.04	-829.6	-711.1	-19.2	-68.6	-726.4
145.8	128.34	130.48	-888.2	-751.5	-13.9	-65.3	-780.3
150.8	132.83	134.62	-923.4	-789.9	-7.7	-60.8	-822.4
155.9	137.87	139.73	-978.2	-831.1	1.2	-54.1	-878.2
160.9	143.11	144.69	-1025.3	-870.4	12.7	-45.0	-931.7
165.9	147.97	149.7	-1078.8	-910.2	25.5	-34.4	-990.0
170.9	152.81	154.73	-1128.8	-951.4	40.6	-21.9	-1049.5
175.9	155.65	156.23	-1151.6	-966.3	50.6	-13.5	-1077.5
181	156.3	156.58	-1159	-973.6	53.0	-11.4	-1087.1
186	156.55	156.77	-1164.6	-974.9	53.9	-10.6	-1091.4
191	156.64	156.86	-1160.9	-975.9	54.3	-10.4	-1090.4
196	156.44	156.88	-1163.4	-977.3	53.5	-11.0	-1091.6
201.1	156.24	155.44	-1161.5	-972.3	52.8	-11.6	-1087.5
206.1	143.16	138.49	-1030.4	-865.2	12.8	-44.9	-931.8
211.1	128.11	123.79	-870.8	-730.5	-14.2	-65.4	-760.8

Wind #23 (Cure Data)

Material: T40/1908 prepreg　　Spool Tension(lb): 5.1
Number of Layers: 3　　Winding Tension(lb): 1.9
Oven Ramp Rate(degC/m): 1.0　　Stress Retention Factor: 0.37

Cure Time (min)	Mand. Temp. (deg C)	Oven Temp. (deg C)	Measured Microstrain Gage 1	Measured Microstrain Gage 2	Apparent Microstrain Gage 1	Apparent Microstrain Gage 2	Actual Microstrain
216.1	114.91	111.21	-714	-608.7	-24.5	-70.8	-613.7
221.2	103.86	100.51	-584.9	-497.2	-25.7	-68.2	-494.1
226.2	94.3	91.19	-466.4	-396.5	-22.8	-62.0	-389.0
231.2	85.74	83.1	-373.1	-314.2	-18.1	-54.1	-307.5
236.2	78.48	76.15	-283.2	-231	-13.2	-46.3	-227.4
241.2	72.11	69.83	-213.2	-160.2	-8.6	-38.9	-162.9
246.3	66.9	65.1	-161	-108	-4.9	-32.7	-115.7
251.3	62.06	60.42	-115.6	-45.4	-1.6	-27.0	-66.2
256.3	57.67	56.24	-75.3	2.4	1.0	-22.0	-26.0
261.3	53.81	52.6	-43.9	59.8	3.0	-17.8	15.3
266.3	50.61	49.45	-18.7	69.9	4.4	-14.4	30.6
271.4	47.8	46.83	23.8	78.4	5.3	-11.7	54.3
276.4	47.19	46.86	39.6	79.2	5.5	-11.1	62.2
281.4	46.41	46.1	136.2	75.6	5.7	-10.4	108.3
286.4	45.8	45.32	139.2	83.6	5.8	-9.8	113.4
291.4	44.77	44.33	132.1	95	6.0	-8.9	115.0
296.5	43.79	43.09	139.5	105.7	6.2	-8.1	123.5
301.5	42.51	41.96	155.9	119.2	6.3	-7.0	137.9
306.6	41.25	40.69	132.4	148.5	6.4	-6.0	140.2
311.6	40.24	39.58	146.5	161.2	6.5	-5.2	153.2
316.6	38.94	38.24	166.8	171.7	6.4	-4.3	168.2
321.7	38.01	37.31	179.1	182.1	6.3	-3.7	179.3
326.7	36.8	36.19	189.7	193.1	6.2	-2.9	189.8
331.7	35.74	35.06	205.5	197.9	6.0	-2.2	199.8
336.8	34.78	34.19	218	208	5.8	-1.7	211.0
341.8	33.79	33.21	222.3	213.7	5.5	-1.2	215.8
346.8	33.03	32.47	231.8	217.7	5.2	-0.8	222.5
351.9	32.06	31.59	251.4	215.5	4.9	-0.3	231.2
356.9	31.47	31.1	260.9	223.5	4.6	-0.1	239.9
361.9	30.82	30.34	263.4	228.3	4.3	0.2	243.6
367	30.19	29.67	266	233.3	4.0	0.4	247.4
372	29.56	29.1	274	238.9	3.7	0.6	254.3
377	29	28.61	282	241.5	3.4	0.8	259.7
382.1	28.3	27.85	284.5	247.2	2.9	1.0	263.9
387.1	27.87	27.43	291.9	253	2.7	1.2	270.5
392.1	27.45	27.06	296.7	254.1	2.4	1.3	273.6
397.2	27.02	26.69	305.7	252.7	2.1	1.4	277.5
402.2	26.62	26.34	310.3	255.7	1.8	1.5	281.4
407.2	26.21	26.12	308	259.2	1.5	1.5	282.1
412.3	26.1	25.81	310.9	259.9	1.4	1.6	283.9
417.3	25.78	25.44	312.5	260.5	1.2	1.6	285.1
422.3	25.33	25.13	321.5	262.4	0.8	1.7	290.7

Wind #23 (Cure Data)

Material: T40/1908 prepreg — Spool Tension(lb): 5.1

Number of Layers: 3 — Winding Tension(lb): 1.9

Oven Ramp Rate(degC/m): 1.0 — Stress Retention Factor: 0.37

Cure Time (min)	Mand. Temp. (deg C)	Oven Temp. (deg C)	Measured Microstrain Gage 1	Measured Microstrain Gage 2	Apparent Microstrain Gage 1	Apparent Microstrain Gage 2	Actual Microstrain
427.3	25.07	24.85	321	267.6	0.6	1.7	293.1
432.3	24.89	24.71	324.5	270.6	0.5	1.7	296.4
437.4	24.64	24.47	323.1	272	0.3	1.8	296.5
442.4	24.44	24.23	327.4	270.6	0.1	1.8	298.0
447.4	24.27	24.13	330.6	275.1	-0.0	1.8	302.0
452.4	24.48	23.91	318.2	277.5	0.1	1.8	296.9
457.5	24.07	23.88	335.6	276.3	-0.2	1.8	305.1
462.5	23.83	23.68	332.3	279.2	-0.4	1.8	305.0
467.5	23.76	23.64	335.6	278.9	-0.5	1.9	306.6
472.6	23.45	23.34	339.1	278.7	-0.8	1.9	308.3
477.6	23.52	23.41	344.5	281	-0.7	1.9	312.2
482.7	23.47	23.31	343.3	280.6	-0.8	1.9	311.4
487.7	23.38	23.24	339.6	280.1	-0.8	1.9	309.3

Wind #24 (Cure Data)

Material: T40/1908 prepreg | Spool Tension(lb): 8.0
Number of Layers: 1 | Winding Tension(lb): 3.0
Oven Ramp Rate(degC/m): 0.5 | Stress Retention Factor: 0.38

Cure Time (min)	Mand. Temp. (deg C)	Oven Temp. (deg C)	Measured Microstrain Gage 1	Measured Microstrain Gage 2	Apparent Microstrain Gage 1	Apparent Microstrain Gage 2	Actual Microstrain
5	22.34	22.48	-53.4	-48.2	-1.8	1.9	-50.8
10.1	22.89	23.15	-53.4	-53.3	-1.3	1.9	-53.6
15.1	23.48	23.49	-55.7	-53.8	-0.7	1.9	-55.3
20.1	24.08	24.21	-55.6	-50.3	-0.2	1.8	-53.8
25.1	27.62	29.02	-64.6	-57.1	2.5	1.2	-62.7
30.1	31.25	32.52	-68.5	-68.6	4.5	0.0	-70.8
35.2	34.03	34.82	-74.9	-72.1	5.5	-1.3	-75.6
40.2	36.59	37.51	-77.7	-78.3	6.1	-2.8	-79.7
45.2	39.2	39.98	-82	-80.8	6.4	-4.5	-82.4
50.2	41.89	42.65	-93.6	-85	6.4	-6.5	-89.2
55.3	44.39	45.09	-103.5	-103	6.1	-8.6	-102.0
60.3	46.97	47.95	-113.6	-108.4	5.5	-10.9	-108.3
65.3	49.36	50.23	-117.1	-116	4.8	-13.2	-112.4
70.3	51.87	52.82	-136.6	-124.2	3.9	-15.7	-124.5
75.4	54.73	55.98	-163.7	-147.1	2.6	-18.8	-147.3
80.4	57.56	58.29	-141.6	-177.1	1.1	-21.9	-148.9
85.4	59.59	60.36	-173.6	-166.6	-0.1	-24.2	-158.0
90.5	62.03	63.01	-185.7	-173	-1.6	-27.0	-165.0
95.5	64.7	65.67	-196.8	-184.7	-3.4	-30.1	-174.0
100.6	67.36	68.27	-199.5	-202.4	-5.2	-33.3	-181.7
105.6	69.95	70.8	-222.6	-215.3	-7.0	-36.4	-197.3
110.6	72.66	73.62	-233.4	-219.9	-9.0	-39.6	-202.4
115.6	75.24	76.22	-249	-231.5	-10.9	-42.6	-213.5
120.6	77.68	78.54	-249.4	-248.1	-12.6	-45.4	-219.7
125.6	79.91	80.89	-273.6	-256.7	-14.2	-47.9	-234.1
130.7	82.67	83.54	-282	-269.2	-16.1	-50.9	-242.1
135.7	85.26	86.1	-296.8	-280.2	-17.8	-53.6	-252.8
140.7	87.82	88.97	-316.4	-295.5	-19.4	-56.2	-268.1
145.8	90.48	91.5	-326.8	-301.6	-20.9	-58.7	-274.4
150.8	92.89	93.79	-340.1	-323.9	-22.2	-60.8	-290.5
155.8	95.52	96.6	-352.7	-323.7	-23.4	-63.0	-295.0
160.8	98.01	99.18	-371.3	-343	-24.3	-64.8	-312.6
165.8	100.72	101.25	-385.8	-376.5	-25.1	-66.5	-335.3
170.9	101.5	101.84	-385.2	-356.9	-25.3	-67.0	-324.9
175.9	99.98	98.08	-377	-352.7	-24.9	-66.1	-319.4
180.9	90.7	87.81	-319.3	-303.1	-21.0	-58.9	-271.2
185.9	81.94	79.48	-271.6	-257.9	-15.6	-50.1	-231.9
191	74.5	72.59	-227.5	-221.2	-10.3	-41.7	-198.3
196	68.14	66.37	-188.3	-186.3	-5.7	-34.2	-167.3
201	62.71	61	-166.2	-166	-2.0	-27.8	-151.2
206.1	58.21	56.89	-140.3	-126.5	0.7	-22.6	-122.4
211.1	54.14	53.31	-113.3	-112.9	2.9	-18.1	-105.5

Wind #24 (Cure Data)

Material: T40/1908 prepreg — Spool Tension(lb): 8.0
Number of Layers: 1 — Winding Tension(lb): 3.0
Oven Ramp Rate(degC/m): 0.5 — Stress Retention Factor: 0.38

Cure Time (min)	Mand. Temp. (deg C)	Oven Temp. (deg C)	Measured Microstrain Gage 1	Measured Microstrain Gage 2	Apparent Microstrain Gage 1	Apparent Microstrain Gage 2	Actual Microstrain
216.1	51.08	50.12	-93.3	-95.8	4.2	-14.9	-89.2
221.1	48.12	47.11	-77.5	-87.4	5.2	-12.0	-79.1
226.1	47.19	46.85	-73.2	-79.8	5.5	-11.1	-73.7
231.2	46.44	46.25	-72.1	-79	5.7	-10.4	-73.2
236.2	45.79	45.63	-66.8	-71.3	5.8	-9.8	-67.1
241.2	44.87	44.46	-68	-71.1	6.0	-9.0	-68.1
246.2	43.65	43.42	-61.7	-62.1	6.2	-8.0	-61.0
251.3	42.55	42.09	-53.1	-62.3	6.3	-7.0	-57.3
256.3	41.38	40.92	-49.6	-57.5	6.4	-6.1	-53.7
261.3	40.21	39.83	-45.2	-48.3	6.5	-5.2	-47.4
266.3	38.95	38.65	-34.7	-39	6.4	-4.3	-37.9
271.4	37.91	37.39	-36.8	-43.8	6.3	-3.6	-41.7
276.4	36.63	36.3	-27.7	-41.4	6.1	-2.8	-36.2
281.4	35.72	35.31	-23.4	-37.6	6.0	-2.2	-32.4
286.4	34.76	34.29	-17.2	-25	5.7	-1.7	-23.1
291.4	33.84	33.41	-15.1	-20.8	5.5	-1.2	-20.1
296.5	32.9	32.67	-15.4	-13.3	5.2	-0.7	-16.6
301.5	32.07	31.72	-10	-17.1	4.9	-0.3	-15.8
306.5	31.26	30.92	-7.7	-20.2	4.5	0.0	-16.2
311.5	30.58	30.49	-0.2	1.9	4.2	0.3	-1.4
316.5	29.81	29.66	1	-14.6	3.8	0.6	-9.0
321.6	29.4	29.2	8.2	-1.1	3.6	0.7	1.4
326.6	28.65	28.69	-1	-3.4	3.2	0.9	-4.2
331.6	28.33	28.16	-5.9	3.7	3.0	1.0	-3.1
336.6	27.73	27.61	11	9.9	2.6	1.2	8.6
341.7	27.25	27.21	6.2	-16.7	2.3	1.3	-7.0
346.7	26.83	26.87	11.6	4.7	2.0	1.4	6.5
351.7	26.63	25.88	9.5	8.2	1.8	1.5	7.2
356.7	26.45	26.26	19.8	1	1.7	1.5	8.8
361.8	25.95	25.85	-1.5	-10.4	1.3	1.6	-7.4
366.8	25.53	25.63	14.3	2.7	1.0	1.7	7.2
371.8	25.16	25.64	10.5	29	0.7	1.7	18.5
376.8	25.06	25.06	13	14.2	0.6	1.7	12.4
381.8	24.95	24.95	13	-1.9	0.5	1.7	4.4
386.9	24.95	24.47	1	23.2	0.5	1.7	11.0
391.9	24.54	23.78	33.5	-5.3	0.2	1.8	13.1
396.9	24.4	24.33	21.1	11.3	0.1	1.8	15.3
401.9	24.16	24.22	31.8	16.9	-0.1	1.8	23.5
407	23.93	23.97	24.5	17.4	-0.3	1.8	20.2
412	23.82	23.98	25.8	16.2	-0.4	1.8	20.3
417	23.78	23.81	25.5	15.3	-0.5	1.9	19.7
422	23.5	23.68	21.7	14.3	-0.7	1.9	17.4

Wind #25 (Cure Data)

Material: T40/1908 prepreg | Spool Tension(lb): 7.9
Number of Layers: 1 | Winding Tension(lb): 4.0
Oven Ramp Rate(degC/m): 0.2 | Stress Retention Factor: 0.51

Cure Time (min)	Mand. Temp. (deg C)	Oven Temp. (deg C)	Measured Microstrain Gage 1	Measured Microstrain Gage 2	Apparent Microstrain Gage 1	Apparent Microstrain Gage 2	Actual Microstrain
5	22.79	22.71	-67.7	-63.5	-1.4	1.9	-65.9
10	23.33	23.47	-65.5	-62.3	-0.9	1.9	-64.4
15.1	23.84	23.94	-63.7	-65.3	-0.4	1.8	-65.2
20.1	24.51	24.5	-68.2	-65	0.2	1.8	-67.6
25.1	25.08	25.11	-68.5	-68.3	0.6	1.7	-69.6
30.1	25.66	25.6	-67.7	-66.5	1.1	1.6	-68.5
35.2	26.05	25.97	-63.4	-66.7	1.4	1.6	-66.5
40.2	26.37	26.28	-65.6	-66.7	1.6	1.5	-67.7
45.2	28.45	28.9	-76.7	-70.2	3.0	1.0	-75.5
50.2	30.08	30.14	-73.3	-73	3.9	0.5	-75.4
55.3	31.25	31.15	-76.2	-76.2	4.5	0.0	-78.5
60.3	32.25	32.23	-77.5	-76.3	4.9	-0.4	-79.2
65.3	33.31	33.39	-79.2	-78.9	5.3	-0.9	-81.2
70.3	34.4	34.4	-83.8	-81.8	5.7	-1.5	-84.9
75.4	35.4	35.42	-85.7	-82.8	5.9	-2.0	-86.2
80.4	36.33	36.36	-84.1	-84.4	6.1	-2.6	-86.0
85.4	37.53	37.57	-87.1	-85.4	6.3	-3.4	-87.7
90.4	38.45	38.49	-94	-90.1	6.4	-4.0	-93.3
95.5	39.51	39.54	-89	-89.9	6.4	-4.7	-90.3
100.5	40.43	40.6	-95	-95	6.5	-5.4	-95.5
105.5	41.54	41.65	-102.5	-96.9	6.4	-6.2	-99.8
110.5	42.65	42.67	-96	-101.1	6.3	-7.1	-98.2
115.5	43.54	43.69	-101.3	-104.1	6.2	-7.9	-101.9
120.6	44.76	44.92	-110.6	-107.8	6.0	-8.9	-107.8
125.6	45.67	45.88	-110.6	-112	5.9	-9.7	-109.4
130.6	46.73	46.92	-120.9	-116.7	5.6	-10.7	-116.3
135.7	47.9	48.18	-127	-117.9	5.3	-11.8	-119.2
140.7	48.58	49.14	-136.6	-129.3	5.1	-12.4	-129.3
145.7	49.66	49.92	-127.2	-127.7	4.7	-13.5	-123.1
150.8	50.71	50.95	-132.8	-133.5	4.3	-14.5	-128.0
155.8	51.86	52.1	-136	-137.1	3.9	-15.7	-130.6
160.8	53.01	53.16	-137	-141.3	3.4	-16.9	-132.4
165.9	53.85	54.23	-148.3	-144.5	3.0	-17.8	-139.0
170.9	54.96	55.29	-148	-150	2.4	-19.0	-140.7
175.9	56.11	56.38	-159.8	-153.9	1.9	-20.3	-147.6
181	56.96	57.38	-163	-158.6	1.4	-21.2	-150.9
186	58.16	58.67	-169.1	-161.8	0.7	-22.6	-154.5
191.1	59.25	59.62	-169.1	-164.1	0.1	-23.8	-154.8
196.1	60.04	60.33	-176.4	-173.5	-0.4	-24.7	-162.4
201.1	61.06	61.37	-183.8	-179.5	-1.0	-25.9	-168.2
206.2	62.1	62.48	-185.1	-186	-1.7	-27.1	-171.2
211.2	63.16	63.51	-191.6	-188.4	-2.3	-28.3	-174.7

Wind #25 (Cure Data)

Material: T40/1908 prepreg   Spool Tension(lb): 7.9
Number of Layers: 1   Winding Tension(lb): 4.0
Oven Ramp Rate(degC/m): 0.2   Stress Retention Factor: 0.51

Cure Time (min)	Mand. Temp. (deg C)	Oven Temp. (deg C)	Measured Microstrain Gage 1	Measured Microstrain Gage 2	Apparent Microstrain Gage 1	Apparent Microstrain Gage 2	Actual Microstrain
216.2	64.23	64.6	-198	-193.4	-3.1	-29.6	-179.4
221.2	65.34	65.62	-203.6	-199.8	-3.8	-30.9	-184.4
226.3	66.35	66.74	-205.2	-202.7	-4.5	-32.1	-185.7
231.3	67.27	67.61	-212.2	-211.6	-5.1	-33.2	-192.7
236.3	68.29	68.9	-215.3	-214	-5.9	-34.4	-194.5
241.4	69.24	69.65	-223.8	-218.1	-6.5	-35.5	-199.9
246.4	70.42	70.84	-230.4	-223.9	-7.4	-36.9	-205.0
251.5	71.56	71.97	-234	-229.9	-8.2	-38.3	-208.7
256.5	72.66	73.08	-238.3	-234.4	-9.0	-39.6	-212.1
261.5	73.48	73.87	-247.5	-240.5	-9.6	-40.5	-218.9
266.5	74.62	75.05	-250.6	-245.4	-10.4	-41.9	-221.9
271.5	75.62	76.01	-256	-249.5	-11.2	-43.0	-225.7
276.5	76.74	77.05	-273.2	-251.8	-12.0	-44.3	-234.4
281.6	77.37	77.8	-275.3	-258.1	-12.4	-45.0	-238.0
286.6	78.62	79.07	-276.7	-263.4	-13.3	-46.4	-240.2
291.6	79.7	80.09	-278.1	-267.2	-14.1	-47.7	-241.8
296.6	80.65	80.98	-285.4	-273.4	-14.7	-48.7	-247.7
301.6	81.6	82.02	-288.2	-278.8	-15.4	-49.8	-250.9
306.6	82.7	83.03	-294.4	-283	-16.1	-50.9	-255.2
311.7	83.81	84.2	-305.5	-288.9	-16.9	-52.1	-262.7
316.7	84.79	85.11	-305.1	-294.4	-17.5	-53.1	-264.4
321.7	85.68	86.03	-318.5	-296.7	-18.1	-54.1	-271.5
326.7	86.69	87.08	-319.8	-302.7	-18.7	-55.1	-274.3
331.7	87.62	87.94	-322.4	-310	-19.3	-56.0	-278.6
336.7	88.65	89.03	-329	-312	-19.9	-57.0	-282.1
341.8	89.8	90.19	-341	-319.3	-20.5	-58.1	-290.8
346.8	90.92	91.27	-342.6	-321.4	-21.2	-59.1	-291.9
351.8	91.76	92.24	-355	-326.8	-21.6	-59.9	-300.2
356.8	92.88	93.42	-349.3	-339	-22.2	-60.8	-302.7
361.8	93.81	94.2	-359.5	-336.3	-22.6	-61.6	-305.8
366.8	94.96	95.35	-361.9	-341.7	-23.1	-62.5	-309.0
371.9	95.96	96.33	-374.3	-346.6	-23.5	-63.3	-317.0
376.9	96.85	97.28	-371.1	-350.3	-23.9	-64.0	-316.8
381.9	97.82	98.25	-374.3	-353.2	-24.2	-64.7	-319.3
387	98.88	99.3	-383.7	-358.5	-24.6	-65.4	-326.1
392	99.96	100.34	-398.7	-364.8	-24.9	-66.1	-336.3
397	100.9	101.37	-396.9	-370.2	-25.1	-66.7	-337.7
402	101.42	101.69	-406.8	-370.9	-25.3	-67.0	-342.7
407.1	101.66	101.24	-397.7	-371.5	-25.3	-67.1	-338.4
412.1	93.61	90.6	-357.1	-333.1	-22.5	-61.4	-303.1
417.1	84.48	81.87	-305	-286.2	-17.3	-52.8	-260.5
422.1	76.94	74.73	-254.6	-244.9	-12.1	-44.5	-221.4

Wind #25 (Cure Data)

Material: T40/1908 prepreg | Spool Tension(lb): 7.9
Number of Layers: 1 | Winding Tension(lb): 4.0
Oven Ramp Rate(degC/m): 0.2 | Stress Retention Factor: 0.51

Cure Time (min)	Mand. Temp. (deg C)	Oven Temp. (deg C)	Measured Microstrain Gage 1	Measured Microstrain Gage 2	Apparent Microstrain Gage 1	Apparent Microstrain Gage 2	Actual Microstrain
427.2	70.39	68.43	-209.9	-212.6	-7.4	-36.9	-189.1
432.2	64.75	63.02	-173	-182.5	-3.4	-30.2	-161.0
437.2	60.06	58.45	-159.7	-156.9	-0.4	-24.7	-145.7
442.3	55.84	54.47	-135.4	-135.1	2.0	-20.0	-126.3
447.3	52.22	51.16	-108.7	-116.1	3.7	-16.1	-106.2
452.3	49.58	48.42	-95.5	-101.8	4.7	-13.4	-94.3
457.4	47.53	47.02	-80	-91.6	5.4	-11.4	-82.8
462.4	47.07	46.66	-89.1	-89.7	5.5	-11.0	-86.7
467.4	39.7	27.36	-44.9	-56.4	6.4	-4.9	-51.4
472.4	29.4	24.65	-3.8	-14	3.6	0.7	-11.0
477.5	25.9	23.93	5.8	0.3	1.3	1.6	1.6
482.5	24.79	23.7	12.1	6.2	0.4	1.8	8.1
487.5	24.32	23.69	24.4	6	0.0	1.8	14.3

Wind #26 (Cure Data)

Material: T40/1908 prepreg — Spool Tension(lb): 8.1

Number of Layers: 1 — Winding Tension(lb): 3.0

Oven Ramp Rate(degC/m): 0.5 — Stress Retention Factor: 0.37

Cure Time (min)	Mand. Temp. (deg C)	Oven Temp. (deg C)	Measured Microstrain Gage 1	Measured Microstrain Gage 2	Apparent Microstrain Gage 1	Apparent Microstrain Gage 2	Actual Microstrain
3	22.96	23.05	-54.7	-46.1	-1.2	1.9	-50.7
6.1	22.9	22.97	-50.6	-40.8	-1.3	1.9	-46.0
9.1	23.06	23.33	-49.3	-44.3	-1.1	1.9	-47.2
12.1	23.5	23.71	-48.9	-44.8	-0.7	1.9	-47.4
15.1	23.96	24.17	-51.3	-37.8	-0.3	1.8	-45.3
18.1	24.37	24.55	-50.7	-41.6	0.0	1.8	-47.1
21.1	25.53	26.76	-52.7	-49.8	1.0	1.7	-52.6
24.1	28.34	29.77	-59.9	-54.1	3.0	1.0	-59.0
27.2	30.63	31.64	-64.1	-64.9	4.2	0.3	-66.7
30.2	32.53	33.4	-68.8	-66.9	5.0	-0.6	-70.1
33.2	34.01	34.7	-71.2	-67.8	5.5	-1.3	-71.6
36.2	35.48	36.33	-76.2	-70.3	5.9	-2.1	-75.2
39.3	37.09	37.91	-78.4	-67	6.2	-3.1	-74.3
42.3	38.63	39.55	-84.4	-73.6	6.4	-4.1	-80.1
45.3	40.31	41.09	-83.7	-73.1	6.5	-5.3	-79.0
48.3	41.83	42.72	-90	-77.5	6.4	-6.5	-83.7
51.3	43.36	44.16	-98.5	-88.6	6.3	-7.7	-92.8
54.4	44.86	45.81	-103.5	-92.1	6.0	-9.0	-96.3
57.4	46.28	47.13	-107.4	-97.7	5.7	-10.3	-100.3
60.4	47.99	48.84	-114.8	-111.9	5.3	-11.9	-110.0
63.5	49.42	50.24	-120.9	-109.9	4.8	-13.3	-111.2
66.5	51.02	51.84	-129.8	-120.2	4.2	-14.9	-119.7
69.5	52.7	53.52	-137.5	-127.5	3.5	-16.6	-126.0
72.6	54.24	55.07	-143.1	-139.3	2.8	-18.2	-133.5
75.6	55.67	56.72	-153.8	-139.4	2.1	-19.8	-137.8
78.7	57.44	58.34	-161.9	-148.4	1.1	-21.7	-144.8
81.7	58.88	59.85	-168.5	-161.1	0.3	-23.4	-153.3
84.7	60.45	61.34	-177.3	-165.1	-0.6	-25.2	-158.3
87.8	61.91	62.97	-182.8	-185	-1.5	-26.9	-169.7
90.8	63.57	64.48	-192.9	-187.1	-2.6	-28.8	-174.3
93.8	65.18	66.19	-194.9	-203.2	-3.7	-30.7	-181.9
96.8	66.38	67.42	-207.6	-196.4	-4.5	-32.1	-183.7
99.9	68.01	68.98	-214.7	-198.1	-5.7	-34.1	-186.5
102.9	69.53	70.51	-224.8	-210.8	-6.7	-35.9	-196.5
105.9	71.01	72.05	-232.9	-224.7	-7.8	-37.6	-206.1
108.9	72.51	73.55	-240.6	-225.6	-8.9	-39.4	-209.0
111.9	74.15	75.19	-251.3	-233.5	-10.1	-41.3	-216.7
115	75.75	76.72	-258.9	-234.4	-11.2	-43.2	-219.4
118	77.2	78.32	-267	-248.2	-12.3	-44.8	-229.0
121	78.79	79.72	-277.2	-259.7	-13.4	-46.6	-238.4
124	80.19	81.28	-282.3	-269.2	-14.4	-48.2	-244.4
127	81.75	82.71	-296.1	-271.1	-15.5	-49.9	-250.9

Wind #26 (Cure Data)

Material: T40/1908 prepreg
Spool Tension(lb): 8.1
Number of Layers: 1
Winding Tension(lb): 3.0
Oven Ramp Rate(degC/m): 0.5
Stress Retention Factor: 0.37

Cure Time (min)	Mand. Temp. (deg C)	Oven Temp. (deg C)	Measured Microstrain Gage 1	Measured Microstrain Gage 2	Apparent Microstrain Gage 1	Apparent Microstrain Gage 2	Actual Microstrain
130	83.27	84.47	-301.4	-282.1	-16.5	-51.6	-257.7
133	84.78	85.75	-309.4	-284.5	-17.5	-53.1	-261.6
136.1	86.38	87.58	-318.9	-289.9	-18.5	-54.8	-267.7
139.1	88.02	89.06	-325.7	-299.4	-19.5	-56.4	-274.6
142.1	89.48	90.39	-331.5	-310.3	-20.4	-57.8	-281.8
145.1	90.77	91.81	-344.1	-317.5	-21.1	-59.0	-290.8
148.1	92.3	93.41	-352.5	-323.1	-21.9	-60.3	-296.7
151.1	93.88	94.89	-361.7	-335.9	-22.6	-61.7	-306.7
154.1	95.37	96.47	-371.1	-332	-23.3	-62.9	-308.5
157.1	96.97	98.01	-378.8	-348	-23.9	-64.1	-319.4
160.2	98.48	99.63	-386.4	-354.1	-24.5	-65.1	-325.5
163.2	100.12	101.09	-395.1	-359.8	-24.9	-66.2	-331.9
166.2	100.97	101.54	-398.9	-367.4	-25.2	-66.7	-337.2
169.3	101.29	101.69	-398.8	-367.3	-25.2	-66.9	-337.0
172.3	101.56	101.53	-402.8	-365.8	-25.3	-67.0	-338.1
175.4	97.68	94.94	-376.3	-346.1	-24.2	-64.6	-316.8
178.4	92.04	89.11	-340.8	-311.7	-21.7	-60.1	-285.3
181.4	86.41	83.77	-310	-285.7	-18.5	-54.8	-261.2
184.4	81.47	79.02	-278.7	-256.1	-15.3	-49.6	-234.9
187.4	77.14	74.8	-250.2	-245.6	-12.2	-44.8	-219.4
190.4	72.84	70.81	-229.6	-209.9	-9.1	-39.8	-195.3
193.5	69.25	67.28	-207.9	-187.9	-6.5	-35.5	-176.9
196.5	65.93	64.15	-183.6	-180.5	-4.2	-31.6	-164.2
199.6	62.68	61.22	-167.1	-159.4	-2.0	-27.8	-148.4
202.6	60.25	58.69	-152.6	-144.3	-0.5	-24.9	-135.7
205.6	58.03	56.63	-140.9	-135.5	0.8	-22.4	-127.4
208.7	55.6	54.34	-127.2	-123.5	2.1	-19.7	-116.6
211.7	53.45	52.24	-114.4	-108.6	3.2	-17.4	-104.4
214.7	51.37	50.23	-101.2	-103.3	4.1	-15.2	-96.7
217.7	49.55	48.44	-94	-94.8	4.8	-13.4	-90.1
220.8	47.78	46.89	-84.8	-78.2	5.3	-11.7	-78.3
223.8	47.28	46.94	-82.3	-79.9	5.5	-11.2	-78.2
226.8	47.06	46.74	-82.1	-79.5	5.5	-11.0	-78.1
229.8	46.72	46.4	-80.7	-76.7	5.6	-10.7	-76.2
232.8	46.31	45.94	-76.3	-70.4	5.7	-10.3	-71.1
235.9	45.76	45.42	-75.3	-70.4	5.8	-9.8	-70.9
238.9	45.28	44.84	-73.5	-70.7	5.9	-9.4	-70.4
241.9	44.61	44.19	-69.4	-70.5	6.1	-8.8	-68.6
244.9	44.13	43.57	-69.2	-65.8	6.1	-8.4	-66.4
248	43.39	42.89	-63.2	-62	6.2	-7.7	-61.9
251	42.83	42.21	-59	-59.4	6.3	-7.3	-58.7
254	42.02	41.43	-57.4	-51.1	6.4	-6.6	-54.1

Wind #26 (Cure Data)

Material: T40/1908 prepreg | Spool Tension(lb): 8.1
Number of Layers: 1 | Winding Tension(lb): 3.0
Oven Ramp Rate(degC/m): 0.5 | Stress Retention Factor: 0.37

Cure Time (min)	Mand. Temp. (deg C)	Oven Temp. (deg C)	Measured Microstrain Gage 1	Measured Microstrain Gage 2	Apparent Microstrain Gage 1	Apparent Microstrain Gage 2	Actual Microstrain
257	41.32	40.72	-52.3	-49.5	6.4	-6.1	-51.1
260	40.61	40.06	-48.8	-42.3	6.4	-5.5	-46.0
263	39.92	39.3	-45.1	-48.1	6.4	-5.0	-47.3
266.1	39.24	38.65	-43.9	-45.8	6.4	-4.5	-45.8
269.1	38.73	38.06	-39.5	-38.8	6.4	-4.2	-40.3
272.1	37.95	37.37	-37.7	-39.3	6.3	-3.6	-39.8
275.1	37.16	36.67	-33.4	-32.2	6.2	-3.1	-34.4
278.1	36.6	36.04	-29.6	-38.5	6.1	-2.8	-35.7
281.2	36.16	35.62	-28.8	-27.8	6.1	-2.5	-30.1
284.2	35.51	34.9	-26.9	-26.3	5.9	-2.1	-28.5
287.2	34.87	34.45	-23.3	-23.1	5.8	-1.7	-25.2
290.2	34.2	33.75	-20.4	-24.3	5.6	-1.4	-24.5
293.2	33.85	33.36	-18.1	-18.7	5.5	-1.2	-20.5
296.2	33.22	32.85	-17.6	-19.5	5.3	-0.9	-20.8
299.3	32.79	32.44	-13.2	-16.1	5.1	-0.7	-16.9
302.3	32.41	31.97	-9.5	-6.8	5.0	-0.5	-10.4
305.3	31.78	31.43	-9.3	-14.7	4.7	-0.2	-14.3
308.3	31.52	31.08	-6.6	-6.6	4.6	-0.1	-8.9
311.3	31.07	30.79	-8	1.4	4.4	0.1	-5.6
314.4	29.01	25.23	3.7	-0.8	3.4	0.8	-0.6
317.4	26.41	23.61	12.6	15.3	1.7	1.5	12.4
320.4	25.16	25.5	19.2	14.3	0.7	1.7	15.5

Wind #27 (Cure Data)

Material: T40/1908 prepreg | Spool Tension(lb): 8.2
Number of Layers: 1 | Winding Tension(lb): 3.9
Oven Ramp Rate(degC/m): 0.5 | Stress Retention Factor: 0.48

Cure Time (min)	Mand. Temp. (deg C)	Oven Temp. (deg C)	Measured Microstrain Gage 1	Measured Microstrain Gage 2	Apparent Microstrain Gage 1	Apparent Microstrain Gage 2	Actual Microstrain
3	23.08	23.64	-74.1	-65.9	-1.1	1.9	-70.4
6.1	23.41	23.62	-71.6	-59.3	-0.8	1.9	-66.0
9.1	23.8	24.04	-70.8	-59.2	-0.5	1.8	-65.7
12.1	24.2	24.31	-70.4	-60.9	-0.1	1.8	-66.5
15.1	24.58	24.6	-70.5	-61	0.2	1.8	-66.8
18.1	25.03	24.96	-71.8	-63.3	0.6	1.7	-68.7
21.2	25.26	25.58	-72.4	-66.3	0.8	1.7	-70.6
24.2	27.63	29.15	-80.5	-70.3	2.5	1.2	-77.3
27.2	30.4	31.45	-88	-77	4.1	0.3	-84.7
30.2	32.29	33.17	-92.4	-81.1	4.9	-0.4	-89.0
33.2	34.04	34.75	-97.1	-88.4	5.5	-1.3	-94.9
36.3	35.56	36.4	-102.4	-90.5	5.9	-2.1	-98.4
39.3	36.96	37.71	-106.6	-98	6.2	-3.0	-103.9
42.3	38.73	39.5	-110.5	-100.4	6.4	-4.2	-106.6
45.4	40.27	40.91	-117.4	-106.5	6.5	-5.3	-112.5
48.4	41.9	42.67	-122.6	-108.7	6.4	-6.5	-115.6
51.4	43.36	44.07	-130.2	-118.8	6.3	-7.7	-123.8
54.5	44.95	45.76	-136.8	-124.5	6.0	-9.1	-129.1
57.5	46.49	47.22	-141.7	-130.7	5.7	-10.5	-133.8
60.5	48.08	48.87	-151.3	-139.8	5.2	-12.0	-142.2
63.6	49.43	50.2	-157.4	-145	4.8	-13.3	-147.0
66.6	51.13	51.96	-166.8	-150.9	4.2	-15.0	-153.5
69.7	52.77	53.67	-176.7	-162.8	3.5	-16.7	-163.2
72.7	54.25	54.96	-183.5	-167.8	2.8	-18.2	-167.9
75.7	55.77	56.62	-192.1	-178.2	2.0	-19.9	-176.2
78.8	57.27	58.06	-199.1	-187.4	1.2	-21.6	-183.1
81.8	58.92	59.89	-207.1	-189.7	0.3	-23.4	-186.8
84.9	60.48	61.24	-217.7	-202.3	-0.6	-25.2	-197.1
87.9	62.26	63.09	-226.7	-209.9	-1.8	-27.3	-203.8
90.9	63.55	64.25	-234.2	-213.3	-2.6	-28.8	-208.1
94	65.21	66.12	-243.5	-231.8	-3.7	-30.7	-220.4
97	66.69	67.33	-254.4	-235.3	-4.7	-32.5	-226.2
100	68.32	69.23	-266.4	-242	-5.9	-34.4	-234.1
103	70	70.36	-263.7	-240.4	-7.1	-36.4	-230.3
106.1	71.09	71.98	-276.5	-256.9	-7.9	-37.7	-243.9
109.1	72.63	73.54	-287.1	-263.9	-9.0	-39.5	-251.2
112.1	74.07	75.1	-294.9	-272.8	-10.0	-41.2	-258.2
115.1	75.69	76.5	-303.1	-282.4	-11.2	-43.1	-265.6
118.1	77.31	78.33	-312.5	-292.8	-12.4	-45.0	-274.0
121.1	78.89	79.71	-320.9	-301.4	-13.5	-46.8	-281.0
124.1	80.31	81.18	-332.4	-305.7	-14.5	-48.3	-287.6
127.2	81.83	82.73	-341.3	-316.3	-15.5	-50.0	-296.0

Wind #27 (Cure Data)

Material: T40/1908 prepreg — Spool Tension(lb): 8.2
Number of Layers: 1 — Winding Tension(lb): 3.9
Oven Ramp Rate(degC/m): 0.5 — Stress Retention Factor: 0.48

Cure Time (min)	Mand. Temp. (deg C)	Oven Temp. (deg C)	Measured Microstrain Gage 1	Measured Microstrain Gage 2	Apparent Microstrain Gage 1	Apparent Microstrain Gage 2	Actual Microstrain
130.2	83.42	84.35	-349.9	-320	-16.6	-51.7	-300.8
133.2	84.94	85.77	-361.3	-327.1	-17.6	-53.3	-308.7
136.2	86.69	87.5	-367.8	-335.5	-18.7	-55.1	-314.7
139.3	88.02	88.9	-373.3	-343.6	-19.5	-56.4	-320.5
142.3	89.75	90.71	-385.9	-352.7	-20.5	-58.0	-330.0
145.3	91.26	92.04	-393.6	-362.9	-21.3	-59.4	-337.9
148.4	92.76	93.81	-406	-365.4	-22.1	-60.7	-344.3
151.4	94.37	95.31	-410.4	-366.9	-22.9	-62.1	-346.2
154.4	95.9	96.86	-422	-386.1	-23.5	-63.3	-360.7
157.5	97.34	98.15	-430.3	-384.2	-24.1	-64.3	-363.1
160.5	98.78	99.86	-444.8	-409.3	-24.5	-65.3	-382.1
163.6	100.11	101.01	-445	-403.3	-24.9	-66.2	-378.6
166.6	101.02	101.5	-451.6	-406.2	-25.2	-66.7	-383.0
169.6	101.3	101.63	-452.5	-408.7	-25.2	-66.9	-384.5
172.6	101.29	100.99	-452.6	-406.7	-25.2	-66.9	-383.6
175.7	97.27	94.81	-427.8	-387.1	-24.0	-64.3	-363.3
178.7	91.42	88.75	-393.6	-358.7	-21.4	-59.6	-335.7
181.7	86.07	83.5	-359.8	-327.8	-18.3	-54.5	-307.4
184.7	80.91	78.71	-330.8	-304	-14.9	-49.0	-285.4
187.8	76.66	74.6	-304.8	-283.4	-11.9	-44.2	-266.0
190.8	72.64	70.69	-278.4	-254.3	-9.0	-39.5	-242.1
193.8	69.07	67.27	-256.3	-239.9	-6.4	-35.3	-227.2
196.9	65.69	63.98	-233.7	-216.9	-4.0	-31.3	-207.6
199.9	62.58	61.07	-220.5	-200.7	-2.0	-27.6	-195.8
202.9	59.86	58.39	-202.3	-186	-0.3	-24.5	-181.8
206	57.19	55.92	-185.5	-170.1	1.3	-21.5	-167.7
209	54.89	53.66	-174.6	-166.7	2.5	-18.9	-162.4
212	52.86	51.66	-159.5	-146.5	3.4	-16.8	-146.3
215.1	50.98	49.9	-152.5	-144.5	4.2	-14.8	-143.2
218.1	48.92	47.97	-141.9	-130.4	5.0	-12.8	-132.3
221.2	47.48	46.78	-130.1	-125.2	5.4	-11.4	-124.7
224.2	47.2	46.78	-131	-124.4	5.5	-11.1	-124.9
227.2	46.85	46.61	-136.3	-128.1	5.6	-10.8	-129.6
230.3	46.59	46.32	-133.8	-109.8	5.6	-10.6	-119.3
233.3	45.92	45.55	-121.1	-130.3	5.8	-9.9	-123.6
236.4	45.75	45.37	-125	-113.4	5.8	-9.8	-117.2
239.4	45.09	44.62	-122.5	-115.4	6.0	-9.2	-117.3
242.4	44.5	44.02	-118.6	-111.1	6.1	-8.7	-113.5
245.5	43.87	43.34	-116.2	-115.2	6.2	-8.1	-114.7
248.5	43.37	42.82	-112.3	-107.2	6.3	-7.7	-109.0
251.5	42.48	41.95	-106.7	-102.5	6.3	-7.0	-104.3
254.6	41.93	41.28	-104.8	-100.3	6.4	-6.5	-102.5

Wind #27 (Cure Data)

Material: T40/1908 prepreg
Spool Tension(lb): 8.2
Number of Layers: 1
Winding Tension(lb): 3.9
Oven Ramp Rate(degC/m): 0.5
Stress Retention Factor: 0.48

Cure Time (min)	Mand. Temp. (deg C)	Oven Temp. (deg C)	Measured Microstrain Gage 1	Measured Microstrain Gage 2	Apparent Microstrain Gage 1	Apparent Microstrain Gage 2	Actual Microstrain
257.6	41.12	40.45	-102.2	-96.6	6.4	-5.9	-99.7
260.6	40.49	39.86	-94.7	-91.9	6.5	-5.4	-93.8
263.6	39.81	39.17	-92.9	-88.2	6.4	-4.9	-91.3
266.6	39.01	38.48	-90.1	-88.6	6.4	-4.4	-90.4
269.6	38.41	37.8	-87.6	-82.7	6.4	-3.9	-86.4
272.7	37.73	37.13	-86.1	-83.6	6.3	-3.5	-86.3
275.7	37.22	36.65	-81.7	-80.7	6.2	-3.2	-82.7
278.7	36.31	35.8	-77.2	-75.9	6.1	-2.6	-78.3
281.7	35.74	35.22	-75	-75.7	6.0	-2.2	-77.2
284.8	35.2	34.71	-72.6	-70.5	5.9	-1.9	-73.5
287.8	34.91	34.4	-68	-67.8	5.8	-1.8	-69.9
290.8	33.98	33.64	-67.8	-69.9	5.5	-1.3	-71.0
293.8	33.64	33.22	-65.3	-62.7	5.4	-1.1	-66.2
296.8	33.21	32.69	-62.5	-60.7	5.3	-0.9	-63.8
299.9	32.58	32.27	-61.4	-58.7	5.1	-0.6	-62.3
302.9	32.11	31.71	-55.9	-58.3	4.9	-0.4	-59.4
305.9	31.76	31.3	-54.4	-59.1	4.7	-0.2	-59.0
308.9	31.44	31.01	-57.1	-49.1	4.6	-0.1	-55.4
311.9	30.91	30.46	-53.8	-54.2	4.4	0.1	-56.3
315	30.66	30.35	-56.1	-45.6	4.2	0.2	-53.1
318	30.25	29.88	-50.5	-48.6	4.0	0.4	-51.8
321	29.89	29.49	-47.4	-50.9	3.8	0.5	-51.3
324	29.5	29.17	-48.4	-48.2	3.6	0.7	-50.5
327.1	29.09	28.89	-46	-47.7	3.4	0.8	-49.0
330.1	28.73	28.49	-43	-48.9	3.2	0.9	-48.0
333.1	28.5	28.24	-44	-37.1	3.1	1.0	-42.6
336.1	28.2	27.89	-38.8	-44.6	2.9	1.1	-43.7
339.1	27.82	27.58	-41.5	-40.5	2.6	1.2	-42.9
342.2	27.71	27.54	-38.7	-38.9	2.6	1.2	-40.7
345.2	27.42	27.19	-37.6	-36.1	2.4	1.3	-38.7
348.2	27.26	26.94	-39	-35.8	2.3	1.3	-39.2
351.2	26.97	26.6	-38.5	-39.5	2.1	1.4	-40.7
354.2	26.81	26.59	-37.3	-32.7	2.0	1.4	-36.7
357.3	26.71	26.41	-34.7	-29.4	1.9	1.4	-33.7
360.3	26.55	26.22	-34.5	-34.4	1.8	1.5	-36.1
363.3	26.14	25.97	-34	-33.5	1.5	1.5	-35.3
366.3	25.98	25.87	-34.7	-35.5	1.3	1.6	-36.6
369.4	26.06	25.79	-30.4	-33.3	1.4	1.6	-33.3
372.4	25.57	25.37	-35.8	-28.6	1.0	1.6	-33.5
375.4	25.53	25.32	-30.7	-32.4	1.0	1.7	-32.9
378.4	25.23	25.14	-29.4	-34.1	0.8	1.7	-33.0
381.4	25.19	25.05	-30.1	-29.5	0.7	1.7	-31.0

Wind #28 (Cure Data)

Material: T40 fiber
Number of Layers: 1
Oven Ramp Rate(degC/m): 1.0
Spool Tension(lb): 5.0
Winding Tension(lb): 4.0
Stress Retention Factor: 0.80

Cure Time (min)	Mand. Temp. (deg C)	Oven Temp. (deg C)	Measured Microstrain Gage 1	Measured Microstrain Gage 2	Apparent Microstrain Gage 1	Apparent Microstrain Gage 2	Actual Microstrain
2	22.59	22.5	-96.8	-86.4	-1.6	1.9	-91.8
4.1	22.49	22.69	-92.2	-83.4	-1.7	1.9	-87.9
6.1	22.67	22.94	-94.1	-81.6	-1.5	1.9	-88.0
8.1	23.69	24.74	-94.1	-84.2	-0.6	1.9	-89.8
10.1	25.38	26.63	-107.4	-89.8	0.9	1.7	-99.9
12.1	27.1	28.55	-110.1	-98.5	2.2	1.4	-106.1
14.2	29.12	30.5	-125.2	-106.5	3.4	0.8	-118.0
16.2	31.11	32.66	-131.7	-113.5	4.4	0.1	-124.9
18.2	33.06	34.57	-141.2	-121.1	5.2	-0.8	-133.4
20.3	35.18	36.76	-148.6	-128.7	5.9	-1.9	-140.6
22.3	37.26	38.8	-155.8	-137	6.2	-3.2	-147.9
24.3	39.08	40.84	-162.2	-145.3	6.4	-4.4	-154.8
26.3	41.22	42.94	-173.5	-152	6.4	-6.0	-163.0
28.3	43.32	44.8	-178.4	-159	6.3	-7.7	-168.0
30.4	45.43	47.04	-187.4	-166.8	5.9	-9.5	-175.3
32.4	47.3	49.01	-197	-176.1	5.5	-11.2	-183.7
34.4	49.53	51.24	-206.5	-183.4	4.8	-13.4	-190.7
36.4	51.59	53.32	-217	-191.9	4.0	-15.4	-198.7
38.5	53.57	55.12	-226.6	-202.4	3.1	-17.5	-207.3
40.5	55.61	57.37	-237.5	-211.4	2.1	-19.7	-215.7
42.6	57.71	59.54	-253.9	-223.9	1.0	-22.0	-228.4
44.6	59.67	61.35	-262.3	-235	-0.1	-24.3	-236.4
46.7	61.9	63.65	-275	-247.2	-1.5	-26.8	-246.9
48.7	63.89	65.7	-291.8	-258.3	-2.8	-29.2	-259.0
50.7	65.99	67.86	-304.5	-271.4	-4.2	-31.7	-270.0
52.7	68.02	69.99	-314.5	-283.8	-5.7	-34.1	-279.3
54.7	69.94	71.91	-332.6	-294.9	-7.0	-36.3	-292.1
56.7	72.17	74.08	-347.5	-309.5	-8.6	-39.0	-304.7
58.7	74.25	76.18	-360.4	-321.7	-10.2	-41.4	-315.3
60.8	76.1	78.18	-374.6	-334.7	-11.5	-43.6	-327.1
62.8	78.17	80.2	-392.8	-345.6	-13.0	-45.9	-339.7
64.8	80.24	82.31	-400.1	-359.3	-14.4	-48.3	-348.3
66.8	82.2	84.22	-420.3	-371.6	-15.8	-50.4	-362.8
68.8	84.46	86.36	-437.8	-384.1	-17.3	-52.8	-375.9
70.8	86.28	88.61	-451	-397.3	-18.5	-54.7	-387.6
72.8	88.43	90.57	-467.7	-409	-19.8	-56.8	-400.1
74.8	90.62	92.74	-475	-420.9	-21.0	-58.8	-408.0
76.9	92.54	94.72	-502.9	-435.8	-22.0	-60.5	-428.1
78.9	94.56	96.76	-514.1	-447	-22.9	-62.2	-438.0
80.9	96.53	98.79	-529.4	-457.3	-23.8	-63.7	-449.6
82.9	98.59	100.72	-535.5	-471	-24.5	-65.2	-458.4
84.9	100.66	102.78	-554.5	-481.8	-25.1	-66.5	-472.4

Wind #28 (Cure Data)

Material: T40 fiber — Spool Tension(lb): 5.0

Number of Layers: 1 — Winding Tension(lb): 4.0

Oven Ramp Rate(degC/m): 1.0 — Stress Retention Factor: 0.80

Cure Time (min)	Mand. Temp. (deg C)	Oven Temp. (deg C)	Measured Microstrain Gage 1	Measured Microstrain Gage 2	Apparent Microstrain Gage 1	Apparent Microstrain Gage 2	Actual Microstrain
87	102.88	104.92	-567.5	-495.4	-25.5	-67.8	-484.8
89	104.58	106.84	-587.3	-510.5	-25.8	-68.6	-501.7
91.1	106.8	108.81	-598.1	-519.1	-25.9	-69.5	-510.9
93.1	108.8	111.27	-619.4	-531.2	-25.8	-70.1	-527.3
95.1	110.93	113.26	-625.9	-542.6	-25.6	-70.6	-536.2
97.2	112.91	115.27	-642.2	-555.4	-25.1	-70.8	-550.8
99.2	115	117.19	-661	-566.6	-24.4	-70.8	-566.2
101.2	117.02	119.52	-675.2	-573.8	-23.5	-70.7	-577.4
103.2	119.06	121.11	-687	-591.2	-22.4	-70.3	-592.8
105.2	120.79	123.65	-707.5	-597.5	-21.2	-69.7	-607.0
107.3	122.55	125.04	-710.9	-610	-19.8	-69.0	-616.0
109.3	124.48	127.08	-725	-621.1	-18.1	-68.0	-630.0
111.3	126.55	129.13	-738.6	-631.4	-16.0	-66.6	-643.7
113.3	128.51	131.05	-751.2	-642.1	-13.7	-65.1	-657.2
115.3	130.48	133.07	-763	-652	-11.1	-63.3	-670.3
117.3	132.66	135.19	-780.2	-662.1	-7.9	-61.0	-686.7
119.3	134.64	137.26	-791.7	-673.2	-4.7	-58.6	-700.8
121.4	136.6	139.09	-803.7	-683.4	-1.2	-56.0	-715.0
123.4	138.72	141.06	-814.6	-691.5	2.9	-52.7	-728.1
125.4	140.53	143.08	-825.8	-702.4	6.7	-49.7	-742.6
127.4	142.6	145.27	-839.1	-710.6	11.4	-45.9	-757.6
129.4	144.55	147.22	-848.3	-719.9	16.3	-42.1	-771.2
131.4	146.77	149.21	-861.5	-729.4	22.2	-37.2	-787.9
133.4	148.7	151.18	-871.5	-738.1	27.7	-32.7	-802.3
135.4	150.68	153.13	-885.3	-745	33.7	-27.7	-818.2
137.5	152.71	155.41	-894.9	-754	40.3	-22.2	-833.5
139.5	154.81	157.27	-907.2	-762.1	47.6	-16.0	-850.4
141.5	156.72	159.47	-914.6	-768.1	54.6	-10.1	-863.6
143.6	158.63	160.71	-924.9	-773	62.0	-3.8	-878.1
145.6	159.7	161.48	-928.7	-779.2	66.3	-0.1	-887.1
147.6	160.25	161.59	-935.4	-781.8	68.6	1.8	-893.8
149.7	160.73	161.89	-934.7	-782.4	70.6	3.6	-895.6
151.7	161.03	162.14	-932.7	-783.1	71.9	4.6	-896.2
153.8	161.06	162	-939.8	-783.2	72.0	4.7	-899.9
155.8	161.15	162.39	-938.6	-784.1	72.4	5.1	-900.1
157.8	160.5	159.06	-933.3	-781.2	69.7	2.7	-893.4
159.9	155.64	151.65	-907.9	-763.5	50.6	-13.5	-854.2
161.9	149.37	144.49	-874.8	-738.2	29.7	-31.0	-805.8
163.9	142.68	137.77	-831.1	-708.2	11.6	-45.8	-752.6
165.9	136.54	131.89	-797.9	-679.8	-1.3	-56.0	-710.2
167.9	130.78	126.42	-756.6	-649.3	-10.7	-63.0	-666.1
170	125.19	121.09	-719.7	-619.3	-17.4	-67.6	-627.0

Wind #28 (Cure Data)

Material: T40 fiber — Spool Tension(lb): 5.0
Number of Layers: 1 — Winding Tension(lb): 4.0
Oven Ramp Rate(degC/m): 1.0 — Stress Retention Factor: 0.80

Cure Time (min)	Mand. Temp. (deg C)	Oven Temp. (deg C)	Measured Microstrain Gage 1	Measured Microstrain Gage 2	Apparent Microstrain Gage 1	Apparent Microstrain Gage 2	Actual Microstrain
172	119.91	115.92	-686.6	-589.4	-21.8	-70.0	-592.1
174	115.18	111.27	-650.3	-561.8	-24.3	-70.8	-558.5
176	110.35	106.83	-620	-535.6	-25.7	-70.5	-529.7
178	106.07	102.48	-582.5	-510.1	-25.9	-69.2	-498.8
180	102.14	98.8	-555.8	-482.9	-25.4	-67.4	-473.0
182.1	98.06	95	-529.4	-458.4	-24.3	-64.8	-449.3
184.1	94.52	91.76	-495.2	-435.3	-22.9	-62.2	-422.7
186.1	91.17	88.1	-473.6	-411.9	-21.3	-59.3	-402.4
188.1	87.72	84.64	-443.8	-388.5	-19.3	-56.1	-378.4
190.1	85.43	82.84	-431.9	-376	-17.9	-53.8	-368.1
192.1	82.43	79.79	-410.4	-355.8	-16.0	-50.7	-349.8
194.1	79.54	77.16	-388	-337.4	-14.0	-47.5	-332.0
196.2	76.8	74.47	-366.1	-317.7	-12.0	-44.4	-313.7
198.2	74.17	71.99	-348.9	-301	-10.1	-41.3	-299.2
200.2	71.94	69.88	-333.3	-285.2	-8.5	-38.7	-285.7
202.2	69.64	67.68	-313	-270.2	-6.8	-36.0	-270.2
204.2	67.33	65.49	-295.8	-257.4	-5.2	-33.2	-257.4
206.2	65.29	63.42	-283.3	-243.6	-3.8	-30.8	-246.2
208.2	63.41	61.71	-262.4	-227.8	-2.5	-28.6	-229.5
210.3	61.55	59.87	-255.3	-219.5	-1.3	-26.4	-223.5
212.3	59.85	58.26	-243.5	-204.6	-0.3	-24.5	-211.7
214.3	58.12	56.57	-235.3	-195.6	0.8	-22.5	-204.6
216.4	56.59	55.17	-218.6	-186.6	1.6	-20.8	-193.0
218.4	55.22	53.82	-210	-176.5	2.3	-19.3	-184.8
220.4	53.73	52.38	-196.1	-168.4	3.0	-17.7	-174.9
222.4	52.36	51.16	-187.8	-157.9	3.7	-16.2	-166.6
224.4	51.21	49.88	-177.5	-149.4	4.1	-15.0	-158.0
226.4	49.82	48.63	-169.7	-145.4	4.7	-13.6	-153.1
228.4	48.65	47.61	-163.3	-136.9	5.1	-12.5	-146.4
230.4	47.81	46.83	-159.7	-132.2	5.3	-11.7	-142.8
232.5	47.49	46.93	-156.8	-129.4	5.4	-11.4	-140.1
234.5	47.09	46.81	-156.7	-130.8	5.5	-11.0	-141.0
236.5	46.94	46.57	-151.2	-125.4	5.6	-10.9	-135.6
238.5	46.68	46.26	-149.2	-127.2	5.6	-10.6	-135.7
240.5	46.48	46.11	-149.4	-125.7	5.7	-10.5	-135.2
242.5	46.13	45.7	-151.3	-123.2	5.8	-10.1	-135.1
244.5	45.69	45.36	-149.1	-119.6	5.9	-9.7	-132.4
246.5	45.58	45.02	-148.9	-120.8	5.9	-9.6	-133.0
248.6	45.1	44.42	-141.8	-116.3	6.0	-9.2	-127.4
250.6	44.9	44.44	-146.6	-108.1	6.0	-9.0	-125.8
252.6	44.72	44.16	-125.6	-110.5	6.0	-8.9	-116.6
254.6	43.66	42.91	-126.6	-109.6	6.2	-8.0	-117.2

Wind #28 (Cure Data)

Material: T40 fiber — Spool Tension(lb): 5.0
Number of Layers: 1 — Winding Tension(lb): 4.0
Oven Ramp Rate(degC/m): 1.0 — Stress Retention Factor: 0.80

Cure Time (min)	Mand. Temp. (deg C)	Oven Temp. (deg C)	Measured Microstrain Gage 1	Measured Microstrain Gage 2	Apparent Microstrain Gage 1	Apparent Microstrain Gage 2	Actual Microstrain
256.7	43.64	43.26	-120.1	-107.1	6.2	-7.9	-112.7
258.7	43	42.07	-140.6	-107.6	6.3	-7.4	-123.5
260.7	42.73	42.01	-124.5	-102.2	6.3	-7.2	-112.9
262.7	42.26	41.48	-121.6	-99.8	6.4	-6.8	-110.5
264.7	41.69	40.93	-120.9	-95.9	6.4	-6.4	-108.4
266.8	41.26	40.64	-117.7	-93.5	6.4	-6.0	-105.8
268.8	40.89	40.13	-115.3	-92.8	6.4	-5.7	-104.4
270.8	40.53	39.71	-111.3	-90.3	6.5	-5.5	-101.3
272.8	39.95	39.2	-106	-87	6.4	-5.0	-97.2
274.8	39.46	38.59	-107.4	-84.2	6.4	-4.7	-96.7
276.9	38.99	38.32	-103.9	-81.9	6.4	-4.3	-93.9
278.9	38.42	37.7	-99.7	-79	6.4	-4.0	-90.6
280.9	38.04	37.36	-98.6	-77.6	6.3	-3.7	-89.4
282.9	37.74	36.99	-93.7	-74	6.3	-3.5	-85.3
284.9	37.22	36.45	-93.1	-73.1	6.2	-3.2	-84.6
287	36.7	35.94	-88.8	-70.6	6.2	-2.8	-81.4
289	36.25	35.52	-88.6	-66.8	6.1	-2.5	-79.5
291	35.98	35.24	-82.6	-65.9	6.0	-2.4	-76.1
293	35.47	34.72	-82.4	-63.2	5.9	-2.1	-74.7
295	35.11	34.45	-79.9	-61.8	5.8	-1.9	-72.8
297.1	34.72	34.12	-75.5	-58.8	5.7	-1.7	-69.2
299.1	32.34	24.73	-59.8	-43.9	5.0	-0.5	-54.1
301.1	28.71	23.17	-44.2	-25.9	3.2	0.9	-37.1
303.1	26.46	22.65	-34.1	-16.4	1.7	1.5	-26.8
305.1	25	22.76	-26.5	-11.2	0.6	1.7	-20.0
307.1	24.26	22.59	-26.1	-10	-0.0	1.8	-18.9

Wind #29 (Cure Data)

Material: T40/1908 prepreg
Spool Tension(lb): 7.7
Number of Layers: 1
Winding Tension(lb): 2.5
Oven Ramp Rate(degC/m): 2.0
Stress Retention Factor: 0.33

Cure Time (min)	Mand. Temp. (deg C)	Oven Temp. (deg C)	Measured Microstrain Gage 1	Measured Microstrain Gage 2	Apparent Microstrain Gage 1	Apparent Microstrain Gage 2	Actual Microstrain
5	23.78	23.64	-43.4	-38.9	-0.5	1.9	-41.8
10	24.38	24.4	-45.2	-40.8	0.1	1.8	-43.9
15.1	33.22	37.13	-66.7	-61.6	5.3	-0.9	-66.4
20.1	44.48	47.93	-94.7	-90.6	6.1	-8.7	-91.4
25.1	54.87	58.28	-135.5	-129.2	2.5	-18.9	-124.1
30.2	65.12	68.45	-186.2	-180.2	-3.7	-30.6	-166.1
35.2	75.32	78.75	-243	-234.7	-10.9	-42.7	-212.0
40.2	85.44	88.91	-300.7	-283.7	-17.9	-53.8	-256.3
45.3	95.3	98.1	-358.5	-335.4	-23.3	-62.8	-303.9
50.3	99.66	100.46	-386.8	-352.1	-24.8	-65.9	-324.1
55.3	100.42	100.94	-390.2	-361.1	-25.0	-66.4	-330.0
60.4	100.88	101.15	-393.1	-363.3	-25.1	-66.6	-332.3
65.4	101.1	101.35	-394.9	-363.4	-25.2	-66.8	-333.2
70.4	101.25	101.38	-395.9	-363.1	-25.2	-66.9	-333.5
75.5	101.4	101.98	-397.3	-366.6	-25.3	-66.9	-335.8
80.5	106.83	109.64	-429.8	-395.3	-25.9	-69.5	-364.9
85.5	115.9	119.31	-478.2	-435.7	-24.0	-70.8	-409.5
90.6	125.83	129.15	-528.6	-476.4	-16.8	-67.1	-460.5
95.6	135.9	139.24	-571.3	-510.6	-2.5	-56.9	-511.2
100.6	145.69	148.93	-614.3	-542.8	19.2	-39.6	-568.3
105.7	152.65	154.53	-638.5	-562.4	40.1	-22.3	-609.3
110.7	155.04	155.89	-645.5	-567.9	48.4	-15.3	-623.2
115.7	155.7	156.34	-648.6	-566.5	50.8	-13.3	-626.3
120.7	156.01	156.58	-648.8	-566.7	51.9	-12.4	-627.5
125.7	156.14	156.76	-647.6	-566.7	52.4	-11.9	-627.4
130.8	156.18	156.74	-648.6	-569.4	52.6	-11.8	-629.4
135.8	148.58	144.73	-620.1	-539.9	27.3	-33.0	-577.2
140.8	133.64	129.52	-558.8	-484.9	-6.4	-59.9	-488.7
145.9	120.71	116.96	-497.4	-438.2	-21.3	-69.8	-422.3
150.9	110.32	107	-440.3	-395	-25.7	-70.5	-369.6
155.9	100.42	97.41	-384.1	-348.3	-25.0	-66.4	-320.5
160.9	91.73	89	-331.8	-305.2	-21.6	-59.8	-277.8
165.9	84.08	81.68	-285.9	-267.4	-17.1	-52.4	-241.9
170.9	77.2	75.12	-247.5	-233.4	-12.3	-44.8	-211.9
176	71.42	69.43	-212.2	-200.3	-8.1	-38.1	-183.2
181	66.07	64.45	-179.8	-173.6	-4.3	-31.8	-158.7
186	61.52	60.1	-154.9	-141.2	-1.3	-26.4	-134.2
191.1	57.6	56.13	-129.6	-121.1	1.1	-21.9	-114.9
196.1	54.33	53.03	-113.1	-110.2	2.8	-18.3	-103.9
201.1	51.08	49.96	-95.5	-92	4.2	-14.9	-88.4
206.1	48.42	47.38	-81	-80.1	5.1	-12.3	-77.0
211.2	46.97	46.55	-74.2	-74.2	5.5	-10.9	-71.5

Wind #29 (Cure Data)

Material: T40/1908 prepreg
Spool Tension(lb): 7.7
Number of Layers: 1
Winding Tension(lb): 2.5
Oven Ramp Rate(degC/m): 2.0
Stress Retention Factor: 0.33

Cure Time (min)	Mand. Temp. (deg C)	Oven Temp. (deg C)	Measured Microstrain Gage 1	Measured Microstrain Gage 2	Apparent Microstrain Gage 1	Apparent Microstrain Gage 2	Actual Microstrain
216.2	46.3	45.65	-71.2	-72.7	5.7	-10.3	-69.7
221.2	34.79	28.19	-15.1	-22	5.8	-1.7	-20.6
226.2	29.7	26.58	5.6	3.7	3.7	0.6	2.5
231.3	27.32	25.3	16.1	12.6	2.3	1.3	12.5
236.3	26.16	24.99	20.5	10.4	1.5	1.5	13.9
241.3	25.72	24.95	23.6	15.2	1.2	1.6	18.0
246.3	25.23	24.55	25.3	22.3	0.8	1.7	22.6
251.4	24.83	24.41	25.5	25.9	0.4	1.7	24.6
256.4	24.58	24.04	27.4	22	0.2	1.8	23.7
261.4	24.45	24.01	29.2	25.2	0.1	1.8	26.2
266.4	24.19	23.83	29.2	22.5	-0.1	1.8	25.0
271.4	23.96	23.65	30.1	20.4	-0.3	1.8	24.5
276.5	23.99	23.76	29.5	19.4	-0.3	1.8	23.7
281.5	24.35	23.82	31.3	22.7	0.0	1.8	26.1

Wind #30 (Cure Data)

Material: T40/1908 prepreg — Spool Tension(lb): 7.8
Number of Layers: 1 — Winding Tension(lb): 2.4
Oven Ramp Rate(degC/m): 1.0 — Stress Retention Factor: 0.31

Cure Time (min)	Mand. Temp. (deg C)	Oven Temp. (deg C)	Measured Microstrain Gage 1	Measured Microstrain Gage 2	Apparent Microstrain Gage 1	Apparent Microstrain Gage 2	Actual Microstrain
5	23.71	23.73	-43.3	-36.5	-0.5	1.9	-40.6
10	24.28	24.53	-42.9	-28.2	-0.0	1.8	-36.4
15.1	25.69	27.22	-47.3	-38	1.1	1.6	-44.0
20.1	32.41	34.76	-70.9	-56.9	5.0	-0.5	-66.1
25.1	38.39	40.22	-88.6	-73.1	6.4	-3.9	-82.1
30.1	43.56	45.27	-105.6	-95.5	6.2	-7.9	-99.7
35.2	48.6	50.19	-123.8	-112.5	5.1	-12.5	-114.5
40.2	53.69	55.37	-143	-136.7	3.1	-17.6	-132.6
45.2	58.83	60.36	-163.2	-153	0.3	-23.3	-146.6
50.3	63.79	65.46	-187.4	-179.8	-2.8	-29.1	-167.7
55.3	68.89	70.59	-213.8	-203.7	-6.3	-35.1	-188.1
60.3	73.58	75.24	-238.1	-222.1	-9.7	-40.6	-204.9
65.3	78.57	80.28	-265.6	-250.5	-13.3	-46.4	-228.2
70.4	83.59	85.26	-293.3	-272.2	-16.7	-51.9	-248.4
75.4	88.58	90.35	-320.3	-295.2	-19.9	-56.9	-269.4
80.4	93.64	95.37	-347.5	-322.7	-22.5	-61.5	-293.1
85.4	98.13	99.23	-370.6	-336.3	-24.3	-64.9	-308.8
90.5	99.49	99.9	-376.9	-344.4	-24.8	-65.8	-315.4
95.5	99.95	100.17	-380.7	-350.3	-24.9	-66.1	-320.0
100.5	99.88	100.06	-380.3	-340.3	-24.9	-66.0	-314.8
105.6	100.1	100.34	-378.9	-344.8	-24.9	-66.2	-316.3
110.6	100.14	100.38	-379.1	-347.7	-24.9	-66.2	-317.8
115.6	100.34	101.17	-381.4	-351.1	-25.0	-66.3	-320.6
120.6	103.91	105.49	-401	-366.5	-25.7	-68.3	-336.8
125.7	108.56	110.38	-425.8	-387.8	-25.9	-70.0	-358.9
130.7	113.38	115.22	-451.5	-407.6	-25.0	-70.8	-381.6
135.7	118.25	120.31	-476	-427.1	-22.9	-70.4	-404.9
140.8	123.4	125.18	-498.5	-442.2	-19.1	-68.6	-426.5
145.8	128.35	130.13	-521.6	-460.8	-13.9	-65.3	-451.6
150.8	133.42	135.19	-541.9	-480.7	-6.7	-60.1	-477.9
155.8	137.53	139.59	-560.9	-492.8	0.5	-54.6	-499.8
160.9	142.27	144.39	-580.8	-508.7	10.7	-46.6	-526.8
165.9	147.31	149.35	-598.4	-520.7	23.7	-36.0	-553.4
170.9	151.58	153.05	-613.6	-531.2	36.6	-25.3	-578.0
176	153.13	153.99	-617.8	-531.9	41.7	-21.0	-585.2
181	153.56	154.22	-618.1	-534.6	43.2	-19.7	-588.1
186.1	153.53	154.26	-619.3	-534.2	43.1	-19.8	-588.4
191.1	153.68	154.36	-619.2	-533.8	43.6	-19.4	-588.6
196.1	153.81	154.43	-620.2	-533.1	44.1	-19.0	-589.2
201.2	149.76	147.2	-605.4	-519.8	30.9	-30.0	-563.0
206.2	139.49	136.42	-564.4	-490	4.5	-51.5	-503.7
211.2	128.55	125.79	-517.1	-451.7	-13.7	-65.1	-445.0

Wind #30 (Cure Data)

Material: T40/1908 prepreg
Number of Layers: 1
Oven Ramp Rate(degC/m): 1.0
Spool Tension(lb): 7.8
Winding Tension(lb): 2.4
Stress Retention Factor: 0.31

Cure Time (min)	Mand. Temp. (deg C)	Oven Temp. (deg C)	Measured Microstrain Gage 1	Measured Microstrain Gage 2	Apparent Microstrain Gage 1	Apparent Microstrain Gage 2	Actual Microstrain
216.2	118.78	116.09	-469.1	-412	-22.5	-70.3	-394.1
221.3	109.81	107.33	-423.2	-373.7	-25.7	-70.3	-350.4
226.3	101.63	99.4	-379.4	-336.3	-25.3	-67.1	-311.7
231.3	94.33	92.28	-338.8	-300.6	-22.8	-62.0	-277.3
236.3	87.65	85.77	-300.8	-267.2	-19.3	-56.0	-246.3
241.3	81.78	79.94	-266.9	-237.9	-15.5	-50.0	-219.7
246.3	76.25	74.52	-234.4	-212.1	-11.6	-43.7	-195.6
251.4	71.71	70.21	-209.6	-184.9	-8.3	-38.4	-173.9
256.4	67.27	66	-185.3	-159.4	-5.1	-33.2	-153.2
261.4	63.31	62.07	-163.1	-138.9	-2.4	-28.5	-135.5
266.5	59.51	58.48	-142.8	-118.8	-0.1	-24.1	-118.7
271.5	56.39	55.43	-125.3	-103	1.7	-20.6	-104.7
276.5	53.56	52.62	-110.2	-88.2	3.1	-17.5	-92.0
281.5	50.82	49.98	-96.8	-75.7	4.3	-14.7	-81.1
286.5	48.65	47.91	-84.3	-64.4	5.1	-12.5	-70.6
291.6	46.48	46.05	-75	-55.1	5.7	-10.5	-62.7
296.6	46.05	45.9	-72.8	-55.7	5.8	-10.1	-62.1
301.6	45.33	45.06	-69.5	-48.7	5.9	-9.4	-57.4
306.6	44.59	44.39	-67	-48.7	6.1	-8.8	-56.5
311.7	43.76	43.42	-61.5	-41.7	6.2	-8.0	-50.7
316.7	42.72	42.32	-57.1	-36.5	6.3	-7.2	-46.4
321.7	41.75	41.25	-52.1	-32.9	6.4	-6.4	-42.5
326.7	40.83	40.29	-47.2	-29.7	6.4	-5.7	-38.8
331.8	39.67	39.18	-42.8	-25.2	6.4	-4.8	-34.8
336.8	38.56	38.12	-37.3	-21.1	6.4	-4.0	-30.4
341.8	37.64	37.21	-32.9	-15.4	6.3	-3.4	-25.6
346.8	36.44	36.06	-27.6	-12.3	6.1	-2.7	-21.7
351.8	35.49	35.08	-23.9	-10	5.9	-2.1	-18.9
356.9	34.47	34.14	-21.3	-6.9	5.7	-1.5	-16.2
361.9	33.8	33.61	-16.8	-4.3	5.5	-1.2	-12.7
366.9	33.22	32.79	-13	3.5	5.3	-0.9	-7.0
371.9	32.33	31.95	-9.8	6	5.0	-0.5	-4.2
377	31.66	31.41	-7	7.4	4.7	-0.2	-2.1
382	30.91	30.61	-4.3	11.7	4.4	0.1	1.4
387	30.29	30.06	-1.6	13.7	4.1	0.4	3.8
392	29.71	29.44	0.5	14.8	3.8	0.6	5.5
397	29.11	28.86	2.7	17.2	3.4	0.8	7.8
402.1	28.72	28.39	4.7	18.5	3.2	0.9	9.5
407.1	28.14	27.87	6.7	20.5	2.8	1.1	11.6
412.1	27.75	27.5	8.3	23.5	2.6	1.2	14.0
417.1	27.28	27.13	10.3	23.2	2.3	1.3	15.0
422.2	26.95	26.8	11.7	24	2.1	1.4	16.1

Wind #30 (Cure Data)

Material: T40/1908 prepreg
Number of Layers: 1
Oven Ramp Rate(degC/m): 1.0

Spool Tension(lb): 7.8
Winding Tension(lb): 2.4
Stress Retention Factor: 0.31

Cure Time (min)	Mand. Temp. (deg C)	Oven Temp. (deg C)	Measured Microstrain Gage 1	Measured Microstrain Gage 2	Apparent Microstrain Gage 1	Apparent Microstrain Gage 2	Actual Microstrain
427.2	26.51	26.44	13	26.7	1.7	1.5	18.2
432.2	26.17	26.04	14.3	26.5	1.5	1.5	18.9
437.2	25.65	25.61	14.9	28.8	1.1	1.6	20.5
442.2	25.58	25.44	16.4	31.1	1.0	1.6	22.4
447.3	25.43	25.25	17.3	30.3	0.9	1.7	22.5
452.3	25.11	24.97	17.8	30.6	0.7	1.7	23.0
457.3	24.65	24.62	18.7	33.2	0.3	1.8	24.9
462.3	24.62	24.47	20	32.4	0.3	1.8	25.2
467.4	24.53	24.3	19.9	33.9	0.2	1.8	25.9
472.4	24.26	24.12	21.1	34.2	-0.0	1.8	26.8
477.4	24.1	23.93	21.7	35.4	-0.2	1.8	27.7
482.4	24.05	23.92	23.5	33.7	-0.2	1.8	27.8
487.4	23.7	23.63	23.2	33.5	-0.5	1.9	27.7
492.5	23.13	23.32	24.5	39.1	-1.1	1.9	31.4
497.5	23.56	23.51	24.1	37.1	-0.7	1.9	30.0
502.5	23.41	23.32	24.9	37	-0.8	1.9	30.4
507.5	23.24	23.2	24.3	37.1	-1.0	1.9	30.2

Wind #31 (Cure Data)

Material: T40/1908 prepreg — Spool Tension(lb): 5.1

Number of Layers: 5 — Winding Tension(lb): 2.6

Oven Ramp Rate(degC/m): 1.0 — Stress Retention Factor: 0.51

Cure Time (min)	Mand. Temp. (deg C)	Oven Temp. (deg C)	Measured Microstrain Gage 1	Measured Microstrain Gage 2	Apparent Microstrain Gage 1	Apparent Microstrain Gage 2	Actual Microstrain
5	23.17	23.36	-85.7	-69.4	-1.0	1.9	-78.0
10	25.91	27.19	-104.6	-83	1.3	1.6	-95.2
15.1	29.43	31.1	-130.2	-103.9	3.6	0.7	-119.2
20.1	34.14	36.13	-158.6	-126.4	5.6	-1.4	-144.6
25.1	39.09	41.22	-183.4	-151.8	6.4	-4.4	-168.6
30.2	44.04	46.32	-201.7	-166.7	6.2	-8.3	-183.1
35.2	49.28	51.55	-225.1	-185.6	4.8	-13.1	-201.2
40.2	54.05	56.49	-247.4	-208.4	2.9	-18.0	-220.3
45.3	59.22	61.49	-281	-235.9	0.1	-23.8	-246.6
50.3	64.42	66.65	-320.3	-271	-3.2	-29.8	-279.2
55.3	69.49	71.68	-368.5	-310.6	-6.7	-35.8	-318.3
60.3	73.85	76.39	-413.1	-353.1	-9.9	-41.0	-357.7
65.3	79.05	81.59	-465.2	-397.2	-13.6	-46.9	-400.9
70.3	84	86.43	-521.3	-443.1	-17.0	-52.3	-447.5
75.4	89.08	91.65	-576.3	-490.3	-20.1	-57.4	-494.5
80.4	93.97	96.52	-634.2	-537.4	-22.7	-61.7	-543.6
85.4	98.25	99.79	-681.8	-574.6	-24.4	-65.0	-583.5
90.4	99.28	100.29	-698.4	-588.6	-24.7	-65.6	-598.3
95.5	100.05	100.56	-702.3	-592	-24.9	-66.1	-601.6
100.5	100.02	100.61	-706.3	-591.8	-24.9	-66.1	-603.5
105.5	100.27	100.72	-704.3	-588.9	-25.0	-66.3	-601.0
110.5	100.28	100.8	-706.6	-589	-25.0	-66.3	-602.2
115.5	100.77	102.17	-714.7	-598.5	-25.1	-66.6	-610.8
120.5	104.42	106.63	-759.7	-633.7	-25.8	-68.5	-649.6
125.6	108.95	111.47	-815.2	-680	-25.8	-70.1	-699.6
130.6	113.84	116.29	-874.8	-725.6	-24.8	-70.8	-752.4
135.7	119.07	121.38	-936.4	-779.1	-22.4	-70.3	-811.4
140.7	123.85	126.18	-997.2	-825.8	-18.7	-68.3	-868.0
145.7	128.77	131.08	-1060.1	-877.7	-13.4	-64.9	-929.8
150.7	133.47	135.87	-1122.1	-927.9	-6.7	-60.1	-991.6
155.8	138.54	140.85	-1190.9	-979.7	2.5	-53.0	-1060.0
160.8	143.1	145.31	-1241.6	-1016.5	12.6	-45.0	-1112.9
165.8	147.83	150.2	-1303.7	-1062.9	25.1	-34.8	-1178.5
170.8	151.93	153.52	-1358.4	-1104.8	37.7	-24.3	-1238.3
175.8	153.16	154.17	-1378.8	-1118.5	41.8	-20.9	-1259.1
180.9	153.71	154.5	-1384.3	-1125.7	43.7	-19.3	-1267.2
185.9	153.81	154.54	-1388.2	-1122.5	44.1	-19.0	-1267.9
190.9	153.81	154.7	-1389.7	-1125.8	44.1	-19.0	-1270.3
195.9	153.92	154.74	-1393.5	-1124.5	44.4	-18.7	-1271.9
200.9	148.6	145.95	-1323	-1067.6	27.4	-32.9	-1192.5
205.9	137.27	134.25	-1163.4	-941.1	0.0	-55.0	-1024.8
211	127.98	124.72	-1027.8	-830.9	-14.3	-65.6	-889.4

Wind #31 (Cure Data)

Material: T40/1908 prepreg Spool Tension(lb): 5.1
Number of Layers: 5 Winding Tension(lb): 2.6
Oven Ramp Rate(degC/m): 1.0 Stress Retention Factor: 0.51

Cure Time (min)	Mand. Temp. (deg C)	Oven Temp. (deg C)	Measured Microstrain Gage 1	Measured Microstrain Gage 2	Apparent Microstrain Gage 1	Apparent Microstrain Gage 2	Actual Microstrain
216	118.09	114.98	-882.7	-712.3	-23.0	-70.5	-750.8
221	109.12	106.29	-746.5	-600.4	-25.8	-70.2	-625.5
226	100.98	98.39	-621.4	-498.4	-25.2	-66.7	-514.0
231.1	93.69	91.23	-505.4	-405.4	-22.5	-61.5	-413.4
236.1	75.61	58.09	-243.9	-143.1	-11.1	-43.0	-166.4
241.1	42.45	32.4	242.3	243.5	6.4	-7.0	243.2
246.2	33.08	27.61	371.2	346.5	5.2	-0.8	356.6
251.2	29.22	26.1	423.8	389.8	3.5	0.8	404.7
256.2	27.25	25.18	448.6	416.5	2.3	1.3	430.8
261.3	26.26	24.52	462.5	427.5	1.6	1.5	443.5
266.3	25.49	24.3	472.1	430.7	1.0	1.7	450.1
271.4	25.09	24.02	477.1	435.5	0.7	1.7	455.1
276.4	24.67	23.7	483.6	443.8	0.3	1.8	462.7
281.4	24.35	23.72	487.7	443.8	0.0	1.8	464.8
286.4	24.08	23.65	491.5	448.9	-0.2	1.8	469.4
291.5	23.86	23.36	494.2	453.5	-0.4	1.8	473.1
296.5	23.57	23.12	494	454.6	-0.7	1.9	473.7

VITA

Paul Michael Northrop was born in 1959 in Los Alamos, New Mexico. He attended high school in El Paso, Texas for three years but graduated from SHAPE American High School in Mons, Belgium in 1977. He graduated from the University of Texas at Austin in 1982 with a Bachelor of Science in Mechanical Engineering.

Mr. Northrop worked for Exxon Company, U.S.A. from 1982-1986 as a drilling engineer, designing and troubleshooting the drilling of deep oil and gas wells in the Rocky Mountain states. He left the petroleum industry in 1986 due to an economic downturn, and worked in residential construction until 1990.

In 1990, Mr. Northrop began studies at Virginia Tech in the area of composite materials. These studies were completed at the date of this writing.

Paul Michael Northrop

Paul Michael Northrop